ANALYSIS OF LOCAL PRESSURE FACTORS ON LOW-RISE INDUSTRIAL BUILDINGS USING COMPUTATION FLUID DYNAMICS

William Davis

UTS 12049262

Table of Contents

List of Figures

List of Appendices

1. Abstract

This report uses CFD modelling to compare the local pressure coefficients for cladding elements and their fixings. Six models were used to simulate typical industrial buildings in Australia, with wind simulated from 0°, 30°, 45°, 60° and 90°. The aim of the modelling was to determine the effect of building dimensions and roof pitch on the local pressure coefficients. In addition, the results were compared to AS1170.2. The design codes AS/NZS 1170.2, EN 1991-1-4:2005+A1 and ASCE/SEI 7-10 were also compared. The comparison of the three design codes shows that AS1170.2 is generally conservative for the magnitude and affected area, with evidence from the modeling that these factors can be reduced. The results yielded that an increase in building dimensions and pitch reduced the magnitude and affected area of local pressure coefficients. Further, the increase of roof pitch induced additional local pressure zones adjacent to the building ridge. It was also found that a squarer building footprint reduces the magnitude of the pressure coefficients.

2. Introduction

Wind loading on structures is a highly technical aspect of structural engineering, with various levels of understanding among structural engineers. As wind loading is generally a governing factor in most structural designs, a vast number of wind testing and analysis has been undertaken to understand and refine the effects of wind on structures.

Local pressure factors are used in the cladding design, and the structural elements directly supporting cladding- to account for pressure increases by wind flow over and around buildings. The areas where these local pressure factors are applied are generally small, although tend to govern the design of cladding and structural elements. The values of the local pressure factors have been derived from multiple wind tunnel tests and Computational Fluid Dynamics (CFD) testing and vary based on the dimensions of the subject building and roof pitch.

This report outlines the local pressure factors from various design codes worldwide, reviews the literature to determine those factors, and compares the magnitude and affected areas. CFD modelling determines the local pressure factors on several structural models, comparing these calculated values to the design codes and the effect of building dimensions and roof pitch on the magnitude of the local pressure factors.

3. Literature Review

A vast number of wind tunnel and CFD testing has been conducted to determine external wind pressures on buildings in an effort to better understand the effects of wind and to ensure design codes are not overly conservative.

Holmes (1994) conducted wind tunnel experiments on gable-roofed tropical houses to determine the effects of elevation, roof pitch and wind direction on the magnitude of external pressures. The experiments were conducted in an open-circuit, boundary layer wind tunnel at James Cook University, Queensland using a 1/50 and 1/100 scale models. The wind pressure applied was similar to a rural terrain in regions C and D in accordance with AS1170.2, with a degree of shielding simulated by model barriers. Figure 1 shows the worst minimum pressure coefficients or "peak suctions", as put by Holmes, for any wind direction.

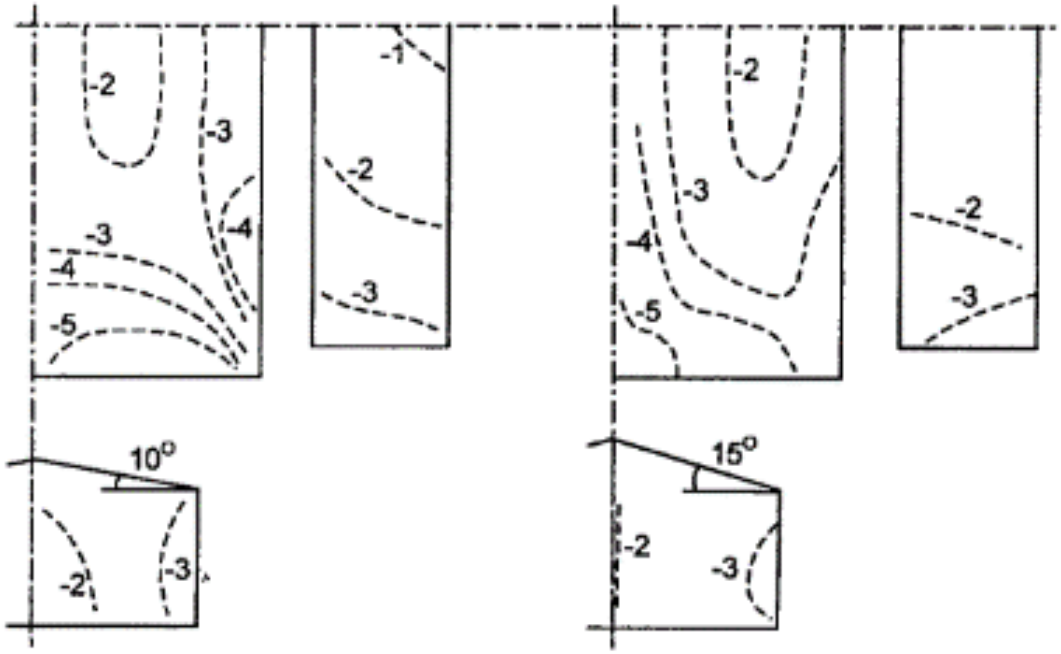

Figure 1: Largest minimum pressure coefficients for houses with roofs of 10 and 15 degrees pitch (for any wind direction) (Holmes, 1994)

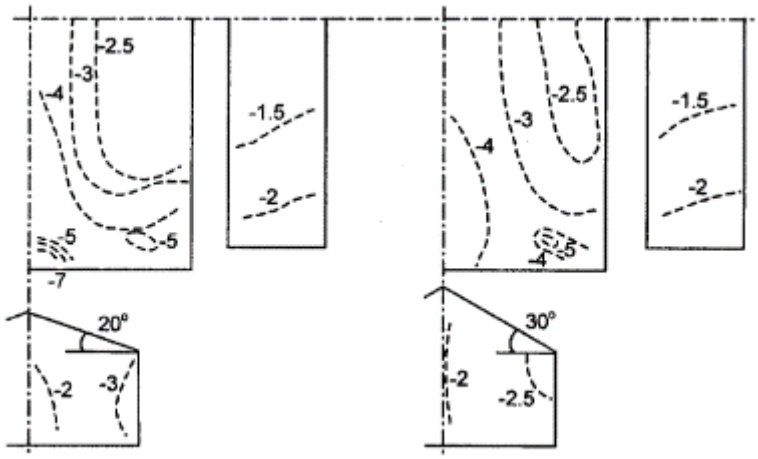

Figure 2: Largest minimum pressure coefficient for houses with roofs of 20 and 30 degrees pitch (for any wind direction) (Holmes, 1994)

The figure above shows peak pressure coefficients of up to 5, with the worst occurring on the model with a roof pitch of 20°. Holmes identifies that the increase of roof pitch intensifies the peak suction at the gable end regions, with the 10° model showing peak suction along the eaves of the long wall.

Stanthopoulos and Saathoff (1991) also conducted wind tunnel testing, to determine the local pressure coefficients for single-span, double-span and multi-span gables roofs with both 4:12 (18.4°) and 12:12 (45°) roof pitches. The experiments were carried out using a boundary layer wind tunnel, with models of 1:400 geometric scale, with the full-scale dimensions being 39m (W) x 61m (L) x 11.6m (H). For the purpose of this report, we will only study the single-span pressure coefficients for the two models.

The figure below shows the maximum negative pressure coefficients recorded for a range of wind directions between 0° and 90°. The top diagram indicates the mean pressure coefficients, and the bottom diagram indicates the instantaneous negative peak coefficients. The data shows that both the mean and instantaneous peak pressures at the ridge edge and corner are greater on the model with a roof slope of 4:12 (18.4°).

Interestingly, Stanthopoulos and Saathoff (1991) compare the peak suction coefficients derived from the wind tunnel testing to that of the Canadian code, with the data obtained from the testing exceeding the value in the code for a single-span building. Similarly, this comparison is done with the data obtained from the double and multi-span buildings and AS1170.2, with the values in the Australian code being less that the testing results.

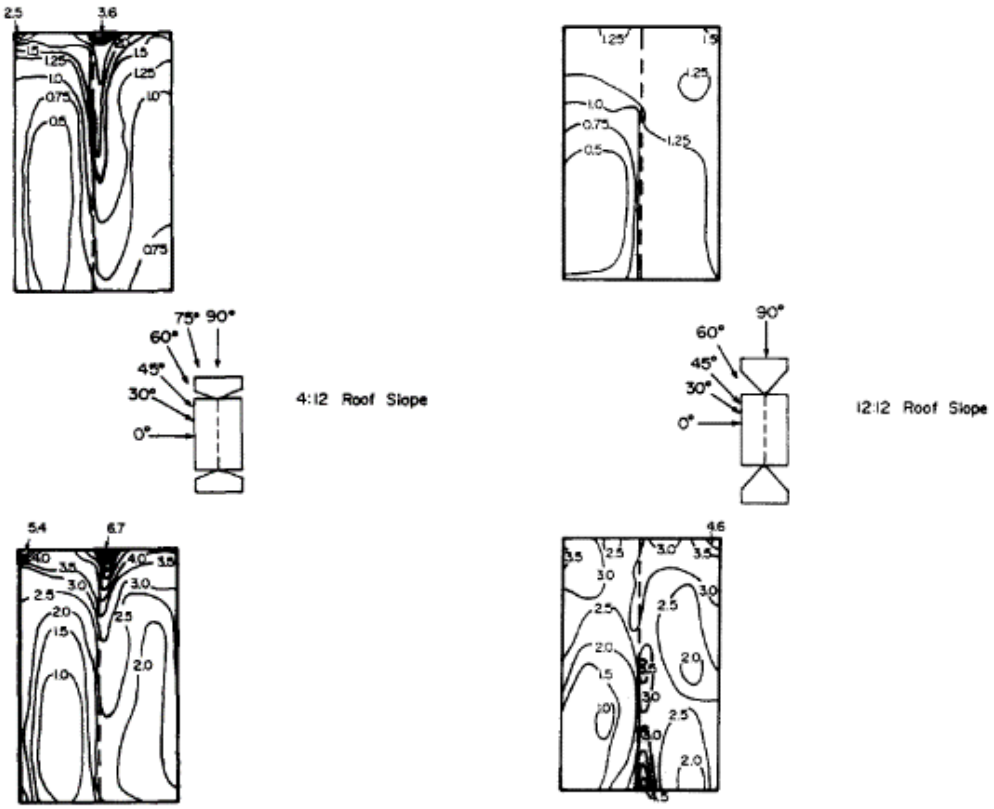

Figure 3: maximum pressure coefficients on roofs with roof slope of 4:12 (18.4°) (left) and 12:12 (45°) (right) (Stanthopoulos and Saathoff, 1991)

Alrawashdeh (2015), under the guidance of Stathopoulos, and using the same wind boundary layer wind tunnel at Concordia University, Canada, underwent testing of nine square building models simulating open-country wind exposure with wind directions ranging from 0° to 90°. The models were of a 1:400 scale with equivalent dimensions of 60m, 120m and 180m, with heights of 5m, 7.5m and 10m. Alrawashdeh's objectives, as outlined in his report, were:

1. To compare the design criteria recommended by four international codes and standards to show the differences between the current wind load provisions in terms of roof zones and design wind loads;
2. To investigate edge and corner zones of large flat roofs having horizontal plan dimensions greater than 10 times their building height;
3. To examine wind-induced suctions on edges and corners of low-rise buildings with large horizontal dimensions; including the effect of the building height and plan dimensions on the local and area-averaged pressure coefficients generated on flat roofs with large dimensions;
4. To assess the current building codes/standards provisions as to their applicability for very large buildings.

The results show that the most critical area-averaged peak wind pressures from the testing are less than the recommended values in the design codes compared. In addition, the corner and edge zones in which the pressure factors are to be applied in accordance with the codes are significantly smaller in the test results. This indicates that the design codes are potentially conservative, in comparison to the test results. Figure 4 shows the comparison of negative peak pressure coefficients on the 60m (W),

60m (L) x 5m (H) model in comparison to the edge and corner zones derived from AS1170.2. As shown, the corner area derived from AS1170.2 is significantly larger than the area in which the peak pressure coefficients occur. Similarly, in figure 4, the results from the 180m (W), 180m (L) x 5m (H) model show the peak pressure coefficients only act on a relatively small area in comparison the code derived areas.

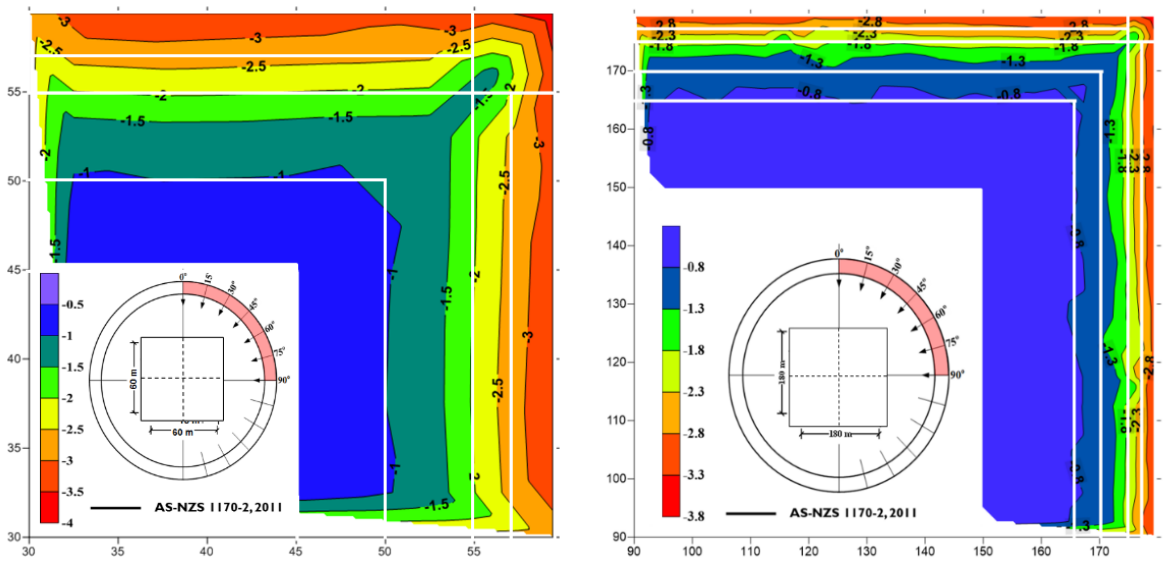

Figure 4: Most critical negative peak pressure coefficient contour (envelope for all wind directions) with roof zones of the current provisions of AS-NZS 1170.2, 2011 for building B7: 60x60x5m (left), for building B9 (right) (Alrawashdeh, 2015)

When discussing the magnitude of the peak pressure, Alrawashdeh (2015) compares the test results (Figure 5) with that of ASCE 7-10 and national building Code of Canada (NBCC) 2010, which are within a range of 0 to +0.5. This gives confidence in not only the calculated peak pressure values, but also the edge and corner zones he derived in his testing.

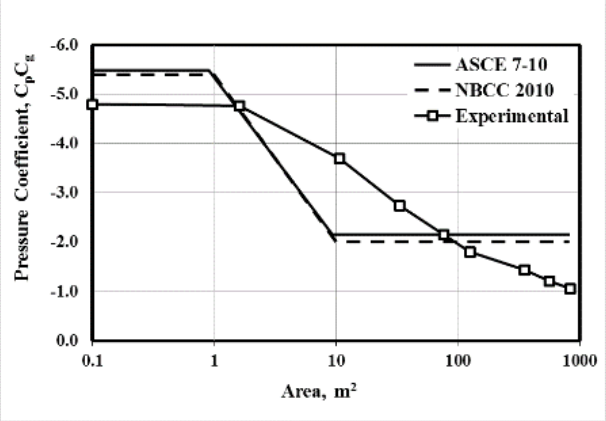

Figure 5: Comparison of most critical pressure coefficients, C_pC_g, between the present study results and the recommended code vales for hte roof corner. (Alrawashdeh, 2015).

The Wind Loading Handbook for Australia and New Zealand, AWES-HB-001-2022, outlines current changes to the local pressure factors in AS1170.2:2021, based on recent wind tunnel tests. Although the testing source is not provided, the results are provided, as shown in figure 6.

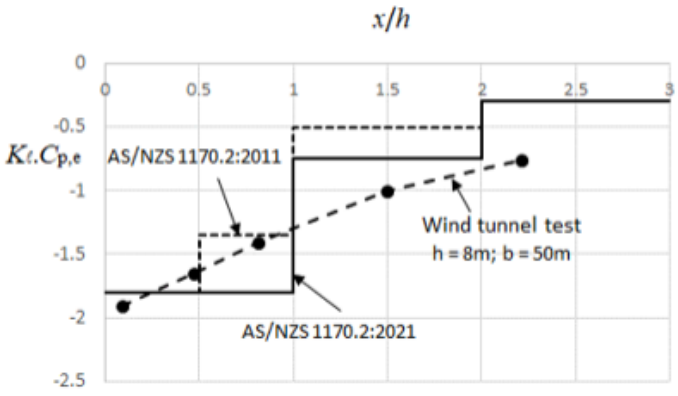

Figure 6: Local pressures on a large flat roof (Australasian Wind Engineering Society, 2022)

This graph shows an increase in the *Kl.CP,e* factors for a certain *x/h* ratio of the building dimensions. Further, the guide links the corner local pressure factor, *RC1*, for roof pitches of less than 10°, to a study conducted by Parackal (2018).

Parackal (2018) underwent CFD modelling, using SAP2000, to examine the load redistribution and progressive failure of batten to rafter connections in light framed structures. His model consisted of a rectangular house with dimensions 9.9m (W) x 8.1m (L), with rafters at 900mm centres, battens at 877mm and a 22.5° roof pitch, to emulate typical older Australian houses. See figure 7.

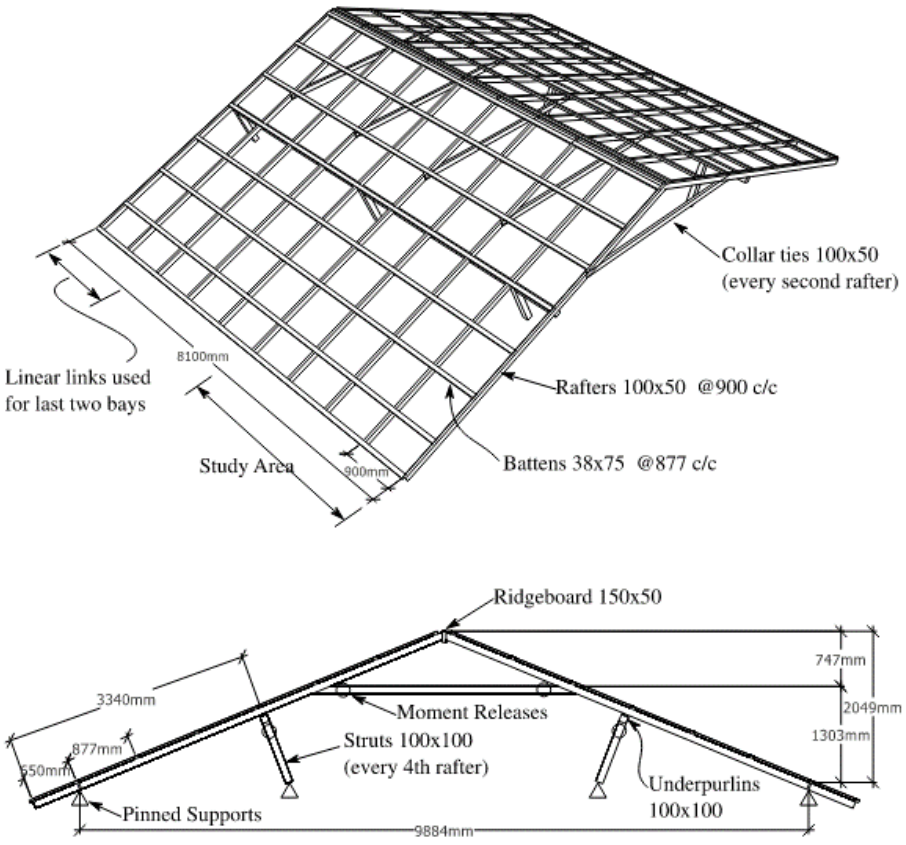

Figure 7: Schematic of the nonlinear structural analysis model (Parackal, 2018)

The results calculated by Parackal (2018) for the pressure distributions (*Cp*) that occur during peak event for differing wind directions are shown in figure 8. These results yield that for a wind direction of 210°, a peak pressure of -2.52 occurs along the gable end of the roof, near the corner. In addition, for a wind direction of 300°, a peak pressure of -2.45 occurs along the long edge, near the eave. These results are extremely specific to the configuration of the model and when compared to other wind tunnel tests explained above, seem relatively similar.

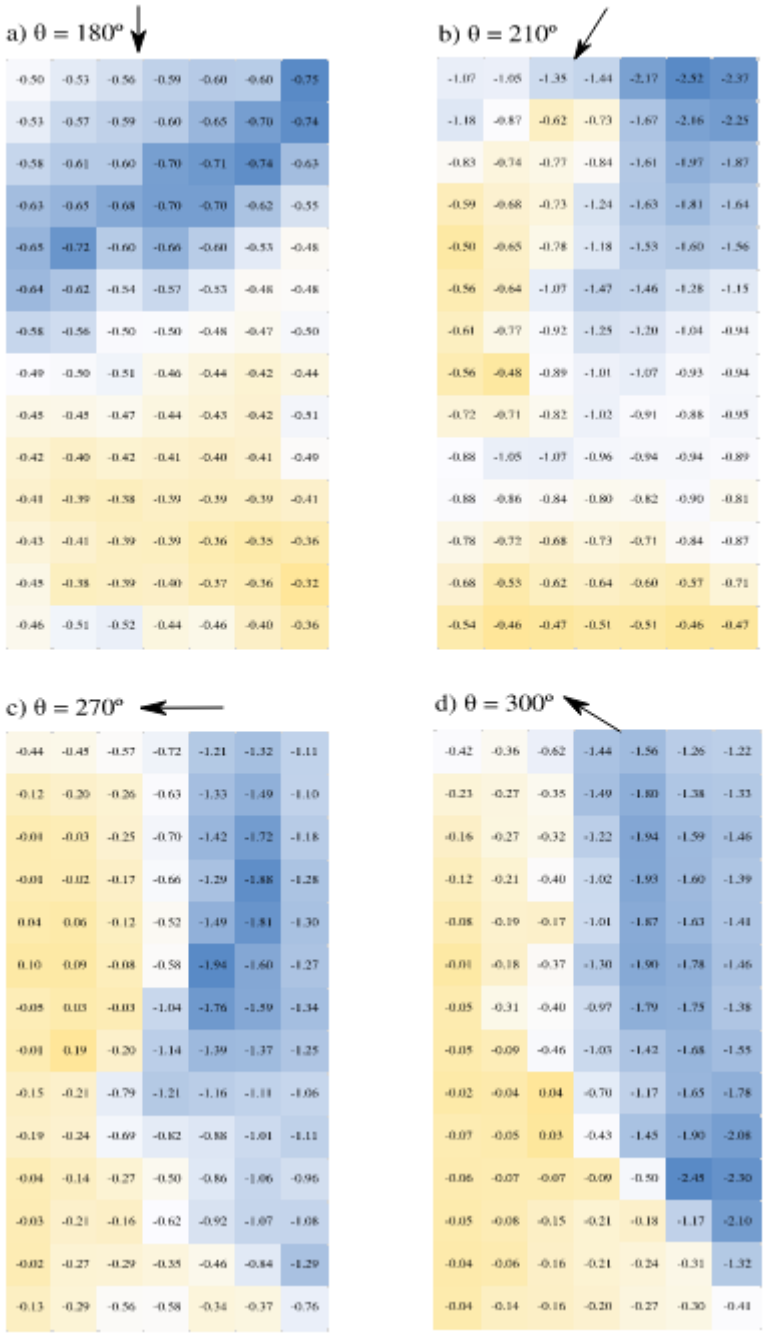

Figure 8: Pressure distributions (Cp) that occur during 'peak events' for selected wind directions (Parackal, 2018)

Singh and Roy (2019) use CFD modelling to determine the effects of roof slope and wind direction on wind pressure distribution on the roof of a square plan pyramidal low-rise building. They describe the efficiencies of CFD modelling in comparison to wind tunnel testing and how CFD reduces both time

and cost in design and research. To calibrate their calculations, they compare their results with that of multiple wind tunnel tests, ensuring the accuracy of CFD modelling for determining wind pressures.

They used ICEM CFD to model their buildings, with a 1:25 scale, using dimensions and enclosures as outlined in Figure 9. The dimensions of the enclosure seemingly suit the recommendations in Franke, Jörg & Baklanov, Alexander (2007) in their paper *Best Practice Guideline for the CFD Simulation of Flows in the Urban Environment*.

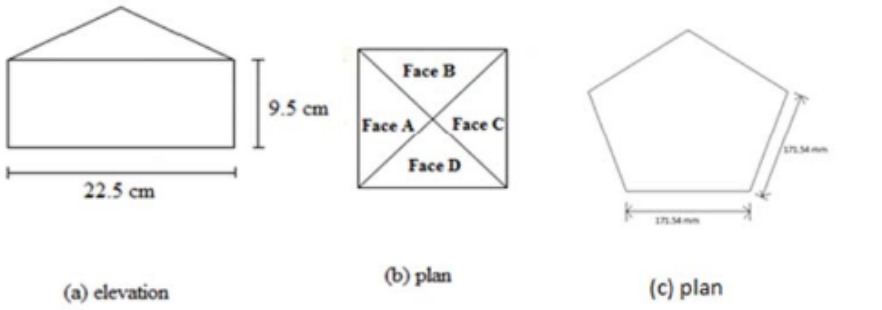

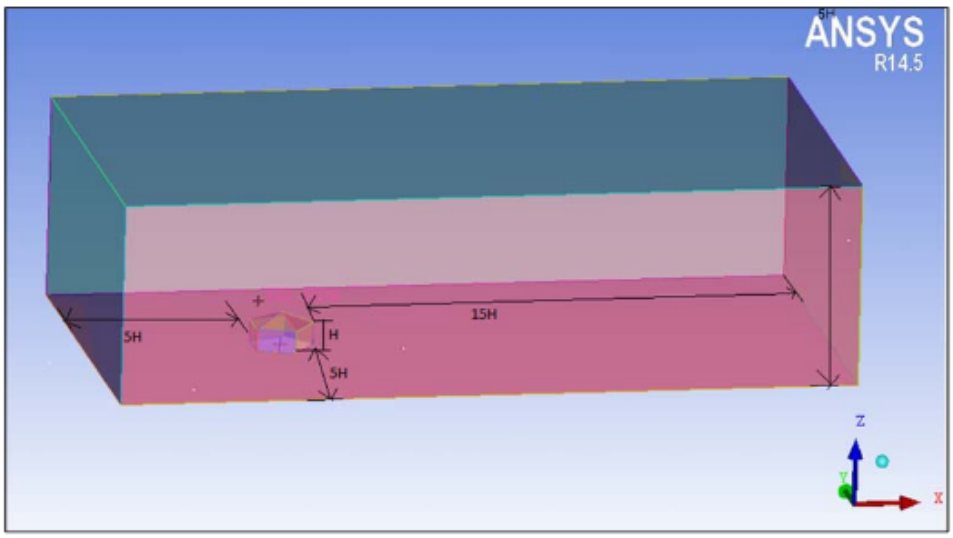

Figure 9: (a) Elevation and (b) plan of rectangular and (c) plan of pentagonal shape building model, and computational domain of building models (Singh and Roy, 2019)

Their paper compares the uplift forces for four pyramidal roof building models with roof slopes of 0°, 10°, 20° and 30°, one set of models with openings at the windward wall and the other without. The results yield that pressure coefficients on the models without openings are double or triple that of models with openings. Figure 10 shows the comparison of results between the calculated pressure coefficients for each model and the figures outlined in IS-875 part 3.

Pressure Value	$C_{p,\,mean}$ on Upper Surface						
	Windward				Leeward		
	Pitched Roof IS-875	Pentagonal Pyramidal Roof CFD	Rectangular Pyramidal Building CFD		Pitched Roof IS-875	Pentagonal Pyramidal Roof CFD	Rectangular Pyramidal Building CFD
Max '-'ve C_P Value	-1.00	-1.16	-0.92		-1.20	-1.1	-1.16

Figure 10: Comparison of Variation of CP, mean on upper roof surface of building roof of 20°roof slope for 0° wind incidence angle (Singh and Roy, 2019).

Mou et al (2017) undergo numerical simulation using CFD modelling to determine the effects building dimensional variation on wind pressure distribution. They compared two situations, adjusting the height-width ratio and the height-thickness ratio. They make note of the importance of various factors that affected the accuracy of results, including computational domain, grid generation, boundary conditions, solar settings, and residual control. Figure 11 shows a graphical representation of their computational domain dimensions and boundary conditions for each model.

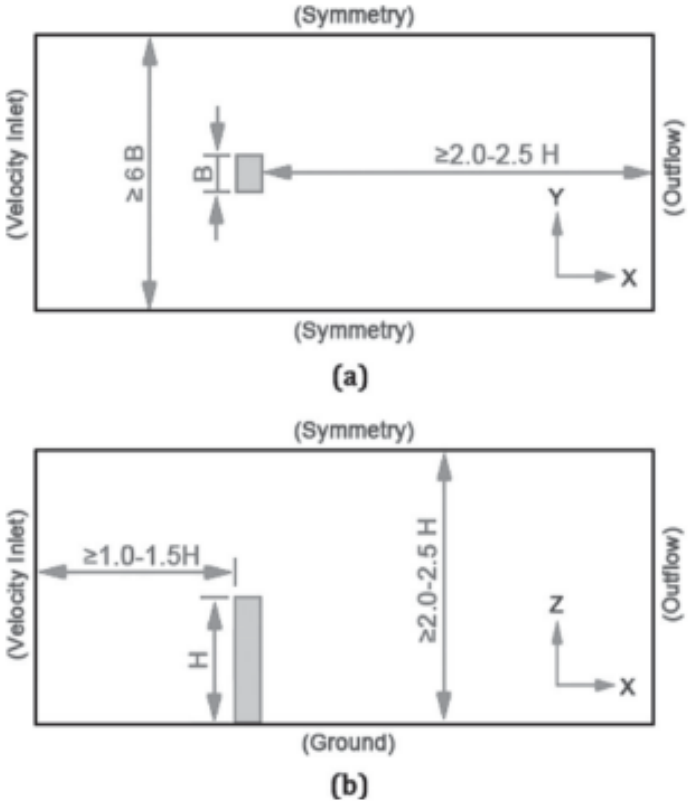

Figure 11: Computational domain and boundary conditions: (a) top view; (b) side view (Mou et al, 2017)

Using Ansys Fluent 14.0 for the simulation, they set the inlet as a velocity inlet, and enclosure walls as symmetry, to accurately portray the real-life conditions. Using the Realizable k− ε turbulent model for the solver, they make note that turbulent kinetic energy and turbulent dissipation rate should be considered.

Their investigations concluded that both the height-width and height-thickness ratios had a great influence on the wind characteristics of buildings. The note that positive pressure on building surfaces varied greatly, with a narrower windward surface was more susceptible to higher wind pressures and a larger surface experiencing a more severe negative wind effect.

The report gives good insight into the power and usefulness of CFD modelling and in particular Ansys Fluent. It also provides guidance on the possible configuration of CFD models to increase the accuracy of simulations.

4. Local pressure factors

This section outlines the local pressure factors for cladding and fixings as found in the following design codes:

- Australia/New Zealand: AS/NZS 1170.2 – Structural Design Actions – Part 2: Wind Actions
- The European Union: EN 1991-1-4:2005+A1 – Eurocode 1: Actions on Structures – Part 1-4: General Actions – Wind Actions
- US: ASCE/SEI 7-10 – Minimum Design Loads for Buildings and Other Structures

The local pressure factors from each design code are compared in magnitude and load area, with diagrams outlining the pressure factors, and how they would be applied according to the codes, to the structural analysis models outlined in Section 5 of this report. Refer to Appendix A for the diagrammatical representations of these local pressure factors.

i. AS/NZS 1170.2:2021 – Structural Design Actions – Part 2: Wind Actions

Section 5.4.4 of AS/NZS 1170.2 provides guidelines for the design of cladding elements, and their fixings. These local pressure factors are to be multiplied with the external pressure coefficient ($C_{p,e}$), area reduction factor (K_a), combination factor applied to external pressures ($K_{c,e}$) and a porous cladding reduction (K_p) to calculate the aerodynamic shape factor (C_{shp}), for external pressures(refer figure 12)

$$C_{\text{shp}} = C_{\text{p,e}} K_{\text{a}} K_{\text{c,e}} K_{\ell} K_{\text{p}}, \text{ for external pressures}$$

Figure 12: Aerodynamic shape factor equation (AS/NZS 1170.2, 2011)

For the building dimensions outlined previously, the relevant local pressure factors include RC1, RA1 and RA2. Refer to Figure 13 for the local pressure factors and Figure 14 for the pressure factor locations. Note the dimension *a* for is the minimum of 0.2*b* or 0.2*d*, if (*h*/*b*) or (*h*/*d*) ≥ 0.2; or 2*h* if both if (*h*/*b*) and (*h*/*d*) < 0.2, and the side ratio of the local pressure factor should not exceed 4.

Columns 4 and 5 of Figure 13, outline the area of the local pressure factor, and the location in relation to the edge of the building. It does not, however, guide where the local pressure factor should be applied. Common assumptions are that it can be applied anywhere within the boundaries or tied to the corner of the building. The former yielded worse effects along the eaves.

Table 5.6 — Local pressure factor (K_ℓ)

Design case	Figure 5.3 reference case	Building aspect ratio (r)	Area (A)	Proximity to edge	K_ℓ
Positive pressures					
Windward wall	WA1	All	$A \le 0.25a^2$	Anywhere	1.5
All other areas	—	All	—	—	1.0
Negative pressures					
Upwind corners of roofs with pitch < 10°	RC1	All	$A \le 0.25a^2$	< a from two edges	3.0
Downwind corners of roofs with pitch ≥ 10°	RC2	All	$A \le 0.25a^2$	< a from both roof edge and ridge	3.0
Upwind roof edges	RA1	All	$A \le a^2$	< a	1.5
	RA2	All	$A \le 0.25a^2$	< $0.5a$	2.0
Downwind side of hips and ridges of roofs with pitch ≥ 10°	RA3	All	$A \le a^2$	< a	1.5
	RA4	All	$A \le 0.25a^2$	< $0.5a$	2.0
Side walls near windward wall edges	SA1	≤ 1	$A \le a^2$	< a	1.5
	SA2		$A \le 0.25a^2$	< $0.5a$	2.0
	SA3	> 1	$A \le 0.25a^2$	> a	1.5
	SA4		$A \le a^2$	< a	2.0
	SA5		$A \le 0.25a^2$	< $0.5a$	3.0
All other areas	—	All	—	—	1.0

NOTE 1 Figure reference numbers and dimension a are defined in Figure 5.3.

NOTE 2 The building aspect ratio (r) is defined as the average roof height (h) divided by the smaller of b or d.

Figure 13: Local pressure factors (Kl) (AS/NZS 1170.2, 2011)

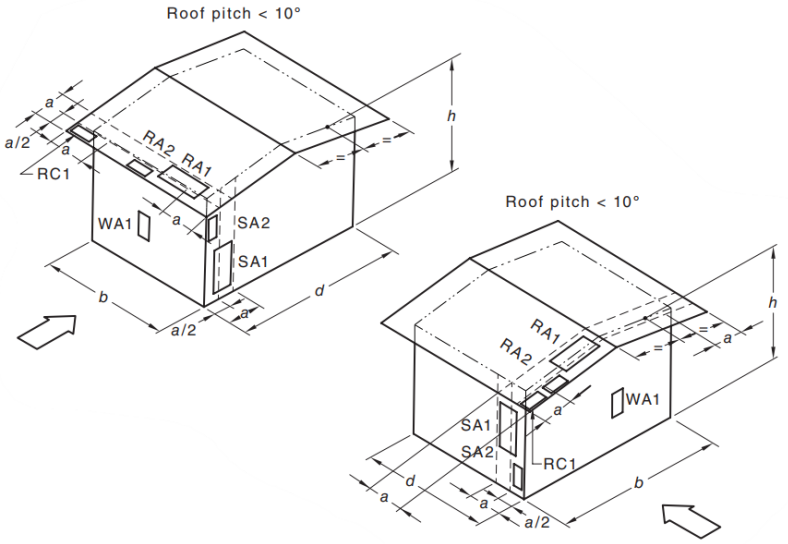

Figure 14: Local pressure factor diagrams (AS/NZS 1170.2, 2011)

ii. EN 1991-1-4:2005+A1 – Eurocode 1: Actions on Structures – Part 1-4: General Actions – Wind Actions

Section 7 of EN 1991-1-4:2005+A1 provides guidelines for applying external wind pressure coefficients for cladding, fixings, and structural parts for loaded areas of $1m^2$ ($C_{pe,1}$) and $10m^2$ ($C_{pe,10}$). The $C_{pe,1}$ coefficient is intended for the design of small elements and fixings with an area per element of $1m^2$ or less (such as cladding and roofing elements) and the $C_{pe,10}$ intended for the design of the overall load bearing structure of buildings. Figure 15 shows a graphical representation for determining the external pressure coefficient c_{pe} for buildings with a loaded area A between 1 m^2 and 10 m^2. Figure 17 outlines pressure coefficient for a range of roof pitches, although for roof pitches between -5° and 5°, data for flat roofs are to be used as per Figure 19. These pressure coefficients for each zone will be applied within the boundaries of $e = b$ or $2h$ (whichever is smaller). Refer Figures 16 and 18. Figures 17 and 19 provide the recommended values of external pressure factors for roof zones for $C_{pe,1}$ and $C_{pe,10}$.

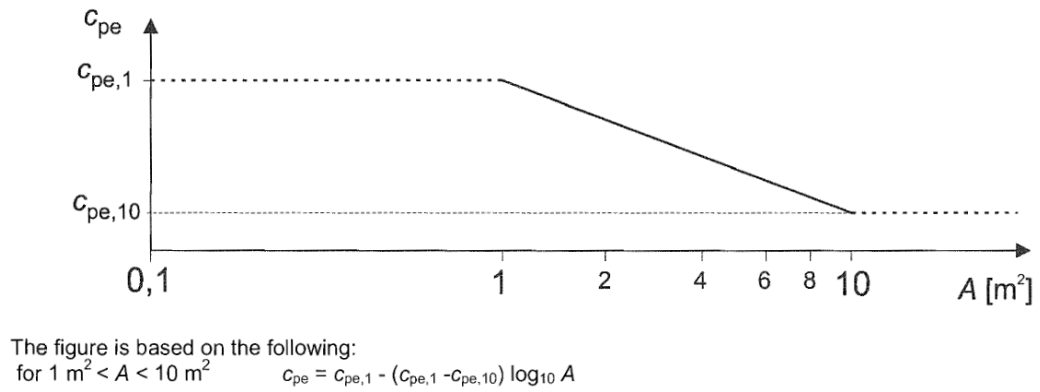

Figure 15: Recommended procedure for determining the external pressure coefficient c_{pe} for buildings with a loaded area A between 1 m^2 and 10 m^2 (EN1991-1-4, 2005)

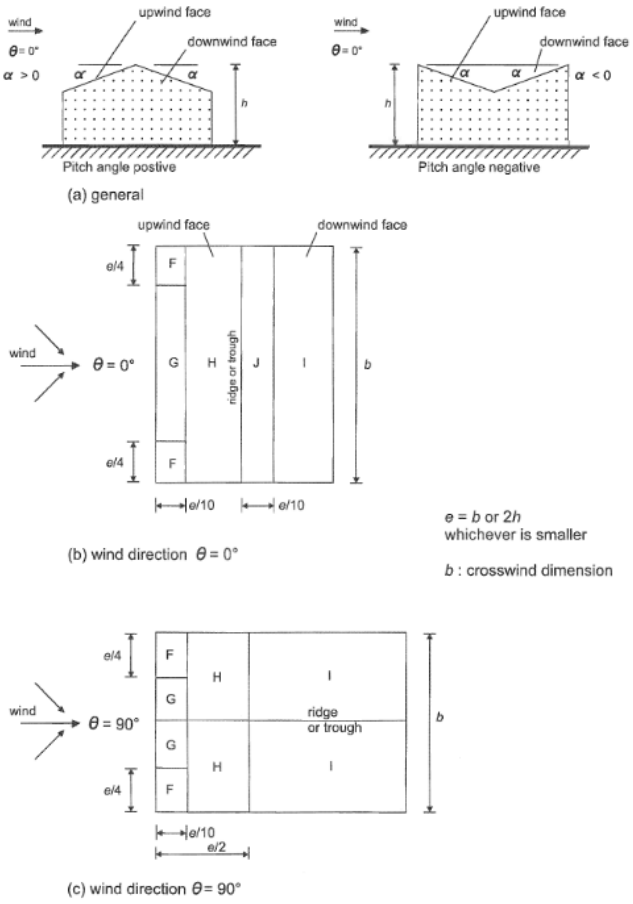

Figure 16: Key for duopitch roofs (EN1991-1-4, 2005)

Pitch Angle α	Zone for wind direction θ = 0 °									
	F		G		H		I		J	
	$c_{pe,10}$	$c_{pe,1}$	$c_{pe,10}$	$c_{pe,1}$	$c_{pe,10}$	$c_{pe,1}$	$c_{pe,10}$	$c_{pe,1}$	$c_{pe,10}$	$c_{pe,1}$
-45°	-0,6		-0,6		-0,8		-0,7		-1,0	-1,5
-30°	-1,1	-2,0	-0,8	-1,5	-0,8		-0,6		-0,8	-1,4
-15°	-2,5	-2,8	-1,3	-2,0	-0,9	-1,2	-0,5		-0,7	-1,2
-5°	-2,3	-2,5	-1,2	-2,0	-0,8	-1,2	+0,2		+0,2	
							-0,6		-0,6	
5°	-1,7	-2,5	-1,2	-2,0	-0,6	-1,2	-0,6		+0,2	
	+0,0		+0,0		+0,0				-0,6	
15°	-0,9	-2,0	-0,8	-1,5	-0,3		-0,4		-1,0	-1,5
	+0,2		+0,2		+0,2		+0,0		+0,0	+0,0
30°	-0,5	-1,5	-0,5	-1,5	-0,2		-0,4		-0,5	
	+0,7		+0,7		+0,4		+0,0		+0,0	
45°	-0,0		-0,0		-0,0		-0,2		-0,3	
	+0,7		+0,7		+0,6		+0,0		+0,0	
60°	+0,7		+0,7		+0,7		-0,2		-0,3	
75°	+0,8		+0,8		+0,8		-0,2		-0,3	

NOTE 1 At θ = 0° the pressure changes rapidly between positive and negative values on the windward face around a pitch angle of α = -5° to +45°, so both positive and negative values are given. For those roofs, four cases should be considered where the largest or smallest values of all areas F, G and H are combined with the largest or smallest values in areas I and J. No mixing of positive and negative values is allowed on the same face.

NOTE 2 Linear interpolation for intermediate pitch angles of the same sign may be used between values of the same sign. (Do not interpolate between α = +5° and α = -5°, but use the data for flat roofs in 7.2.3). The values equal to 0,0 are given for interpolation purposes

Figure 17: Recommended values of external pressure coefficients for duopitch roofs (EN1991-1-4, 2005)

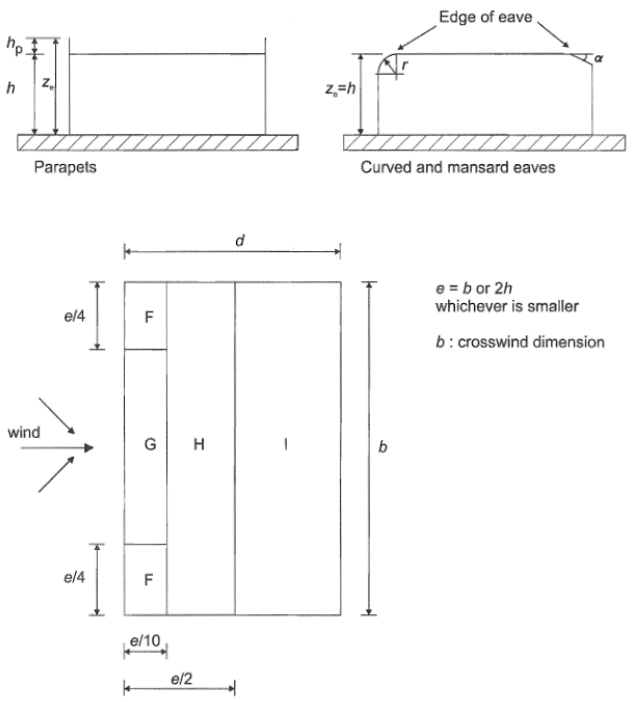

Figure 18: Key for flat roofs (EN1991-1-4, 2005)

Roof type		Zone F		Zone G		Zone H		Zone I	
		$c_{pe,10}$	$c_{pe,1}$	$c_{pe,10}$	$c_{pe,1}$	$c_{pe,10}$	$c_{pe,1}$	$c_{pe,10}$	$c_{pe,1}$
Sharp eaves		-1,8	-2,5	-1,2	-2,0	-0,7	-1,2	+0,2	
								-0,2	
With Parapets	h_p/h=0,025	-1,6	-2,2	-1,1	-1,8	-0,7	-1,2	+0,2	
								-0,2	
	h_p/h=0,05	-1,4	-2,0	-0,9	-1,6	-0,7	-1,2	+0,2	
								-0,2	
	h_p/h=0,10	-1,2	-1,8	-0,8	-1,4	-0,7	-1,2	+0,2	
								-0,2	
Curved Eaves	r/h = 0,05	-1,0	-1,5	-1,2	-1,8	-0,4		+0,2	
								-0,2	
	r/h = 0,10	-0,7	-1,2	-0,8	-1,4	-0,3		+0,2	
								-0,2	
	r/h = 0,20	-0,5	-0,8	-0,5	-0,8	-0,3		+0,2	
								-0,2	
Mansard Eaves	α = 30°	-1,0	-1,5	-1,0	-1,5	-0,3		+0,2	
								-0,2	
	α = 45°	-1,2	-1,8	-1,3	-1,9	-0,4		+0,2	
								-0,2	
	α = 60°	-1,3	-1,9	-1,3	-1,9	-0,5		+0,2	
								-0,2	

NOTE 1 For roofs with parapets or curved eaves, linear interpolation may be used for intermediate values of h_p/h and r/h.

NOTE 2 For roofs with mansard eaves, linear interpolation between α = 30°, 45° and α = 60° may be used. For α > 60° linear interpolation between the values for α = 60° and the values for flat roofs with sharp eaves may be used.

NOTE 3 [A1] In Zone I, where positive and negative values are given, both values should be considered. [A1]

NOTE 4 For the mansard eave itself, the external pressure coefficients are given in Table 7.4a "External pressure coefficients for duopitch roofs: wind direction 0° ", Zone F and G, depending on the pitch angle of the mansard eave.

NOTE 5 For the curved eave itself, the external pressure coefficients are given by linear interpolation along the curve, between values on the wall and on the roof.

[A1] NOTE 6 For mansard eaves with horizontal dimension less than e/10,the values for sharp eaves should be used. For the definition of e see Figure 7.6. [A1]

Figure 19: Recommended values of external pressure coefficients for flat roofs (EN1991-1-4, 2005)

iii. ASCE/SEI 7-10 – Minimum Design Loads for Buildings and Other Structures

Chapter 30 of ASCE/SEI 7-10 outlines the procedures to determine wind loads on components and cladding. Part 1 refines the calculations for enclosed or partially enclosed low-rise buildings with $h \leq$ 18.3m (relevant to the structural analysis models).

The external pressure coefficients C*p* are combined with the gust effect factor *G* and applied to the corners of buildings, along the eaves, and general roof areas. Dimension *a* is 10 percent of the least horizontal dimension or 0.4*h*, whichever is smaller, but no less than 4 percent of the least horizontal dimension or 3 ft (0.9m), ASCE/SEI 7-10 (2002). Refer Figure 20 for the external pressure coefficients as shown in ASCE/SEI 7-10 for gable roofs with pitch < 7° and Figure 21 for gable roofs with pitches between 7° and 17°. Refer Appendix A for the external pressure factors on the structural analysis models in accordance with ASCE/SEI 7-10.

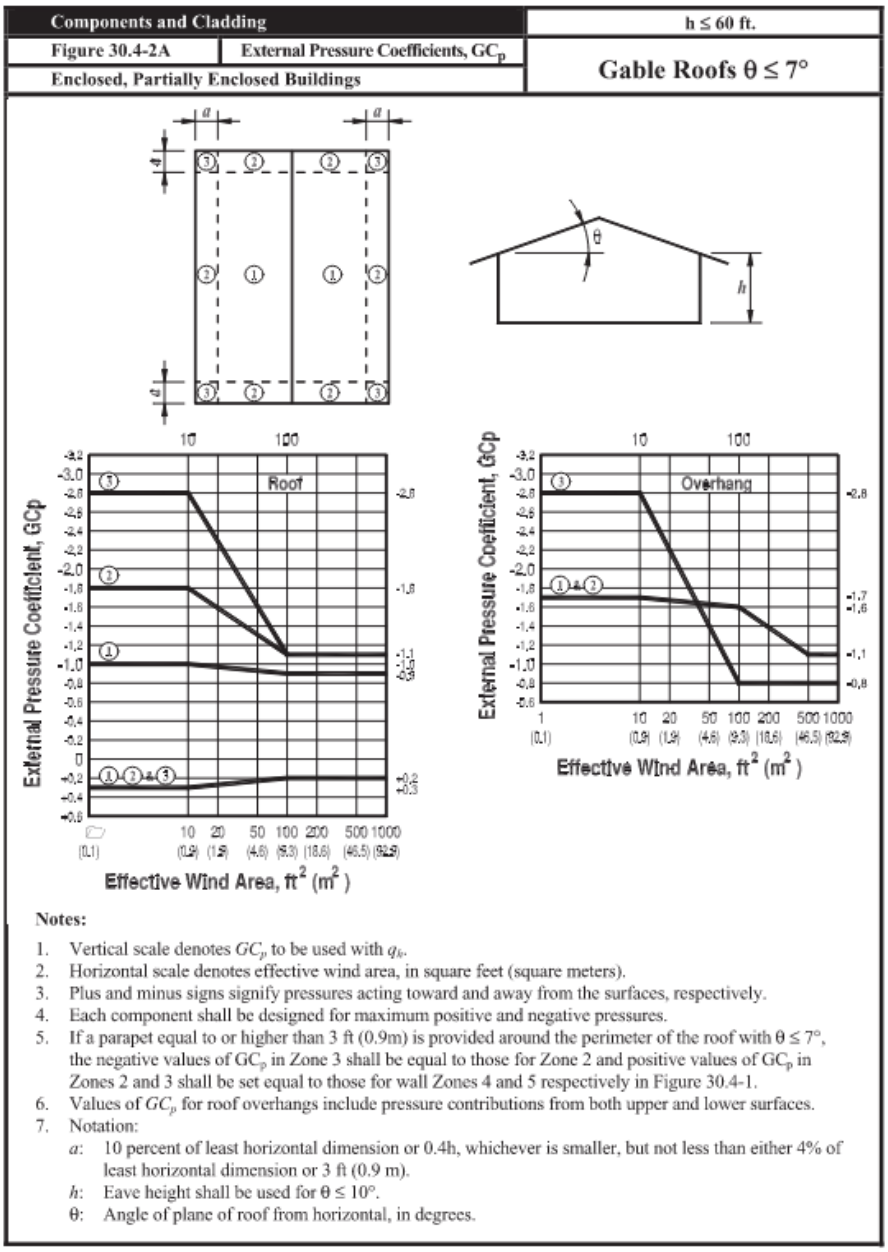

Figure 20: External pressure coefficients for gable roofs with pitch <7° (ASCE/SEI 7-10, 2002)

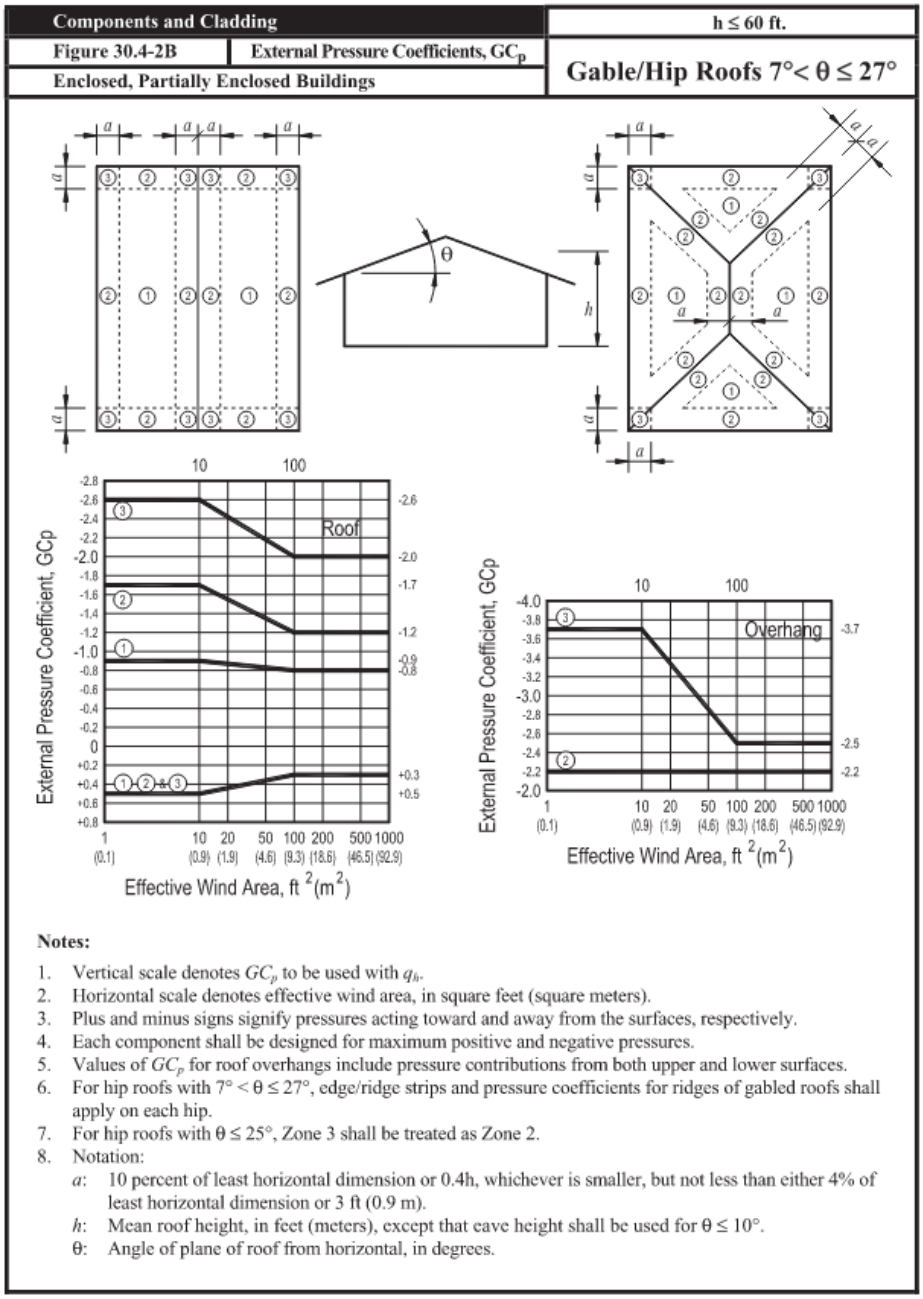

Figure 21: External pressure coefficients for gable roofs with pitch between 7° and 17° (ASCE/SEI 7-10, 2002)

iv. Comparison of design codes

Local pressure coefficients have been calculated using the design codes design codes AS/NZS 1170.2, EN 1991-1-4:2005+A1 and ASCE/SEI 7-10 for each of the 6 models outline in Section 5 of this report. Refer to Appendix A for the diagrammatical representations of these local pressure factors.

The governing factors of the design of cladding elements and their fixings are generally the corner uplift factors, which are described in terms of magnitude and affected area. For the three design codes described above, the maximum corner uplift coefficients for the design models is -3.0, in accordance with AS1170.2. This factor does not vary with the building dimensions. EN 1991-1-4:2005+A1 and ASCE/SEI 7-10 have corner uplift coefficient ranging from -2.0 to -2.5, depending on the building

dimensions. The area of affect is based on a dimension '*a*' for AS170.2 and ASCE/SEI 7-10 and '*e*' for EN 1991-1-4:2005+A1, as described above.

For wind pressures along the windward edges, AS1170.2 recommends two patch loads, RA1 and RA2 for upwind roof edges, with magnitudes of -1.5 and -2.0, respectively. These factors are to be applied as a moving load along the eave, to represent uplift forces for all wind directions. EN 1991-1-4:2005 and ASCE/SEI 7-10 use pressure areas in lieu of patch loading. In comparison to AS1170, the pressure areas are generally smaller than the zones in which the RA1 and RA2 factors are applied. The upwind roof edge pressure coefficient in EN 1991-1-4:2005 for the design models is -2.0, with the ASCE/SEI 7-10 factors ranging from -1.1 to -1.5. EN 1991-1-4:2005 and has a secondary pressure zone, similar to RA2 in AS1170.2, with a pressure coefficient ranging from -0.7 to -1.2 for the design models.

Pressure coefficients for central areas on roofs are outlined in both EN 1991-1-4:2005 and ASCE/SEI 7-10 with factors ranging from -0.2 to -1.2 and -0.9, respectively. AS1170.2 does not outline additional local pressure factors for these areas, relying on the typical external pressure coefficients for upwind and downwind slopes.

For roof pitches of 10° or greater, all three codes add pressure coefficient zones around the ridge of the building. These are generally similar to the upwind roof edges as described above.

5. Structural Analysis Models

Six models have been used to depict typical industrial buildings in Australia, to determine the maximum negative local pressure factors, the size of the area these pressures occur and to determine the effect of roof pitch and building dimensions on these pressure factors. The model dimensions are as follows:

1. 50m (W) x 100m (L) x 14m (H) – Roof pitch 3°
2. 100m (W) x 200m (L) x 14m (H) – Roof pitch 3°
3. 150m (W) x 150m (L) x 14m (H) – Roof pitch 3°
4. 50m (W) x 100m (L) x 14m (H) – Roof pitch 10°
5. 100m (W) x 200m (L) x 14m (H) – Roof pitch 10°
6. 100m (W) x 100m (L) x 14m (H) – Roof pitch 10° (note smaller dimensions were used for this model to depict a more realistic building shape compared to a 150m (W) x 150m (L) x 14m (H) with a 10°roof pitch.)

The design wind speed and wind pressures have been calculated in accordance with AS1170.2:2021 for the six models, assuming the buildings are located in Region 2 with a terrain category of TC1 (Very exposed open terrain with very few or no obstructions) and a regional wind speed of 45m/s (V_{500}). See below example of calculations for Model 1.

Site Wind Speed

$$V_{\mathrm{sit},\beta} = V_{\mathrm{R}} M_{\mathrm{c}} M_{\mathrm{d}} \left(M_{\mathrm{z,cat}} M_{\mathrm{s}} M_{\mathrm{t}} \right)$$

V_R = 45m/s

M_c = 1.0

M_d = 0.95 (North, East, South); 1.00 (West)

$M_{z,cat}$ = 1.11 (H_{avg} = 13.35m)

M_s = 1.00

Mt = 1.00

$V_{sit,\beta}$ = $V_{des,\theta}$ = 47.5m/s (North, East, South); 50.0m/s (West)

Note the inlet velocity magnitude of 50.0m/s was assumed for all wind directions

Design Wind pressure

$$p = \left(0.5\rho_{\mathrm{air}}\right)\left[V_{\mathrm{des},\theta}\right]^2 C_{\mathrm{shp}} C_{\mathrm{dyn}}$$

ρ_{air} = 1.2kg/m3

$V_{des,\theta}$ = 47.5m/s (North, East, South); 50.0m/s (West)

C_{shp} = $C_{p,e}K_aK_{c,e}K_lK_p$ – note the Aerodynamic shape factors will not be calculated here

All models are assumed to be fully enclosed. This is done as industrial buildings typically do not have windows or have non-opening windows and the assumption that all roller doors would most likely be closed during a high wind event. Wind loads were then applied at 0°, 30°, 45°, 60° and 90°.

6. Method of Analysis

As described in the literature review, CFD modelling is an extremely powerful and useful tool for simulating wind flow and its effect on buildings. For this study, the Ansys Fluent package has been used to model, simulate, and analyse the structural models.

Modelling

Using the Design Modeler module, a scale sketch of the building end wall was drawn and extruded to the required length. Refer Figure 22 for 100m (W) x 200m (L) x 14m (H) – Roof pitch 3° model.

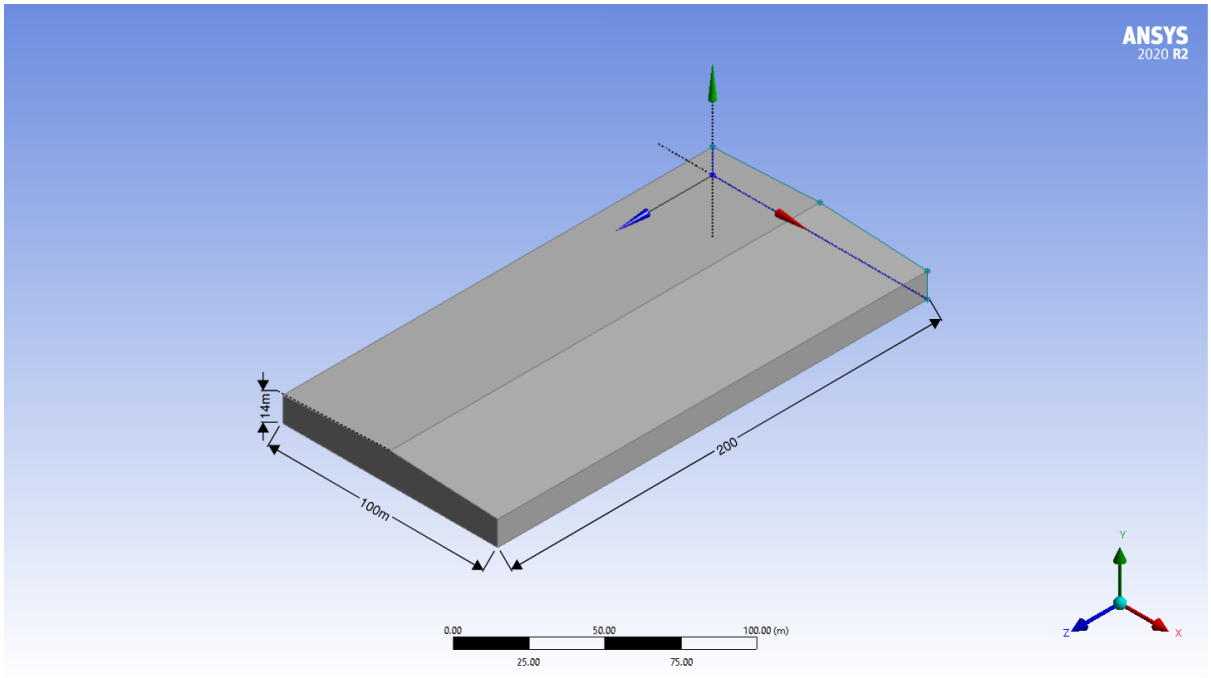

Figure 22: Orthogonal view of Model 2

Once the model had been extruded, a rectangle was sketched around the model in the XZ plane to depict the base of a wind tunnel for the fluid to be directed through, which was later extruded around the model to form the enclosure. The dimensions of the enclosure were based on the work from Franke, Jörg & Baklanov, Alexander (2007) in their paper *Best Practice Guideline for the CFD Simulation of Flows in the Urban Environment*. The dimensions of the enclosure were set to 5H from the windward edge and side walls, 5H above the ridge line and 15H from the leeward edge to ensure the fluid flow had sufficient room to prevent turbulence interference, refer Figure 23. The Boolean function was used the 'subtract' the model of the building from the enclosure. This step prevents the meshing of the interior of the building, which is unnecessary for this experimentation. The outer faces of the building remain in the fluid body of the enclosure and the software can record the forces and pressures applied to these faces.

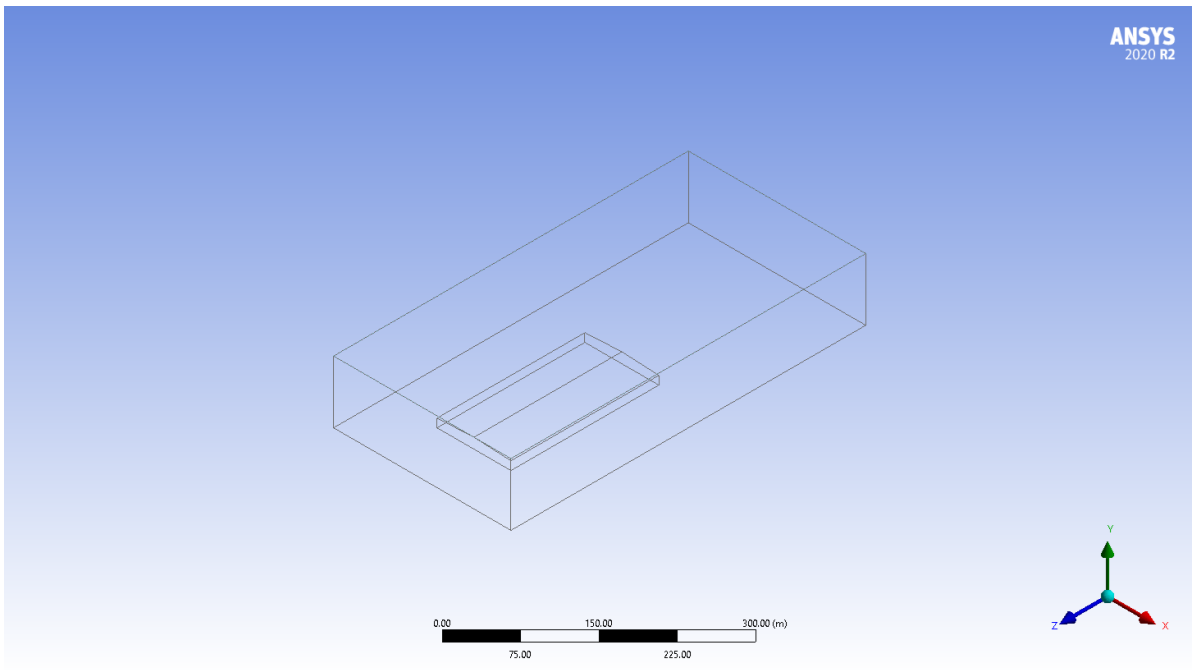

Figure 23: Wireframe view of Model 2 showing typical configuration of enclosure.

Meshing

Meshing is the process of dividing the surface of a geometry into smaller areas to allow the software to solve the governing equations efficiently. The design models were transferred to the *Fluent (with fluent meshing)* module to take advantage of the "watertight geometry" workflow, which is more reliable in producing faster and higher quality meshing in comparison to the typical Ansys meshing tool. Figure xx shows the "watertight geometry" workflow tree.

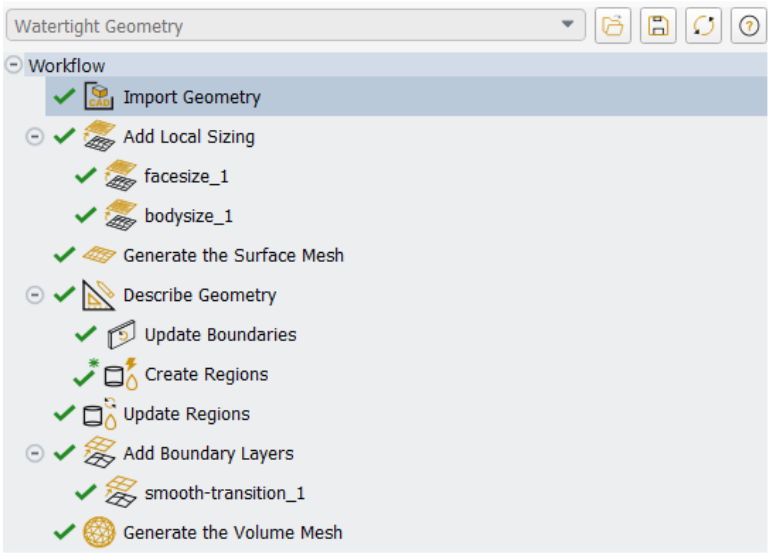

Figure 24: Fluent (with Fluent Meshing) "Watertight Geometry" workflow tree

In the "add local sizing" stem, a facesize was added on the building walls, with a target mesh size of 10m, and similarly, a bodyside was added for the fluid domain with a target mesh size of 10m. This size was determined through an iterative process based on mesh quality and the solver reaching convergence. It was notice that different target mesh sizes between the face and body sixes caused the solver to not reach convergence. When generating the surface meh, no changes were made to the

default settings. The geometry type was set to “consists of both fluid and solid regions and/or voids” and the wall boundary conditions were changed to “Symmetry”. Finally, three boundary layers were added with a smooth transition offset method, which was the default setting in the workflow and the mesh was generated with a poly-hexcore fill type. The Polyhedrons are also less sensitive to stretching in comparison to Tetrahedrons, with results in better mesh quality and improved numerical stability of the model (Sosnowski, *Et al*, 2017).

Figure 25 shows the original mesh using the Fluent meshing tool, and Figure 26 shows the mesh using the Watertight Geometry process. The Watertight Geometry portrays a much cleaner and structured mesh in comparison to the output from the Fluent meshing tool.

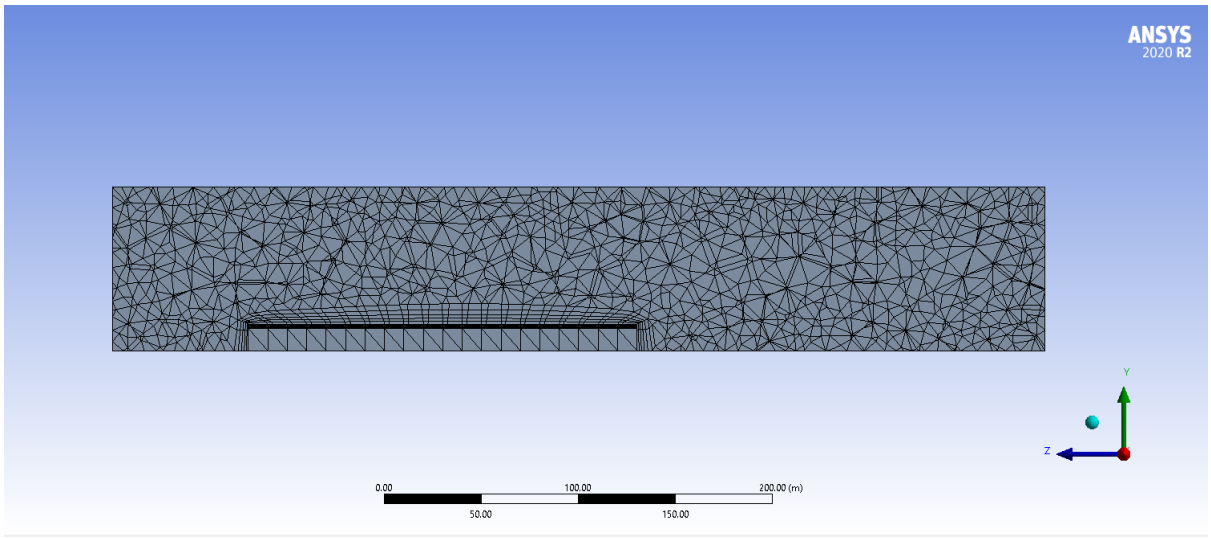

Figure 25: mesh elevation output from Fluent Meshing Tool

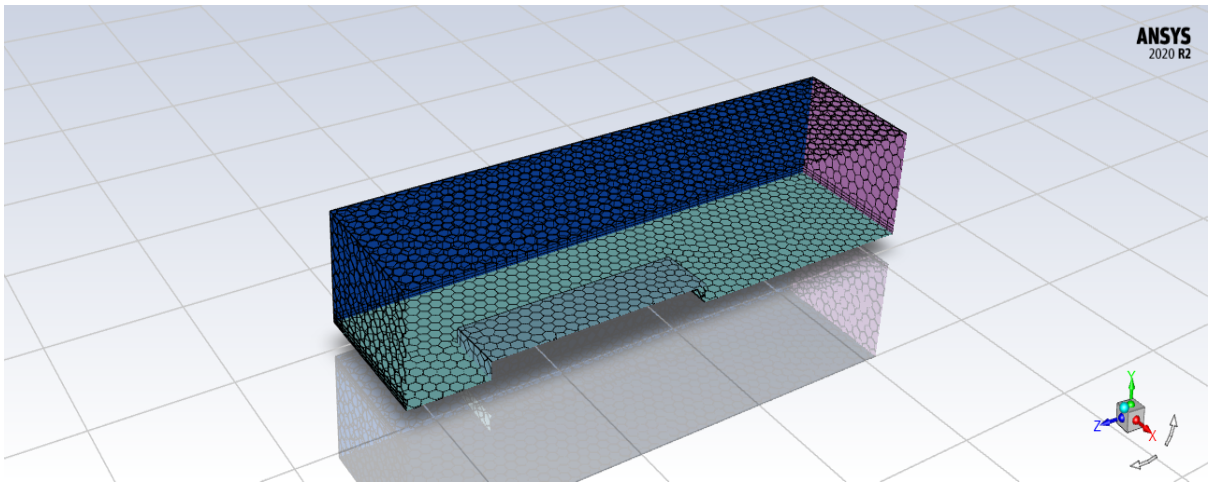

Figure 26: Orthogonal view of output from Watertight Geometry Meshing tool

To ensure the quality of the created mesh, the Ansys Fluent User Guide (2023) outlines a range of metrics that can be checked. For this study, two metrics were used:

- Skewness – defined in the user guide as *the difference between the shape of the cell and the shape of an equilateral cell of equivalent volume. Highly skewed cells can decrease accuracy and destabilize the solution.* The guide suggests the skewness ratio is kept between 0.33 and 0.95.

- Orthogonal quality - defined in the user guide as *a measure that combines a variety of quality measures, including: the orthogonality of a face relative to vectors from the cell centroid to the face centroid and to the neighboring cell centroid; a metric that detects poor cell shape at a local edge (such as twisting and/or concavity); and the variation of normals between the faces that can be constructed from the cell face. This definition is optimal for evaluating thin prism cells.* The guide suggests a minimum orthogonal quality of 0.1.

Solver Setup

The viscous model was set to SST k-omega to allow more accurate results for the pressure coefficients that are required. This model is suitable for aerodynamic applications. The boundary conditions can also be adjusted in this step. For the Inet boundary condition, the velocity magnitude is set as the design site wind speed, calculated in Section 6, as 50m/s. This velocity magnitude was adopted for all wind directions to calculate the worst-case uplift coefficients. The outlet condition is automatically set as a pressure outlet, allowing the fluid to pass through the enclosure. Prior to initializing and running the solver function, solution reports must be setup. Here, the lift coefficient report is setup to record the uplift pressure on the building in the positive Y direction. Various other reports can be generated in this section for flow rates, drag forces and pressures, heat transfer, etc.

During the solution process, it is necessary to monitor the progress on the solver function, to ensure the solution is tending towards convergence. For this experimentation the scaled residuals and the lift coefficient plots were monitored. Refer figures 27and 28. At the end of each solver iteration, the residual sum for each of the conserved variables is computed and stored, thereby recording the convergence history. This history is also saved in the data file. The residual sum is defined below. On a computer with infinite precision, these residuals will go to zero as the solution converges. On an actual computer, the residuals decay to some small value ("round-off") and then stop changing ("level out"). For single-precision computations (the default for workstations and most computers), residuals can drop as many as six orders of magnitude before hitting round-off. Double-precision residuals can drop up to twelve orders of magnitude. Ansys Fluent User's Guide (2023).

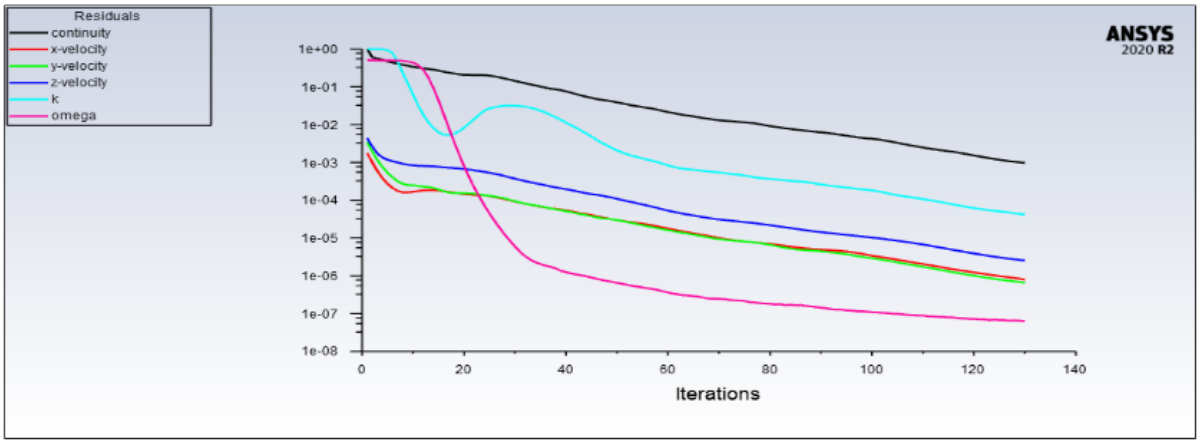

Figure 27: Scaled residuals for Model 2

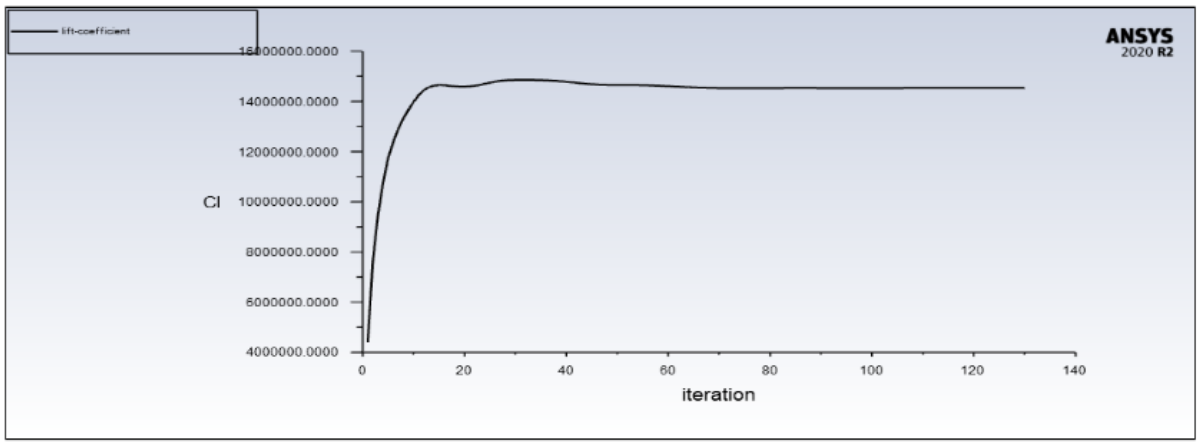

Figure 28: Lift Coefficient plot for Model 2

During the modelling process, there were cases where the scaled residuals and the life coefficient plots showed errors. The errors were noticed firstly in the slope of the scaled residuals graphs, there the line trends would not be tending downwards, which indicates that the calculations were not converging. Similarly in the life coefficient plots, the graph would not flatten, showing the solution was not converging. In an attempt to rectify the issues in the solver processes, adjustments were made to the meshing to simplify the problem. By increasing the minimum size of mesh element size, a simpler model was transferred to the solver, allowing the calculation to converge. Although this process allowed for convergence, the results were less accurate, and the lift coefficient areas were larger than the areas calculated with the smaller mesh element size.

To maintain the smaller mesh element size and still work towards convergence, there is an option in the solver setup to adjust the Pseudo Transient Explicit Relaxation or “under-relaxation” factors. As described in the Ansys Fluent User’s Guide (2023), the pressure-based solver uses under-relaxation of equations to control the update of computed variables at each iteration. By reducing the factors shown in Figure 29 by 0.1 to 0.3, the residuals would begin to reduce, and the lift coefficient plot would flatten out until convergence, while still maintaining the accuracy of the smaller mesh element size. This process was adopted for all models with convergence issued (generally all models with a wind direction of 90°) to maintain a consistent mesh element size throughout the structural analysis models. Examples of this process can be found in the Analysis and Results section of this report.

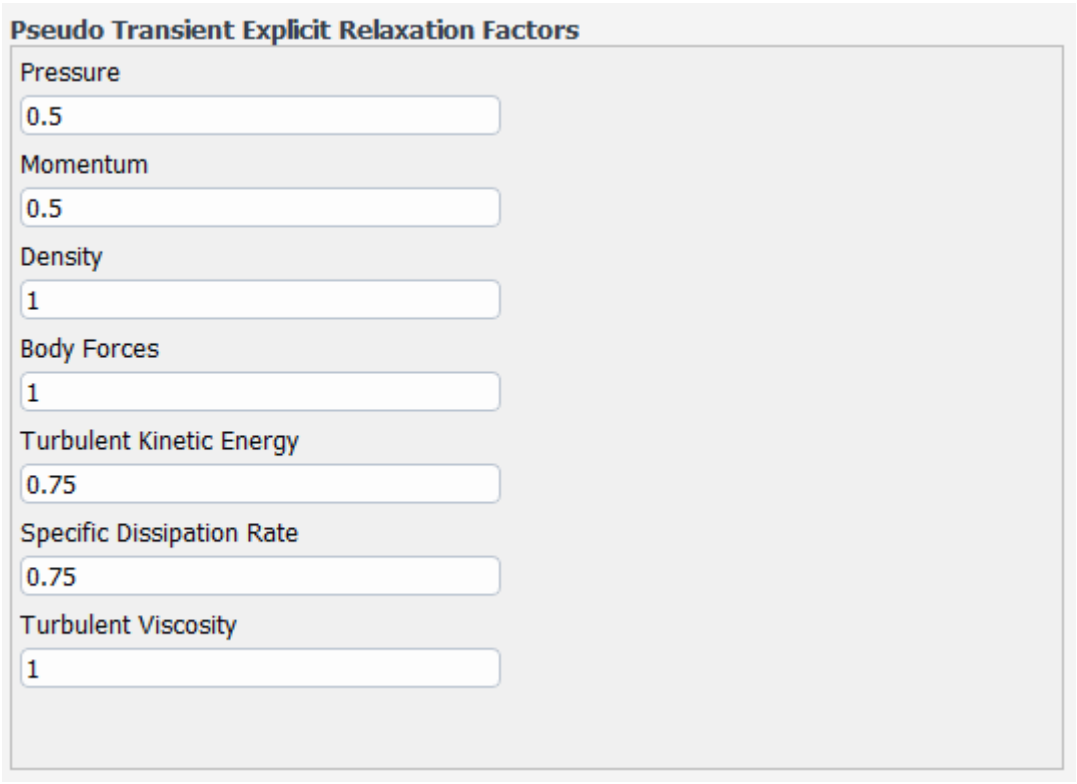

Figure 29: "under-relaxation" factors

7. Analysis and Results

The aim of this report is to compare the CFD modelling results with the local pressure factors and affected areas outlined in the design codes AS/NZS 1170.2, EN 1991-1-4:2005+A1 and ASCE/SEI 7-10. In addition, an analysis was undertaken of the effects of building dimensions and roof pitches on the local pressure factors.

The figures below show the pressure coefficients on the roof of each model for each wind direction, with the cooler colours representing negative pressures (uplift) and the warmer colours representing positive pressures. Note in some cases, the change in pressures seem quite acute with a hard edge, especially near the eaves and corners. This is due to the size and positioning of the mesh elements in each model, along with the number of contour lines added in CFD-Post analysis. Although the wind pressures will not necessarily act as shown (generally a more uniform distribution of forces), the number of contours helps to display the area affected by the peak uplift pressures. This also shows that there is an opportunity to rationalize the meshing process to show more realistic results.

Each figure has been overlayed with the equivalent local pressure factor areas, as calculated using AS1170.2, denoted as dashed lines. Refer to Appendix B for the diagrams of these areas for each model, for 0°, 30°, 45°, 60° and 90° wind directions.

Model 1 - 50m (W) x 100m (L) x 14m (H) – Roof pitch 3°

- 0° wind direction: the maximum calculated pressure coefficient is -2.673, located within the 5m eave zone at the windward edge denoted by the dashed line in figure 30. In comparison to AS1170.2, this pressure is -.673 larger than the equivalent RA2 pressure of -2, although this pressure acts in a small area close to the eave. In the pressure zone between 5m and 10m from the windward wall, the pressure ranges from -1.918 to –1.541, approximately -.4 greater than the equivalent RA1 pressure factor of -1.5.
- 30° wind direction: the maximum calculated pressure coefficient is -4.051, located within the 5m eave zone near the building ridge. This is double the RA2 pressure factor calculated from AS1170.2, although the area affected is relatively small. The average pressure within the 5m eave zone is approximately -2, which is similar to the RA2 pressure in AS1170.2. The maximum pressure coefficient calculated along the long edge of the building, within the 5m zone, is -1.233, marginally less than RA2, and ranging from -0.7629 to -1.271 within the 5m-10m zone.
- 45° wind direction: the maximum calculated pressure coefficient in the 0m-5m zone along the short edge was -3.401, located at the ridge. This is approximately -0.9 greater than the RA2 pressure. The average pressure in that zone was approximately -2.2, marginally larger than RA2. In the 5m-10m zone along the short edge, the average pressure is approximately -1.4, equivalent to the RA1 pressure. In the 0m-5m zone along the long edge, the maximum pressure is -3.007, -1kPa larger than RA2, although only affecting small areas near the eave. The average pressure in this zone is approximately -1.628, equivalent to RA1. There is also a pressure coefficient in the corner zone of -2.219, which is less than the RC1 pressure coefficient as per AS1170.2.
- 60° wind direction: the pressure coefficients calculated along the short edge are relatively insignificant, with an average of approximately -1. There is a small area of the roof which experiences a pressure coefficient of -3.199 near the leeward corner, although similarly insignificant. The maximum pressure coefficients calculated along the long edge is -4.166 in relatively small areas. The average pressure coefficient within the 0m-5m zone along the long edge is approximately -2.279, marginally larger than RA2. In the 5m-10m zone from the long edge, the average pressure coefficient is -1.5, equivalent to RA1.

- 90° wind direction: the maximum calculated pressure coefficient is -2.39, located between 0m and 10m at the side wall eaves. This pressure coefficient is less than the RC1 coefficient of -3.0 as per AS1170.2. The average pressure coefficient in the 0m-5m zone along the long edge is approximately -0.95, significantly less than RA2. Similarly, in the 5m-10m zone, the average pressure coefficient is approximately -.84, less than RA1. As seen in the scaled residuals and lift coefficient graphs in Appendix B, this model did not quite reach convergence, even with reducing the under-relaxation factors. This leads to a reduction in the accuracy of the results, although the results have been taken at 80% accurate based on the lift coefficient shape.
- Comments: the model 1 output of pressure coefficients showed some similarity to AS1170.2 in terms of magnitude and location, in some cases exceeding the Australian standard figures. Interestingly, the pressure coefficient magnitude localized at the ridge line was higher than the RC1 pressure factor located at the corner of the building. AS1170.2 does not allow for a significant pressure coefficient of that magnitude in this location for a roof pitch less than 10°.

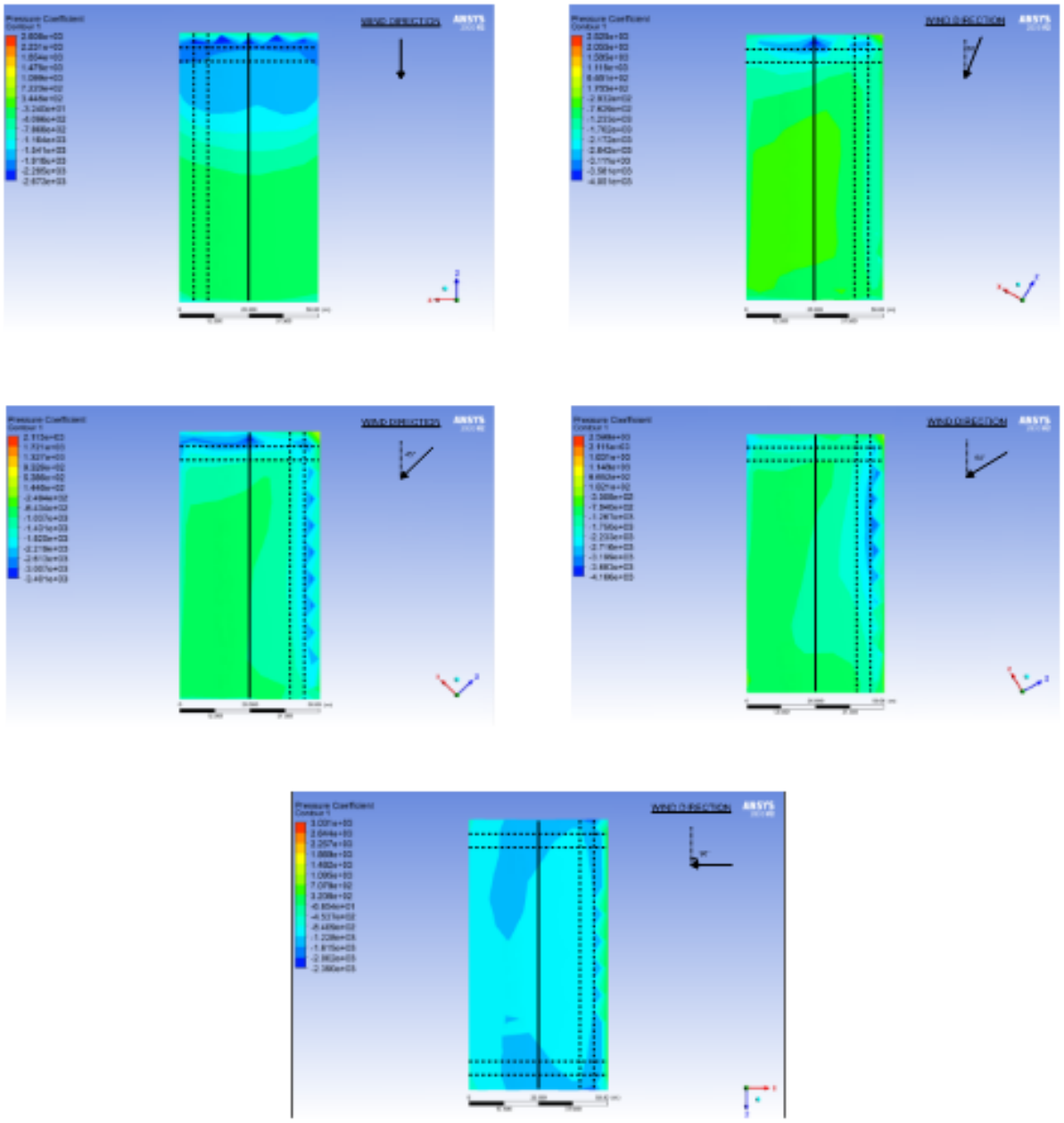

Figure 30: Pressure coefficient outputs for wind directions 0°, 30°, 45°, 60° and 90° for Model 1

Model 2 - 100m (W) x 200m (L) x 14m (H) – Roof pitch 3°

- 0° wind direction: The maximum calculated pressure coefficient is -3.154, located in the corner zones between 0m-12.7m from the windward edge and 0m-25.4m from the side wall edges. This pressure coefficient and affected area is similar to the RC1 factor. For the 0m-12.7m zone from the windward edge, the average pressure coefficient is approximately -2.2, marginally larger than the RA2 factor. For the 12.7m-25.4m zone from the windward edge, the average pressure coefficient is approximately -1.85, marginally larger than the RA1 factor.
- 30° wind direction: the maximum calculated pressure coefficient in -3.606, located within the 0m-12.7m zone from the short edge and 12.7m-25.4m zone from the long edge. Notably, a pressure coefficient of -3.176 is found within the 0m-12.7m zone from the short edge near the ridge. The average pressure coefficient in the 0m-12.7m zone from the short edge is approximately -2.5, 0.5 higher than the RA2 factor. For the 12.7m-25.4m zone from the short edge, the average pressure coefficient is approximately -1.24, marginally less than the RA1 factor. The 30° wind direction does not affect the long edge zones significantly.
- 45° wind direction: the maximum calculated pressure coefficient is -2.981, located in the corner zones between 0m-12.7m from the short edge and 12.7m-25.4m from the side wall edges. This pressure coefficient and affected area is similar to the RC1 factor. For the 0m-12.7m zone from the short edge, the average pressure coefficient is approximately -1.5, marginally smaller than the RA2 factor. For the 12.7m-25.4m zone from the short edge, the average pressure coefficient is approximately -1.03, 0.5 less than the RA1 factor. For the 0m-12.7m zone from the long edge, the average pressure coefficient is approximately -1.7, marginally less than the RA2 factor, although the affected area is less than outlined in AS1170.2. For the 12.7m-25.4m zone from the long edge, the average pressure coefficient is approximately -0.6775, significantly less than the RA1 factor.
- 60° wind direction: the maximum calculated pressure coefficient is -3.32, located in the 0m-12.7m zone from the long edge, although the size of the affected area is small. The average pressure coefficient in this zone is approximately -2.2, similar to RA2. In the 12.7m-25.4m zone from the long edge, the average pressure coefficient is approximately 1.5, similar to RA1. Note there is also a pressure coefficient on -3.32 affecting the leeward corner.
- 90° wind direction: the maximum calculated pressure coefficient is -3.425, although the affected area is miniscule. For a more accurate comparison, the maximum pressure coefficient for this wind direction is taken as -2.927, occurring at both corners between 0m-12.7m from the windward edge and 0m-12.7m from the side walls. This pressure coefficient is similar to the RC1 factor. For the 0m-12.7m zone from the windward edge, the average pressure coefficient is approximately -1.7, with higher coefficients of approximately -2.7 near the corners. For the 12.7m-25.4m zone form the windward edge, the average pressure coefficient is approximately -1.2, although there is an affected area further towards the leeward wall with an average pressure coefficient of -1.7. similar to the 90° wind direction in Model 1, this model did not reach full convergence, see Appendix B for the scaled residual and lift coefficient graphs. Results have been taken at 80% accurate based on the lift coefficient shape.
- Comments: This model shows similar results to what is documented in AS1170.2, although the ‘a’ distance, and subsequently the affected area, is significantly smaller in the model than the Australian Standard.

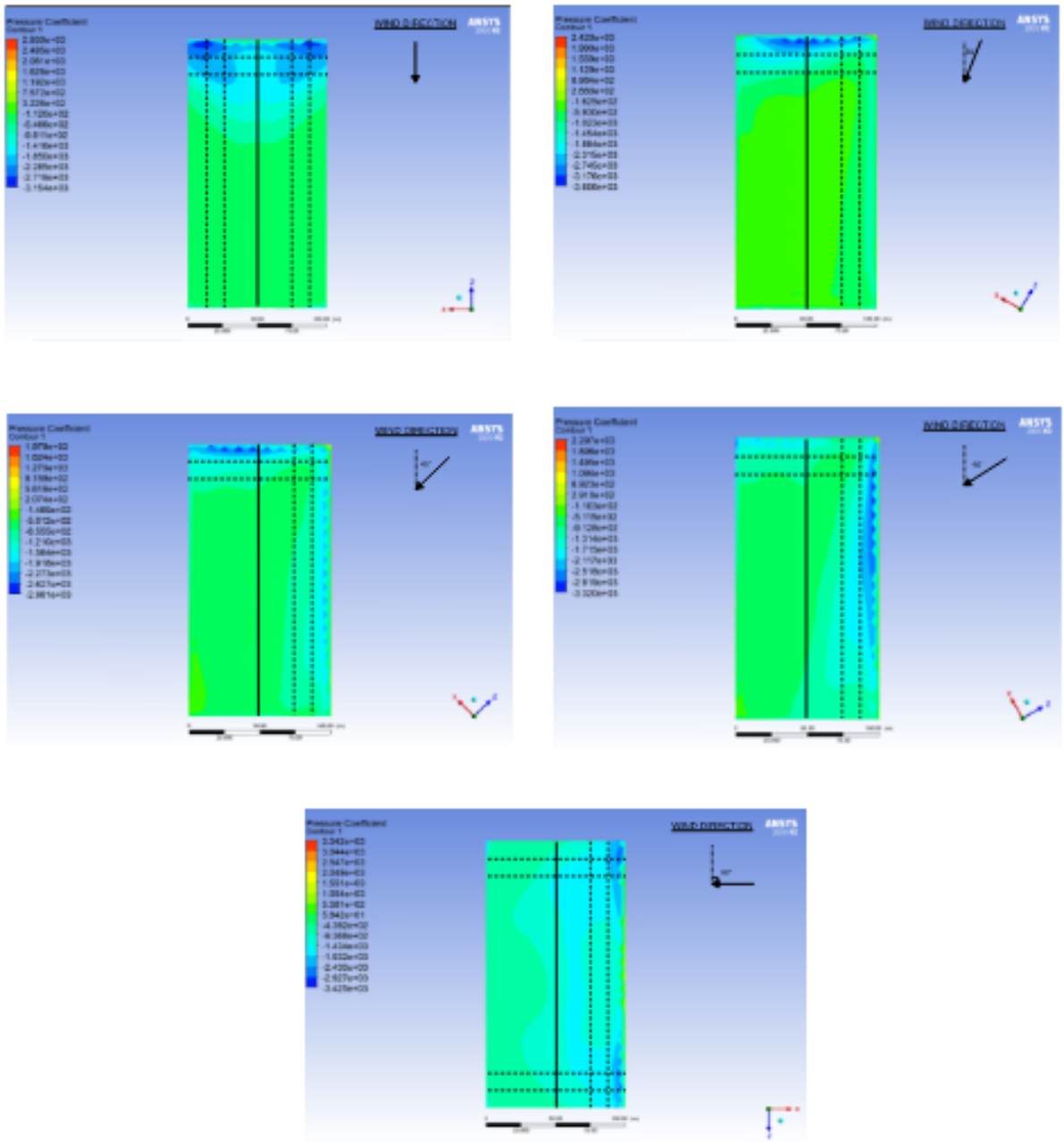

Figure 31: Pressure coefficient outputs for wind directions 0°, 30°, 45°, 60° and 90° for Model 2

Model 3 - 150m (W) x 150m (L) x 14m (H) – Roof pitch 3°

- 0° wind direction: the maximum calculated pressure coefficient is -4.21 affecting a relatively small area in the both corner zones between 0m-12m form the windward edge and 12m-24n from the side walls. In the same areas a pressure coefficient of -3.686 affected a more prominent area can be seen. The average pressure coefficient in the 0m-12m zone from the windward edge is approximately -2.4, marginally higher than the RA2 factor. In the zone between 12m-24m from the windward edge, the average pressure coefficient is approximately -1.25, marginally less than the RA1 factor. The magnitude and affected areas of the calculated pressure coefficients are generally in line with AS1170.2.

- 30° wind direction: the maximum calculated pressure coefficient is -3.538, located in the 0m-12m zone from the windward edge, although no further than 6m from that edge. The average pressure coefficient in the 0m-12m zone is approximately -2.5, marginally higher than the RA2 factor, although affecting a smaller area. The average pressure coefficient in the 12m-24m zone is approximately -1.4, similar to the RA1 factor. The average pressure coefficient in the 0m-12m zone of the long edge is approximately 1.6, less than the RA2 factor. The pressure coefficient in the 12m-24m zone of the long edge is insignificant for this wind direction. Interestingly, there is a small area of uplift in the opposite corner of approximately -3.5.
- 45° wind direction: the maximum calculated pressure coefficient is -3.04, located in the 0m-12m zone near the ridge. The average pressure coefficient in this zone is approximately -2.2, similar to the RA2 factor. The average pressure coefficient in the 12m-24m zone from the top edge is approximately 1.0, 0.5 less than the RA1 factor. The average pressure coefficient for the 0m-12m zone from the side edge is approximately -1.6, marginally less that the RA2 factor. The average pressure coefficient for the 12m-24m zone from the side edge is approximately -0.8, 0.7 less than the RA1 factor.
- 60° wind direction: the maximum calculated pressure coefficient is -2.98, located in the 0m-12m zone between the ridge and the side edge. The average pressure coefficient in this zone is approximately -2.0, similar to RA2. The average pressure coefficient in the 12m-24m zone from the top edge is approximately 1.0, 0.5 less than the RA1 factor. The average pressure coefficient for the 0m-12m zone from the side edge is approximately 1.7, with a small area at the corner showing a pressure coefficient of -2.98. The average pressure coefficient for the 12m-24m zone from the side edge is approximately -0.8, significantly less than the RA1 factor. Interestingly, the areas in which the pressure coefficient are highest tend towards the top edge, not the side edge thought to experience more wind loading.
- 90° wind direction: the maximum calculated pressure coefficient is -3.58, located in small areas within the 0m-12m zone from the windward edge and the 12m-24m zone from the side walls. The average pressure coefficient in the 0m-12m zone from the windward edge is approximately 2.3, similar to the RA2 factor. The average pressure coefficient in the 12m-24m zone from the windward edge is approximately 1.7, marginally higher than the RA1 factor.
- Comments: Similar to model 2, the calculated pressure coefficients are generally in line with the local pressure factors in AS1170.2, although the ‘a’ distance, and subsequently the affected area, is significantly smaller in the model than the Australian Standard. The results tend to show that there could be an opportunity to reduce the extent of the ‘a’ distance to something similar to the minimum of 0.2b or 0.2d.

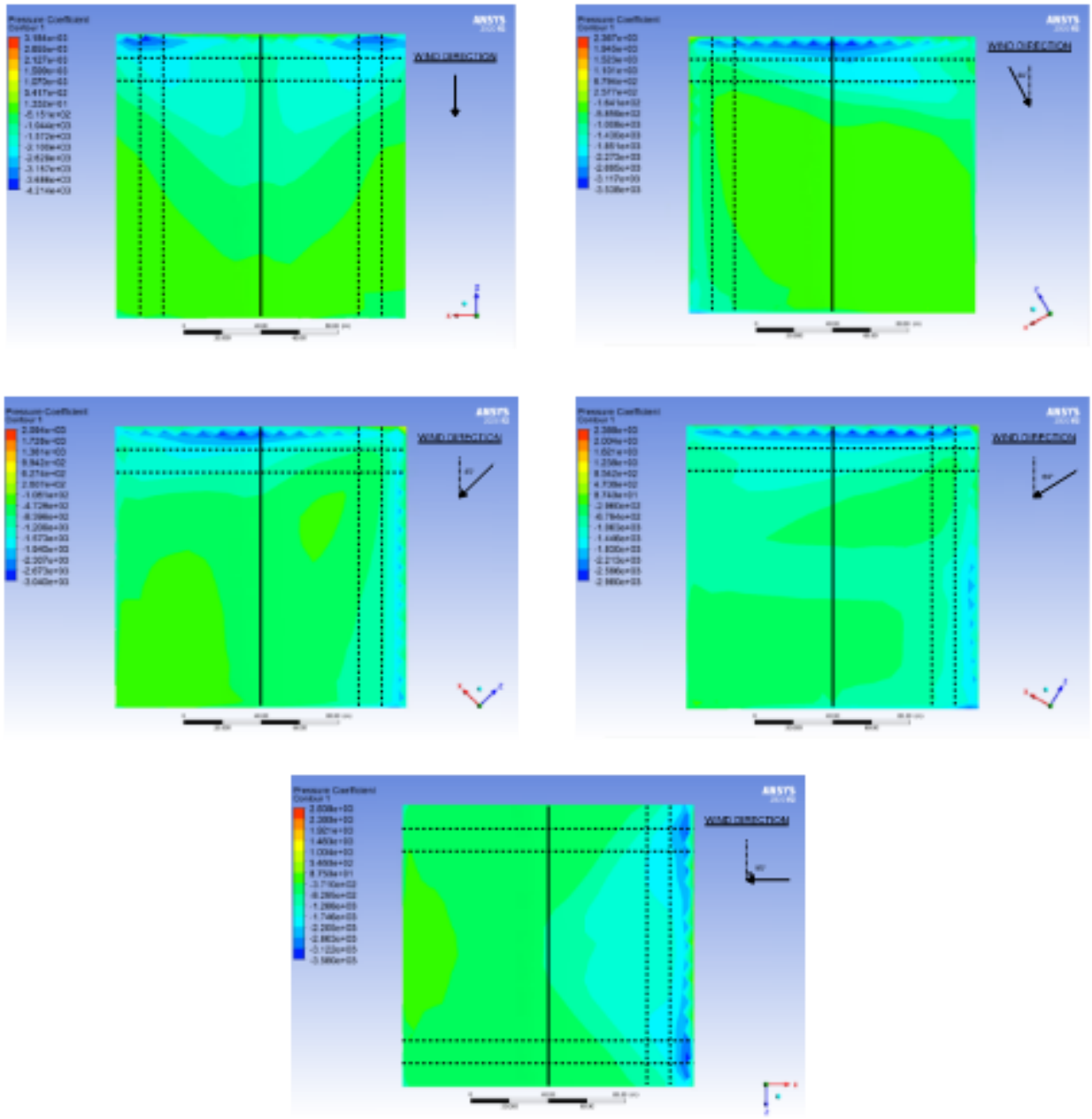

Figure 32: Pressure coefficient outputs for wind directions 0°, 30°, 45°, 60° and 90° for Model 3

<u>Model 4 - 50m (W) x 100m (L) x 14m (H) – Roof pitch 10°</u>

- <u>0° wind direction:</u> the maximum calculated pressure coefficient is -2.294 affecting the central portion of the roof within the 0m-5 zone form the windward wall. The average pressure coefficient in this zone is approximately -2, generally in line with AS1170.2, for the 5m-10m zone form the windward edge, the average pressure coefficient is approximately -1.8, marginally higher than the figures in AS1170.2. A non-symmetrical patch of pressure of -1.954 can be seen near the side wall edge of the building, past the 5m-10m zone. This is assumed to be an error from the model, most likely attributed to the meshing size and shape. A symmetrical pressure pattern is assumed, similar to the pattern on the right-hand side of the model.

- 30° wind direction: the maximum calculated pressure coefficient is -3.689, occurring in two small areas within the 0m-5m zone from the windward edge. The average pressure coefficient in this zone is approximately -2.1, marginally higher than the figures in AS1170.2. for the 5m-10m zone from the windward edge, the average pressure coefficient is approximately -1.8, marginally higher than AS1170.2. The pressure coefficient along the long edge of the building, between 0m-10m from the eave is approximately -1.0.
- 45° wind direction: the maximum calculated pressure coefficient is -3.511, affected a small area within the 0m-5m zone. The average pressure coefficient in this zone is approximately -1.9, although a relatively larger area shows a pressure coefficient of -0.233 or greater on the downwind slope of the roof. The average pressure coefficient for the 5m-10m zone is approximately -1.8, again with a localized pressure on the downwind slope of the roof. The average pressure coefficient along the long edge of the building in the 0m-5m zone is approximately -1.8, and -1.2 in the 5m-10m zone. In the 0m-10m zone from the ridge, on the downwind slope of the roof, the average pressure coefficient is approximately -1.3.
- 60° wind direction: the maximum calculated pressure coefficient is -2.848, occurring in the 0m-50m zone from the long edge of the building, with a small patch of occurring in the 0m-5m zone from the short edge eave, on the downwind slope of the roof. The average pressure coefficient in the 0m-5m zone from the long edge is approximately -1.9. In the 5m-10m zone from the long edge, the average pressure coefficient is approximately -1.8. in the 0m-5m zone from the short edge at the downwind slop of the roof, the average pressure coefficient is approximately -2.3.
- 90° wind direction: the maximum calculated pressure coefficient in the 0m-5m zone from the windward edge is -3.567, occurring along the majority of the zone. The average pressure coefficient in this zone is approximately -3.0. For the 5m-10m zone, the average pressure coefficient is approximately 2.4. in the 0m-5m zone from the ridge, the average pressure coefficient is approximately -1.4, and -1.0 in the 5m-10m zone from the eave. Interestingly, the pressure coefficient in the zone between the 10m line and the ridge on the windward slope is approximately -1.5, which is relatively high in comparison to AS1170.2.
- Comments: the results from the CFD modelling generally align with the factors in AS1170.2 in magnitude and affected area. Some models showed greater maximum pressure coefficients, but generally the affected areas were relatively small.

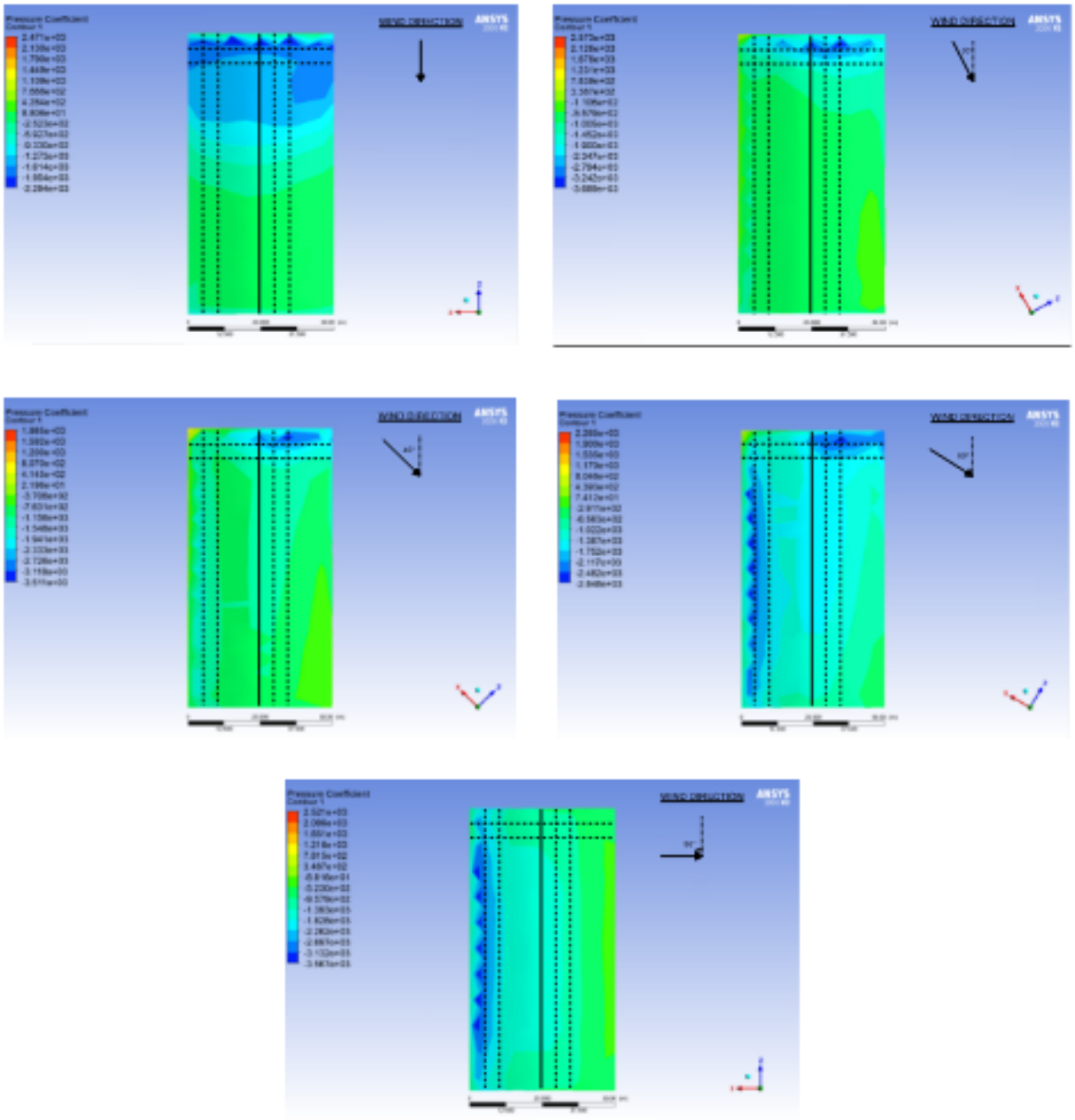

Figure 33: Pressure coefficient outputs for wind directions 0°, 30°, 45°, 60° and 90° for Model 4

Model 5 - 100m (W) x 200m (L) x 14m (H) – Roof pitch 10°

- 0° wind direction: the maximum calculated pressure coefficient is -2.624, occurring in the corner zones 0m-12.7m from the windward edge and 0m-25.4m from the side walls. The average pressure coefficient in the 0m-12.7m zone from the windward edge is approximately -1.8, and in the 12.7m-25.4m zone from the windward edge, approximately -1.3. The calculated values are generally smaller than the factors in AS1170.2 and affecting a smaller area from the windward edge.
- 30° wind direction: the maximum calculated pressure coefficient is -2.94, occurring in the square zone 0m-12.7m from the windward edge and 0m-12.7m from the ridge line. The average pressure coefficient in the 0m-12.7m zone from the windward edge is approximately

2.0. The average pressure coefficient in the 12.7m-25.4m zone from the windward edge is approximately 1.2. A small area of uplift is present in the leeward corner of the building, within the 0m-12.7m corner zone, with a pressure coefficient of -2.5. There is no significant uplift recorded along the long edge of the building for this wind direction. Similarly to the 0° wind direction, the affected areas are generally smaller than in AS1170.2.

- 45° wind direction: the maximum calculated pressure coefficient is -2.692, occurring in the square zone 0m-12.7m from the short edge and 0m-12.7m from the ridge line. The average pressure coefficient in the 0m-12.7m zone is approximately -1.5, and -0.865 in the 12.7m-25.4m zone. The average pressure coefficient in the 0m-12.7m zone from the long edge is approximately -1.1, with no significant uplift recorded in the 12.7m-25.4m zone from the long edge.
- 60° wind direction: the maximum calculated pressure coefficient is -2.716, occurring in the corner zone between 0m-12.7m from the windward long edge and the downwind side wall. The zone between 0m-12.7m experiences is same maximum pressure coefficient close to the long edge eave, with the average pressure coefficient in the zone being approximately 1.2. In the zone between 0m-12.7m from the short windward edge and 0m-25.4m on the downwind slope from the ridge, a small area of uplift with pressure coefficient of -2.0 occurs. The downwind slope zone between 0m-12.7m from the short windward edge experiences an average pressure coefficient of -1.5.
- 90° wind direction: the maximum calculated pressure coefficient in the 0m-12.7m zone from the windward edge is -3.377, occurring close to windward eave. The average pressure coefficient in this zone is approximately -1.8. The average pressure coefficient in the 12.7m-25.4m zone is approximately -0.7, nearly half that of the factor in AS1170.2. the 0m-12.7m zone from the ridge on the downwind slope experiences an average pressure coefficient of -0.9
- Comments: the calculated pressure coefficients for Model 5 were generally smaller than the factors in AS1170.2. Further to this, the areas in which these pressures occur is significantly smaller than the projected areas in AS1170.2.

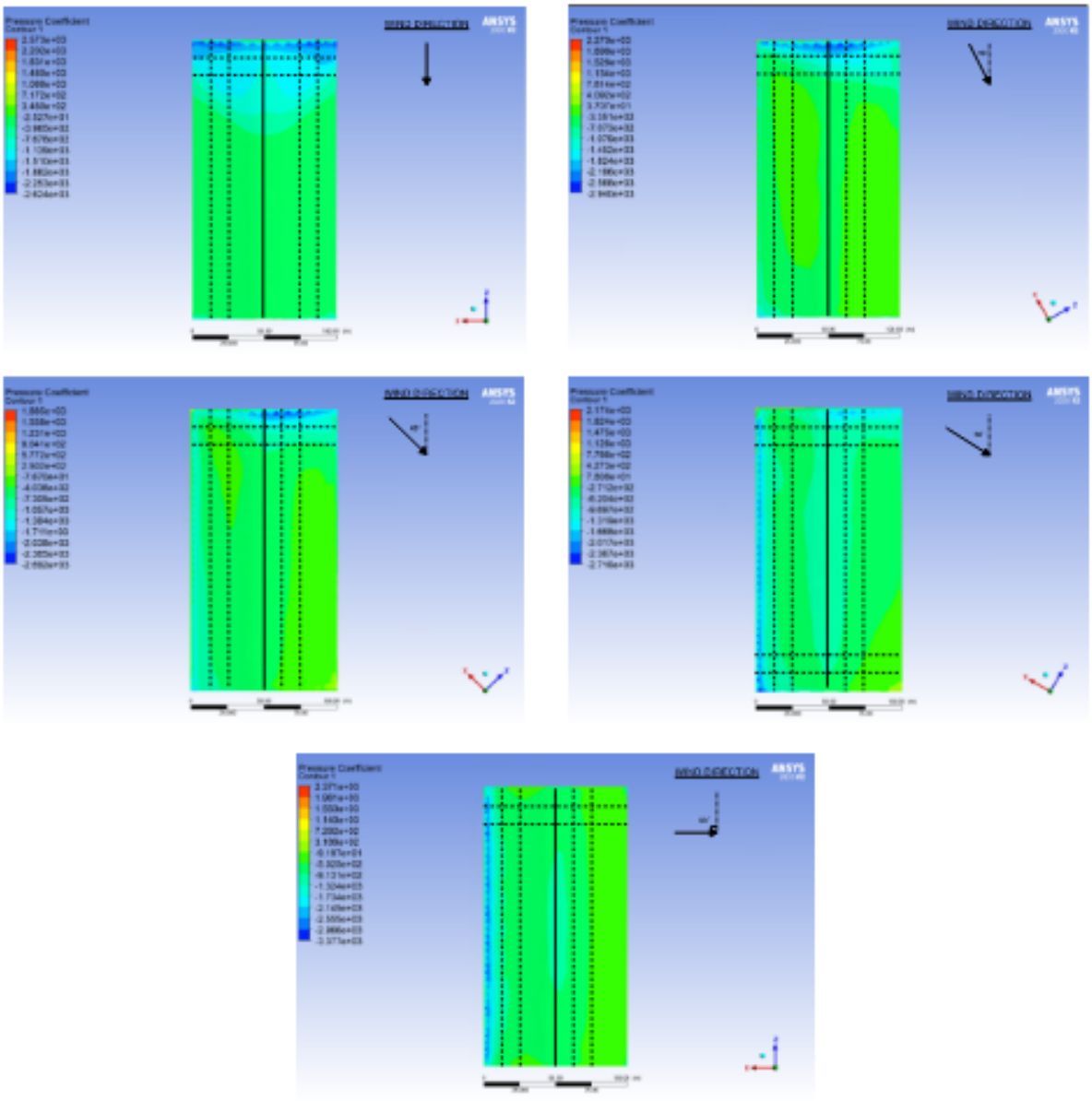

Figure 34: Pressure coefficient outputs for wind directions 0°, 30°, 45°, 60° and 90° for Model 5

Model 6 - 100m (W) x 100m (L) x 14m (H) – Roof pitch 10°

- 0° wind direction: the maximum calculated pressure coefficient is -3.442, occurring in both corner zones between 0m-9.6m. The average pressure coefficient in 0m-9.6m zone from the windward edge is approximately -2.0. For the 9.6m-19.2m zone from the windward edge, the average pressure coefficient is approximately -1.8.
- 30° wind direction: the maximum calculated pressure coefficient is -4.031, occurring in a small area between 0m-9.6m from the short edge and 0m-19.6m from the ridge. The average pressure coefficient in the 0m-9.6m zone from the short edge is approximately -2.2. In the 9.6m-19.6m zone from the short edge, the average pressure coefficient is approximately -1.7.
- 45° wind direction: the maximum calculated pressure coefficient is -4.462, occurring in small areas between 0m-9.6m from the short edge and 0m-19.6m from the ridge. Due to the size of affected area, the maximum pressure coefficient here is assumed to be -3.2. The average

pressure coefficient in the 0m-9.6m zone from the short edge is approximately -2.2. in the 9.6m-19.6m zone from the short edge is approximately -1.4. No significant pressure was recorded in the 0m-19.6m zone from the long edge.

- 60° wind direction: the maximum calculated pressure coefficient is -4.211, occurring in the corner zone between 0m-9.6m from the windward long edge and the downwind side wall. The affected area is insignificantly small. In the 0m-9.6m zone on the downwind slope for the roof, an average pressure coefficient of -2.2 is seen. No other significant pressure is noted.
- 90° wind direction: the maximum calculated pressure coefficient is -2.745, occurring in small areas of both windward corner zones. The average pressure coefficient in the 0m-9.6m zone from the windward edge is approximately -1.8, with the average in the 9.6m-19.6m zone being approximately -0.8. For the 0m-9.6m zone from the ridge on the downwind slope of the roof, the average pressure coefficient is approximately -1.4, and -0.9 in the 9.6m-19.6m zone from the ridge.
- Comments: similar to Model 5, the calculated pressure coefficients for Model 6 were generally smaller than the factors in AS1170.2. Further to this, the areas in which these pressures occur is significantly smaller than the projected areas in AS1170.2. There were incidences of pressure coefficients higher than AS1170.2, although only affected small areas of the roof.

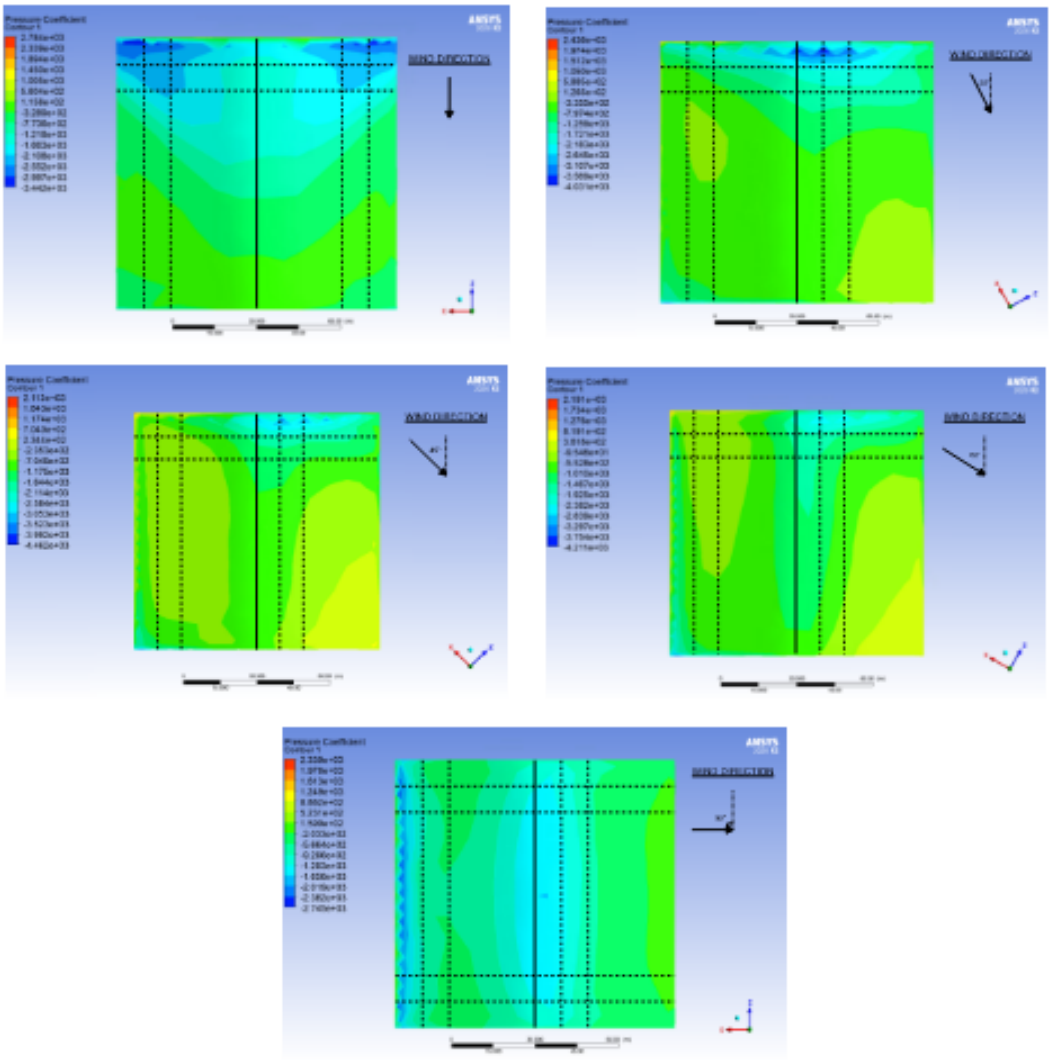

Figure 35: Pressure coefficient outputs for wind directions 0°, 30°, 45°, 60° and 90° for Model 6

8. Discussion

The aim of this report is to compare the calculated pressure coefficients experienced by each modelled building, comparing the effects dimension and roof pitch have on the magnitude, location, and size of the uplift forces. In addition, the calculated pressure coefficients are compared to the factors outlined in the design codes AS/NZS 1170.2.

Evidence of results accuracy

As outlined in section 7, for the majority of the models and wind directions, the magnitude of pressure coefficients was generally in line with the three design codes. In addition, the external pressure factors for each model were compared to the factors outlined in AS1170.2. The calculated pressures were also within a range of 0.2 of the design code factors. As discussed previously, the models do not incorporate any surface roughness factors at the ground surface. This would only tend to reduce the pressure factors induced on the building models. For these reasons it is assumed that the results are generally accurate and somewhat conservative. Additional modelling, incorporating surface roughness would be the logical next stage of research.

Effect of building dimensions

The results outlined in section 7 of this report show that for Model 1, the calculated pressure coefficients are generally similar to the local pressure factors in AS1170.2. Similarly, the Model 2 and Model 3 outputs are generally in line with the factors in AS1170.2, although the affected area is seemingly reduced when the width and breadth of the building is increased. This is most evident in the outputs for wind direction 30°, 45°, 60° and 90°. For models 2 and 3, the affected area is approximately half the distance of the '*a*' value calculated from 1170.2. interestingly, this figure has changed in the most recent amendment of AS1170.2, with the value increasing from the minimum of 0.2b or 0.2d, if (h/b) or (h/d) >= 0.2 to 2*h* if both (h/b) and (h/d) < 0.2. The results from the CFD modelling show that this increase in '*a*' is somewhat conservative.

When analyzing the maximum calculated pressure coefficients to the factors in AS1170.2 for each model, it is evident that the calculated figures are marginally higher than the code factors although the affected areas are generally less, with only a small area experiencing the higher-pressure value. When averaging the pressure coefficients in each zone, the values are generally smaller than the factors in AS1170.2. When comparing the maximum pressure coefficients between models 1-3, it can be seen that the magnitude and location is more consistent with the larger building dimensions. This tends to show that the turbulence eddies at the eaves of the building are developed more consistently over a larger area. In addition, it must be noted that the wind pressure in the design models has been applied evenly throughout the enclosure, with no allowance for the ground surface roughness and variance for wind speed with height. This, in turn, would reduce the design wind pressure induced on the building, reducing the magnitude of the pressure coefficients. With this in mind, it can be confidently assumed that the output pressure coefficients would be reduced in real life scenarios.

For Model 4, pressure coefficient outputs were generally in line with AS1170, although the outputs for mode 5 and 6 showed a reduced magnitude and affected area of pressure coefficients. Similar to models 2 and 3, models 5 and 6 showed the '*a*' value to be approximately half that of the calculated figure in AS1170.2. Interestingly, this occurred for Model 6 even though the dimensions (100m (W) x 100m (L) x 14m (H)) were similar to the Model 1 Dimensions (50m (W) x 100m (L) x 14m (H)). This would seemingly be due to the rectangular shape of Model 1 compared to the square shape of Model 6, with the distance between the windward eave and the leeward eave having an altering the wind

flow over the building, affecting the uplift at the windward edge. This shows that in terms of uplift pressure on cladding and fixings, a squarer footprint is a more desirable design.

Effect of roof slope

When comparing models 1 and 4, the maximum calculated pressure coefficients can be seen to be greater for the 3° roof pitch, although only marginally. In terms of the area size affected by high uplift forces, both models were relatively similar. The main difference between the two models is the pressure coefficient at the downward slope near the short edge of the building, with the steeper pitched roof experiencing a higher uplift force over a larger area in that zone. This is in line with AS1170.2, with the addition of the RA3 and RA4 pressure zones for the downwind side of ridges for roofs with roof pitches greater than 10°.

In the comparison of models 2 and 5, the increase of maximum calculated pressure coefficients is more prevalent, with the average increase in pressure coefficients nearly 0.5. In addition, the affected area of the pressure coefficients is generally less for the 10° roof pitch. Similarly, in the comparison of models 3 and 6, although not the same building dimensions but the same shape, the maximum calculated pressure coefficients were greater by an average factor of 0.4.

Additional comments

It can be seen in the output diagrams that local pressure factors along the eave zone of the building models occur at a certain distance back from the edge. This phenomenon is caused by the turbulence eddies that are formed when the wind interacts with the wall and roof junction. Interestingly, in all three of the studies design codes, there is emphasis on the corner zones, with the pressure coefficients being the larger in those areas. In AS1170.2, the RC1 factor is given as an area that acts in with a proximity of $<a$ from two edges. Previous to this research it was understood that the corner pressures, especially the RC1 factor in AS1170.2, were effectively locked or pinned to the corner point. Whereas the results in this report tend toward the corner local pressure factor being less prevalent directly in the corner, and affecting the areas away from the corner, by a nominal distance.

9. Conclusion

A range of CFD modelling, using the Ansys Fluent CFD program, was completed to gain an understanding of the effects of building dimensions and roof pitch on the negative local pressure coefficients in the corner and eaves zones of buildings, with particular interest in the design of cladding elements and their fixings. Six models were used to simulate typical warehouse buildings in Australia, with wind applied at 0°, 30°, 45°, 60° and 90°. The aim was to compare the uplift forces calculated to the factors provided in the three design codes AS/NZS 1170.2, EN 1991-1-4:2005+A1 and ASCE/SEI 7-10. In addition, the three design codes were also compared.

The CFD modelling program is a powerful tool, although once understood, was effective in providing accurate results to compare and analyze. The results showed that the building dimensions and roof slope have significant effects on the local pressure factors. It was found that the magnitude and affected area of the local pressure factors generally decreased with the increase in building size. The increase of roof pitch also tended to reduce the magnitude and affected area of the pressure coefficients, although induce higher pressures around the ridge of the roof.

The comparison of the design codes showed that the Australian code is generally more conservative than that of the European and American codes in both magnitude and size of affected area of the local pressure coefficients. It was concluded based on the results in this report that there is a possibility of reducing the 'a' value in AS1170.2. In addition, it was also concluded that the local pressure factors is AS1170.2, especially the RC1 factor, can be reduced. This is based on the relatively small areas in which these high pressure coefficients were observed to act.

This research, using CFD modelling for modelling the effects of wind on low-rise industrial buildings, has the potential to refine the current design codes to achieve more accurate and realistic pressure factors, which can result in more efficient building designs in the future.

10. References

Holmes, J. D. and Syme, M.J. (1994). *Wind loads on steel steel-framed low-rise buildings*. Steel Construction (Australian Institute of Steel Construction).

Holmes, J. D. (2001). *Wind loading of structures.* Spon Press

Stathopoulos, T. and Saathoff, P. (1991). *Wind pressure on roofs of various geometries.* Journal of Wind Engineering and Industrial Aerodynamics. Elsevier Science Publishers.

Alrawashdeh, H. (2015). *Wind pressures on flat roof edges and corners of large low buildings.* (Thesis, Concordia University, Canada). https://spectrum.library.concordia.ca/id/eprint/980473/

Australasian Wind Engineering Society (2022). *Wind Loading Handbook For Australia And New Zealand - Background to AS/NZS 1170.2 Wind Actions - AWES-HB-001-2022.* https://www.awes.org/product/wind-loading-handbook-for-australia-new-zealand-background-to-as-nzs-1170-2-wind-actions-wind-loading-handbook/

Parackal, K. I. (2018). *The Structural Response and Progressive Failure of Batten to Rafter Connections under Wind Loads*. (PhD Thesis, James Cook University, QLD). https://researchonline.jcu.edu.au/62277/

ASCE/SEI 7-10, (2010). *Minimum Design Loads for Buildings and Other Structures*. Structural Engineering Institute of ASCE, Reston, VA. https://www.waterboards.ca.gov/waterrights/water_issues/programs/bay_delta/california_waterfix/exhibits/docs/dd_jardins/DDJ-148%20ASCE%207-10.pdf

The European Union (2005). *EN 1991-1-4:2005+A1 – Eurocode 1: Actions on Structures – Part 1-4: General Actions – Wind Actions. https://www.phd.eng.br/wp-content/uploads/2015/12/en.1991.1.4.2005.pdf*

Standards Australia (2021). *AS/NZS 1170.2 – Structural Design Actions – Part 2: Wind Actions.* https://store.standards.org.au/product/as-nzs-1170-2-2021

Roy, A. et al. (2018). *Wind Pressure Variation On Pyramidal Roof Of Rectangular And Pentagonal Plan Low Rise Building Through CFD Simulation.* https://www.researchgate.net/publication/323343127_WIND_PRESSURE_VARIATION_ON_PYRAMIDAL_ROOF_OF_RECTANGULAR_AND_PENTAGONAL_PLAN_LOW_RISE_BUILDING_THROUGH_CFD_SIMULATION

Muo et al. (2017). *Numerical simulation of the effects of building dimensional variation on wind*

Pressure distribution. Engineering Applications of Computational Fluid Mechanics. https://doi.org/10.1080/19942060.2017.1281845

Ansys (2023). *Ansys Fluent User's Guide*. https://forum.ansys.com/forums/topic/ansys-fluent-2020-r1-theory-guide-user-guide-full-pdf/

Cochran, L. S. and Cermak, J. E. (1992). *Full- and model-scale cladding pressures on the Texas Tech university experimental building*. Journal of Wind Engineering and Industrial Aerodynamics. https://www.sciencedirect.com/science/article/pii/016761059290374J

Franke, J. and Baklanov, A. (2007). *Best Practice Guideline for the CFD Simulation of Flows in the Urban Environment: COST Action 732 Quality Assurance and Improvement of Microscale Meteorological Models.*
https://www.researchgate.net/publication/257762102_Best_Practice_Guideline_for_the_CFD_Simulation_of_Flows_in_the_Urban_Environment_COST_Action_732_Quality_Assurance_and_Improvement_of_Microscale_Meteorological_Models

Holmes, J. D. (1988). *Distribution of peak wind loads on a low-rise building.* Journal of Wind Engineering and Industrial Aerodynamics.
https://www.sciencedirect.com/science/article/pii/0167610588901456

Roy, A. and Singh, J. (2019). *Effects of roof slope and wind direction on wind pressure distribution on the roof of a square plan pyramidal low-rise building using CFD simulation.*
https://link.springer.com/article/10.1007/s40091-019-0227-3

Xu, Y. L. and Reardon, G. F. (1998). *Variations of wind pressure on hip roofs with roof pitch.* Journal of Wind Engineering and Industrial Aerodynamics. https://www.sciencedirect.com/journal/journal-of-wind-engineering-and-industrial-aerodynamics

Stathopoulos, T. (1982). *Wind loads on low-rise buildings: a review of the state of the art.* Centre of Building Studies, Concordia University, Canada.
https://www.sciencedirect.com/science/article/pii/0141029684900051

Stathopoulos, T. and Alrawashdeh, H. (2015). *Wind pressures on large roofs of low buildings and wind codes and standards.* Department of Building, Civil and Environmental, Concordia University, Canada. https://www.sciencedirect.com/science/article/pii/S0167610515300209

Holmes, J. D. (1994). *Wind Pressures on tropical housing*. Journal of Wind Engineering and Industrial Aerodynamics. https://www.sciencedirect.com/science/article/pii/0167610594900213

Stathopoulos, T. (2003*). Wind loads on low buildings: in the wake of Alan Davenport's contributions*. Journal of Wind Engineering and Industrial Aerodynamics.
https://www.sciencedirect.com/science/article/pii/S0167610503001302

APPENDIX A

Local pressure factors - AS/NZS 1170.2 – Structural Design Actions – Part 2: Wind Actions

MODEL 1 - 50m (W) x 100m (L) x 14m (H) – Roof pitch 3°

AREA	PRESSURE COEFFICIENTS
RC1	-3.0
RA1	-1.5
RA2	-2.0

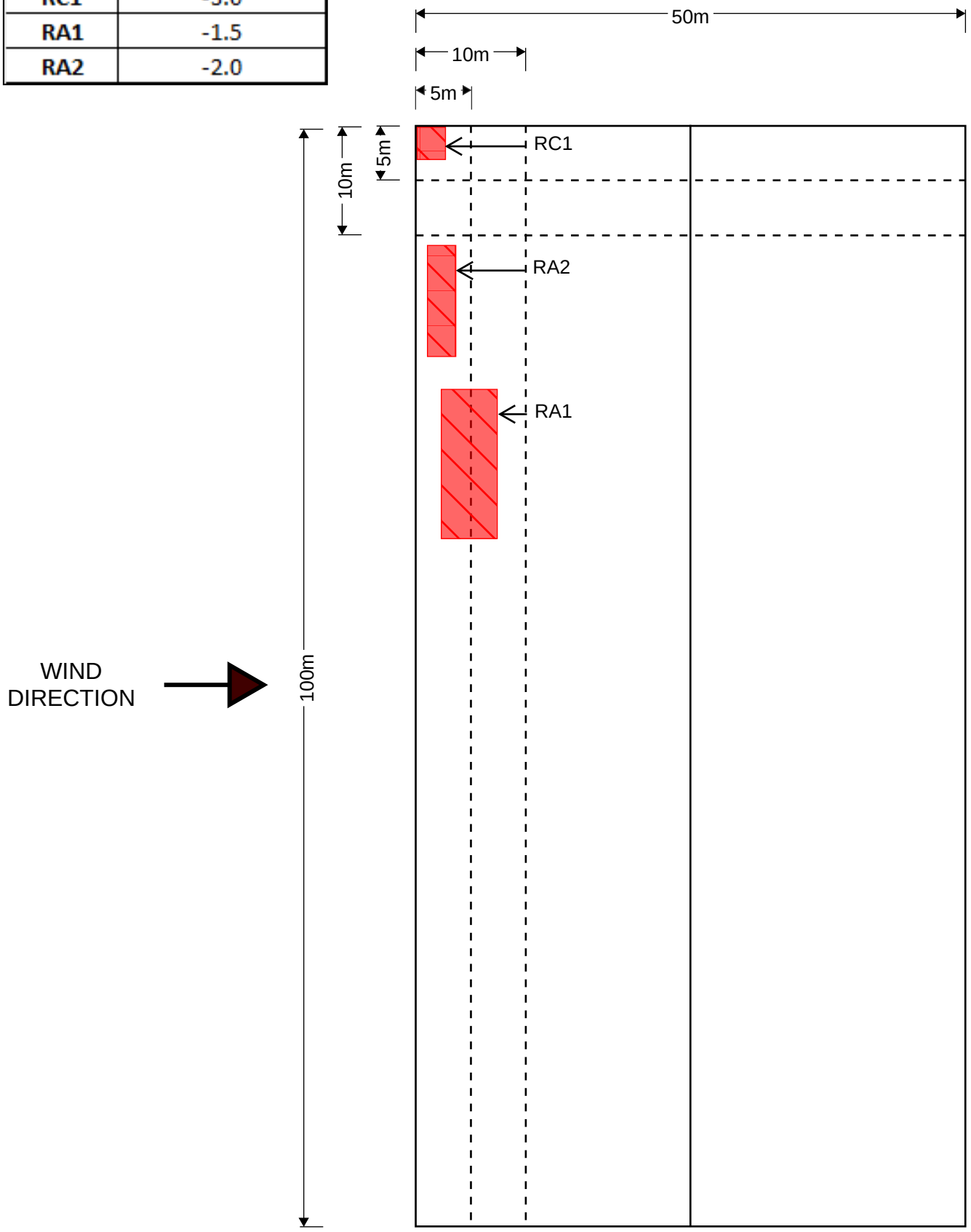

MODEL 1 - 50m (W) x 100m (L) x 14m (H) – Roof pitch 3°

AREA	PRESSURE COEFFICIENTS
RC1	-3.0
RA1	-1.5
RA2	-2.0

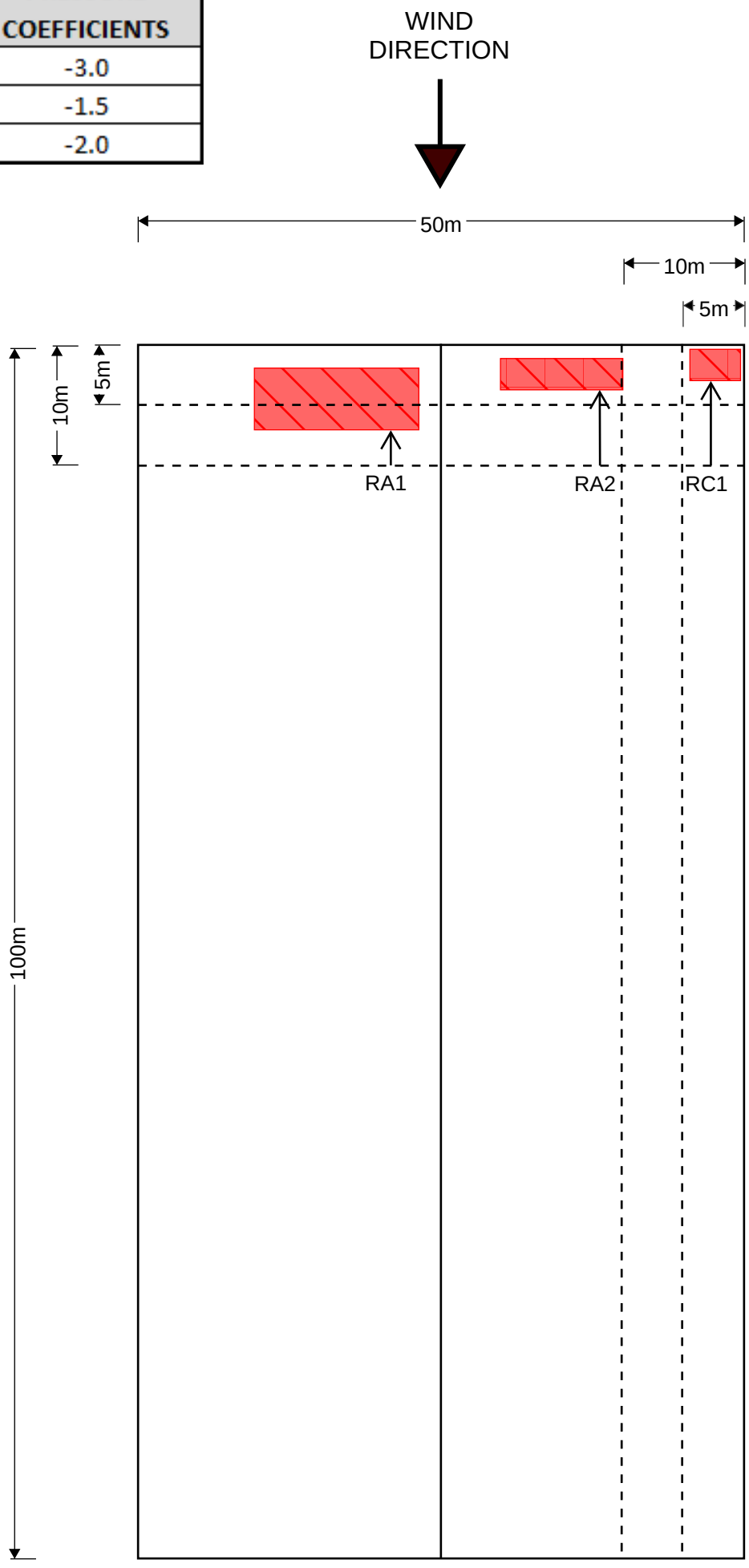

MODEL 2 - 100m (W) x 200m (L) x 14m (H) – Roof pitch 3°

AREA	PRESSURE COEFFICIENTS
RC1	-3.0
RA1	-1.5
RA2	-2.0

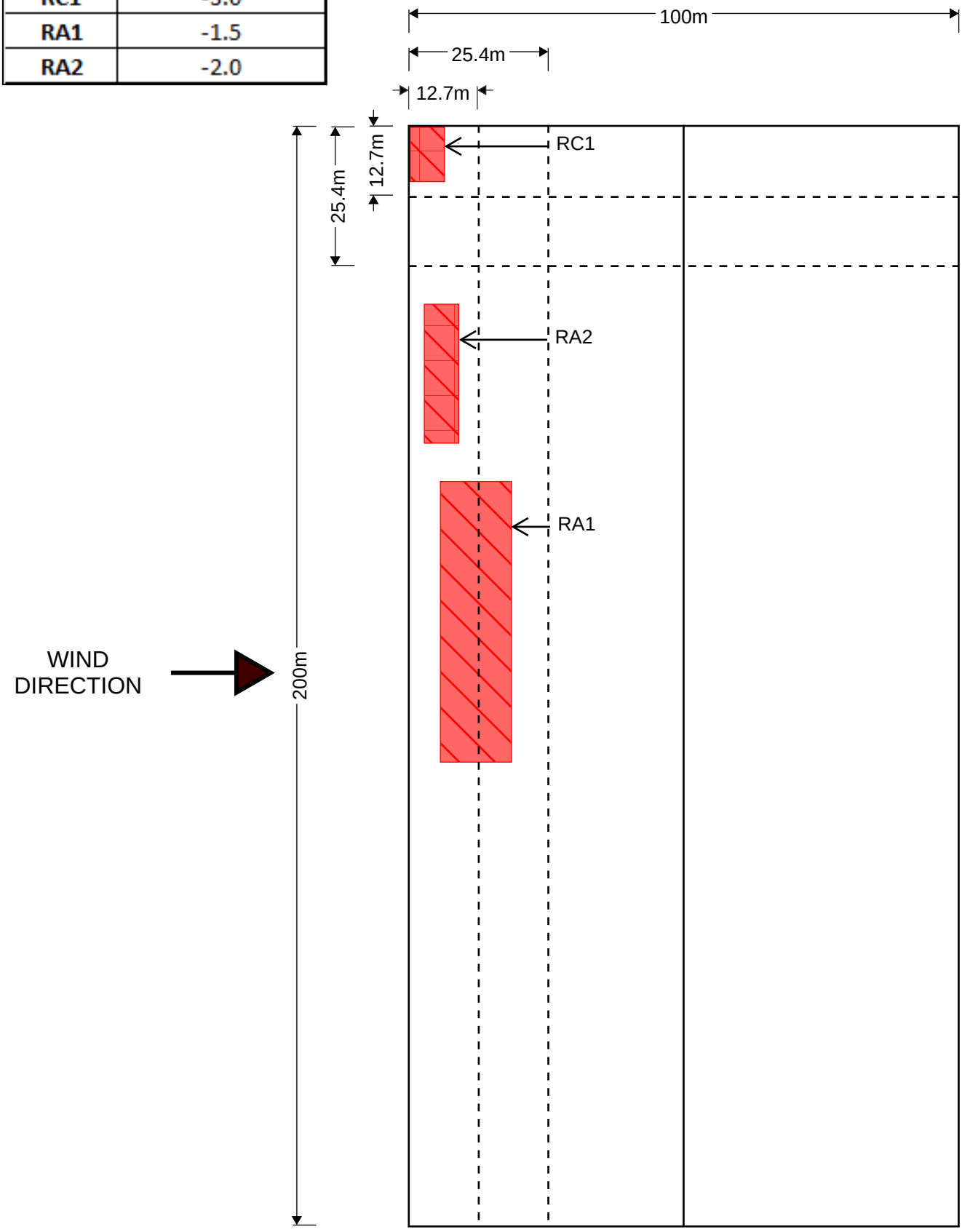

MODEL 2 - 100m (W) x 200m (L) x 14m (H) – Roof pitch 3°

AREA	PRESSURE COEFFICIENTS
RC1	-3.0
RA1	-1.5
RA2	-2.0

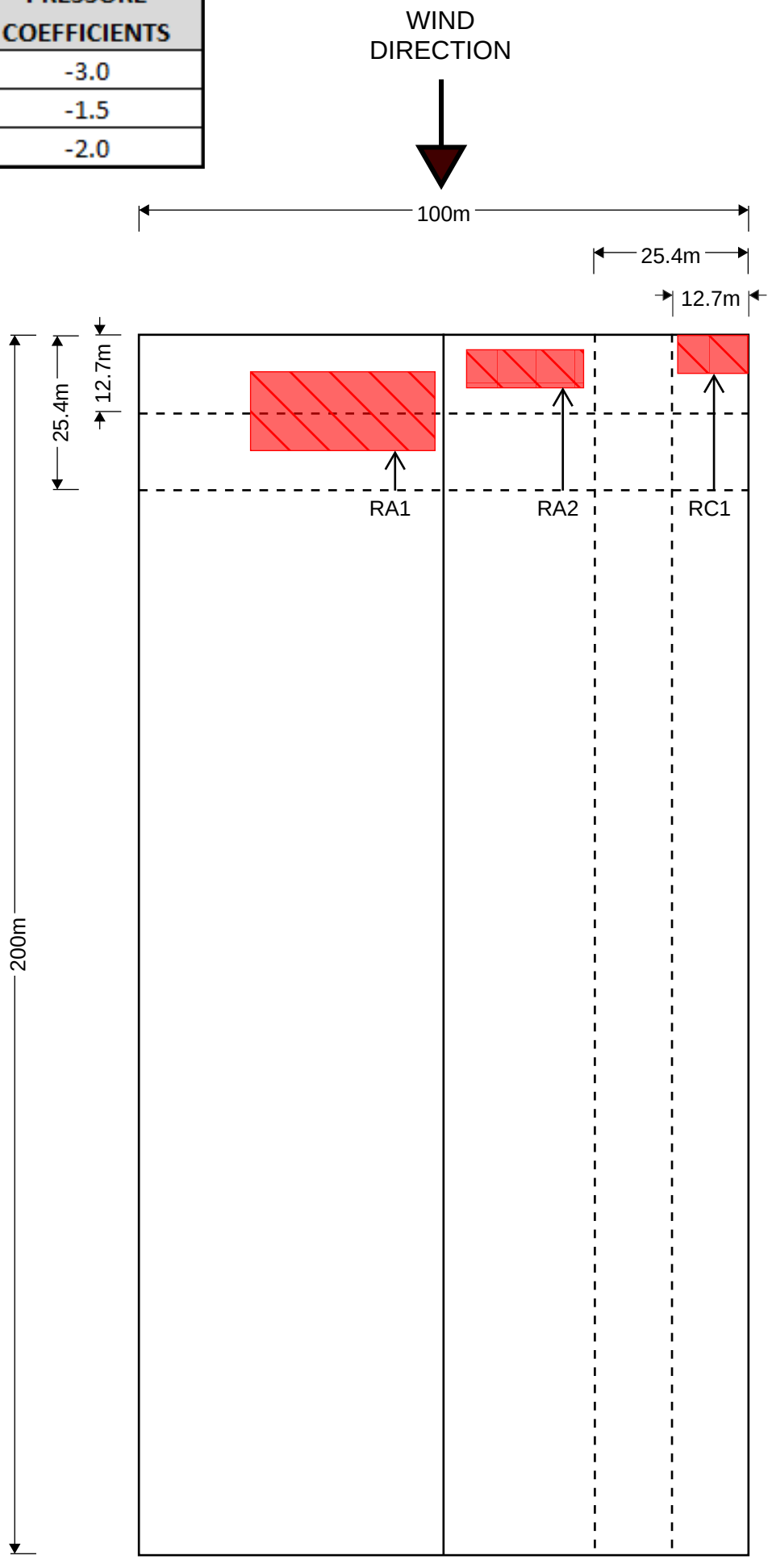

MODEL 3 - 150m (W) x 150m (L) x 14m (H) – Roof pitch 3°

AREA	PRESSURE COEFFICIENTS
RC1	-3.0
RA1	-1.5
RA2	-2.0

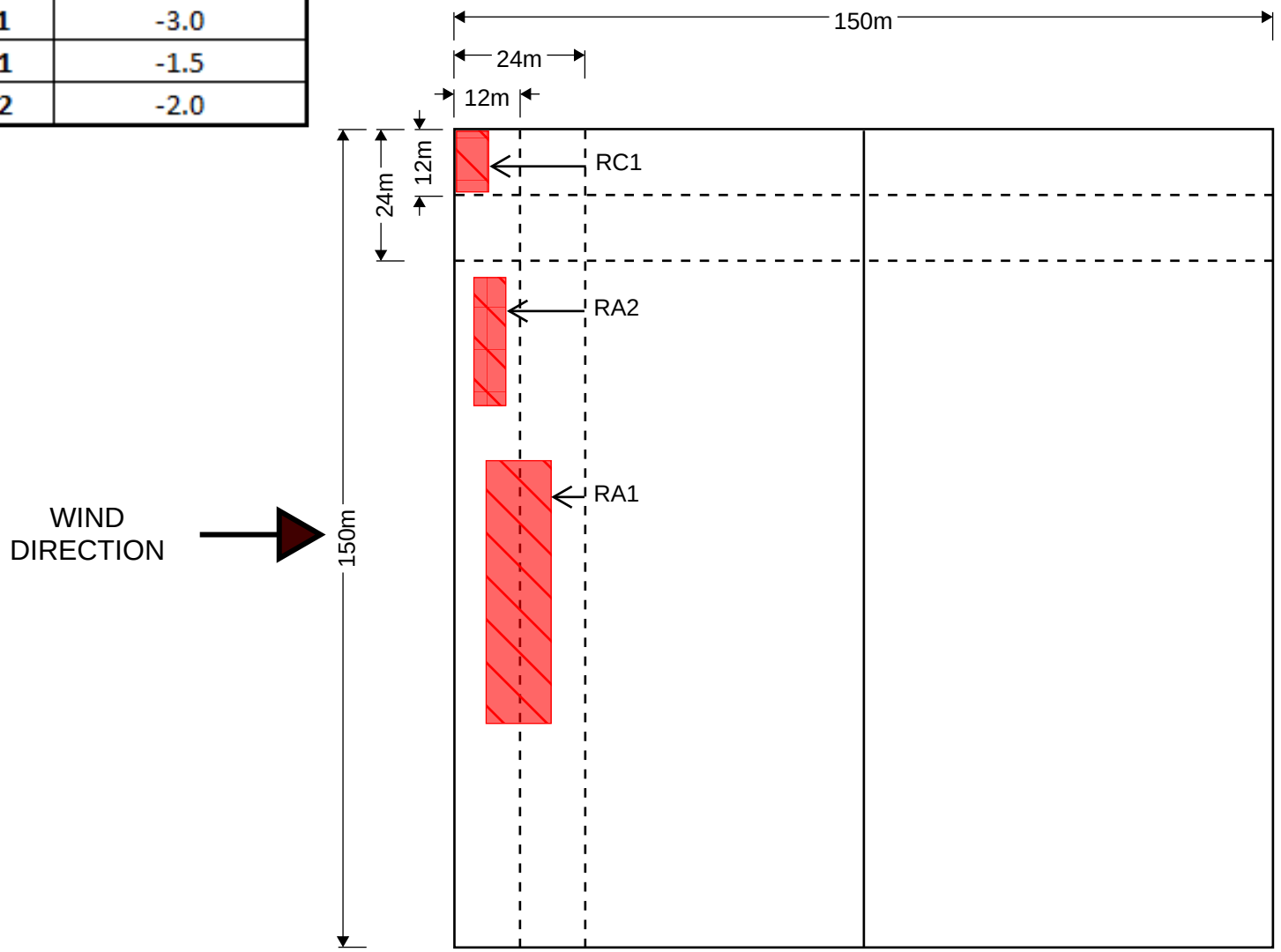

MODEL 3 - 150m (W) x 150m (L) x 14m (H) – Roof pitch 3°

AREA	PRESSURE COEFFICIENTS
RC1	-3.0
RA1	-1.5
RA2	-2.0

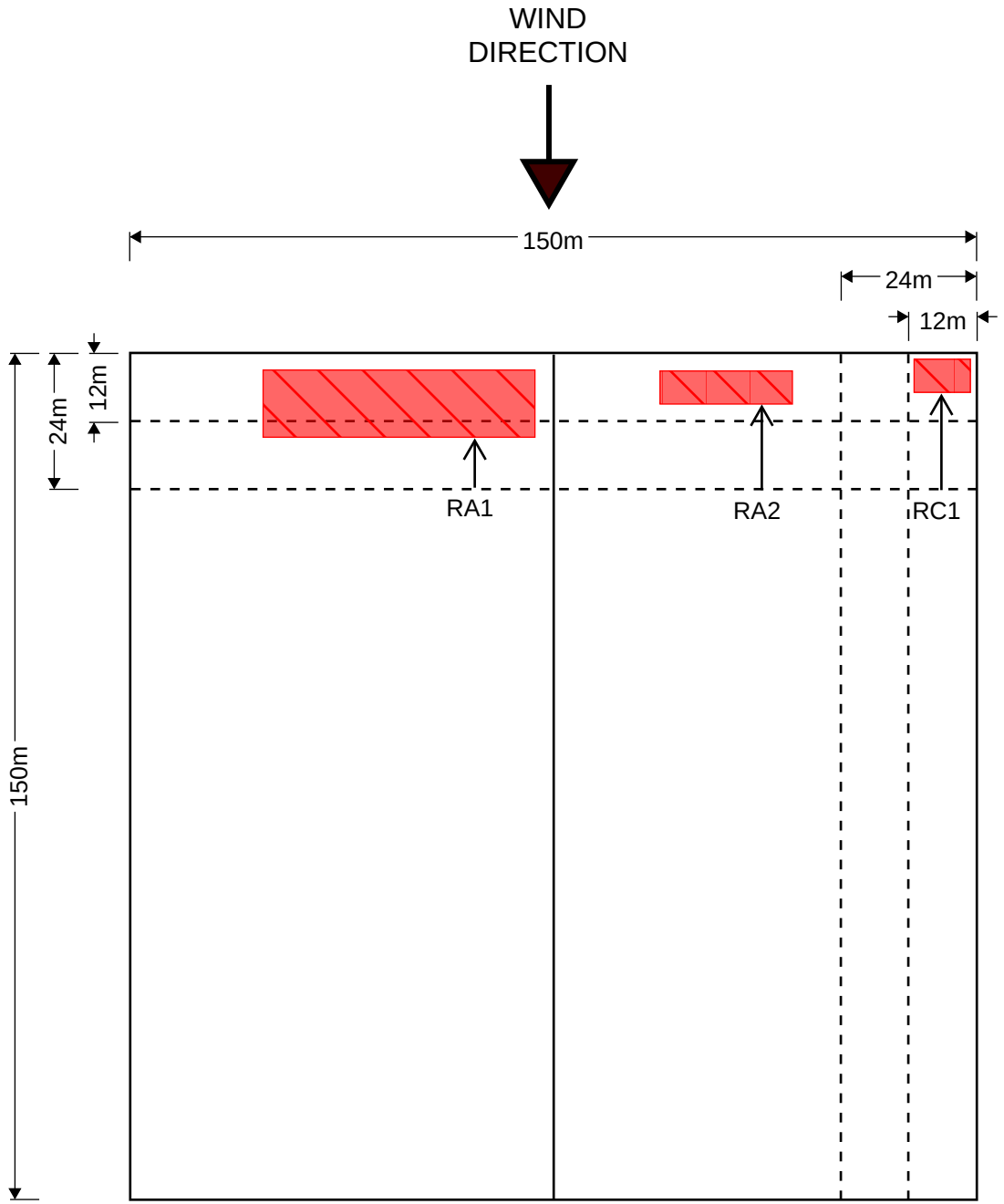

MODEL 4 - 50m (W) x 100m (L) x 14m (H) – Roof pitch 10°

AREA	PRESSURE COEFFICIENTS
RC1	-3.0
RA1	-1.5
RA2	-2.0
RA3	-1.5
RA4	-2.0

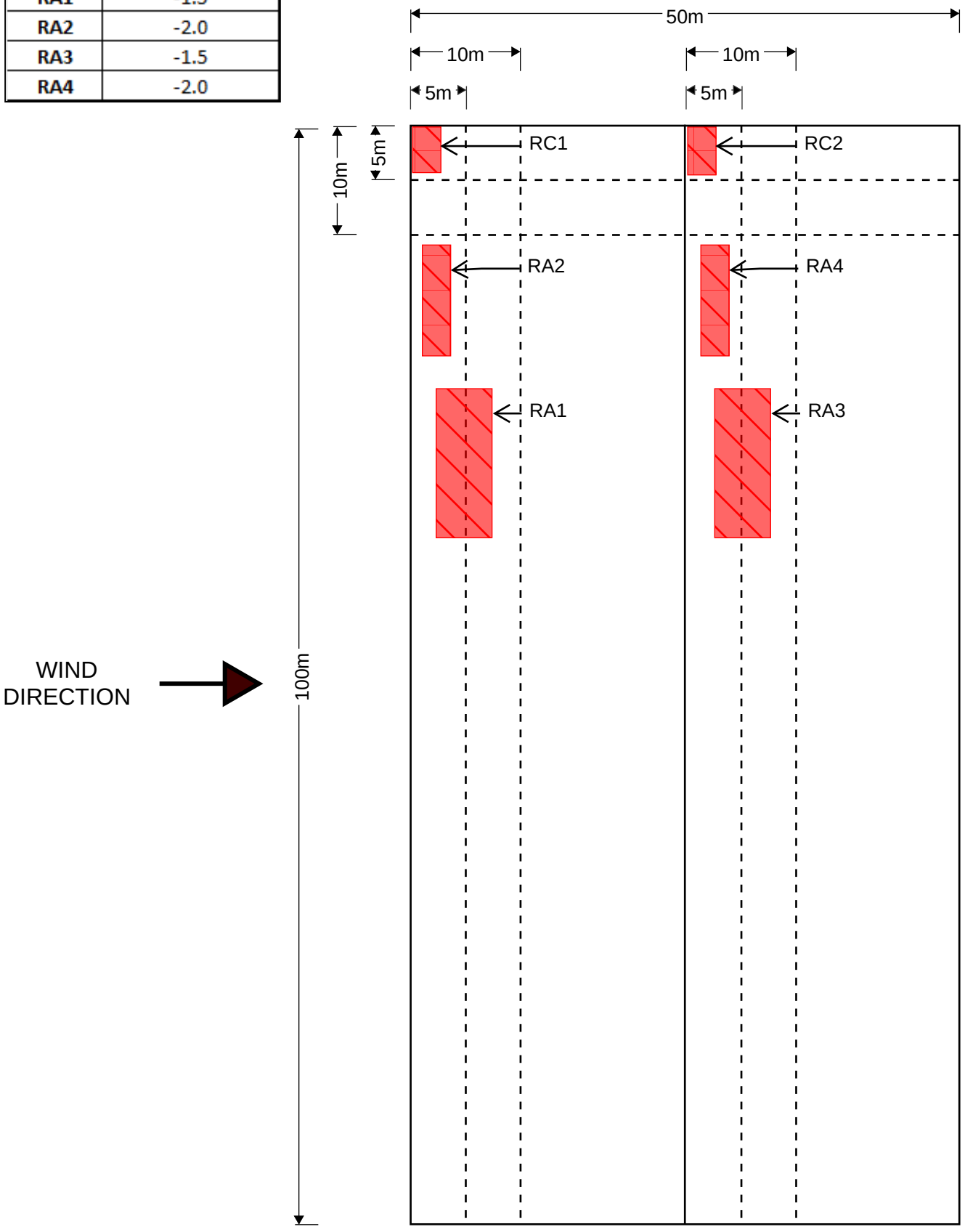

MODEL 4 - 50m (W) x 100m (L) x 14m (H) – Roof pitch 10°

AREA	PRESSURE COEFFICIENTS
RC1	-3.0
RA1	-1.5
RA2	-2.0

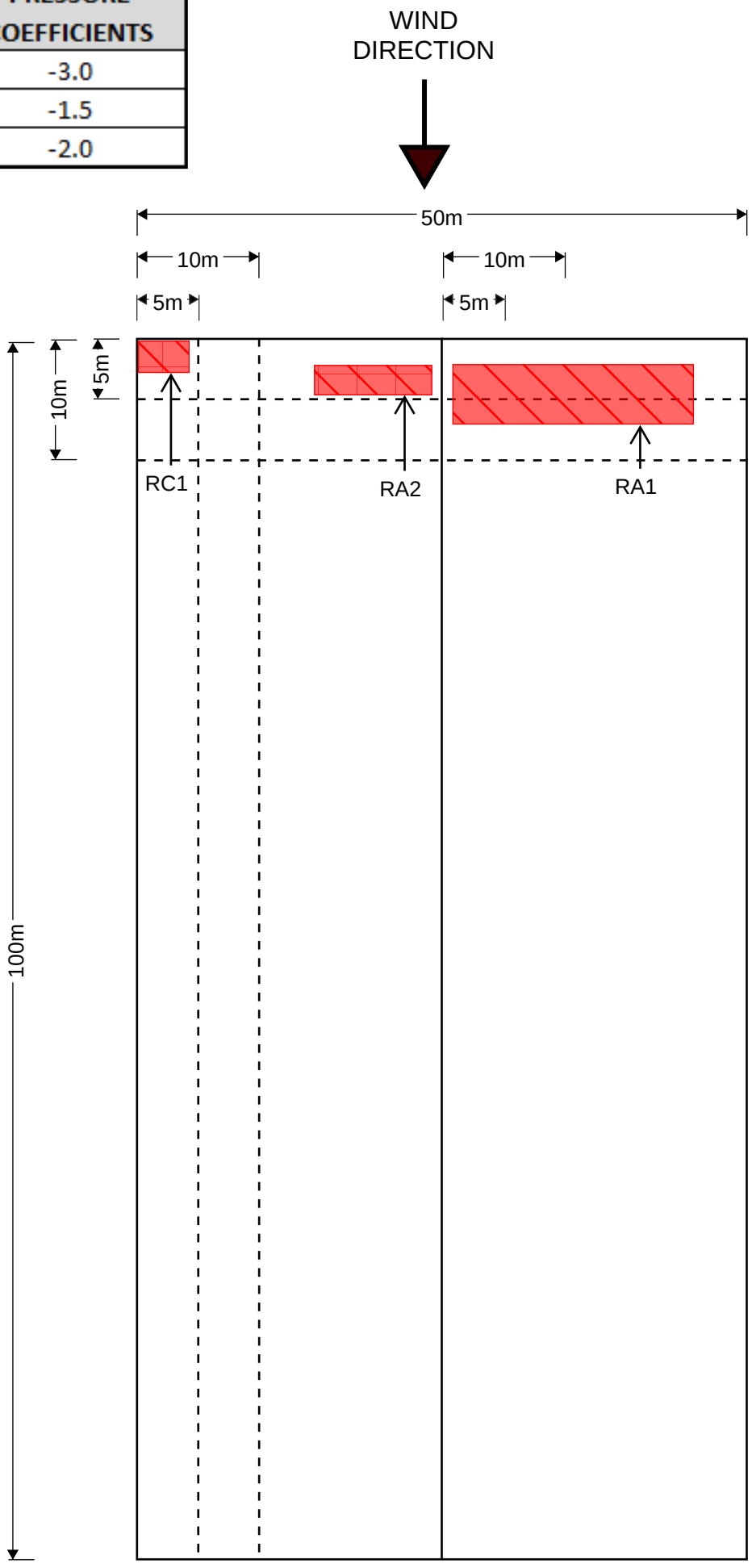

MODEL 5 - 100m (W) x 200m (L) x 14m (H) – Roof pitch 10°

AREA	PRESSURE COEFFICIENTS
RC1	-3.0
RA1	-1.5
RA2	-2.0
RA3	-1.5
RA4	-2.0

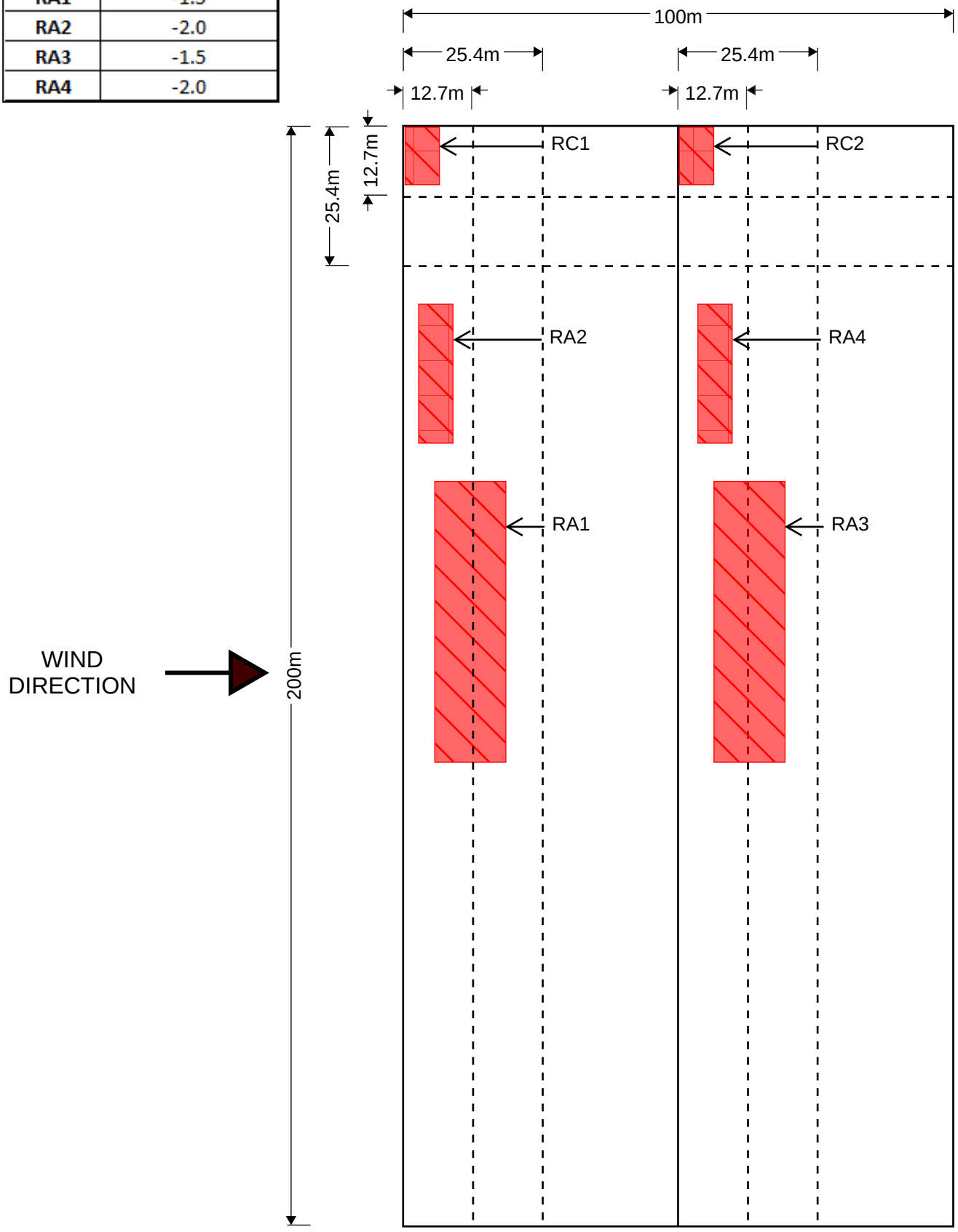

MODEL 5 - 100m (W) x 200m (L) x 14m (H) – Roof pitch 10°

AREA	PRESSURE COEFFICIENTS
RC1	-3.0
RA1	-1.5
RA2	-2.0

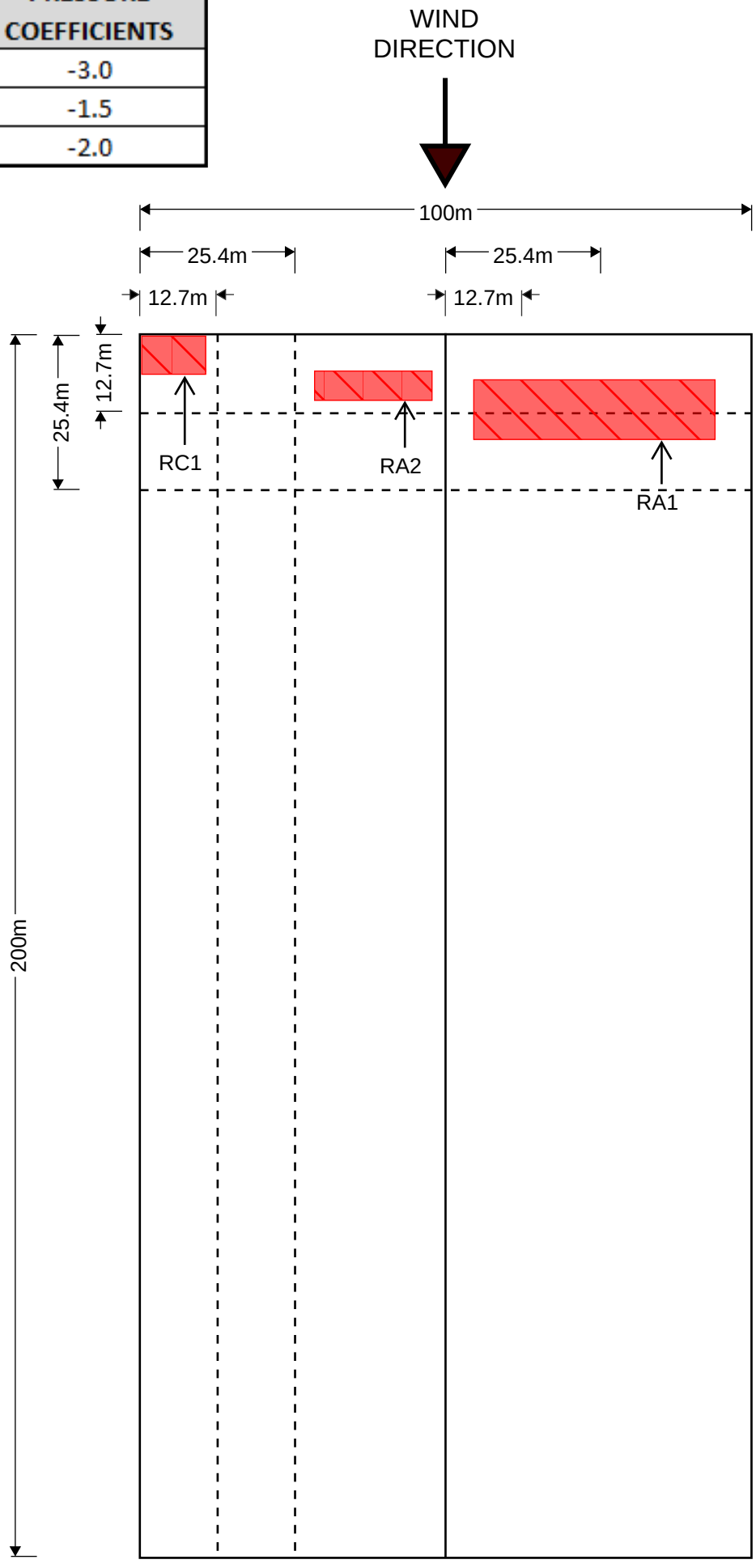

MODEL 6 - 100m (W) x 100m (L) x 14m (H) – Roof pitch 10°

AREA	PRESSURE COEFFICIENTS
RC1	-3.0
RA1	-1.5
RA2	-2.0
RA3	-1.5
RA4	-2.0

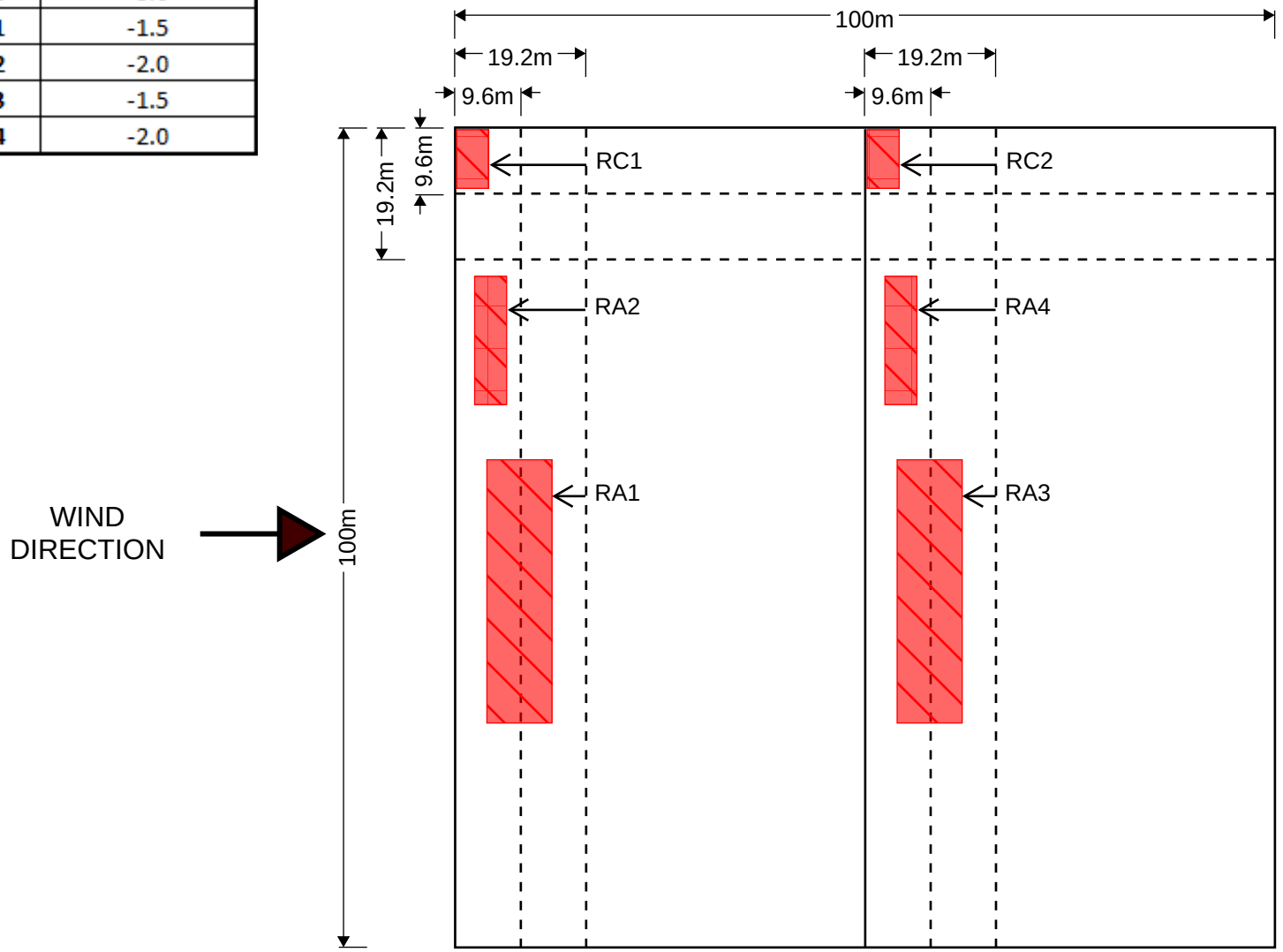

MODEL 6 - 100m (W) x 100m (L) x 14m (H) – Roof pitch 10°

AREA	PRESSURE COEFFICIENTS
RC1	-3.0
RA1	-1.5
RA2	-2.0

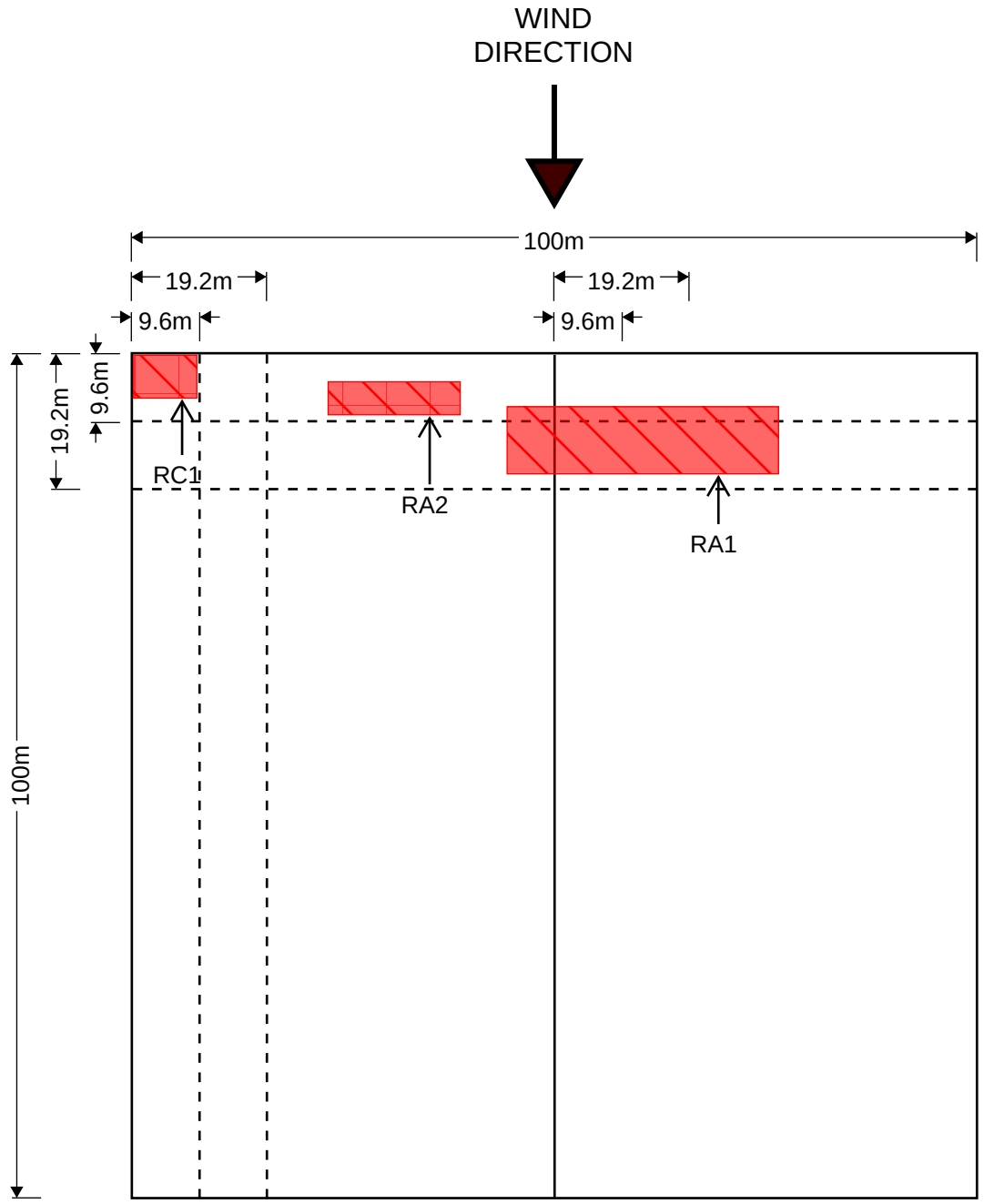

Local pressure factors - EN 1991-1-4:2005+A1 – Eurocode 1: Actions on Structures – Part 1-4: General Actions – Wind Actions

MODEL 1 - 50m (W) x 100m (L) x 14m (H) – Roof pitch 3°

AREA	PRESSURE COEFFICIENTS
F	-2.5
G	-2.0
H	-0.7
I	-0.2

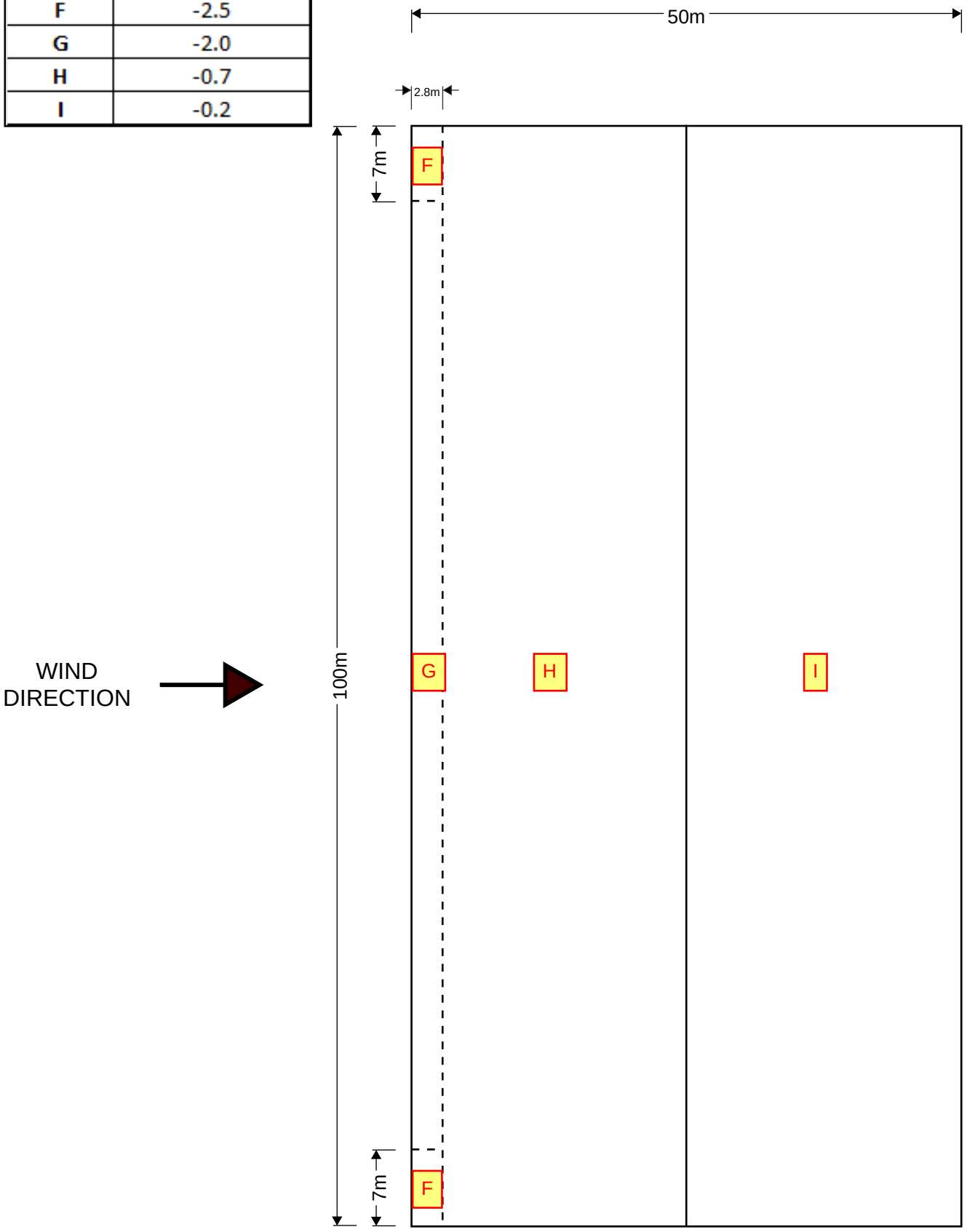

MODEL 1 - 50m (W) x 100m (L) x 14m (H) – Roof pitch 3°

AREA	PRESSURE COEFFICIENTS
F	-2.5
G	-2.0
H	-0.7
I	-0.2

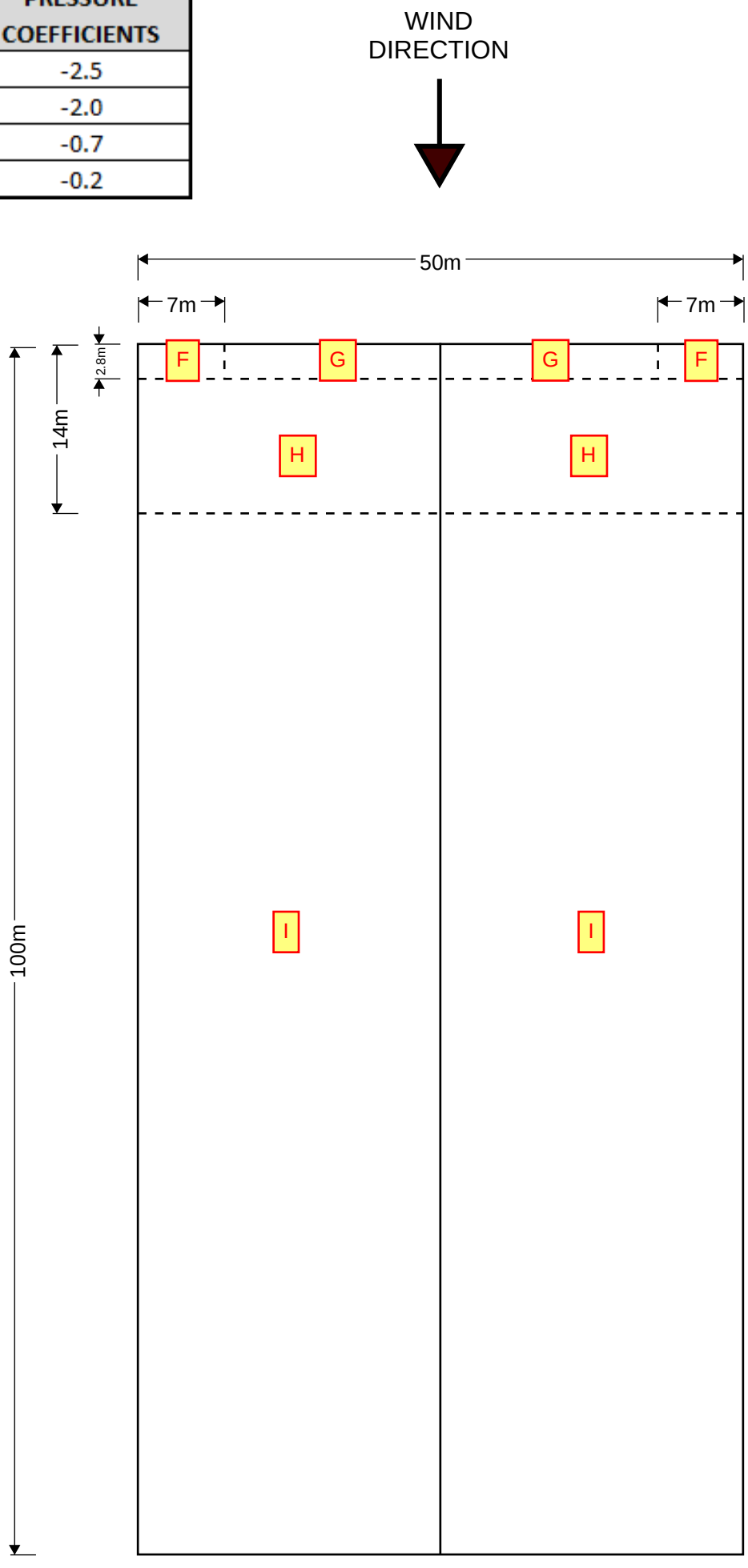

MODEL 2 - 100m (W) x 200m (L) x 14m (H) – Roof pitch 3°

AREA	PRESSURE COEFFICIENTS
F	-2.5
G	-2.0
H	-0.7
I	-0.2

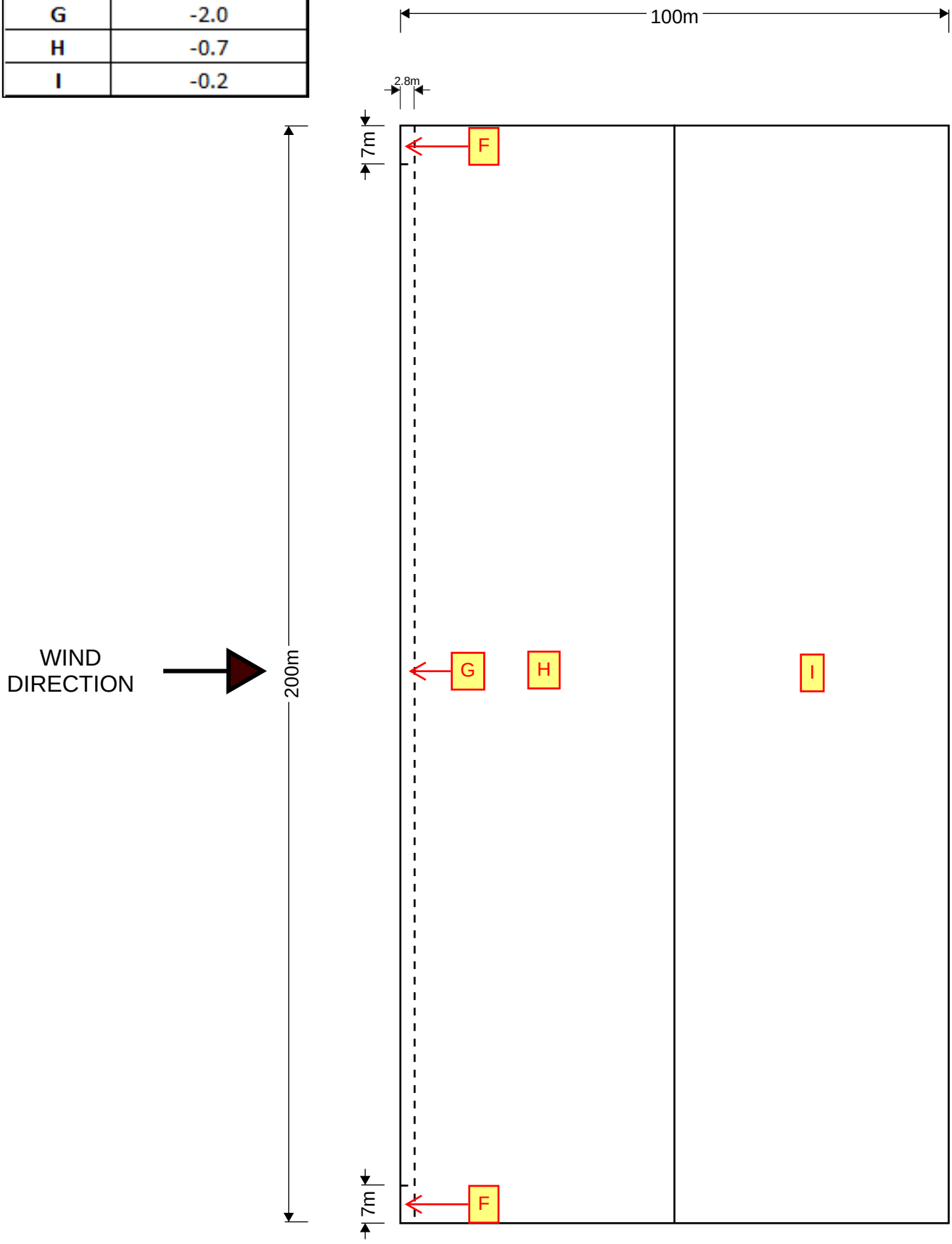

MODEL 2 - 100m (W) x 200m (L) x 14m (H) – Roof pitch 3°

AREA	PRESSURE COEFFICIENTS
F	-2.5
G	-2.0
H	-0.7
I	-0.2

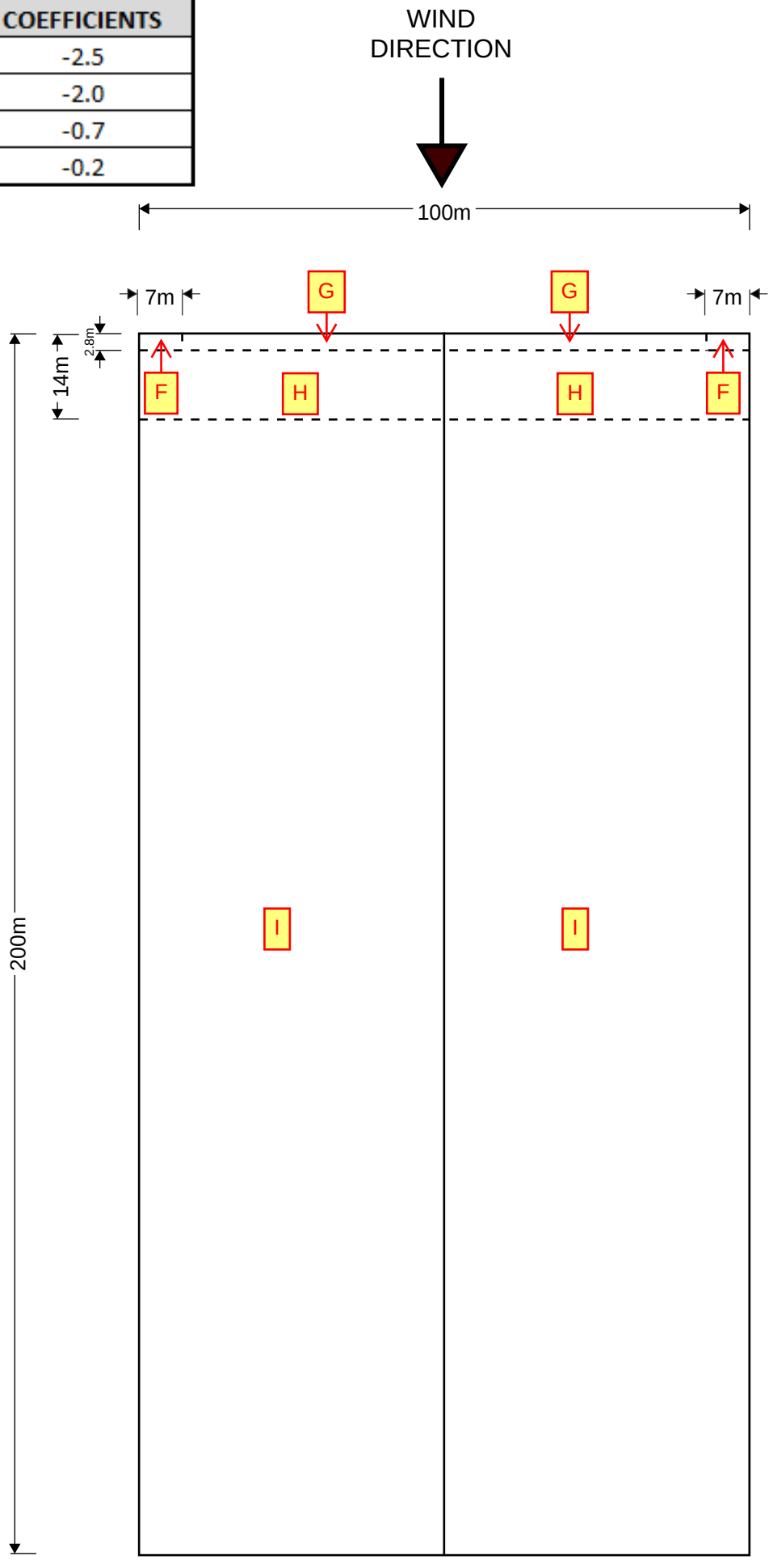

MODEL 3 - 150m (W) x 150m (L) x 14m (H) – Roof pitch 3°

AREA	PRESSURE COEFFICIENTS
F	-2.5
G	-2.0
H	-0.7
I	-0.2

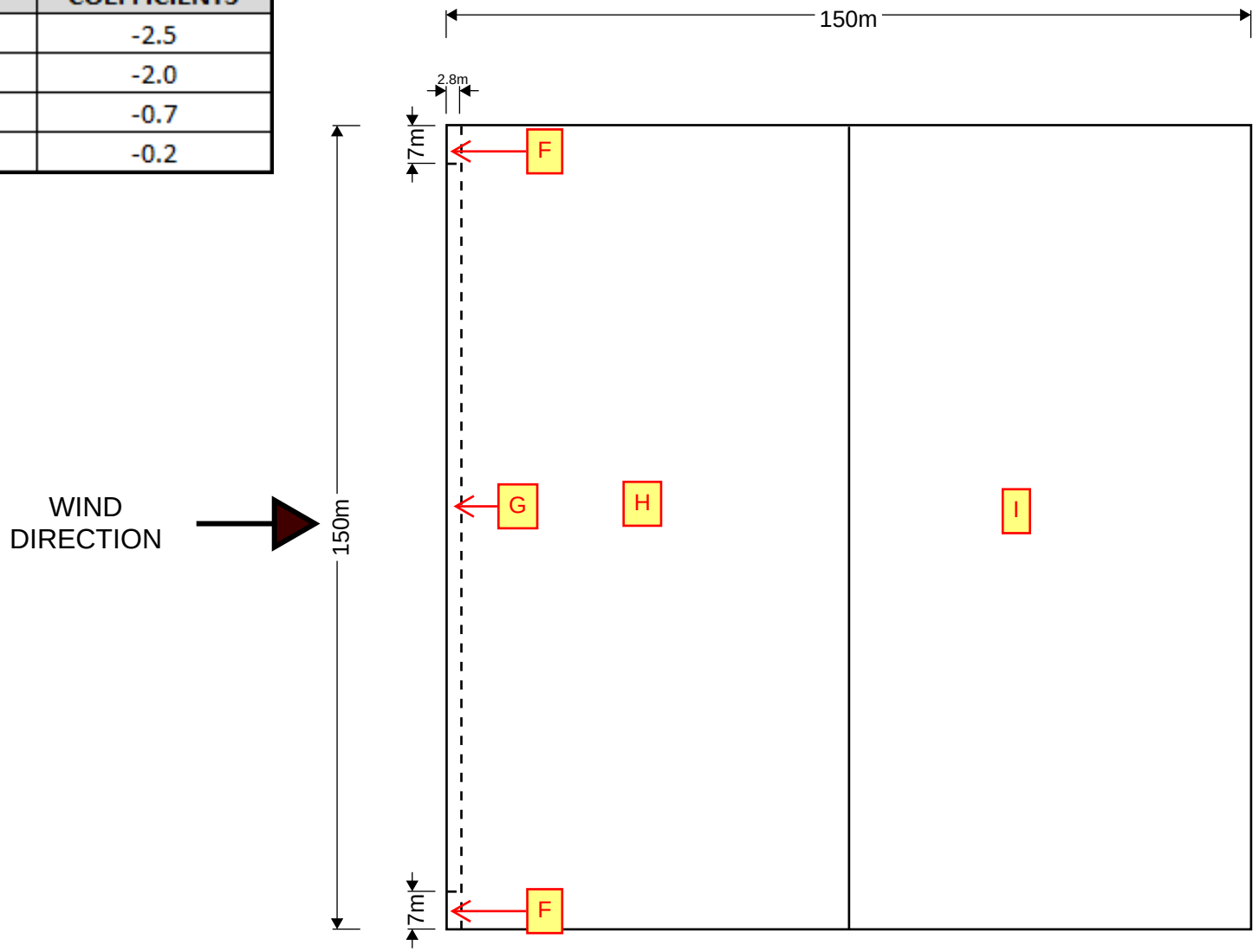

MODEL 3 - 150m (W) x 150m (L) x 14m (H) – Roof pitch 3°

AREA	PRESSURE COEFFICIENTS
F	-2.5
G	-2.0
H	-0.7
I	-0.2

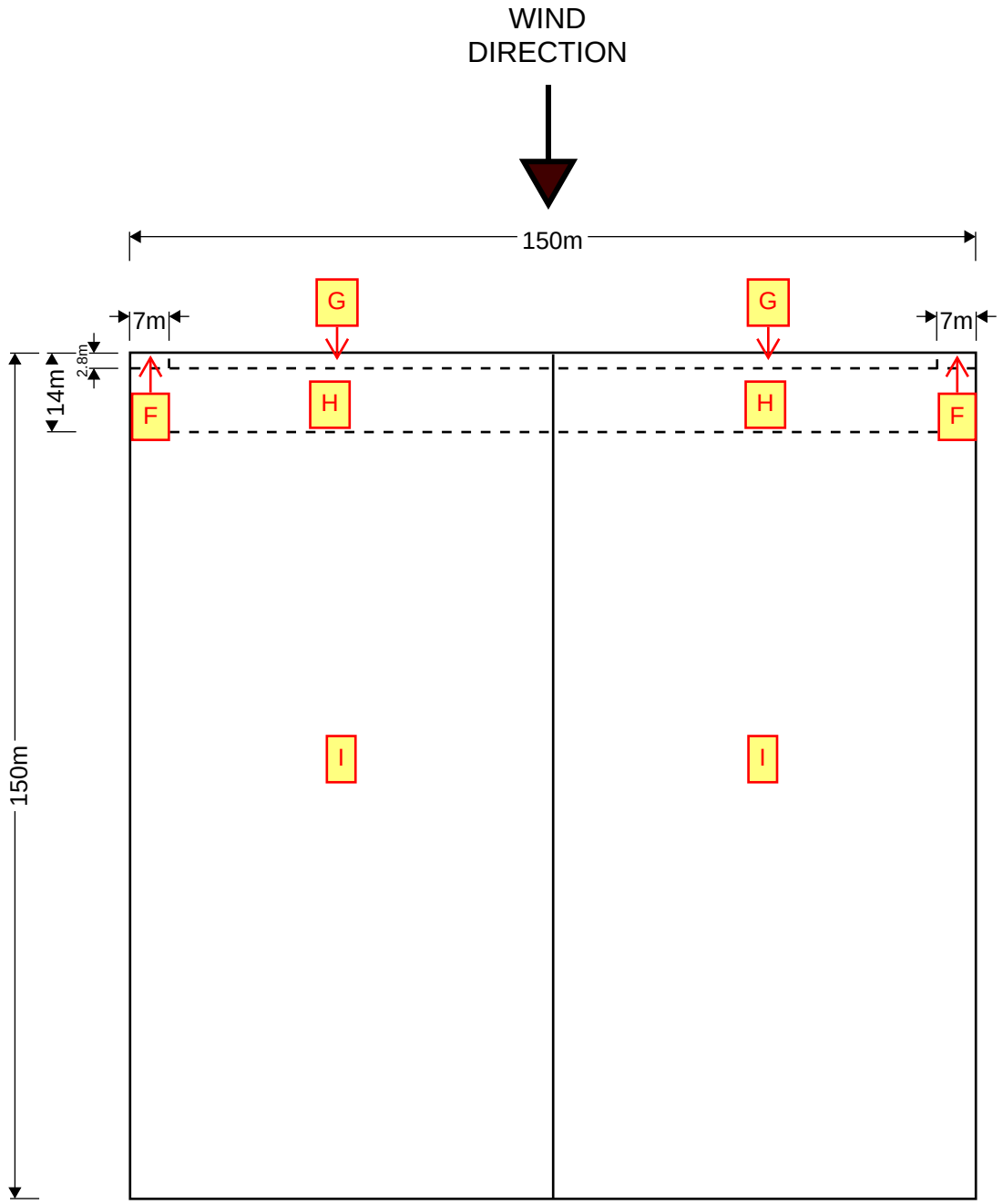

MODEL 4 - 50m (W) x 100m (L) x 14m (H) – Roof pitch 10°

AREA	PRESSURE COEFFICIENTS
F	-2.25
G	-2.0
H	-1.2
I	-0.5
J	-1.05

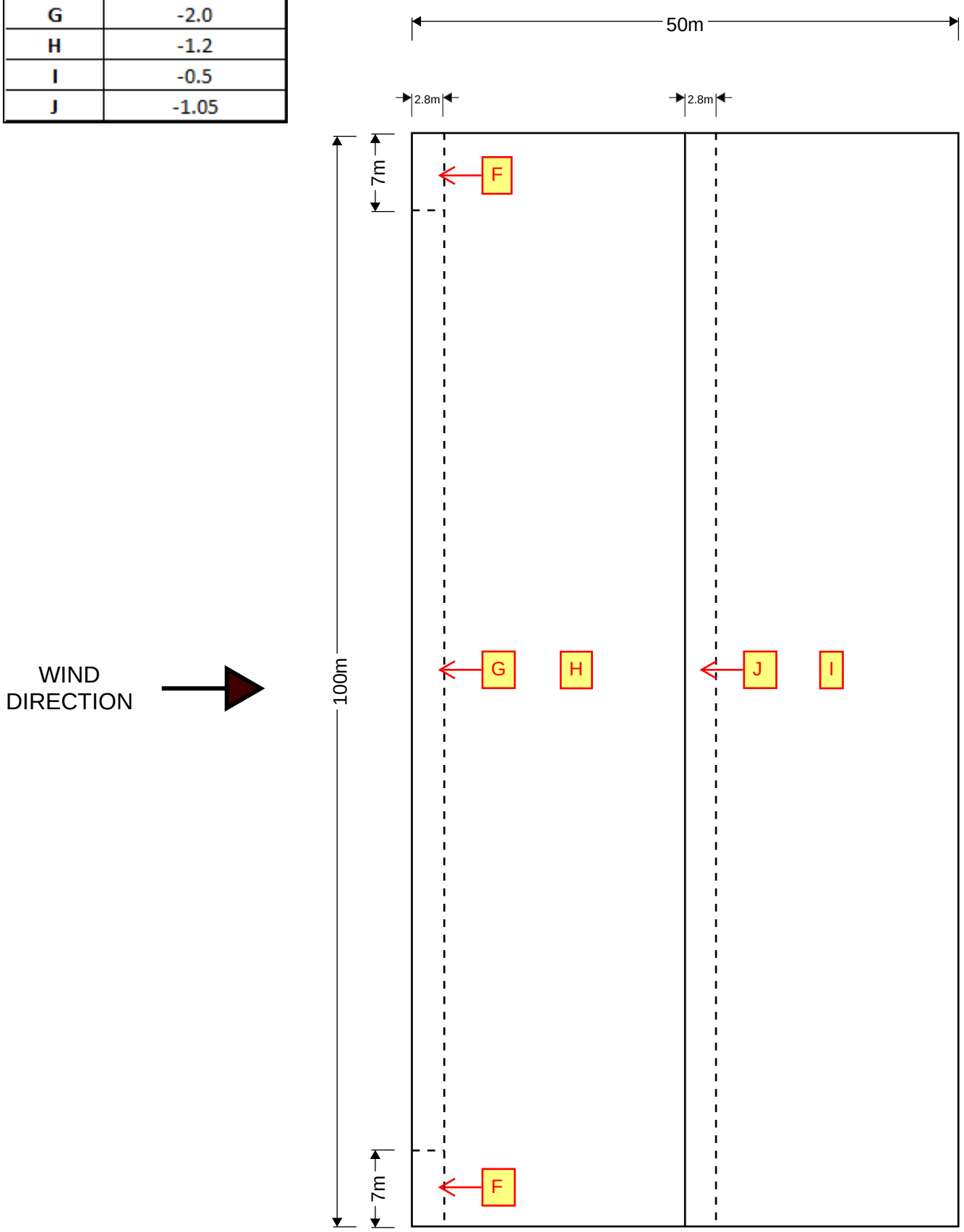

MODEL 4 - 50m (W) x 100m (L) x 14m (H) – Roof pitch 10°

AREA	PRESSURE COEFFICIENTS
F	-2.25
G	-2.0
H	-1.2
I	-0.5
J	-1.05

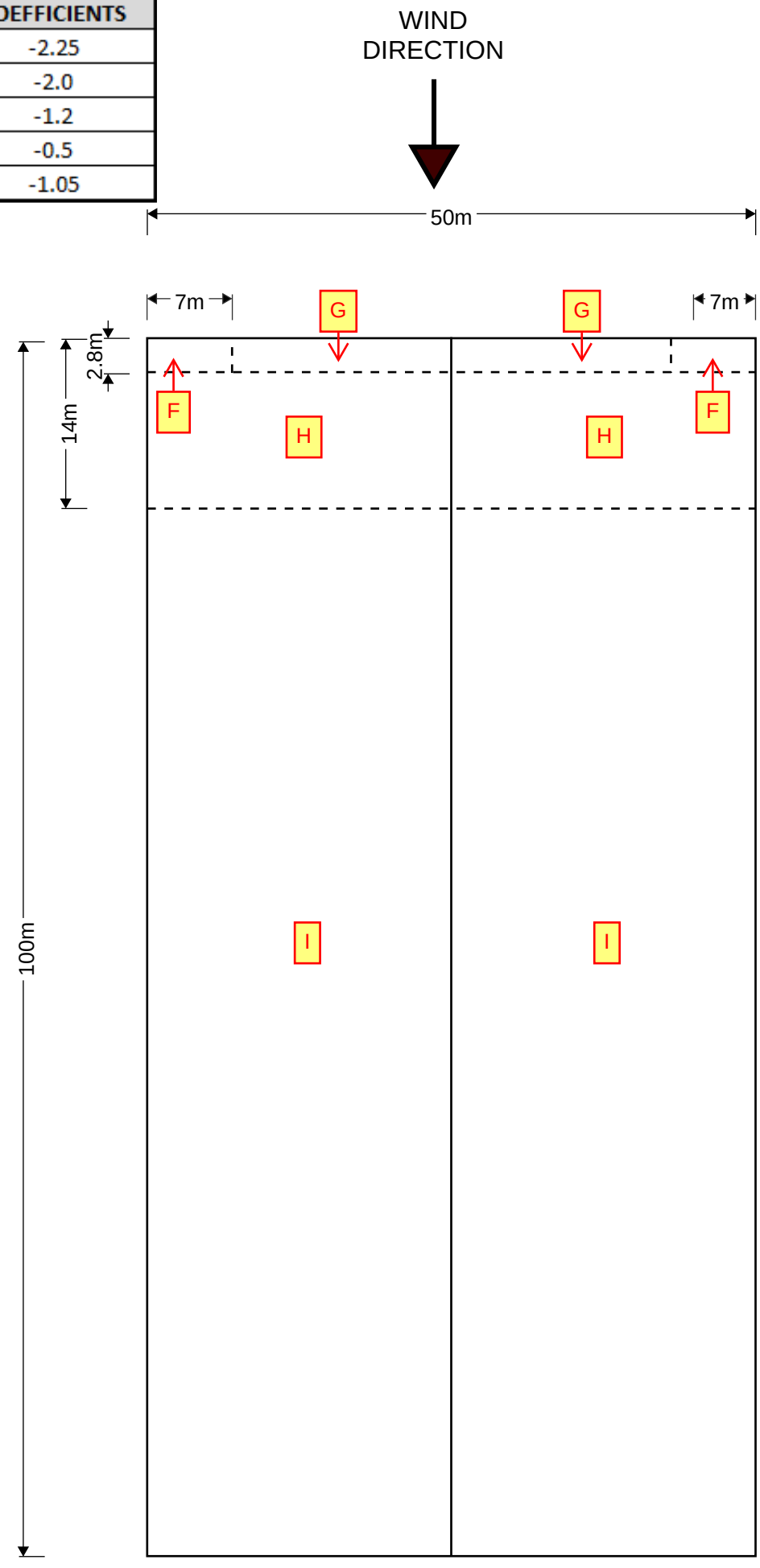

MODEL 5 - 100m (W) x 200m (L) x 14m (H) – Roof pitch 10°

AREA	PRESSURE COEFFICIENTS
F	-2.25
G	-2.0
H	-1.2
I	-0.5
J	-1.05

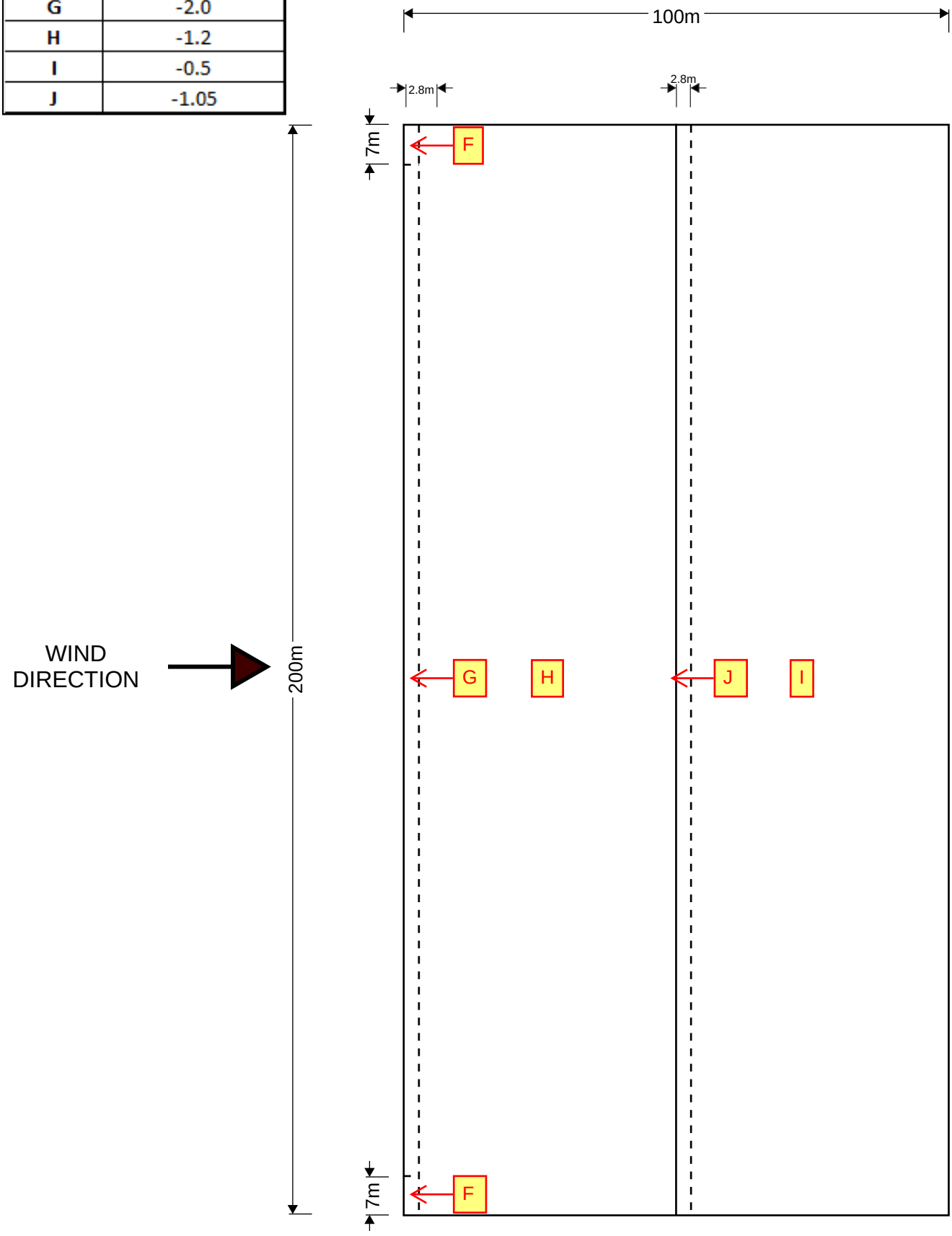

MODEL 5 - 100m (W) x 200m (L) x 14m (H) – Roof pitch 10°

AREA	PRESSURE COEFFICIENTS
F	-2.25
G	-2.0
H	-1.2
I	-0.5
J	-1.05

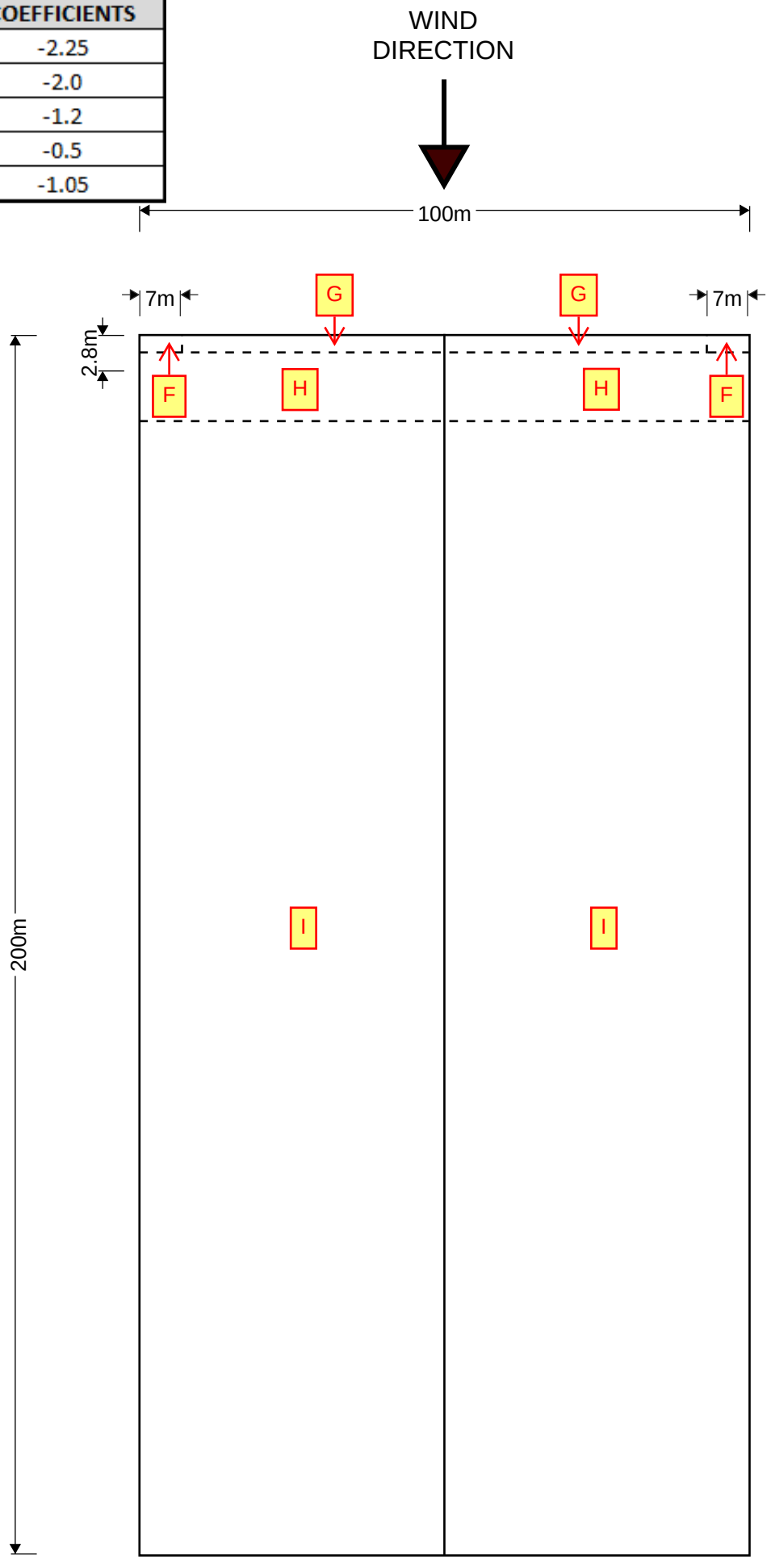

MODEL 6 - 100m (W) x 100m (L) x 14m (H) – Roof pitch 10°

AREA	PRESSURE COEFFICIENTS
F	-2.25
G	-2.0
H	-1.2
I	-0.5
J	-1.05

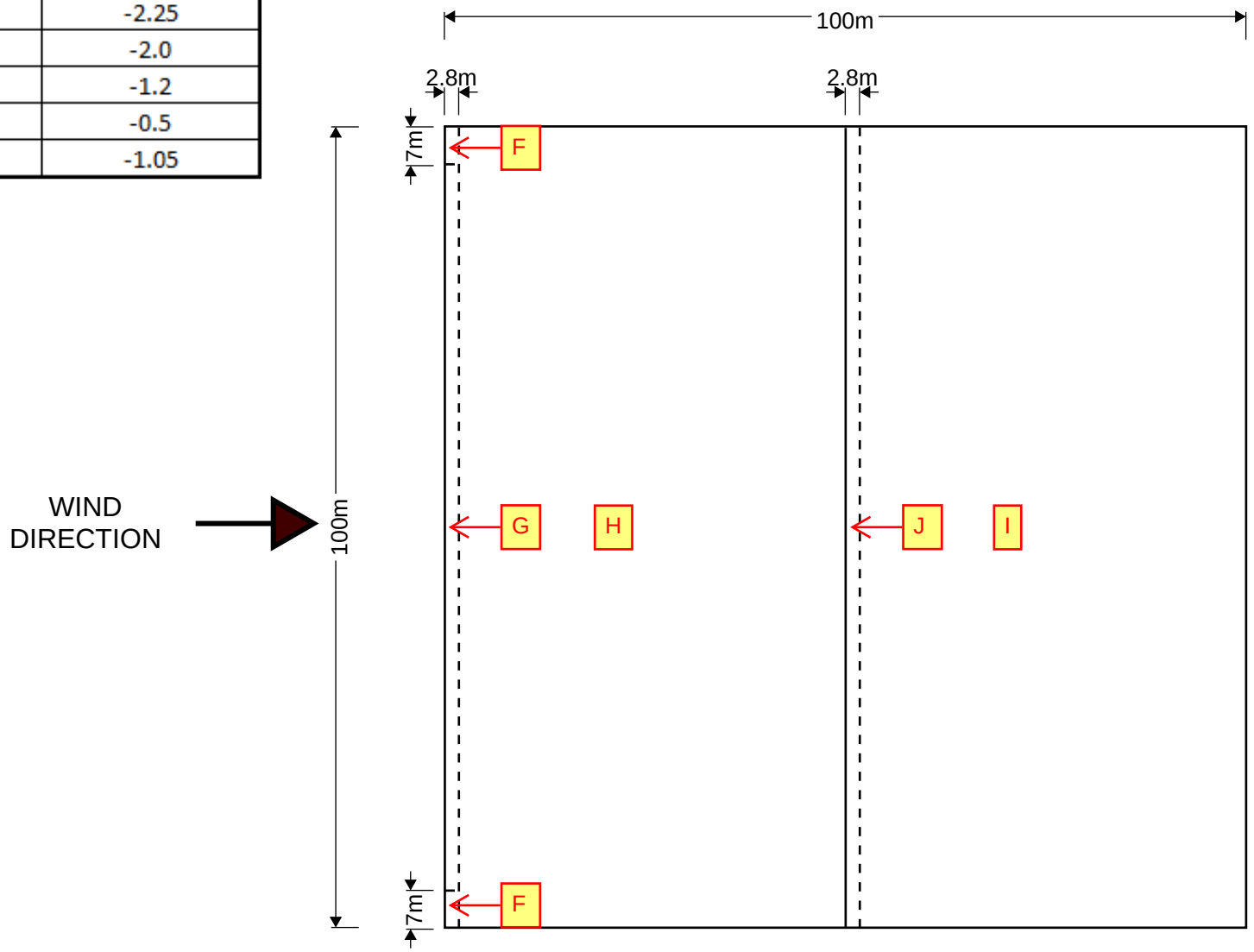

MODEL 6 - 100m (W) x 100m (L) x 14m (H) – Roof pitch 10°

AREA	PRESSURE COEFFICIENTS
F	-2.25
G	-2.0
H	-1.2
I	-0.5
J	-1.05

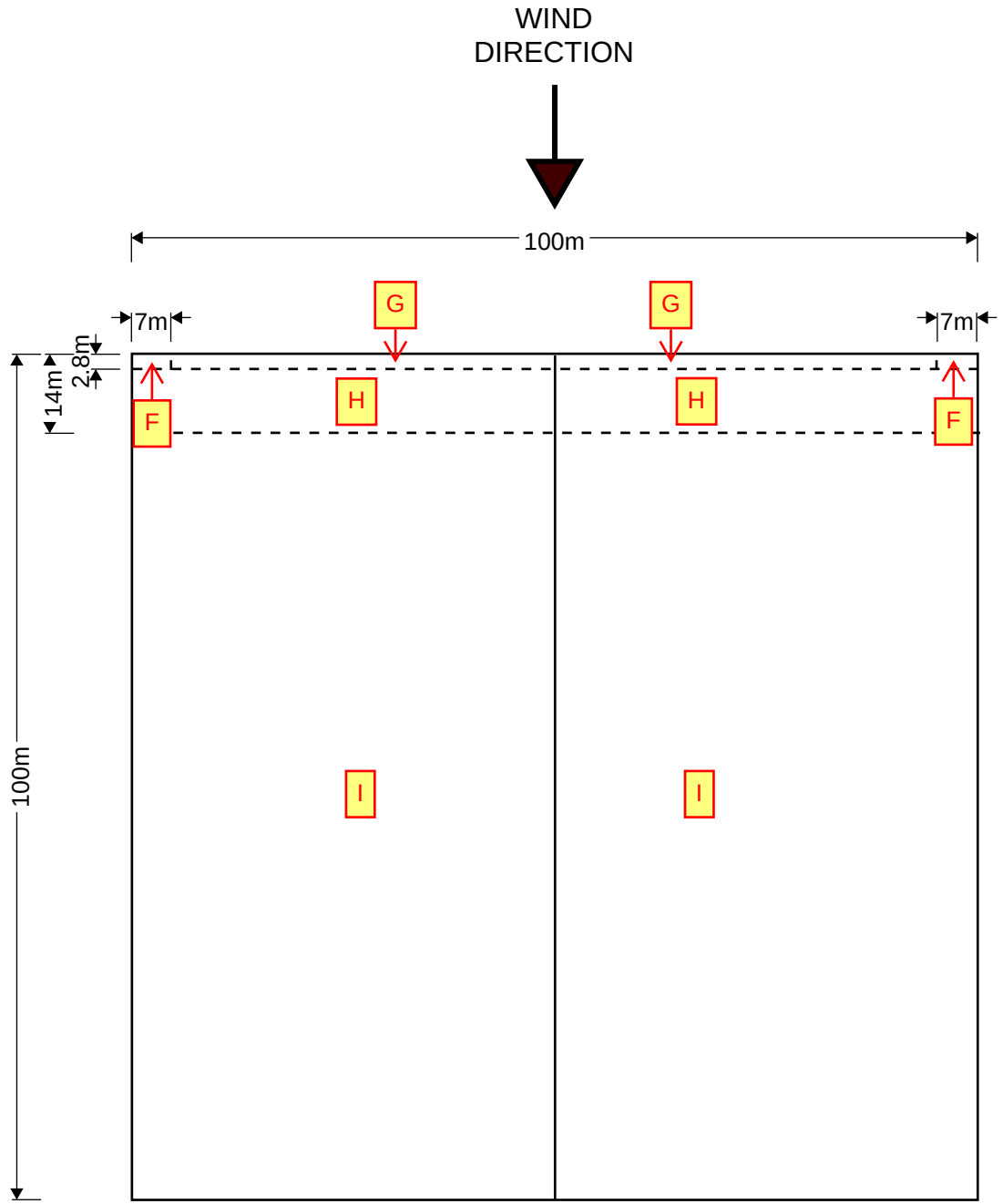

Local pressure factors - ASCE/SEI 7-10 – Minimum Design Loads for Buildings and Other Structures

MODEL 1 - 50m (W) x 100m (L) x 14m (H) – Roof pitch 3°

AREA	PRESSURE COEFFICIENTS
3	-2.2
2	-1.1
1	-0.9

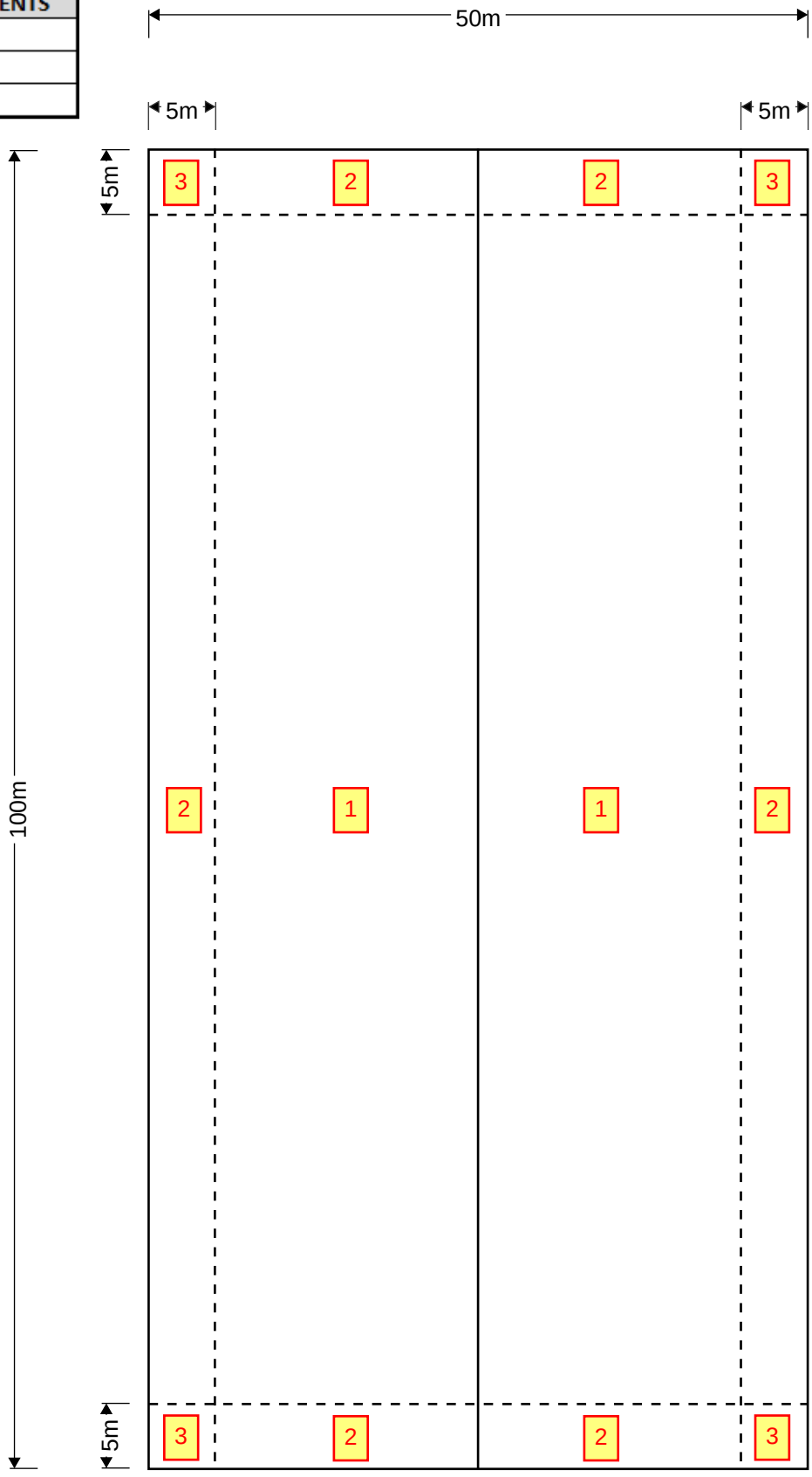

MODEL 2 - 100m (W) x 200m (L) x 14m (H) – Roof pitch 3°

AREA	PRESSURE COEFFICIENTS
3	-2.0
2	-1.1
1	-0.9

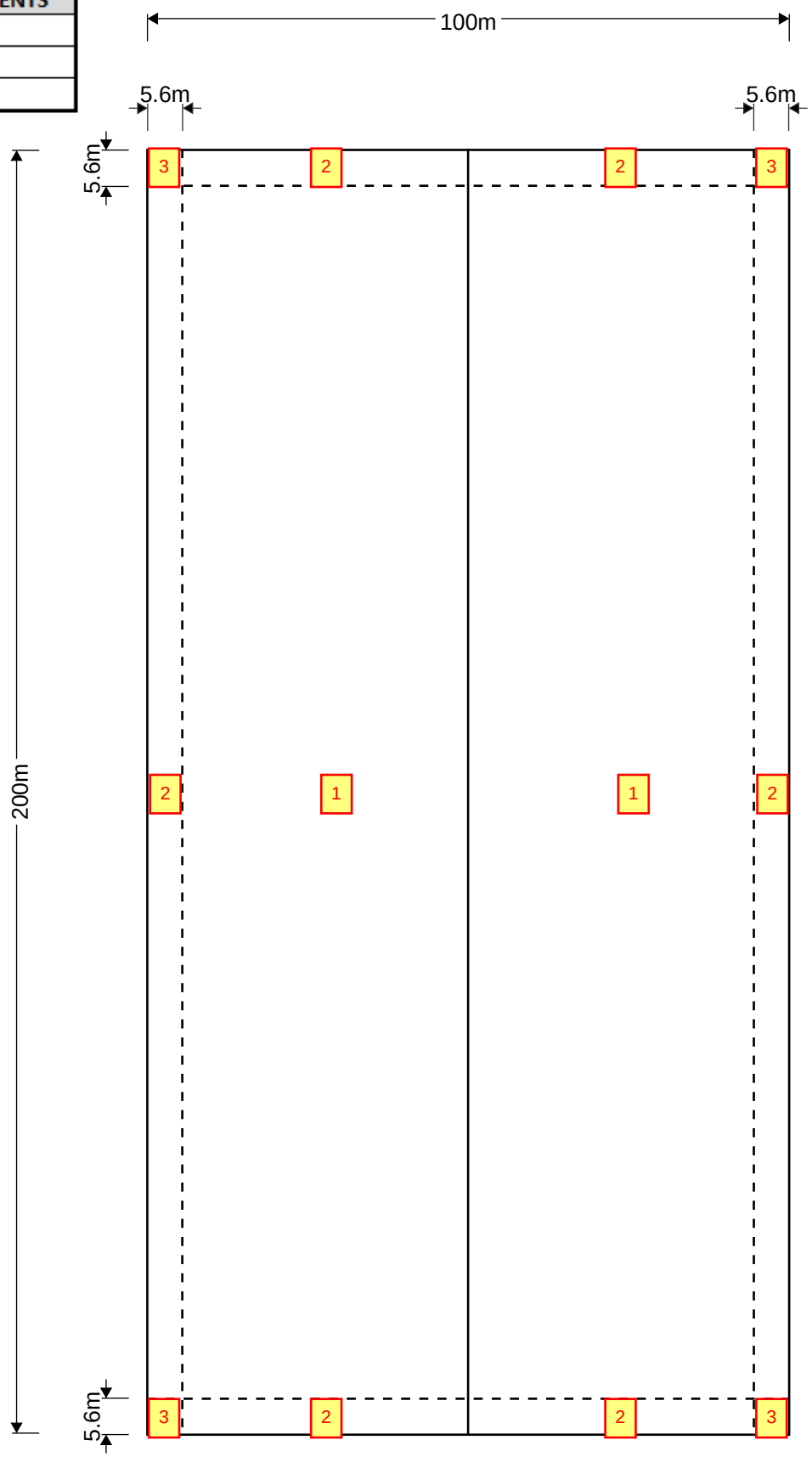

MODEL 3 - 150m (W) x 150m (L) x 14m (H) – Roof pitch 3°

AREA	PRESSURE COEFFICIENTS
3	-2.0
2	-1.1
1	-0.9

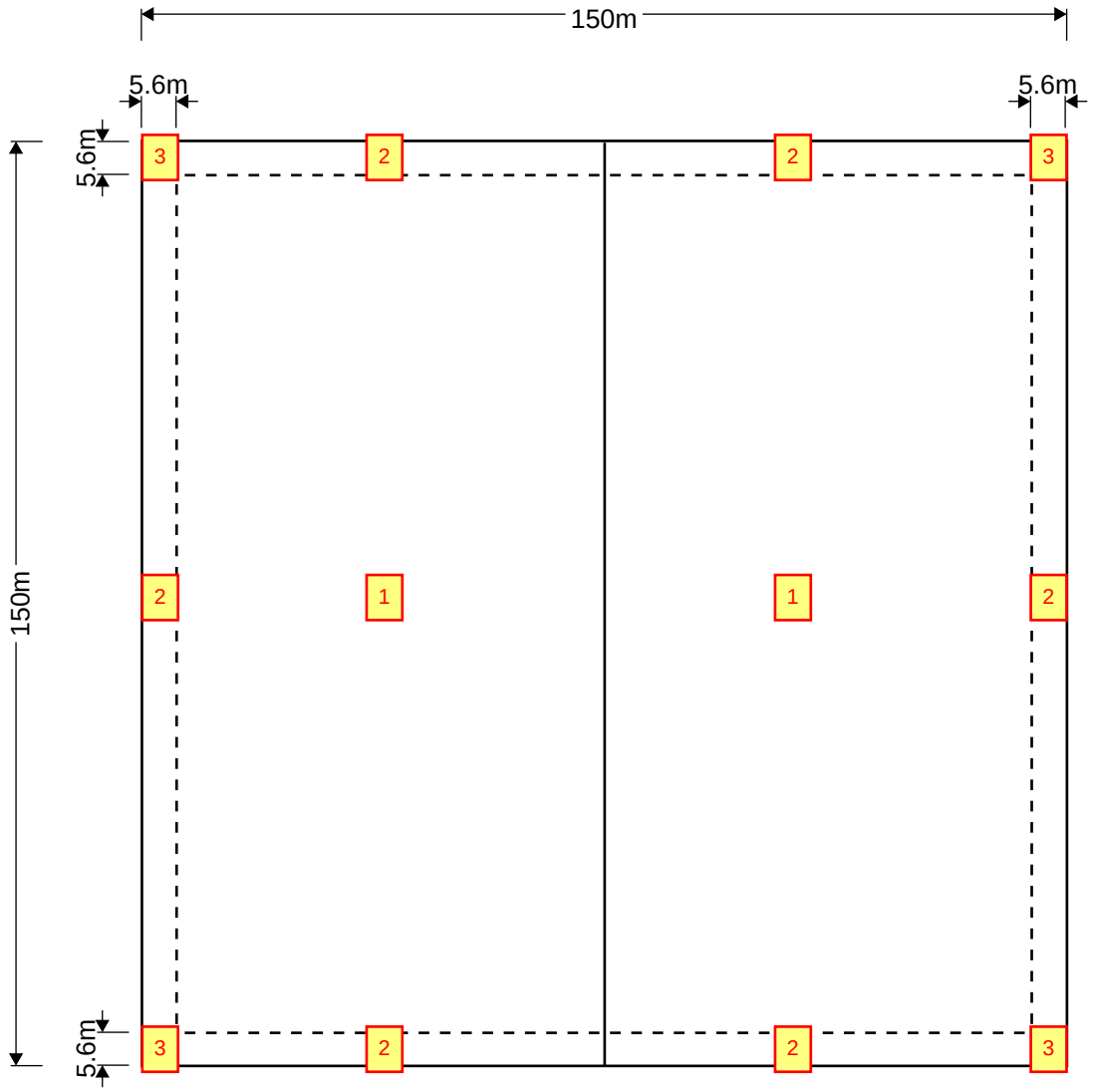

MODEL 4 - 50m (W) x 100m (L) x 14m (H) – Roof pitch 10°

AREA	PRESSURE COEFFICIENTS
3	-2.4
2	-1.5
1	-0.9

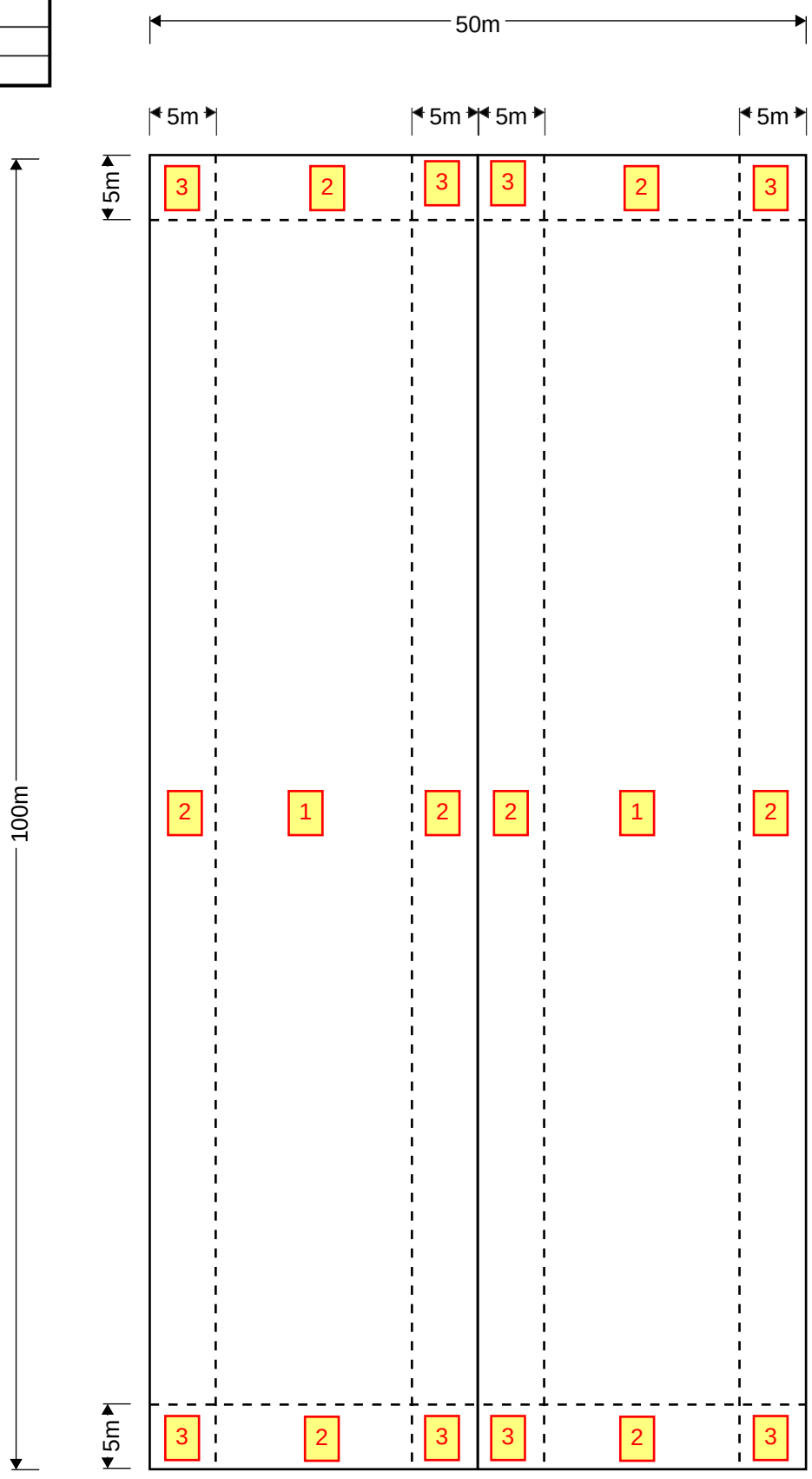

MODEL 5 - 100m (W) x 200m (L) x 14m (H) – Roof pitch 10°

AREA	PRESSURE COEFFICIENTS
3	-2.3
2	-1.5
1	-0.9

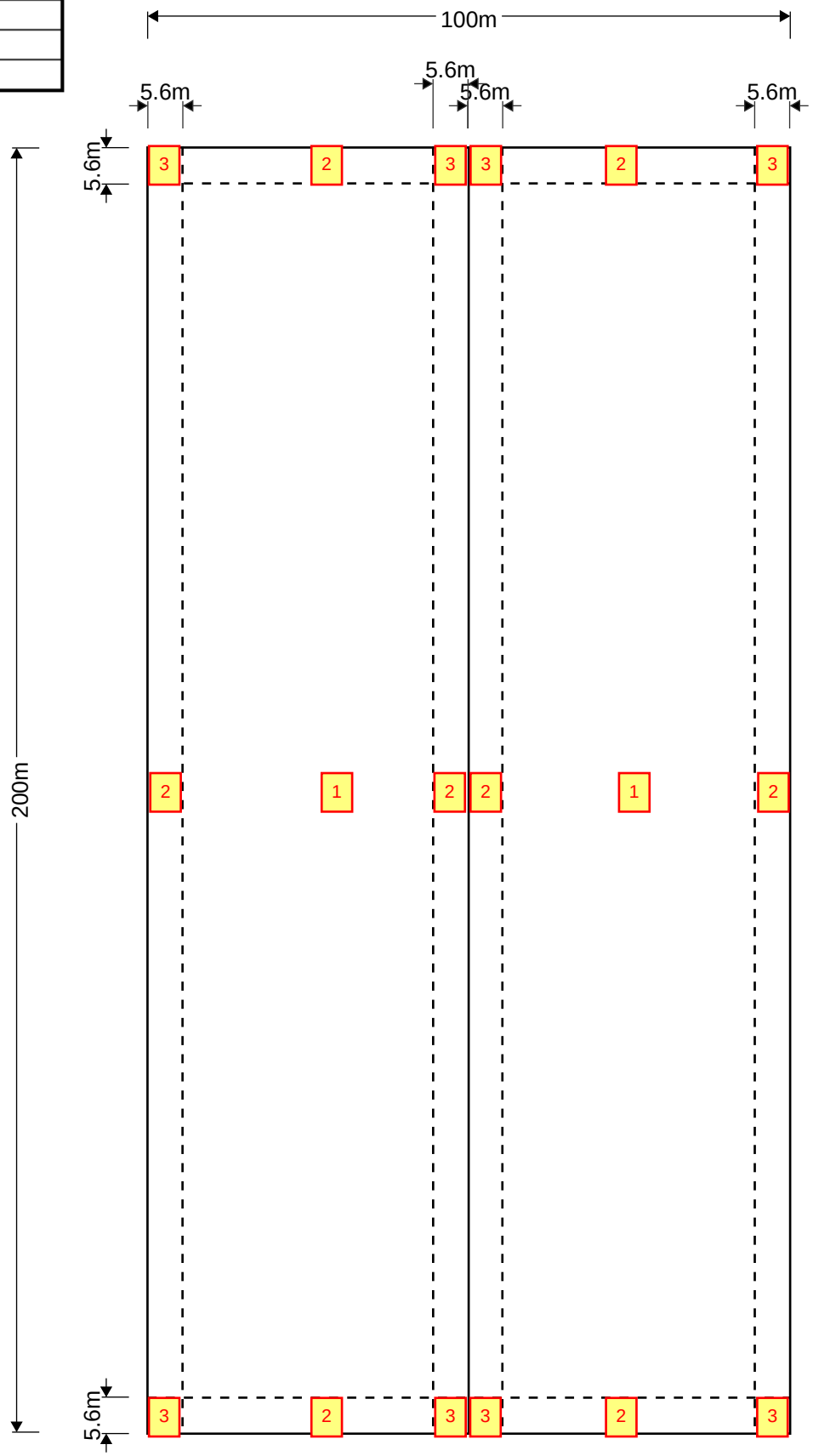

MODEL 6 - 100m (W) x 100m (L) x 14m (H) – Roof pitch 10°

AREA	PRESSURE COEFFICIENTS
3	-2.3
2	-1.5
1	-0.9

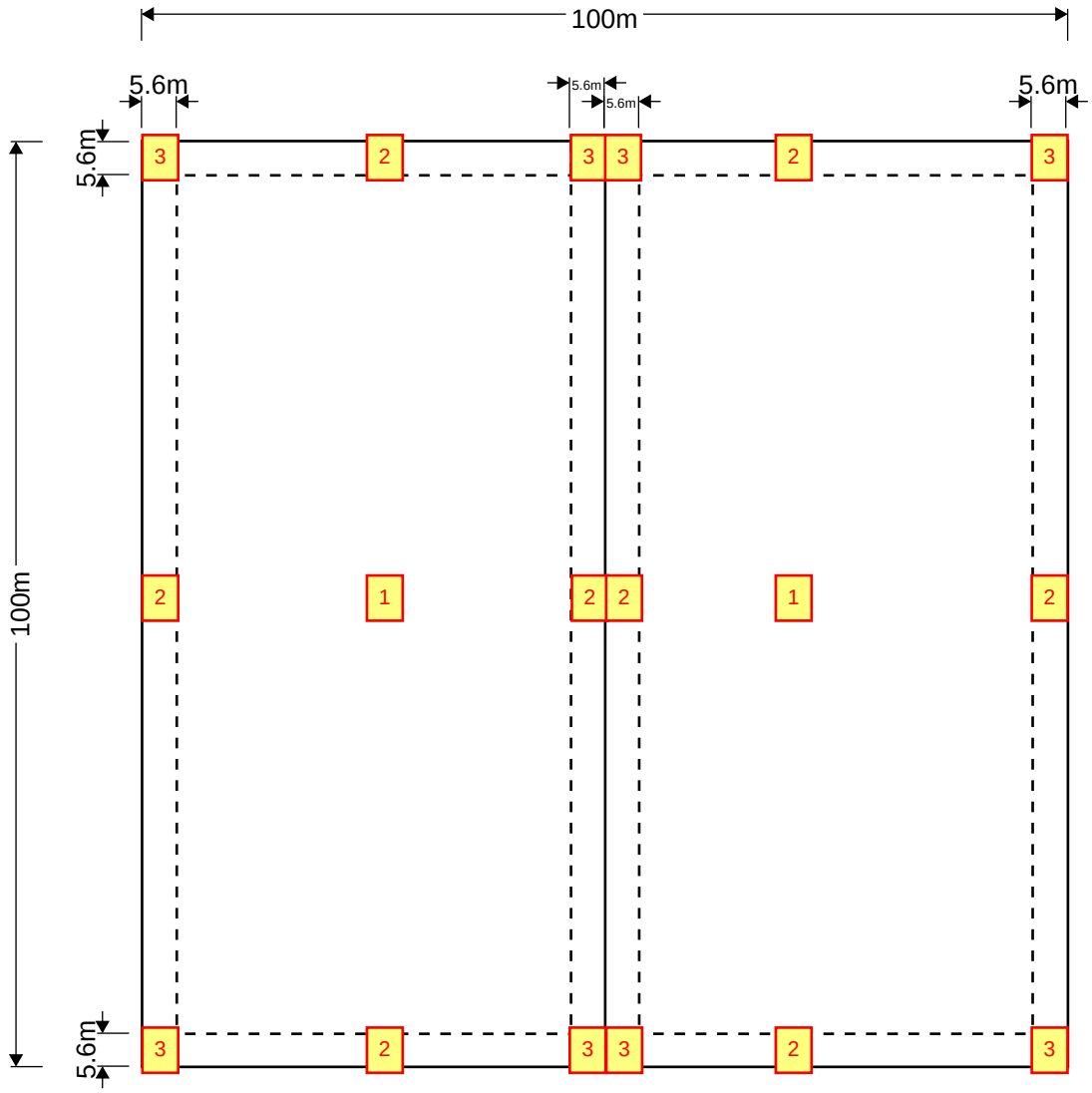

APPENDIX B

Model 1 Outputs

MODEL 1 - 0° SCALED RESIDUALS AND LIFT COEFFICIENT GRAPHS

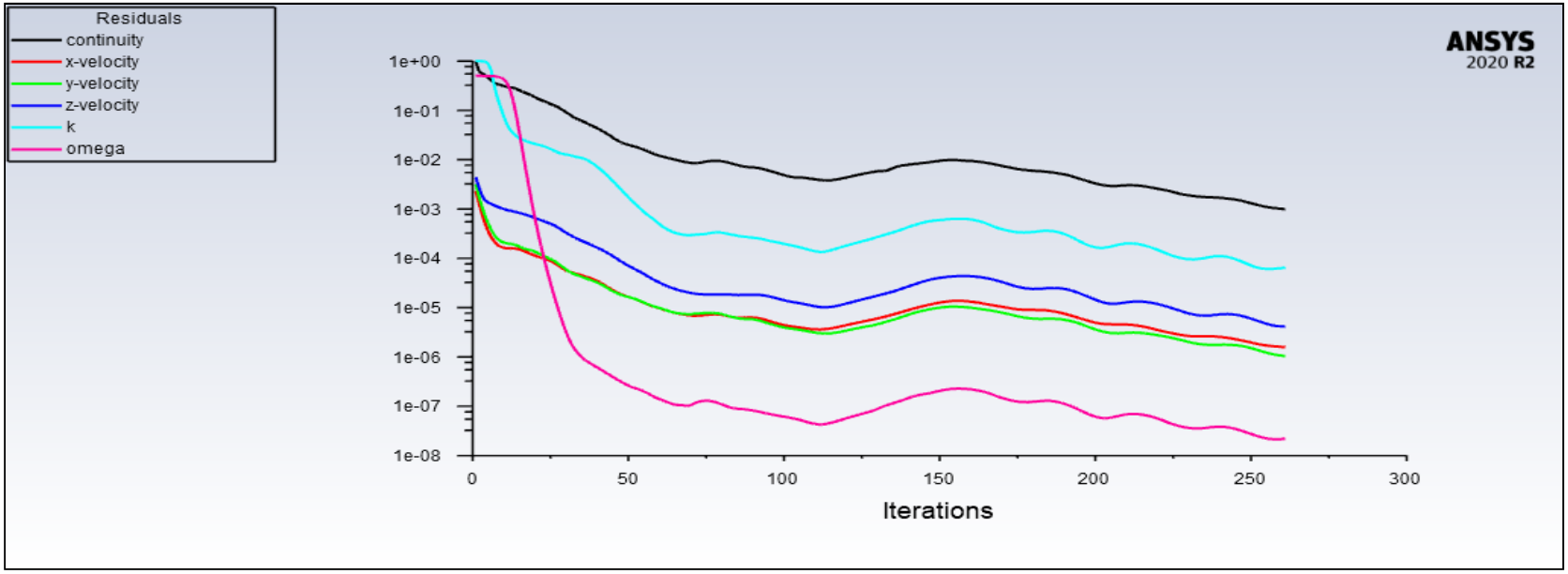

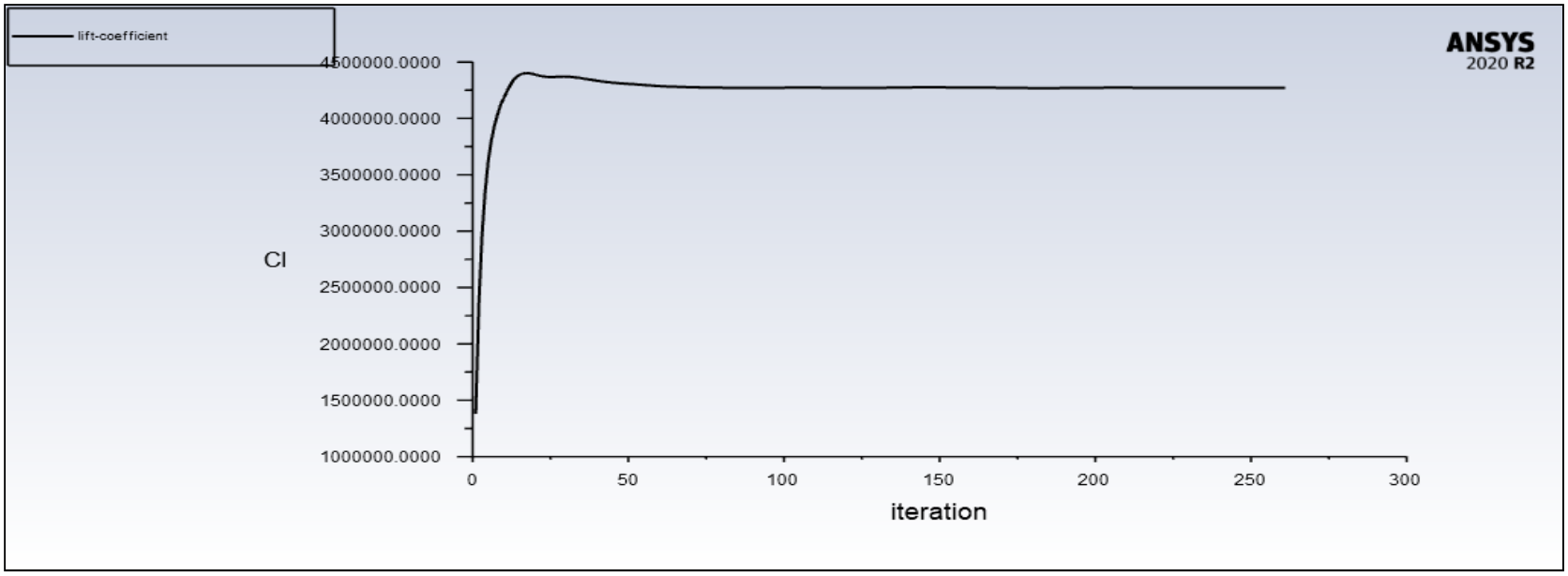

MODEL 1 - 0° PRESSURE COEFFICIENTS

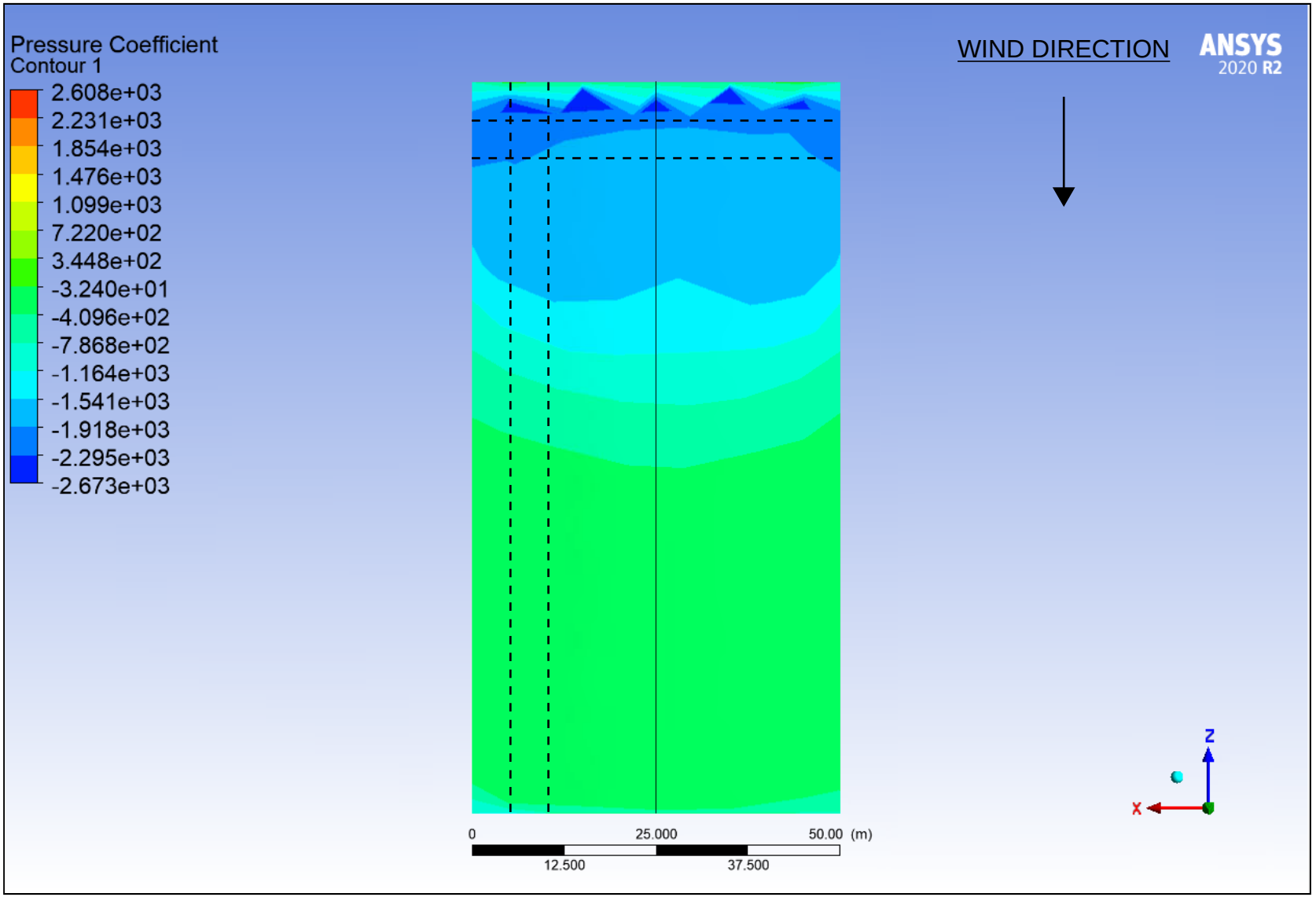

MODEL 1 - 30° SCALED RESIDUALS AND LIFT COEFFICIENT GRAPHS

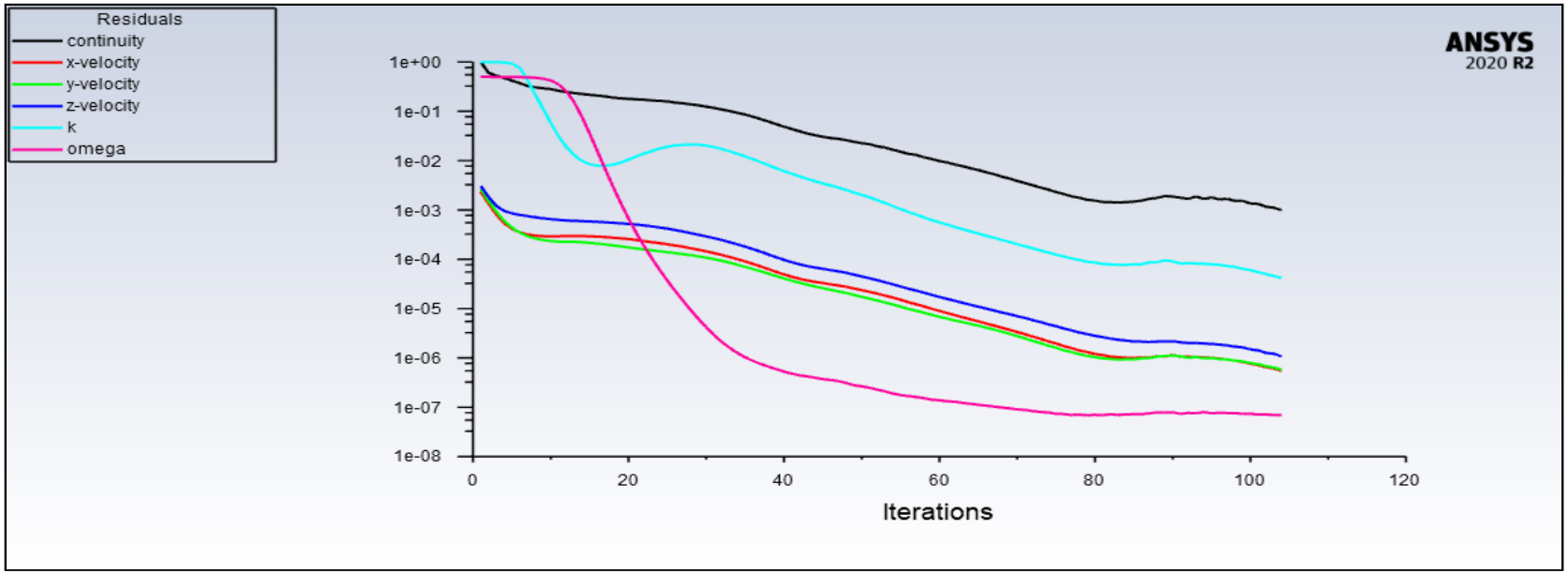

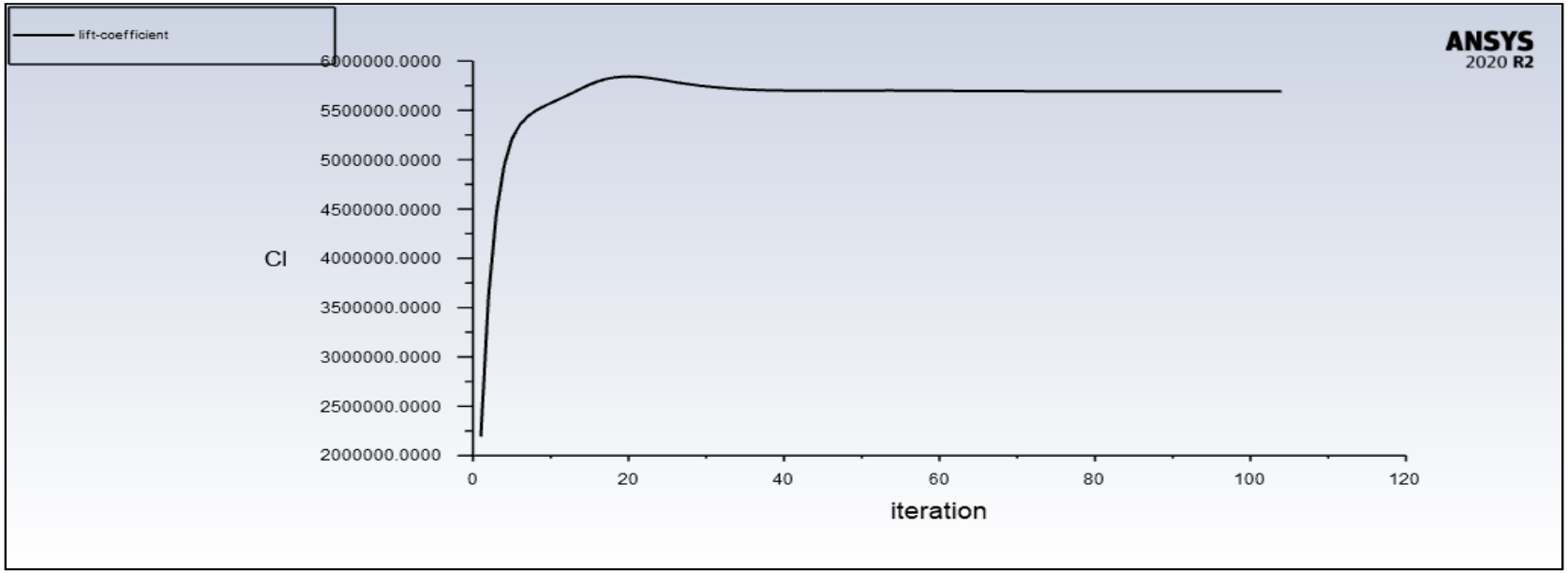

MODEL 1 - 30° PRESSURE COEFFICIENTS

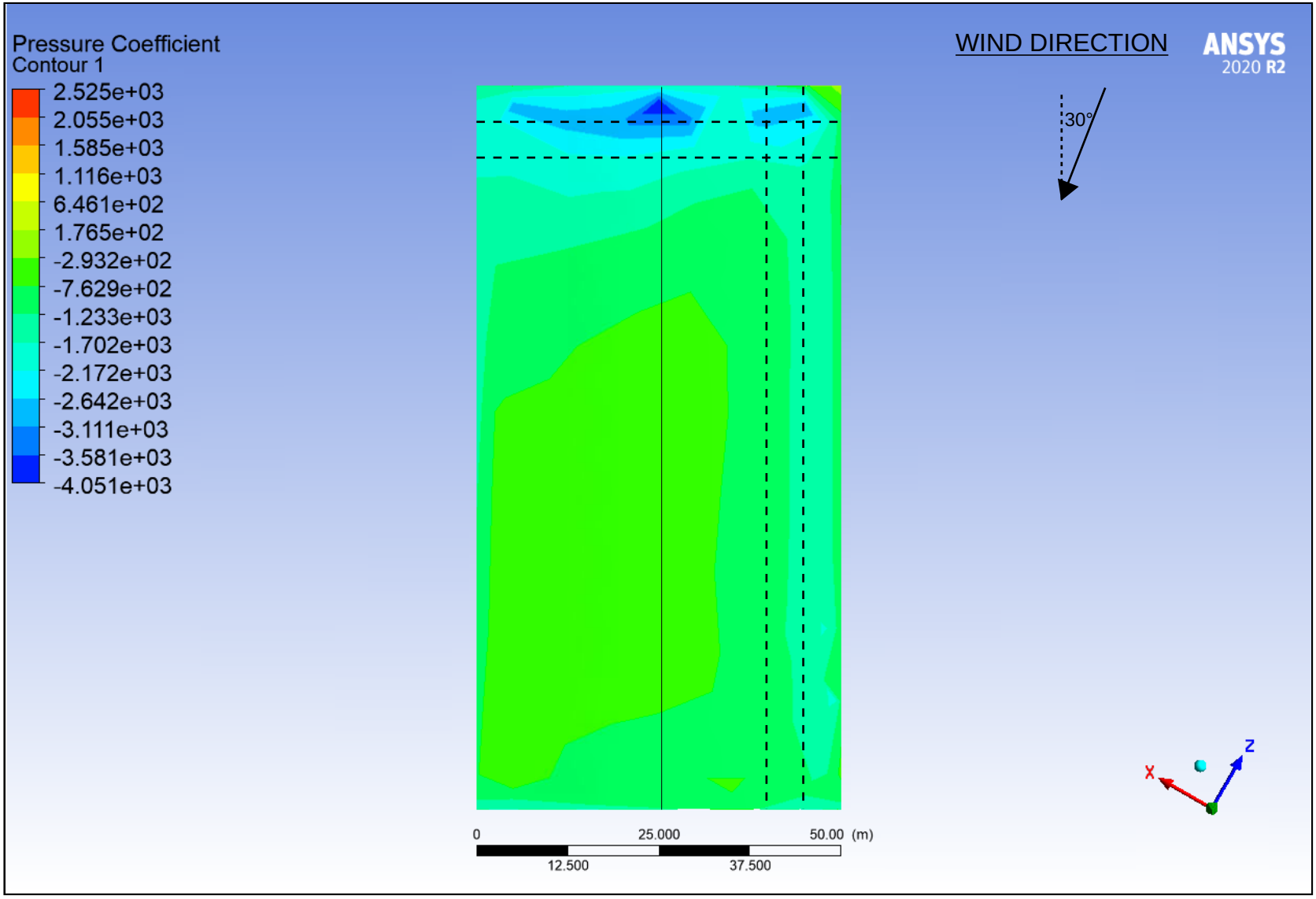

MODEL 1 - 45° SCALED RESIDUALS AND LIFT COEFFICIENT GRAPHS

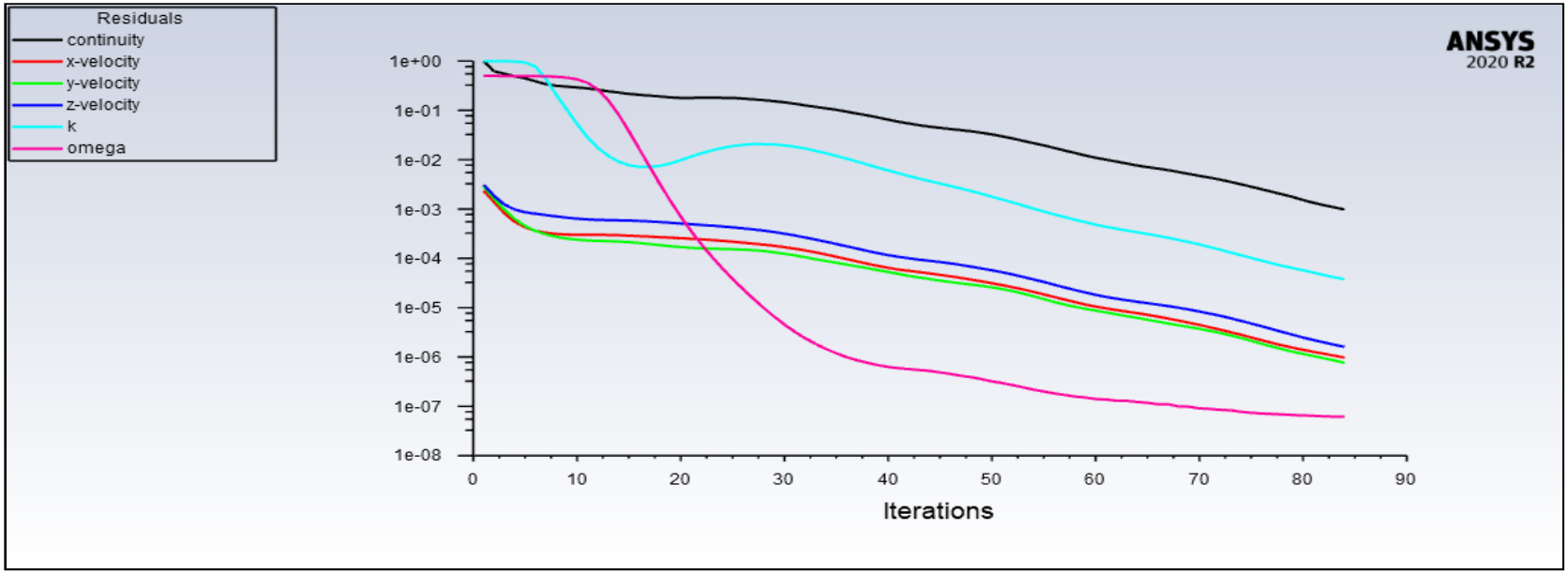

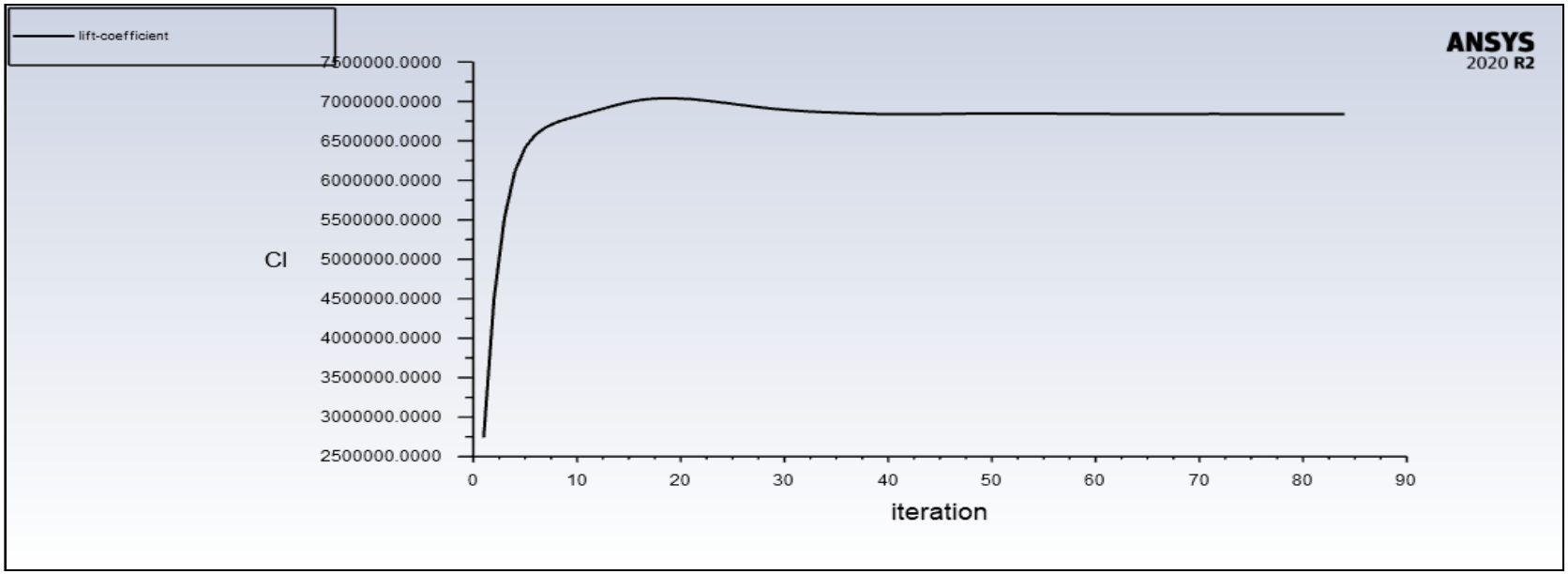

MODEL 1 - 45° PRESSURE COEFFICIENTS

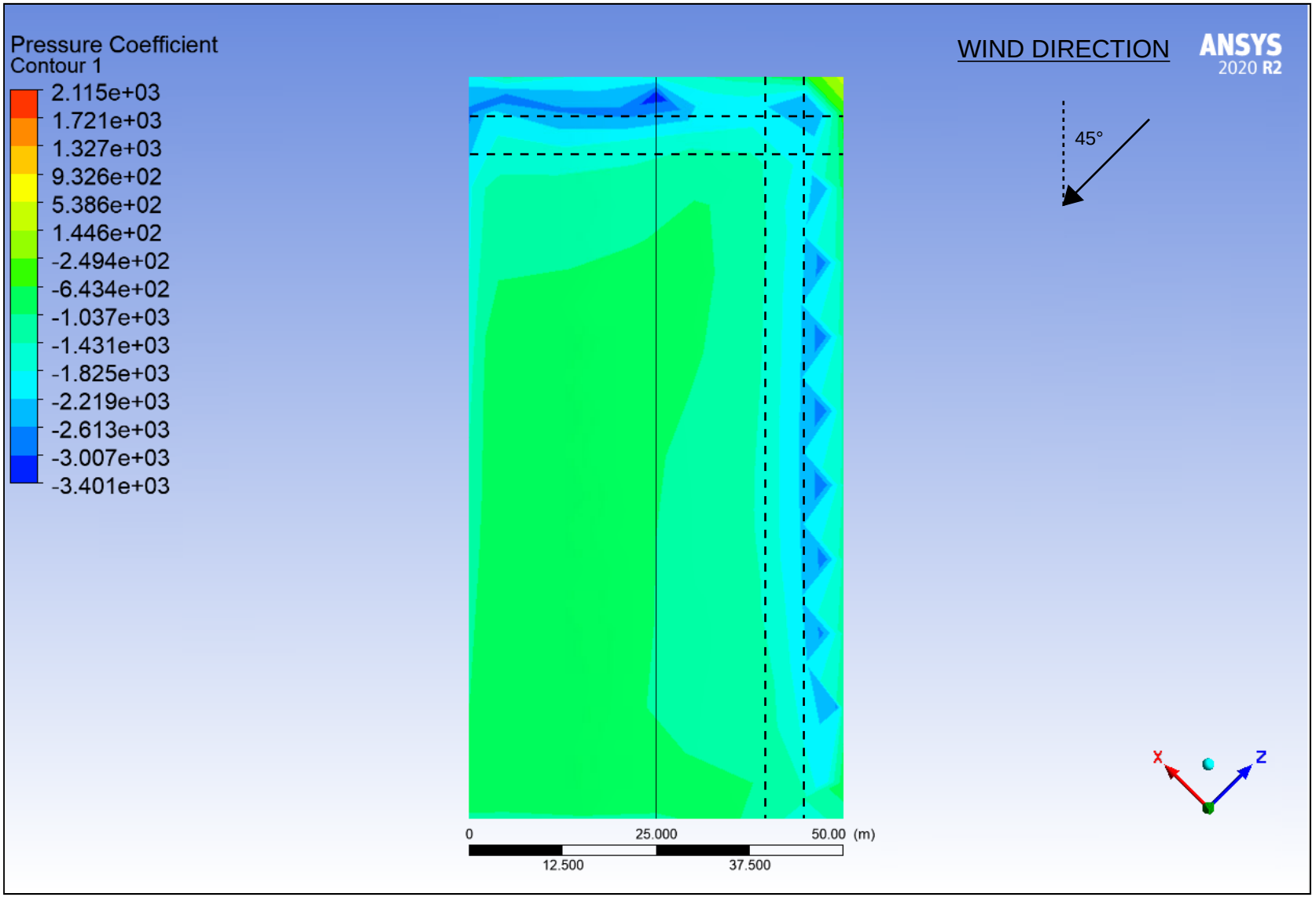

MODEL 1 - 60° SCALED RESIDUALS AND LIFT COEFFICIENT GRAPHS

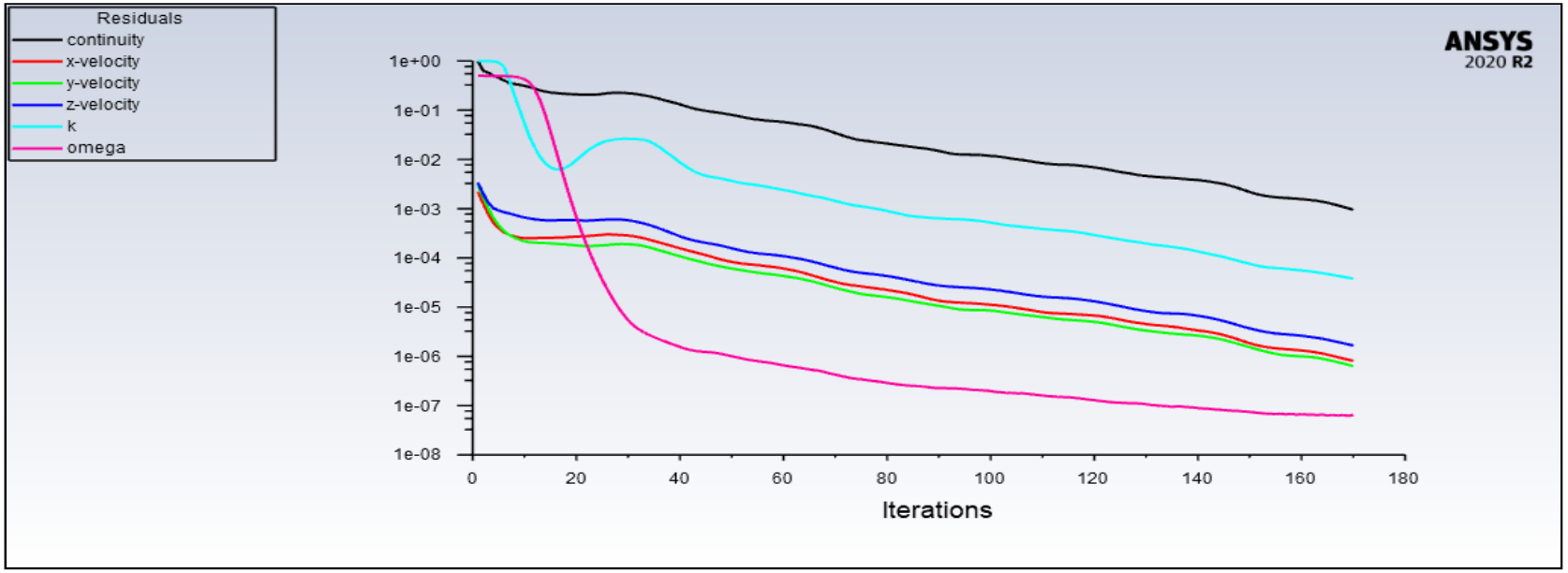

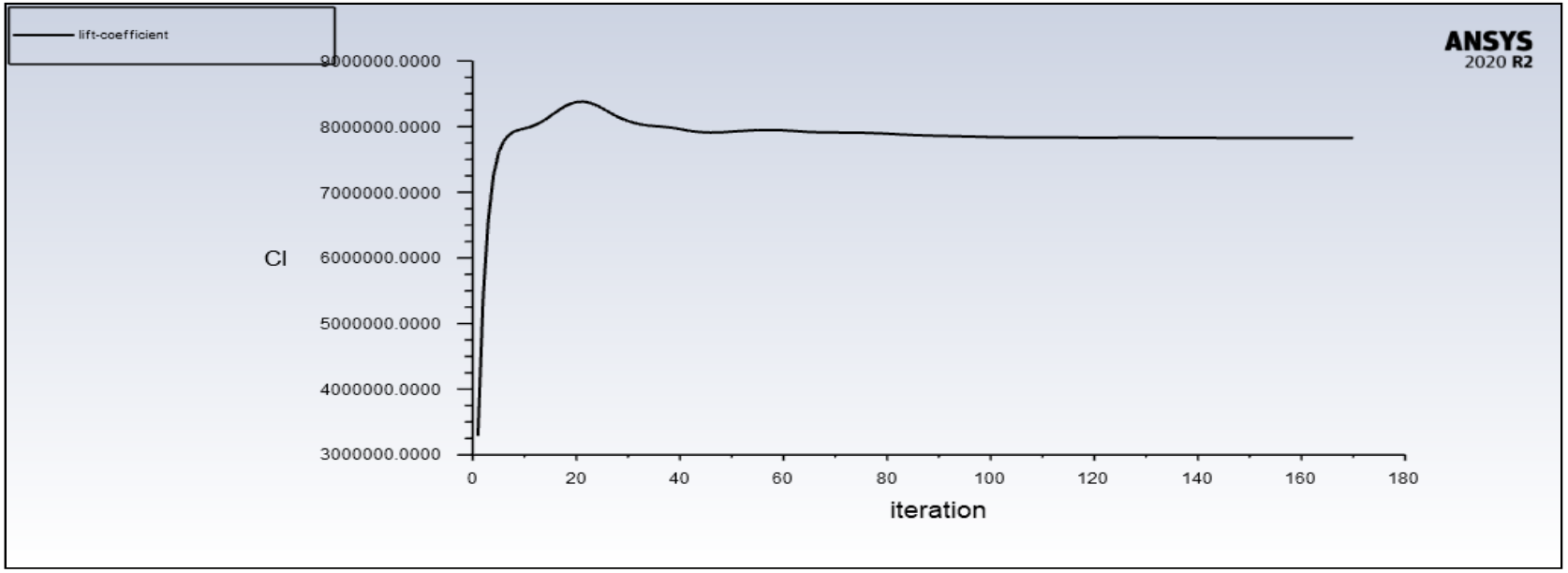

MODEL 1 - 60° PRESSURE COEFFICIENTS

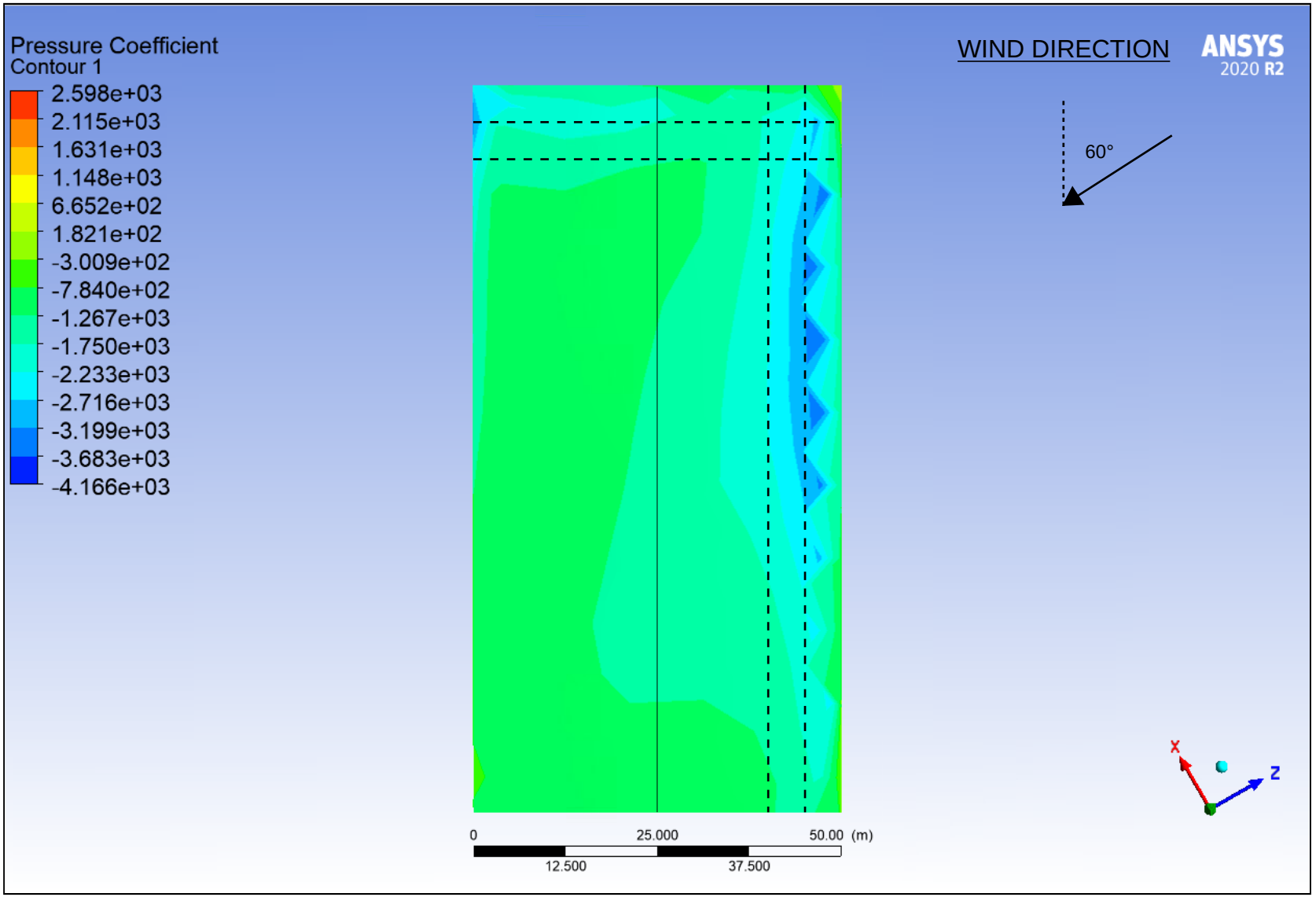

MODEL 1 - 90° SCALED RESIDUALS AND LIFT COEFFICIENT GRAPHS

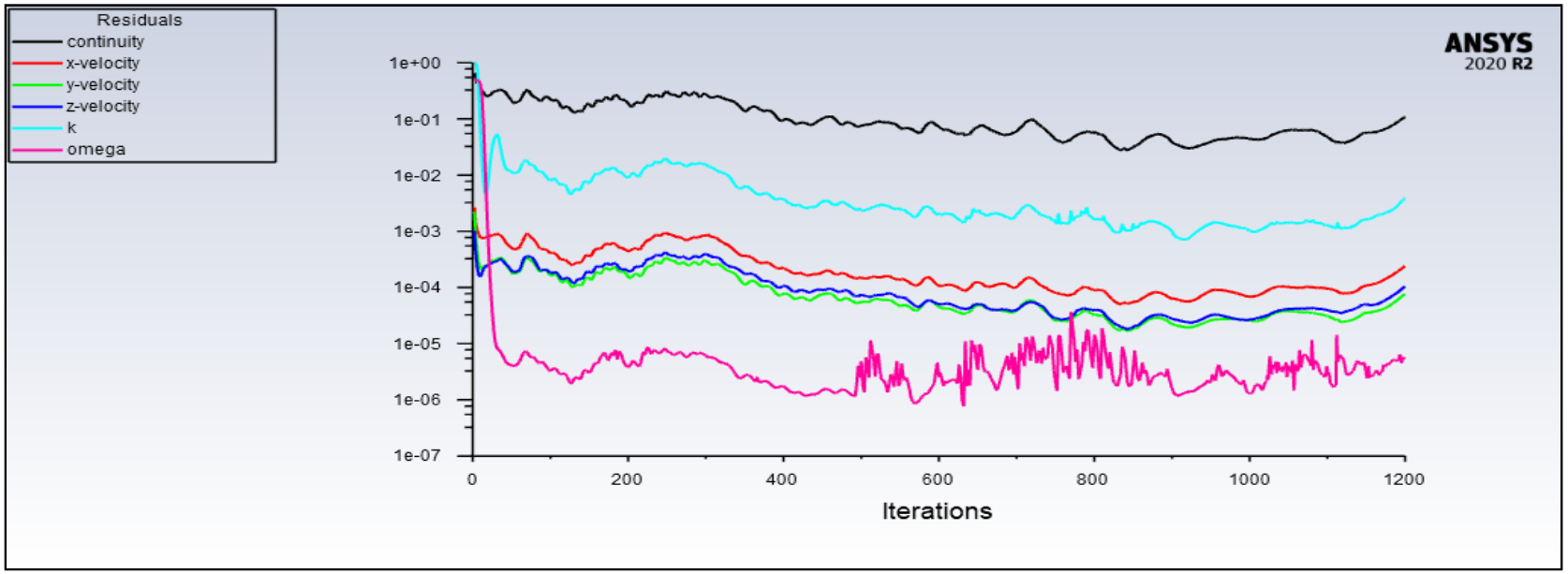

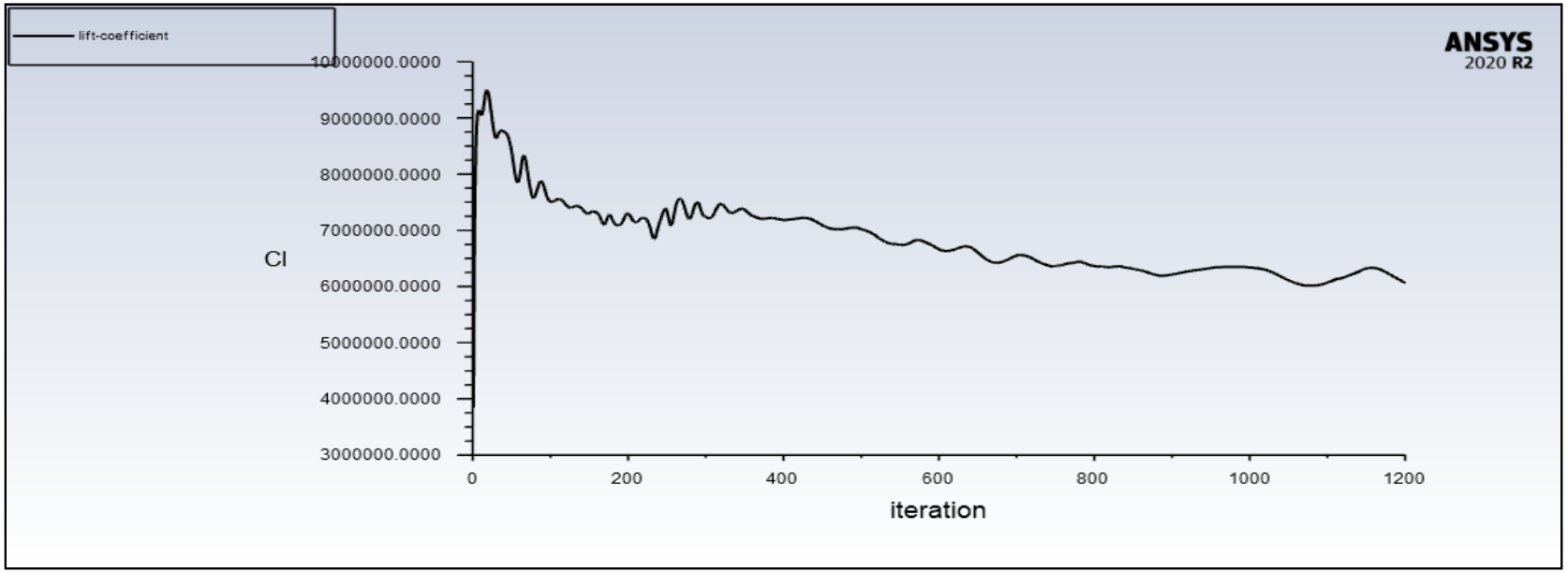

MODEL 1 - 90° PRESSURE COEFFICIENTS

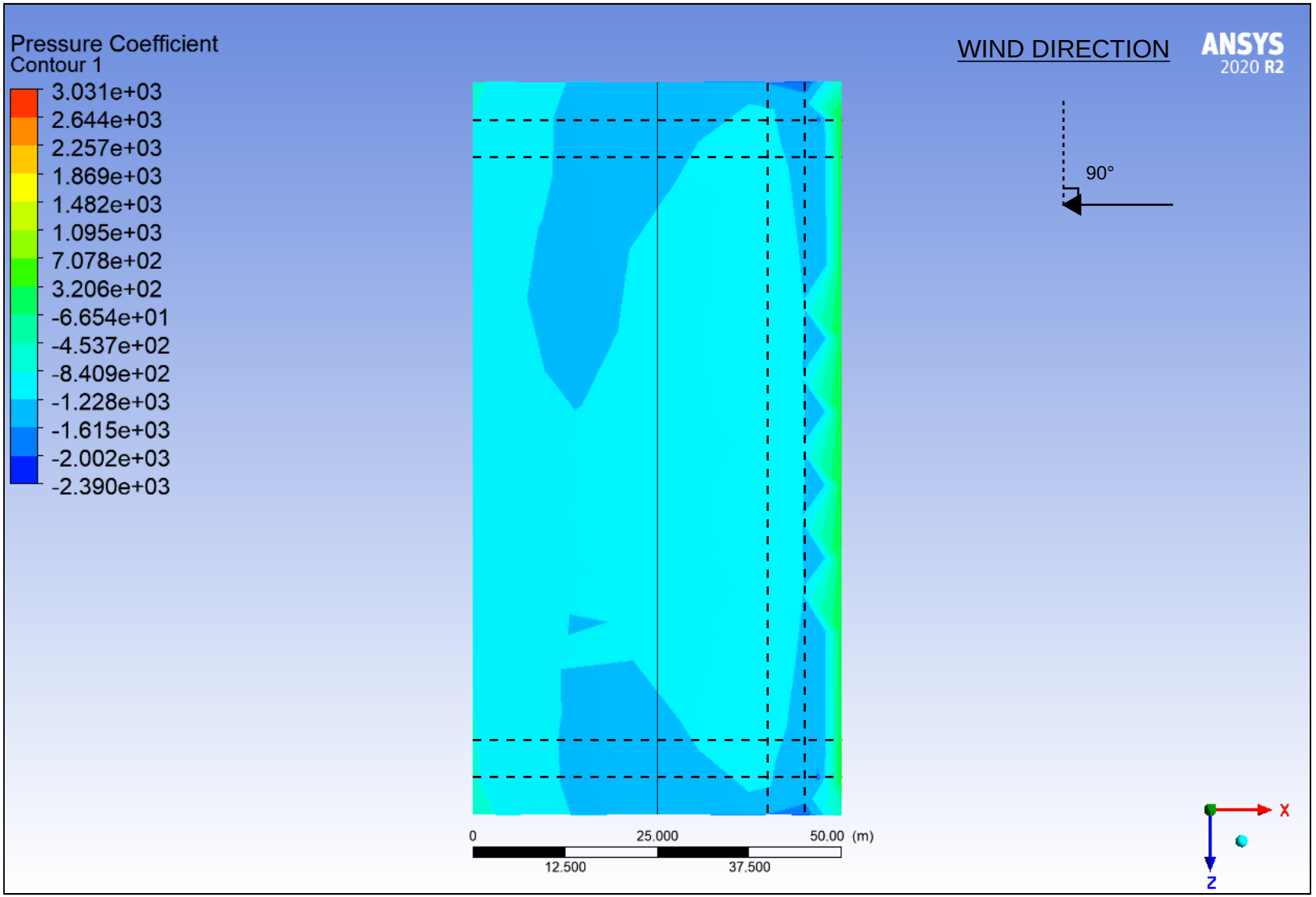

Model 2 Outputs

MODEL 2 - 0° SCALED RESIDUALS AND LIFT COEFFICIENT GRAPHS

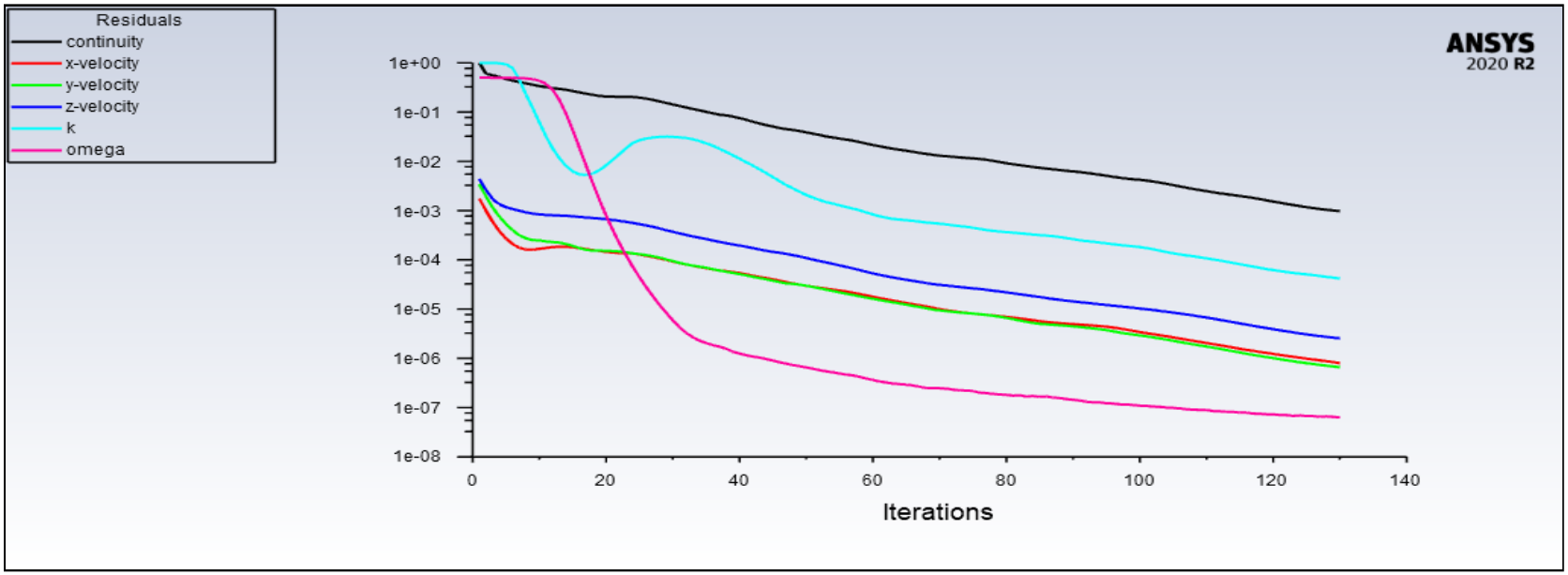

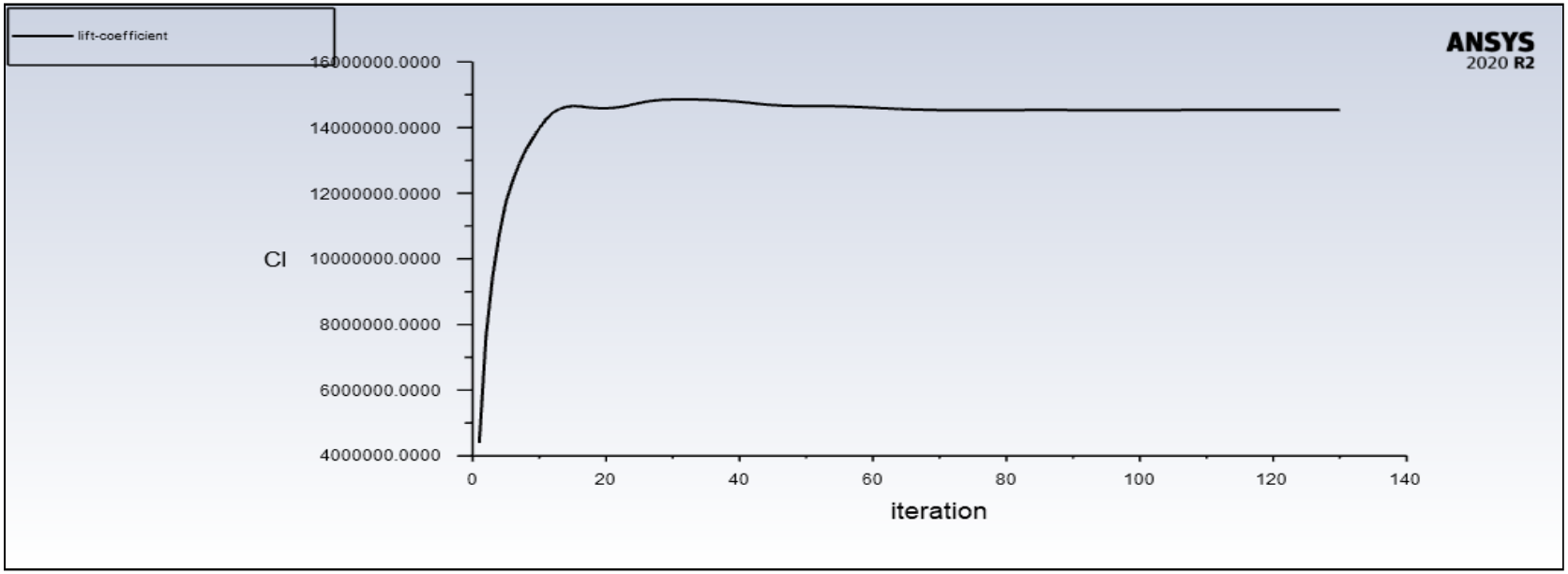

MODEL 2 - 0° PRESSURE COEFFICIENTS

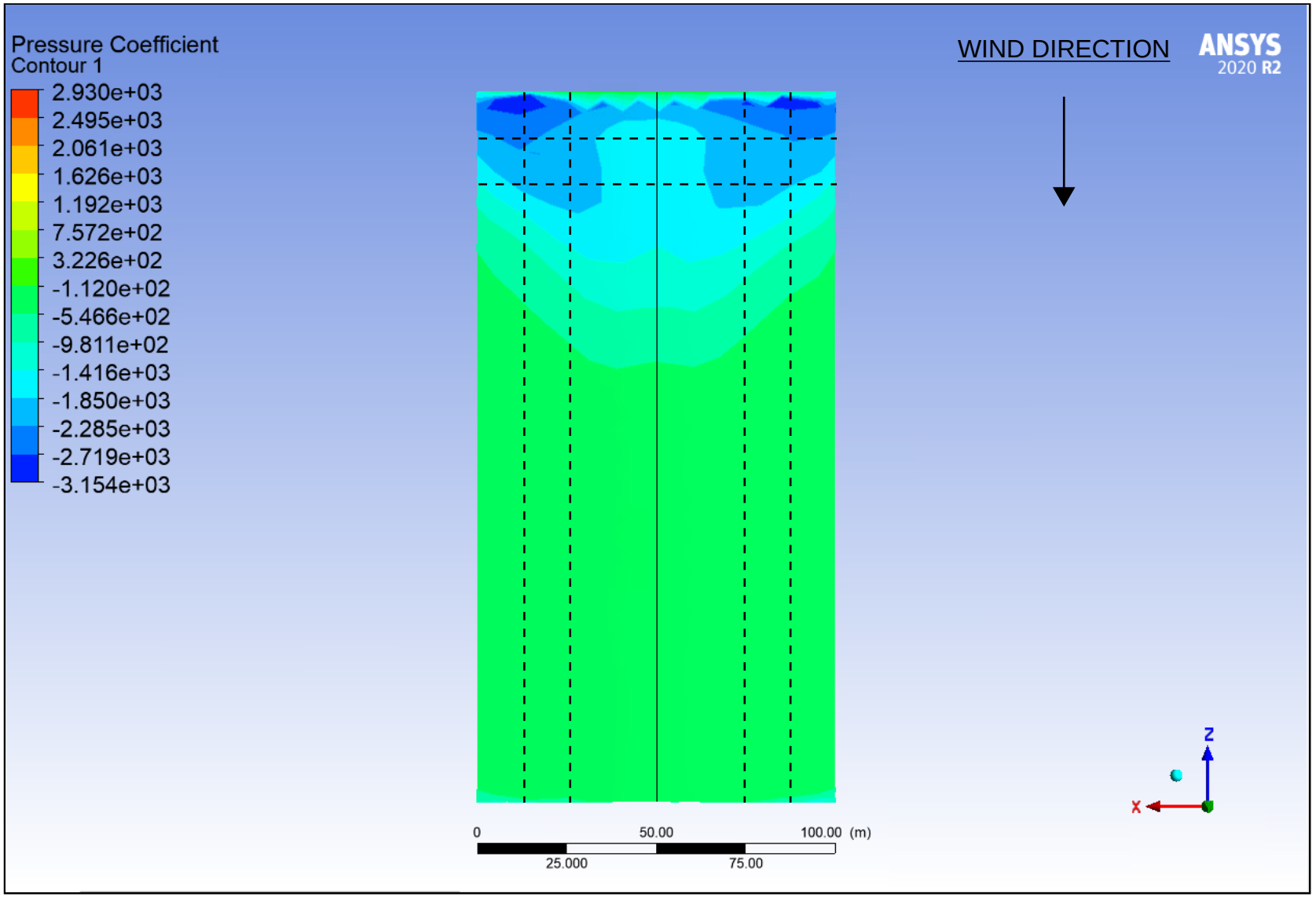

MODEL 2 - 30° SCALED RESIDUALS AND LIFT COEFFICIENT GRAPHS

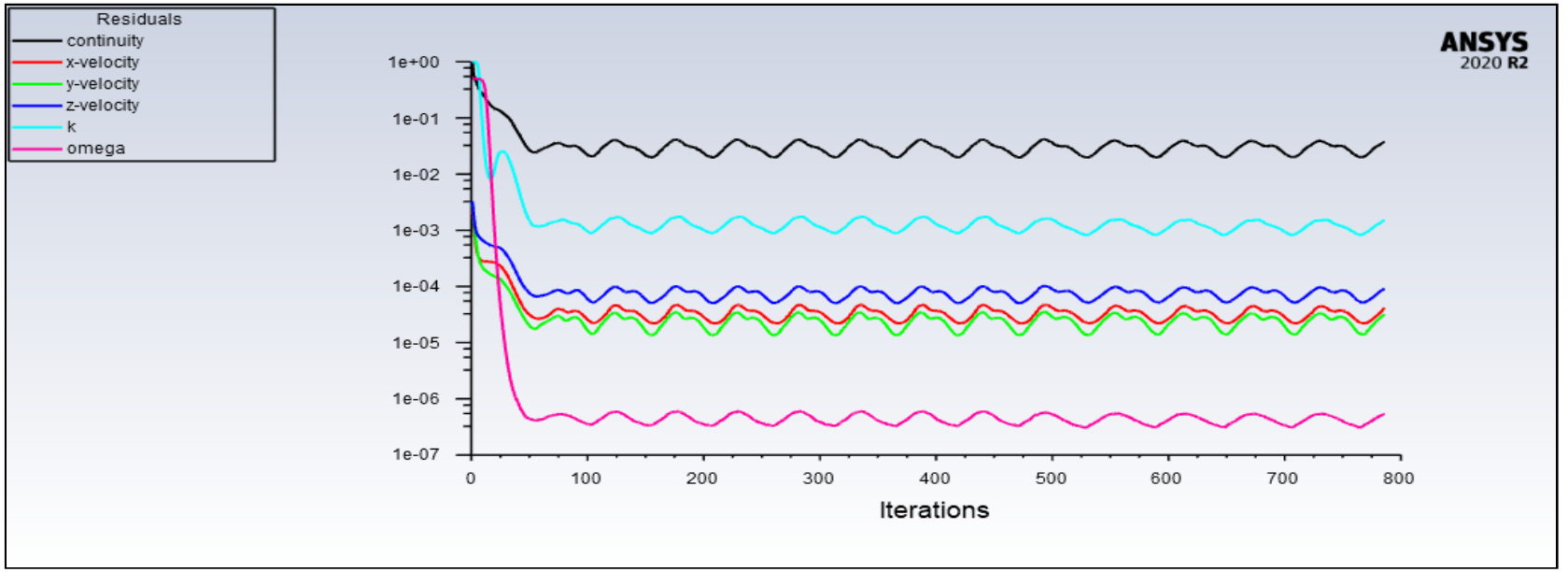

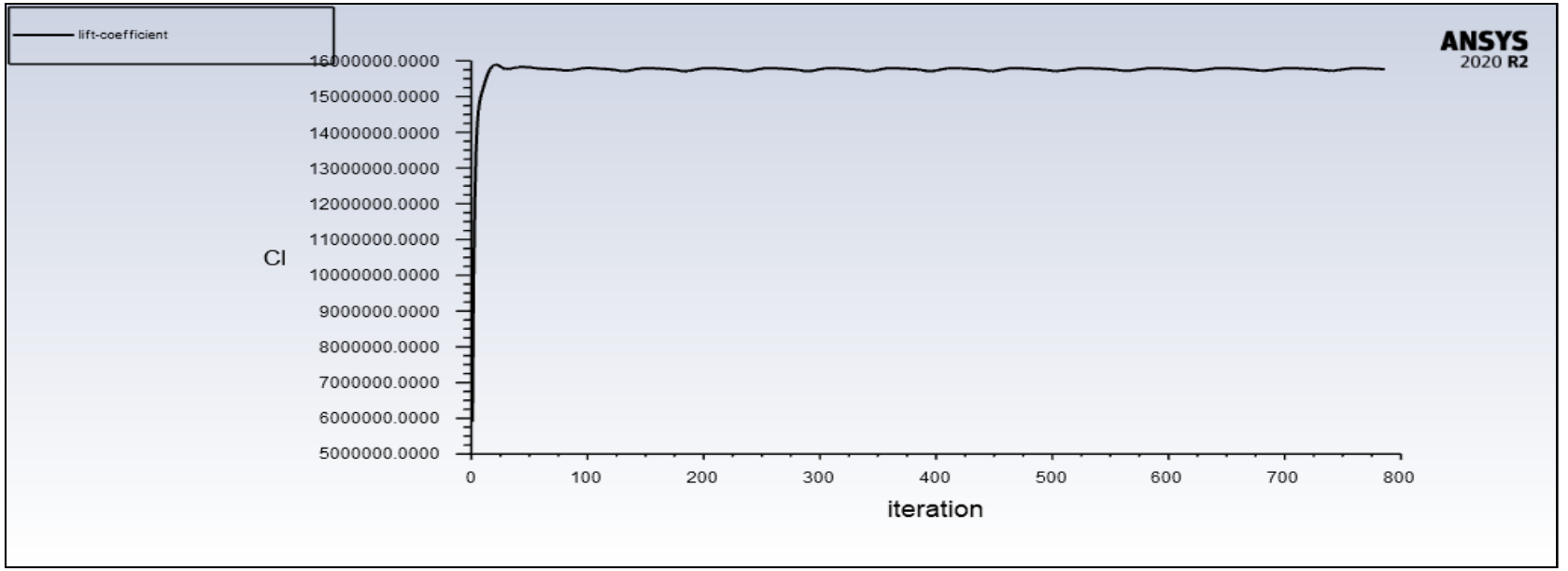

MODEL 2 - 30° PRESSURE COEFFICIENTS

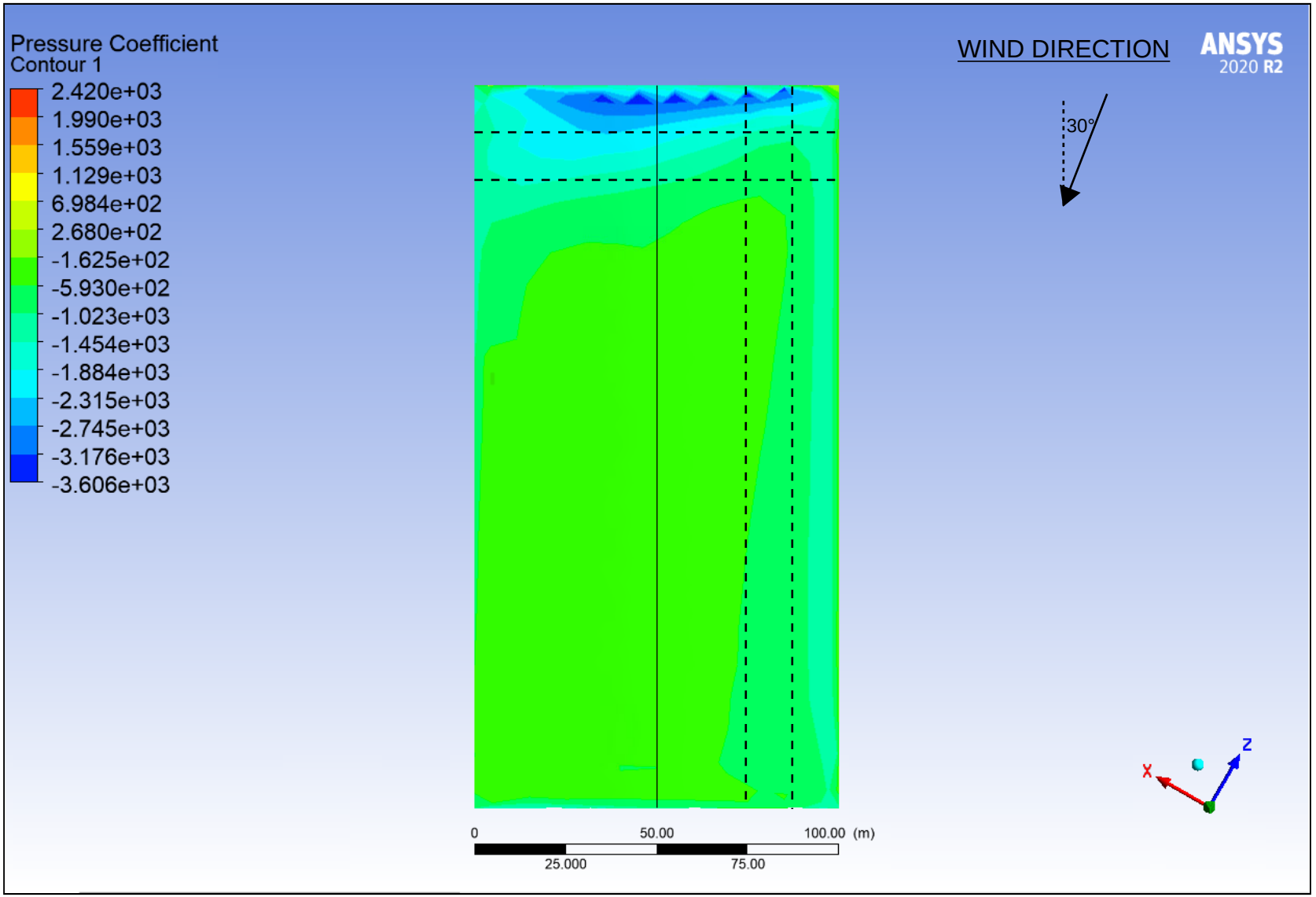

MODEL 2 - 45° SCALED RESIDUALS AND LIFT COEFFICIENT GRAPHS

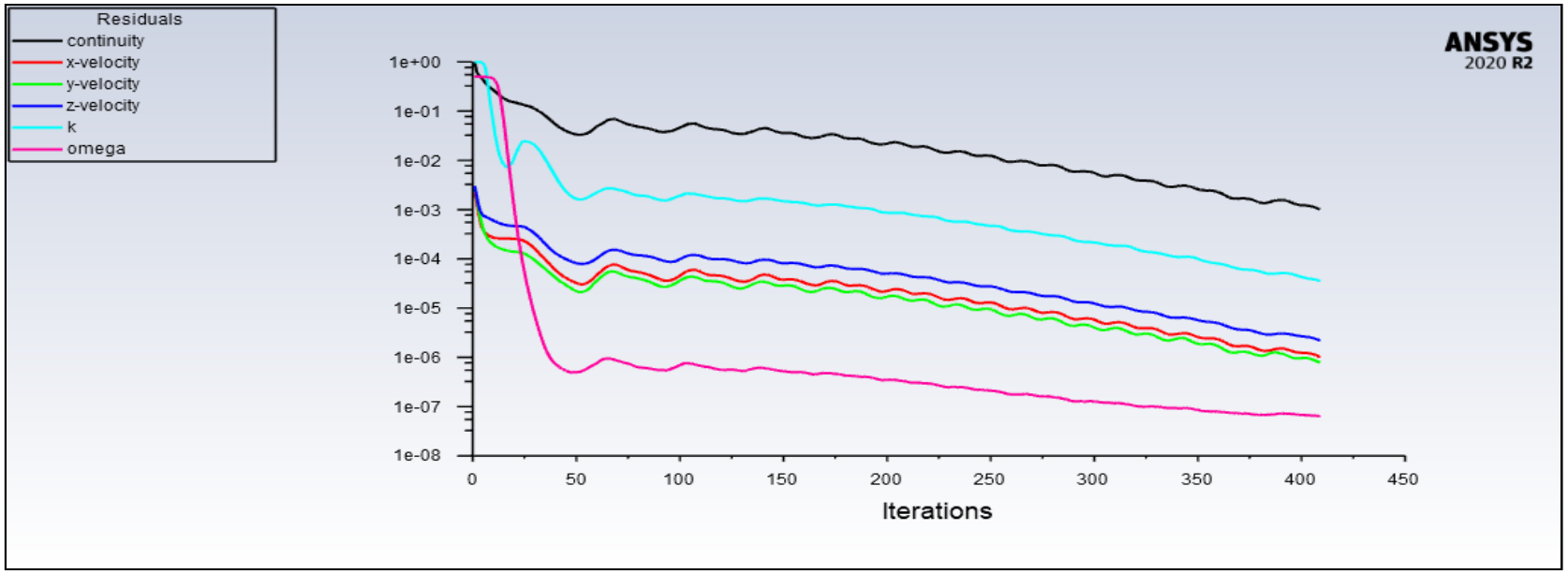

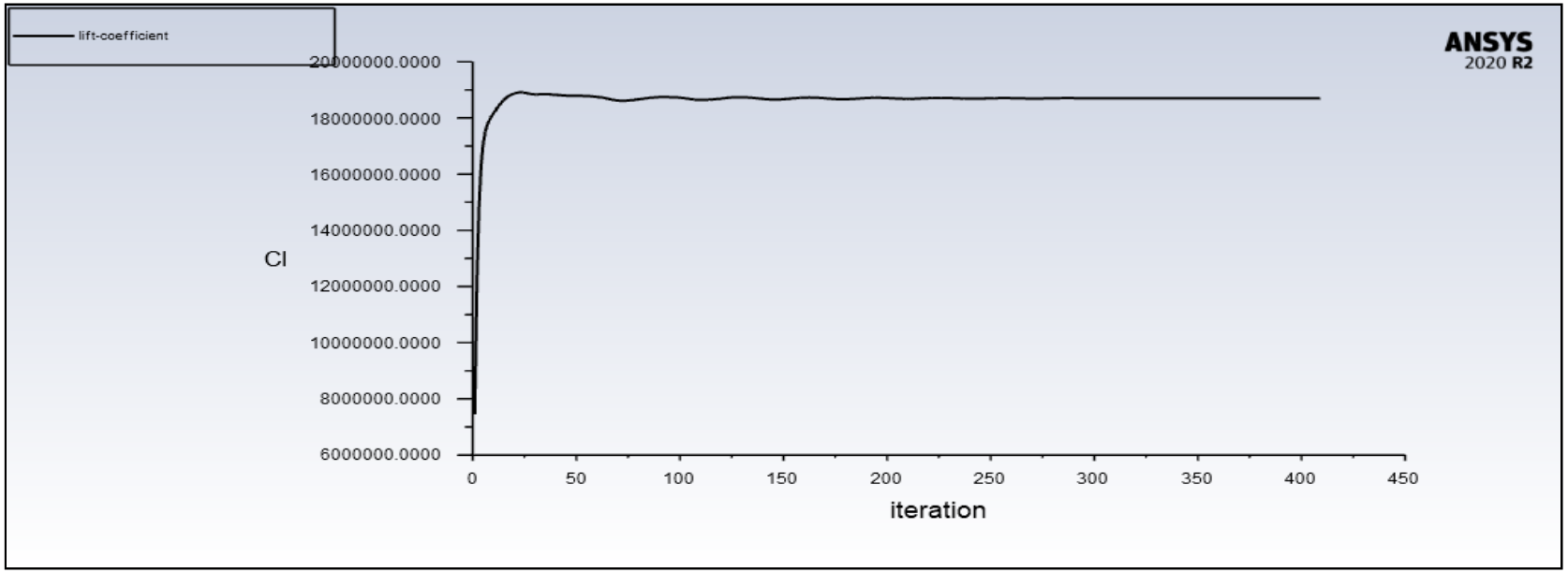

MODEL 2 - 45° PRESSURE COEFFICIENTS

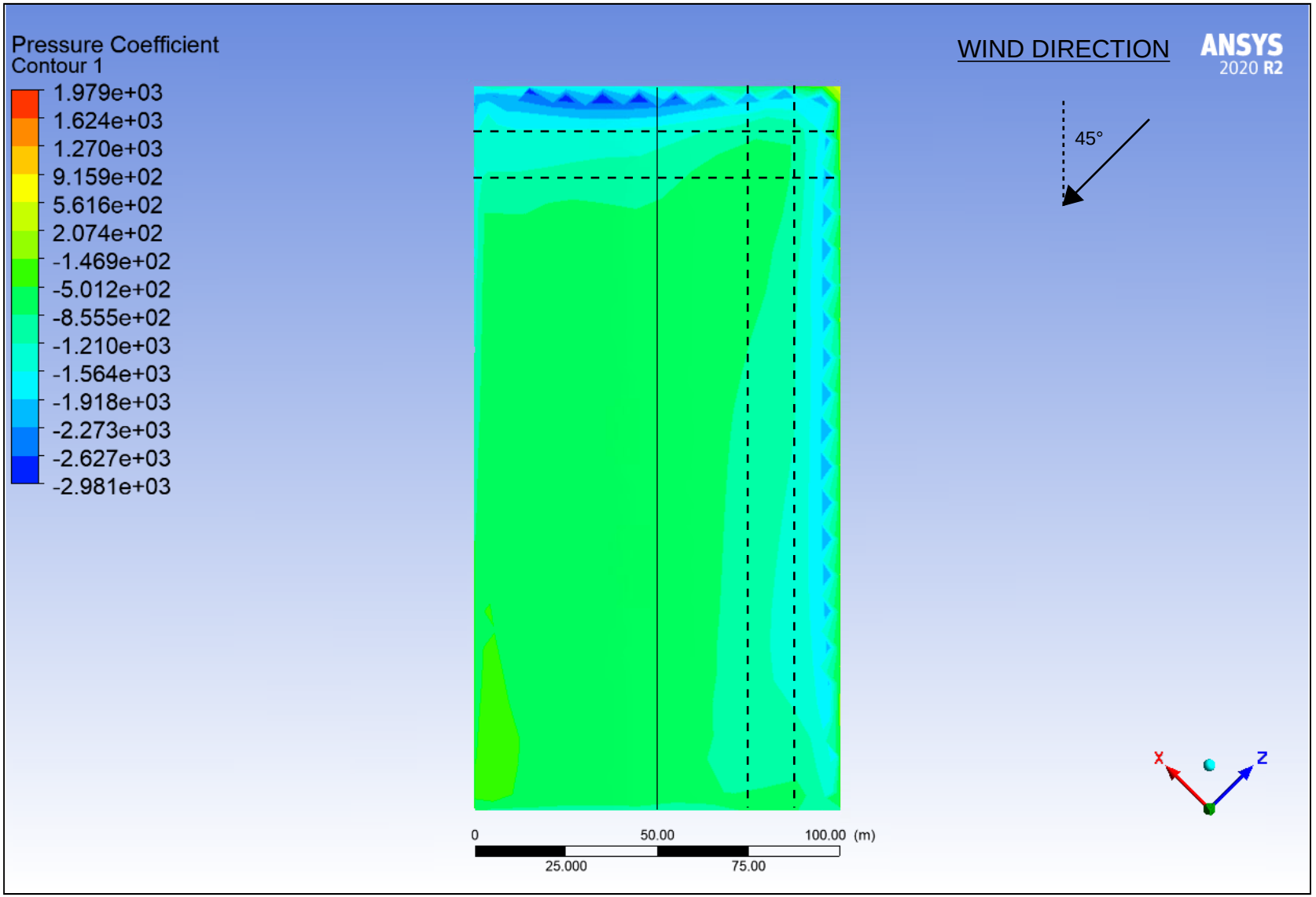

MODEL 2 - 60° SCALED RESIDUALS AND LIFT COEFFICIENT GRAPHS

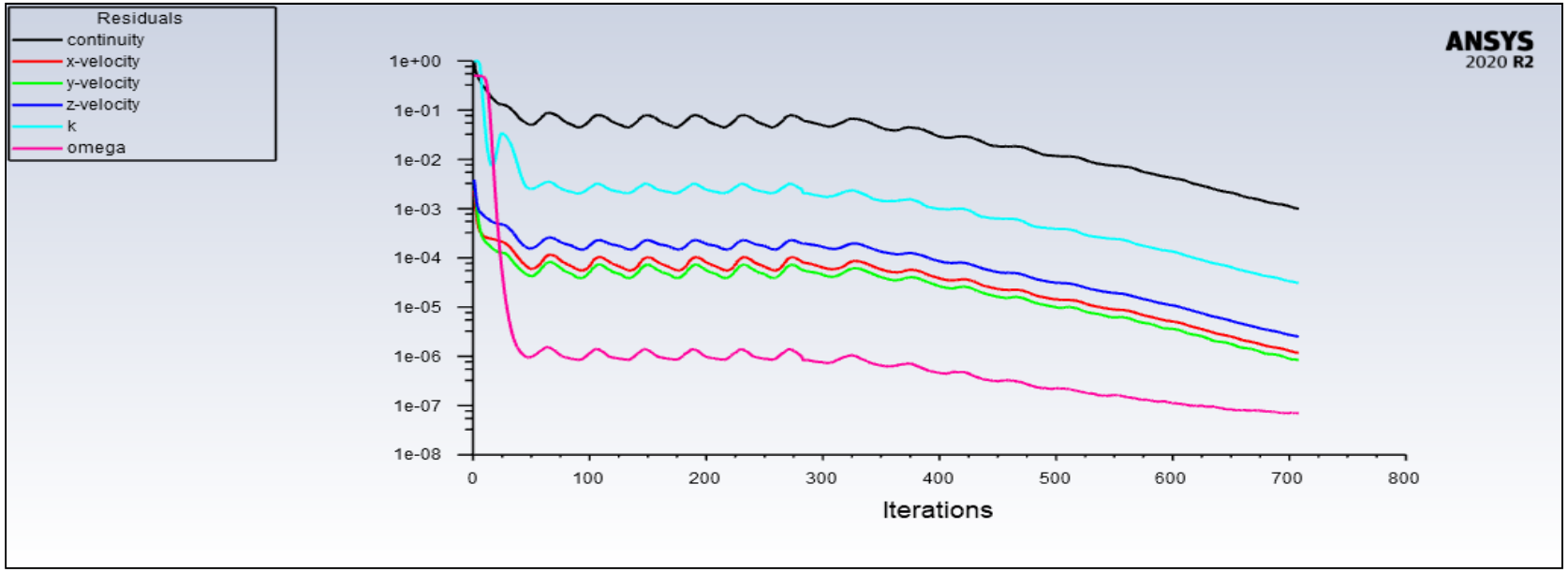

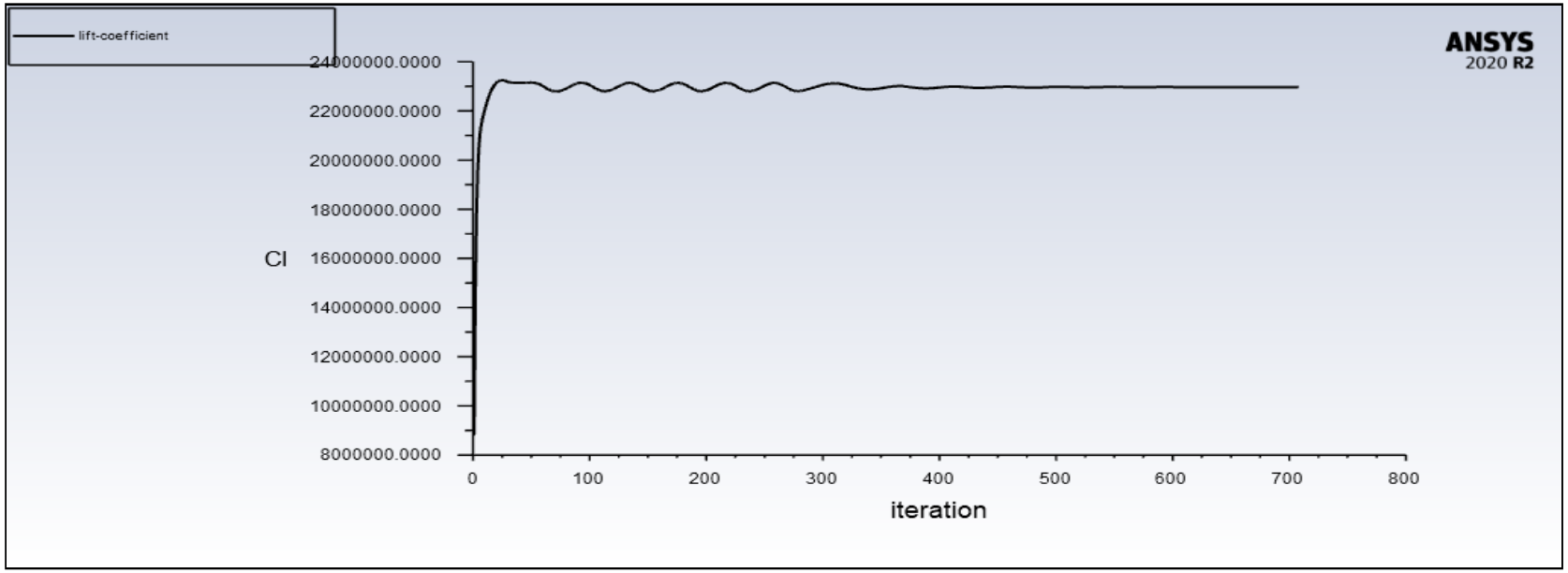

MODEL 2 - 60° PRESSURE COEFFICIENTS

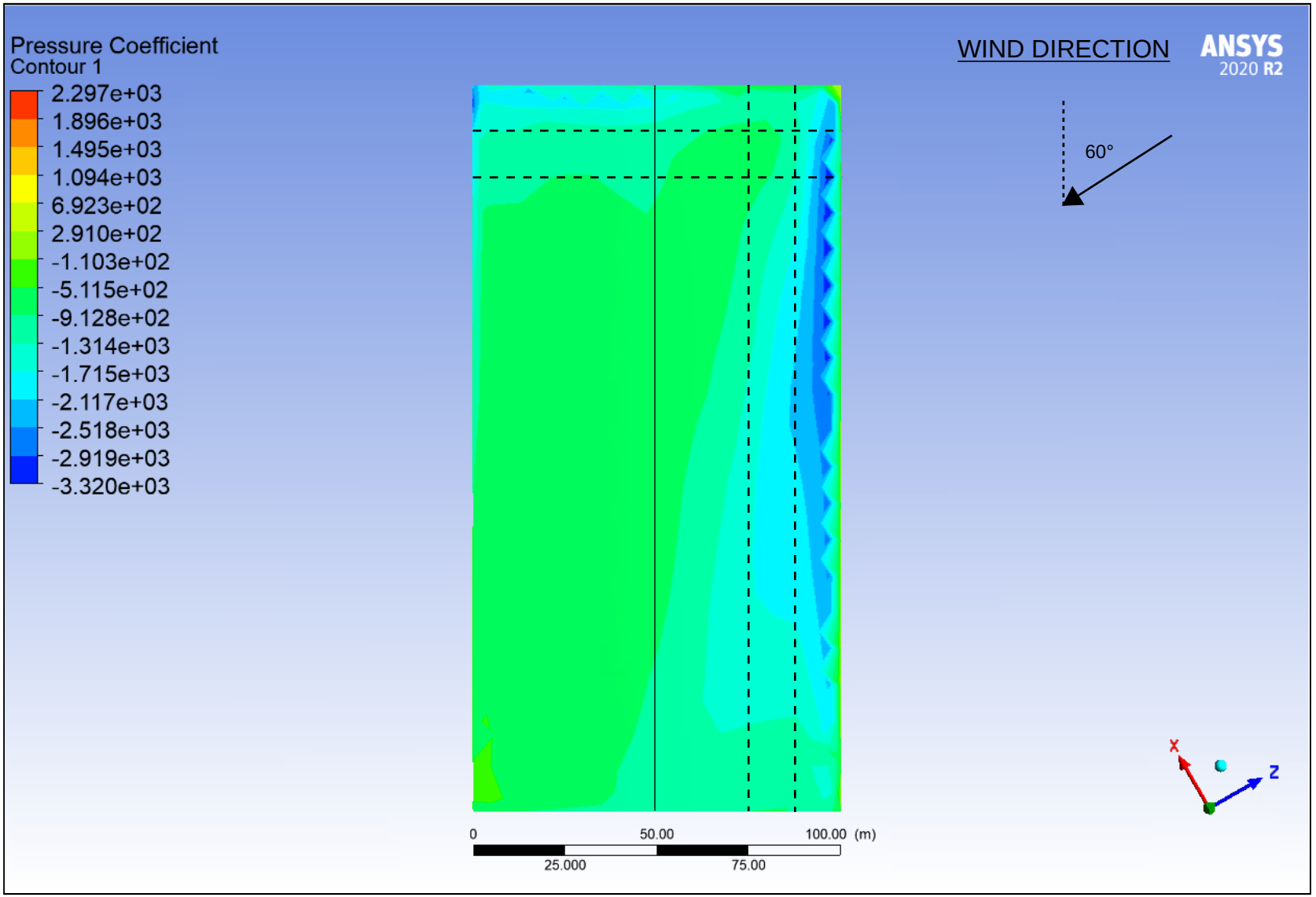

MODEL 2 - 90° SCALED RESIDUALS AND LIFT COEFFICIENT GRAPHS

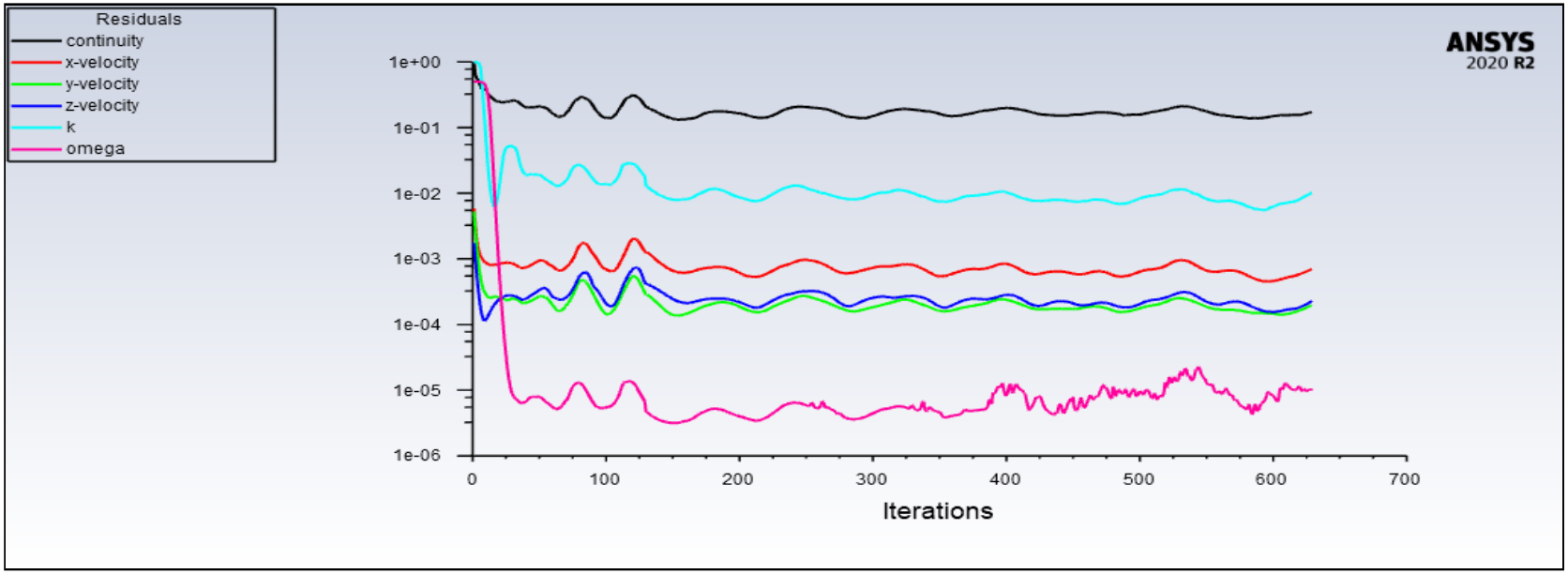

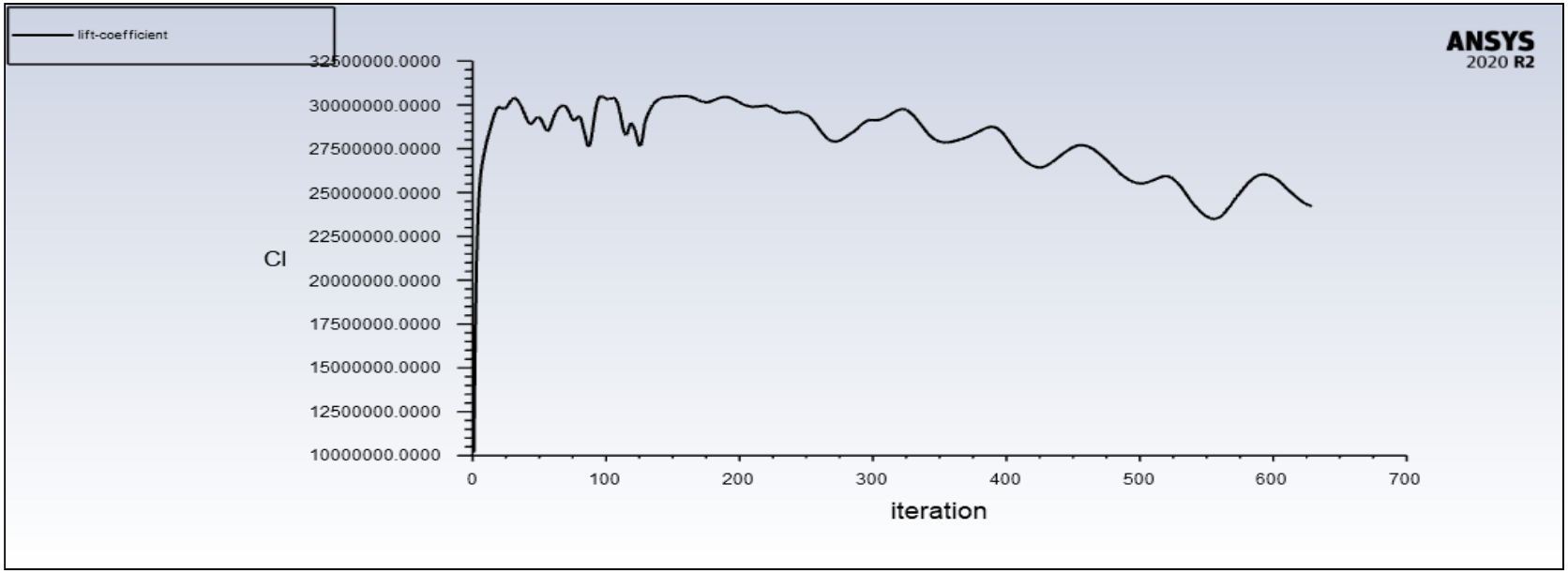

MODEL 2 - 90° PRESSURE COEFFICIENTS

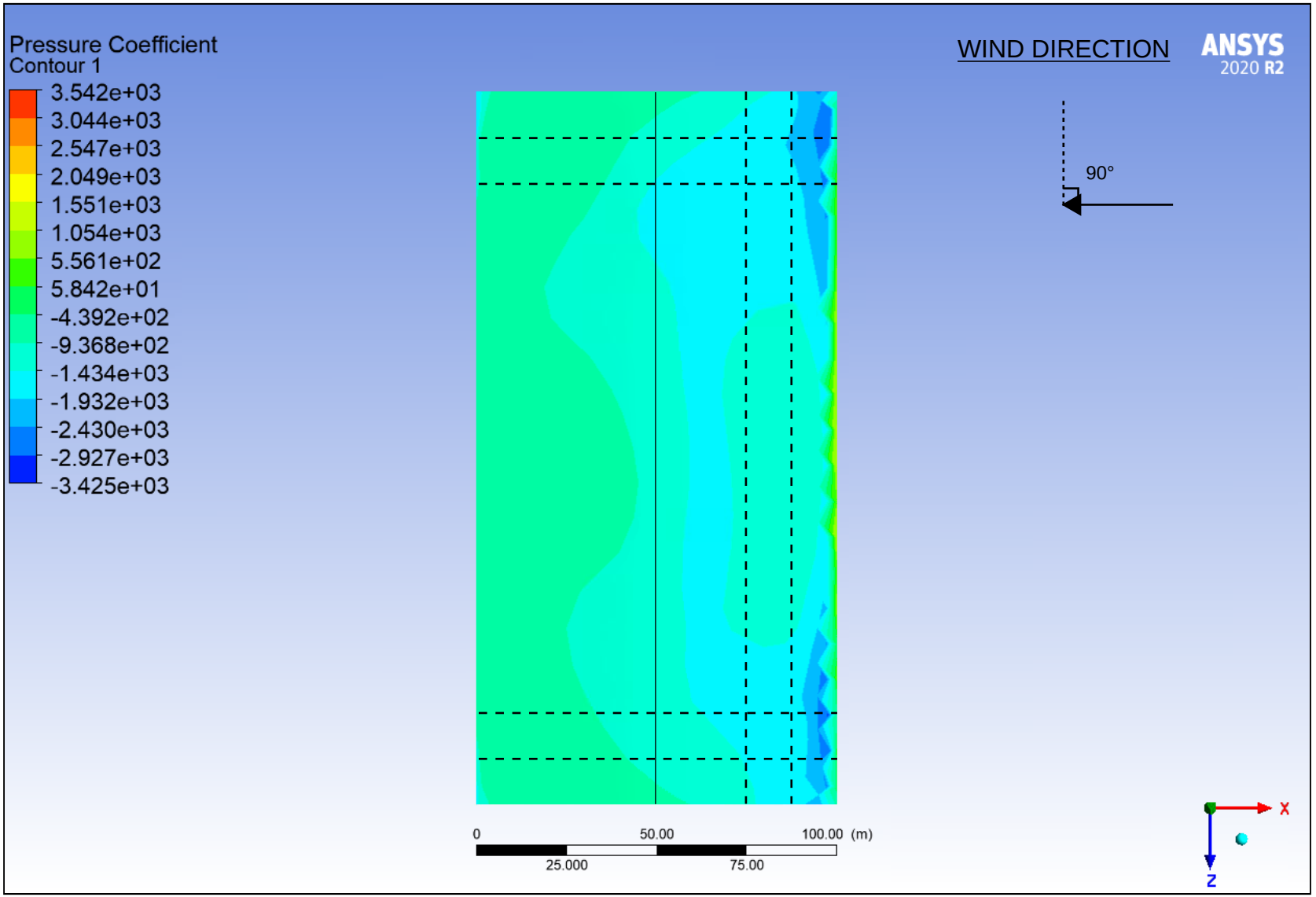

Model 3 Outputs

MODEL 3 - 0° SCALED RESIDUALS AND LIFT COEFFICIENT GRAPHS

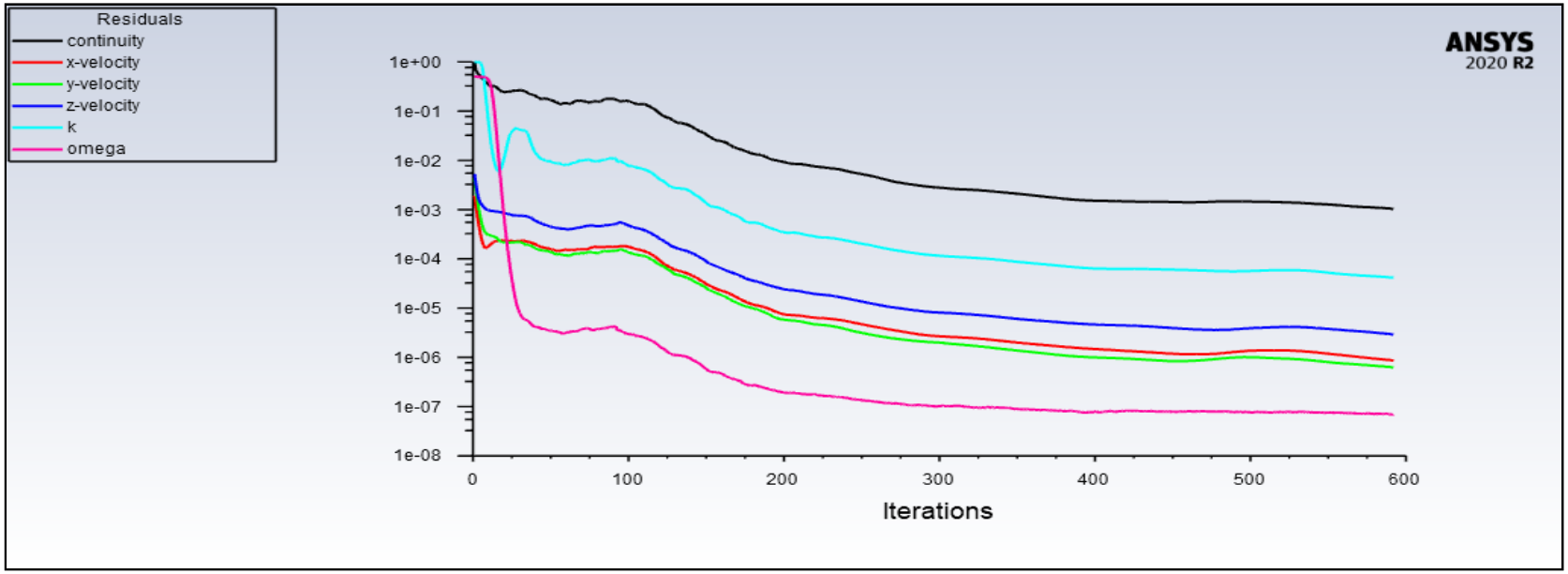

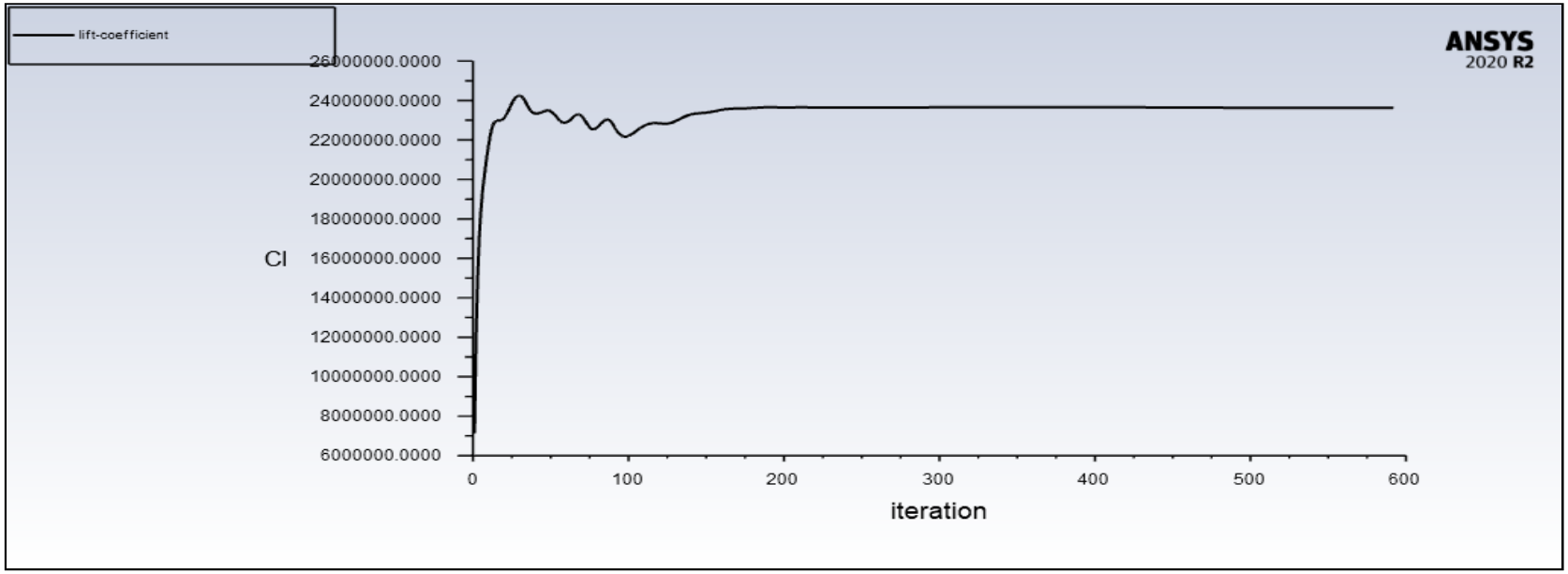

MODEL 3 - 0° PRESSURE COEFFICIENTS

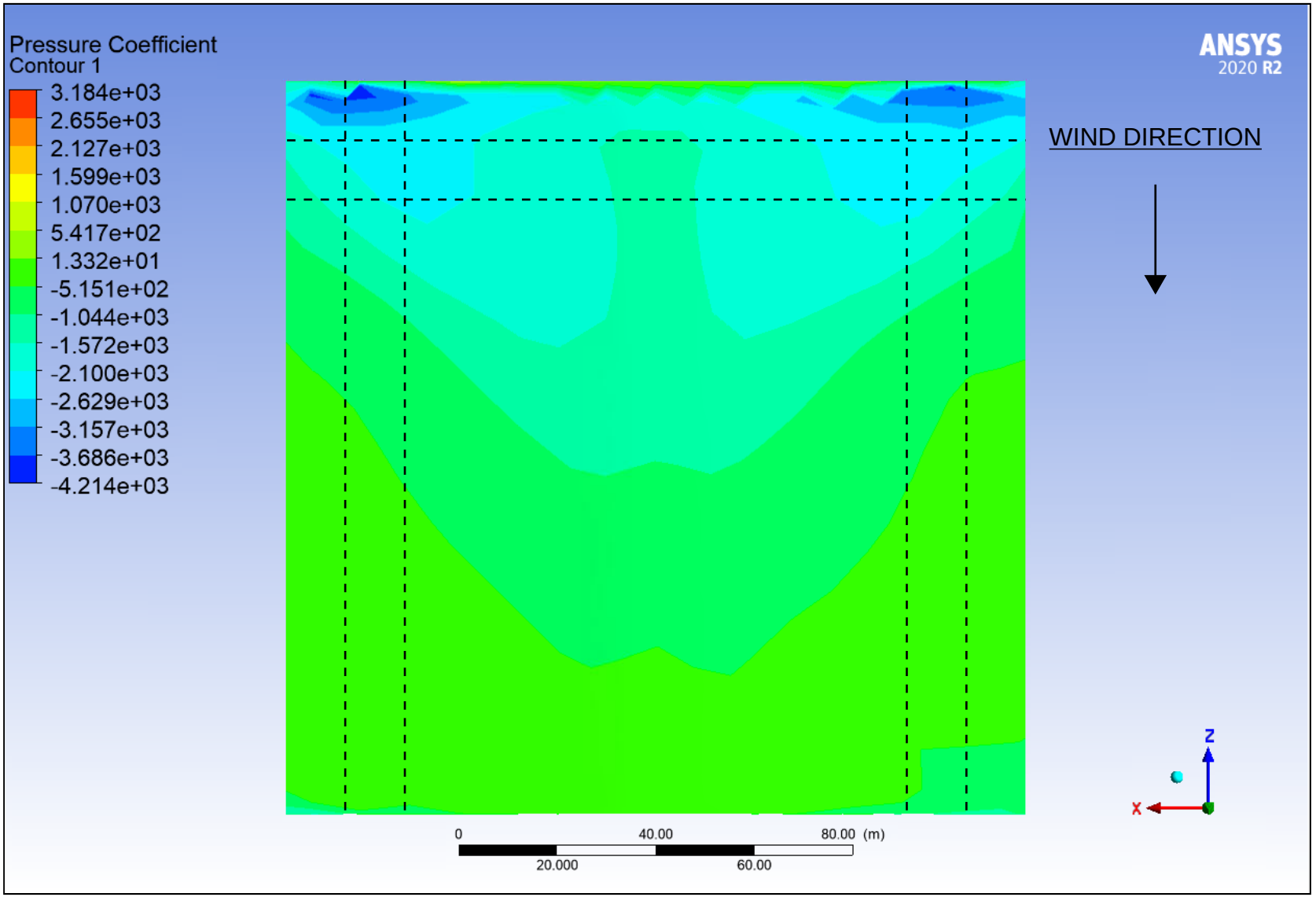

MODEL 3 - 30° SCALED RESIDUALS AND LIFT COEFFICIENT GRAPHS

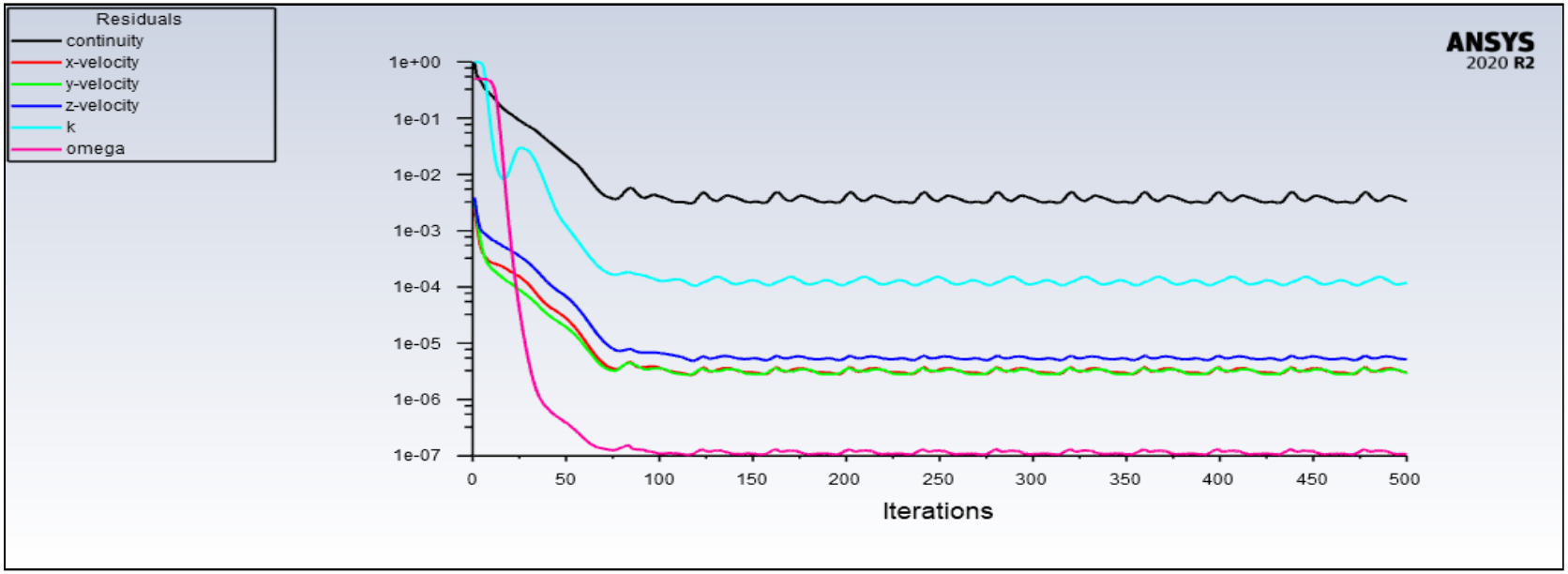

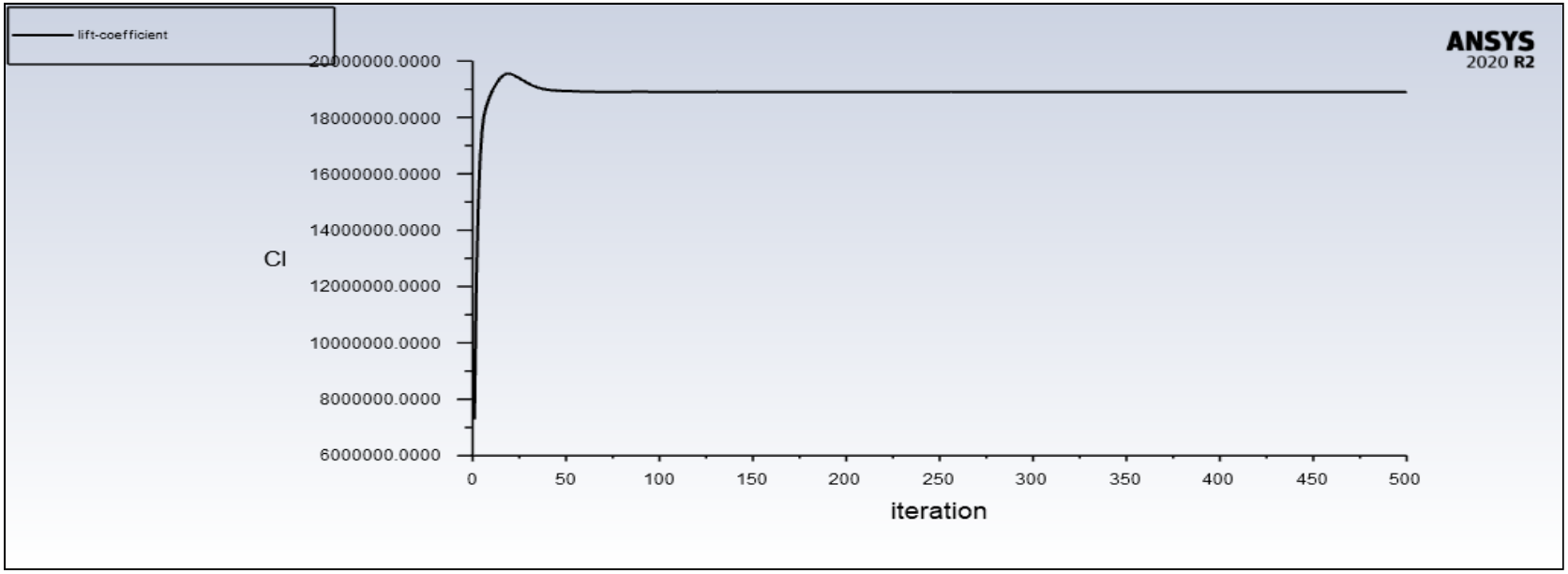

MODEL 3 - 30° PRESSURE COEFFICIENTS

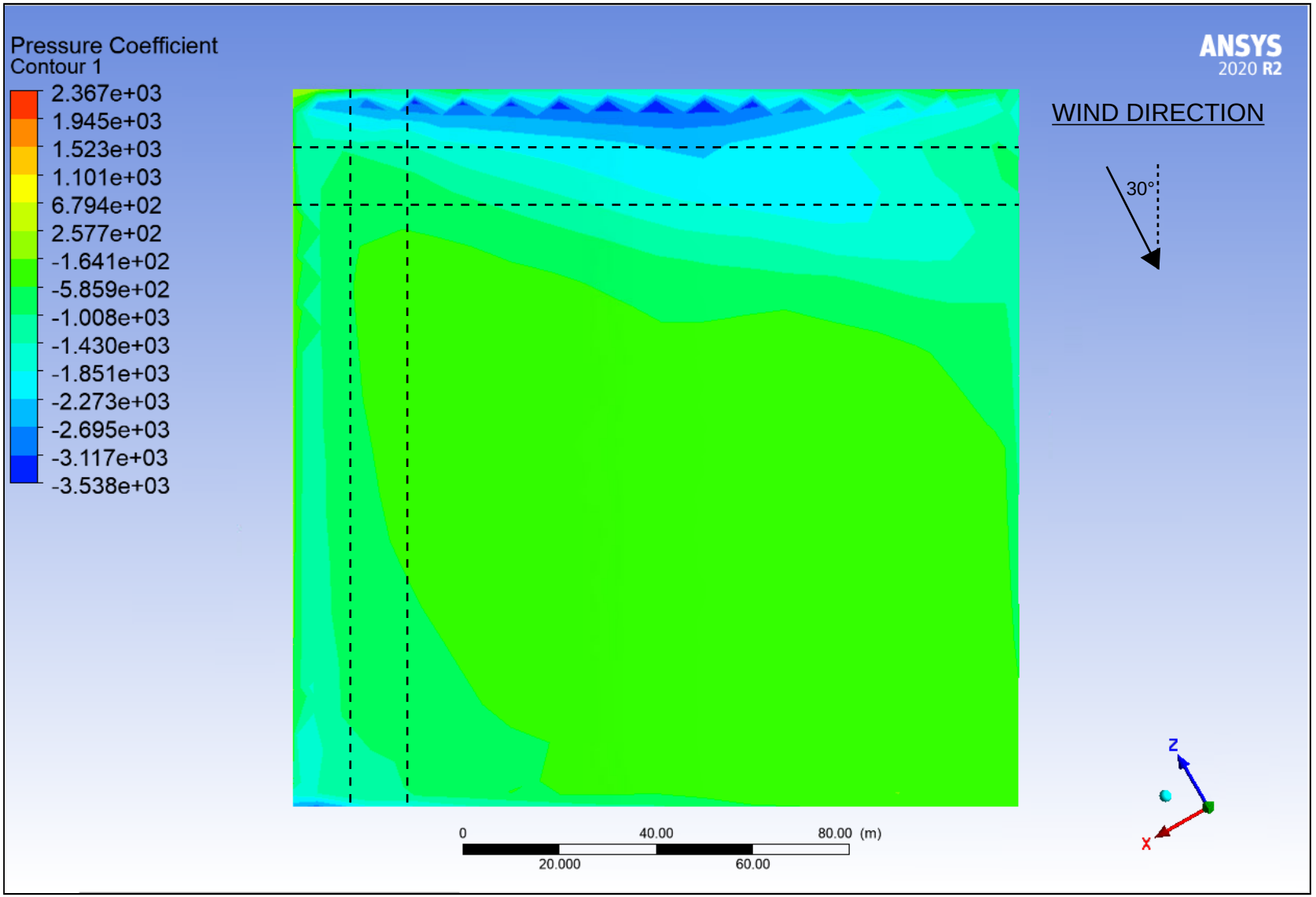

MODEL 3 - 45° SCALED RESIDUALS AND LIFT COEFFICIENT GRAPHS

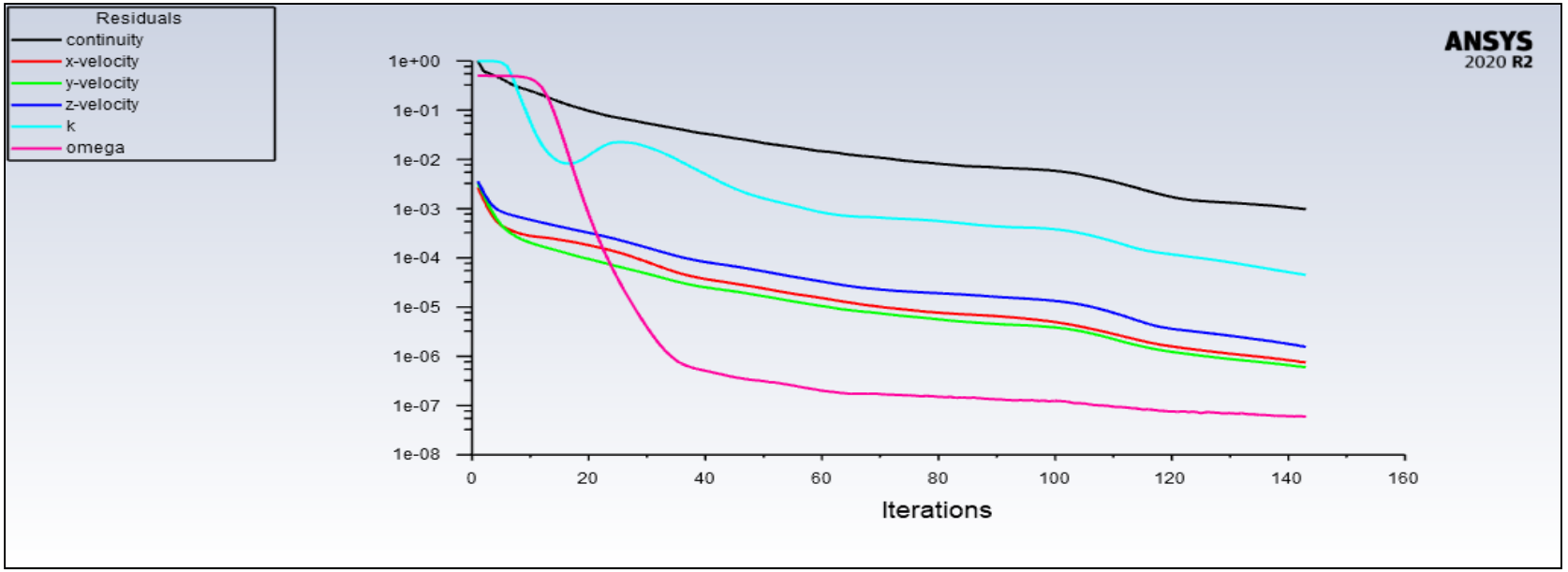

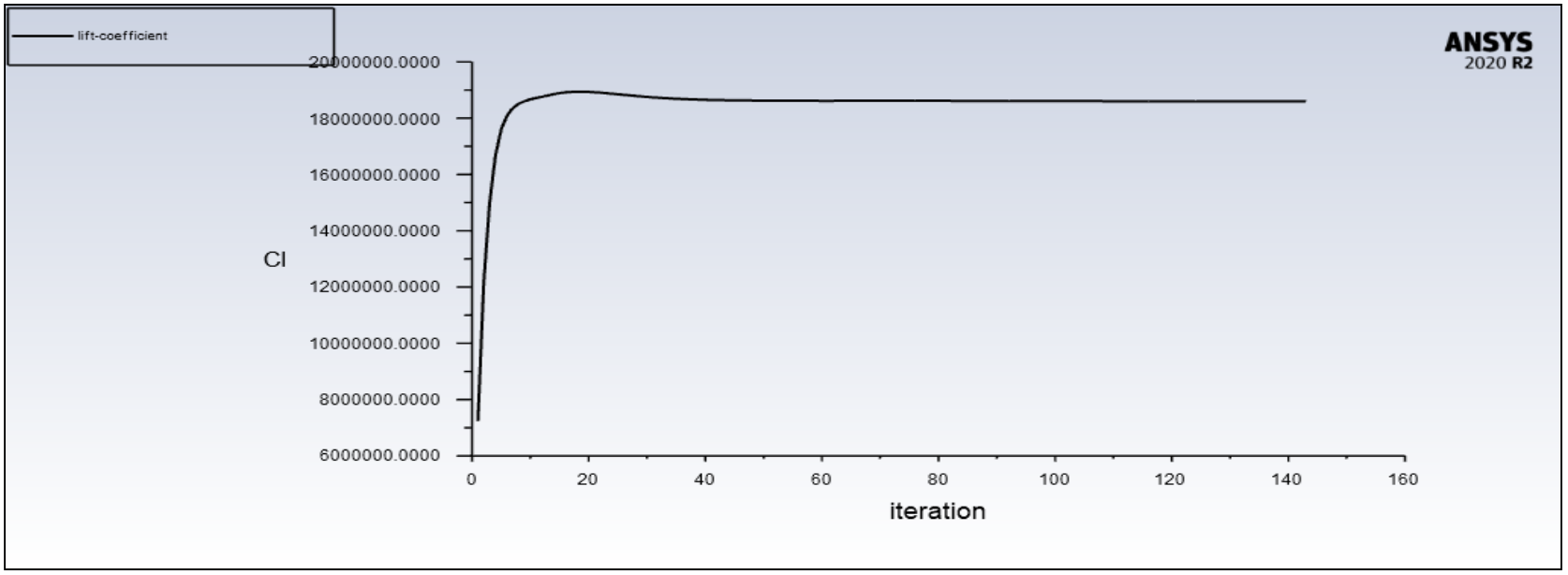

MODEL 3 - 45° PRESSURE COEFFICIENTS

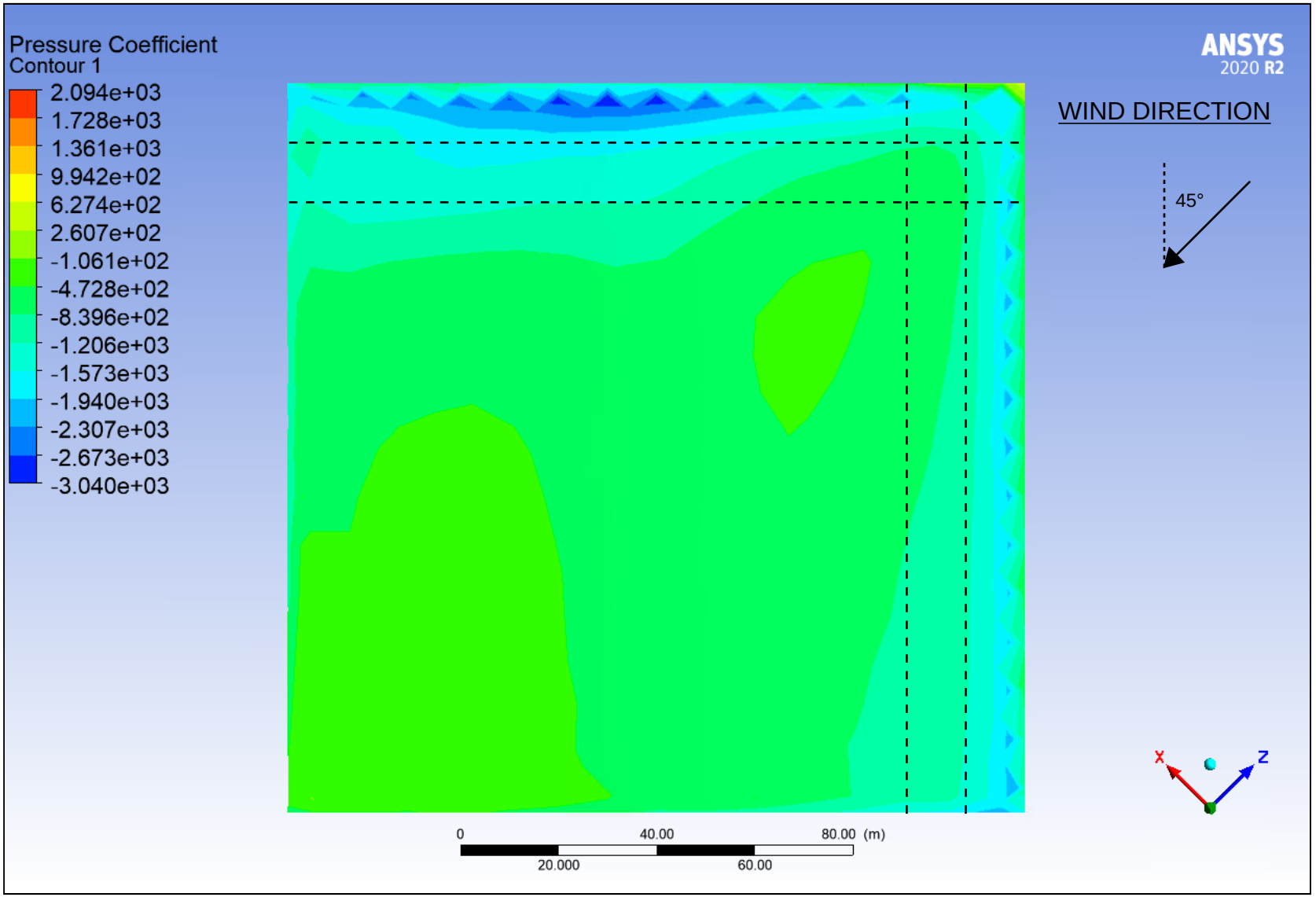

MODEL 3 - 60° SCALED RESIDUALS AND LIFT COEFFICIENT GRAPHS

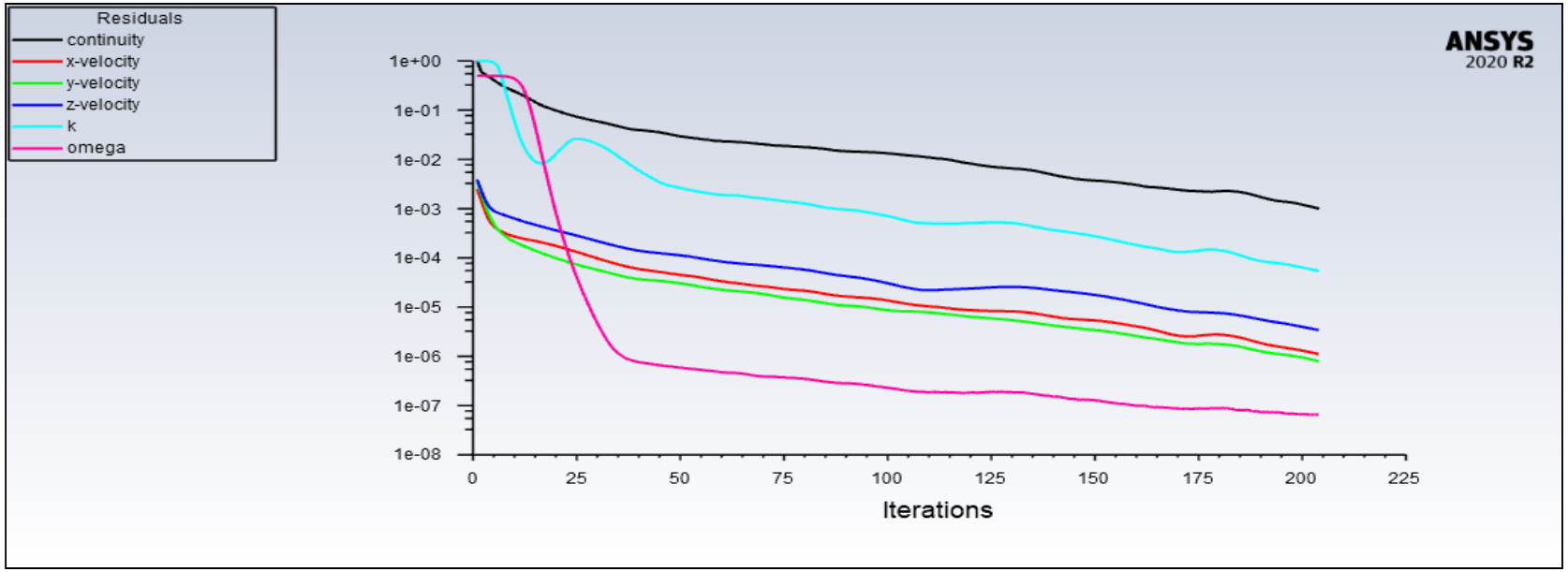

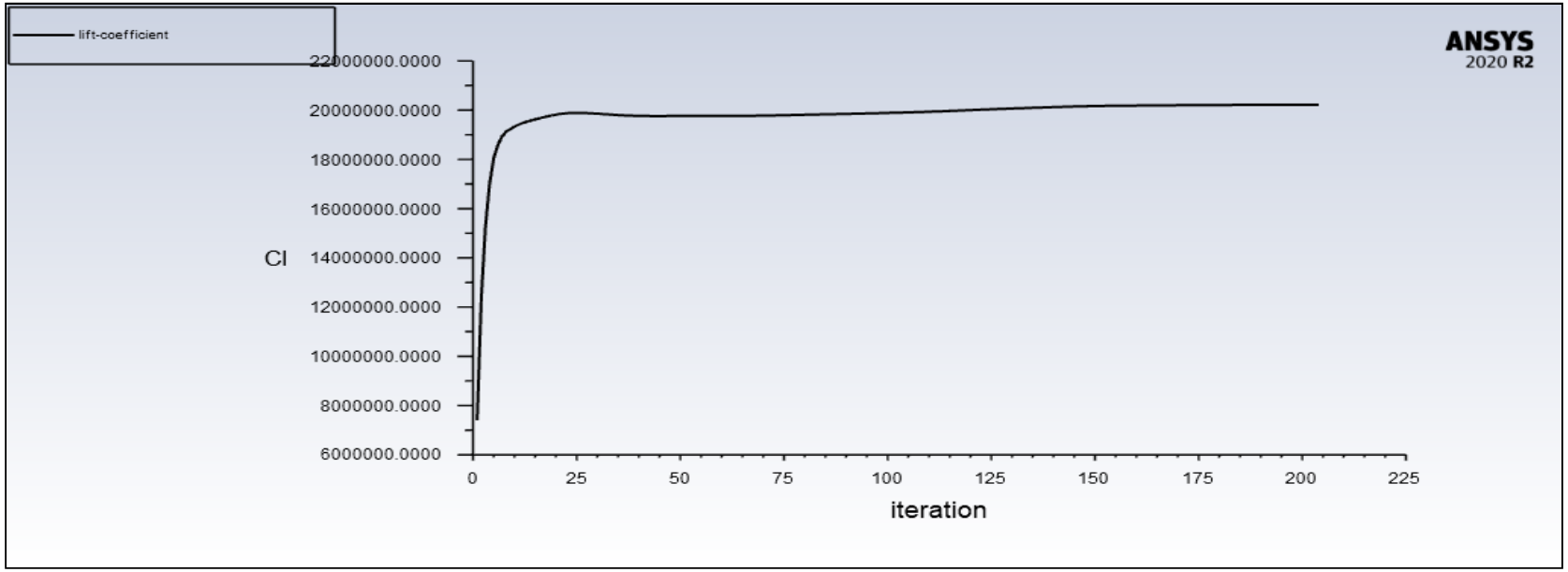

MODEL 3 - 60° PRESSURE COEFFICIENTS

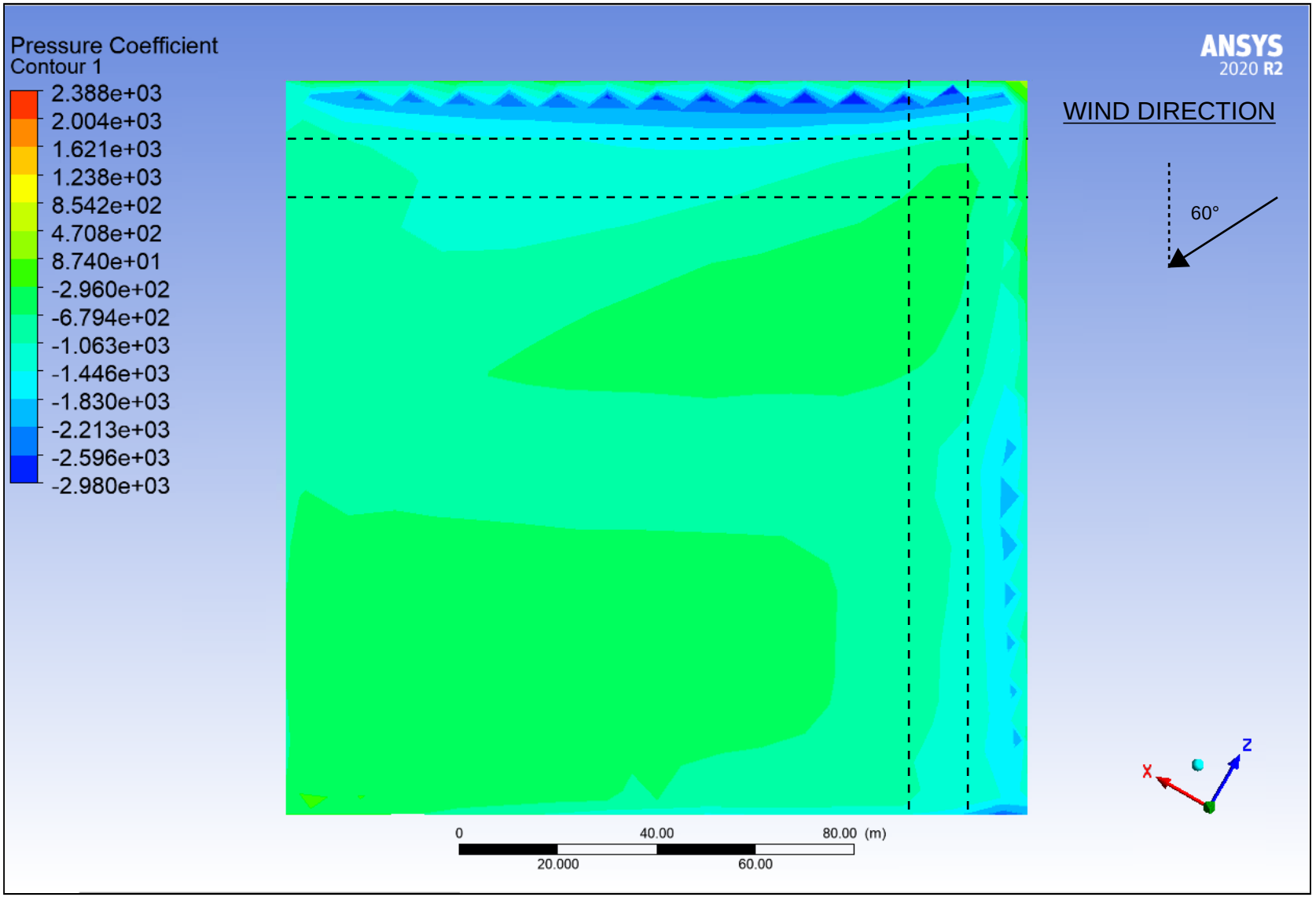

MODEL 3 - 90° SCALED RESIDUALS AND LIFT COEFFICIENT GRAPHS

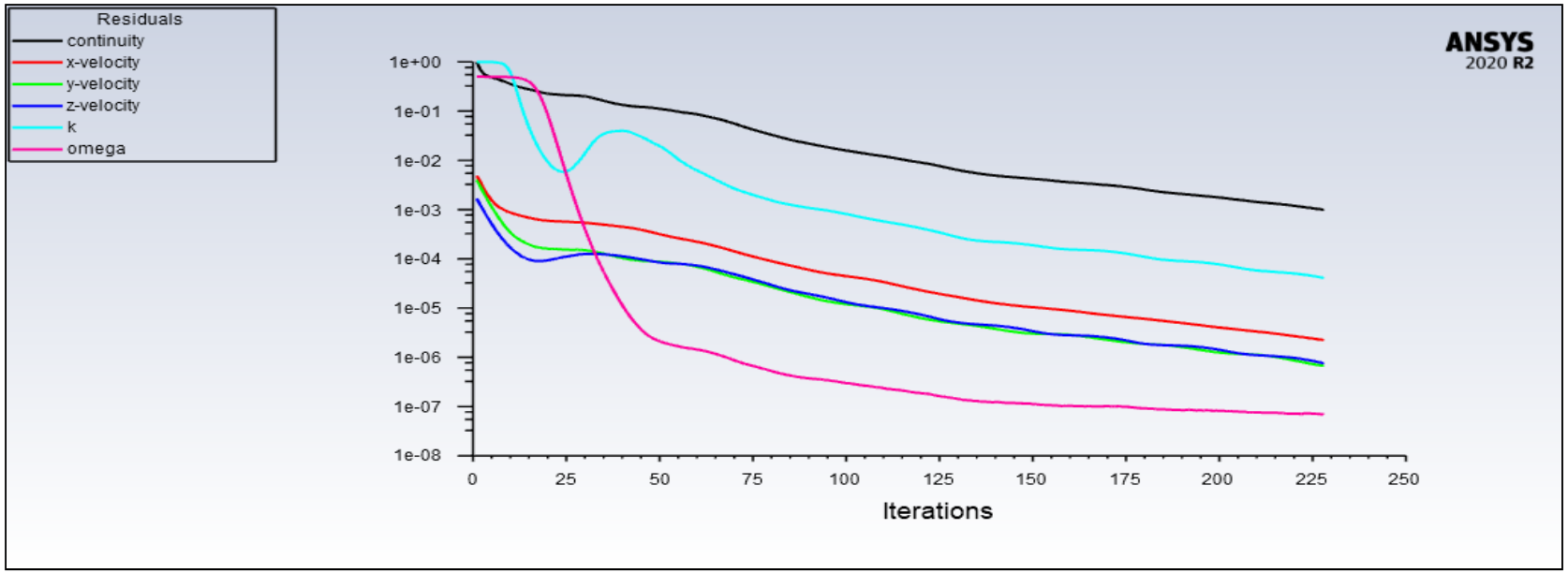

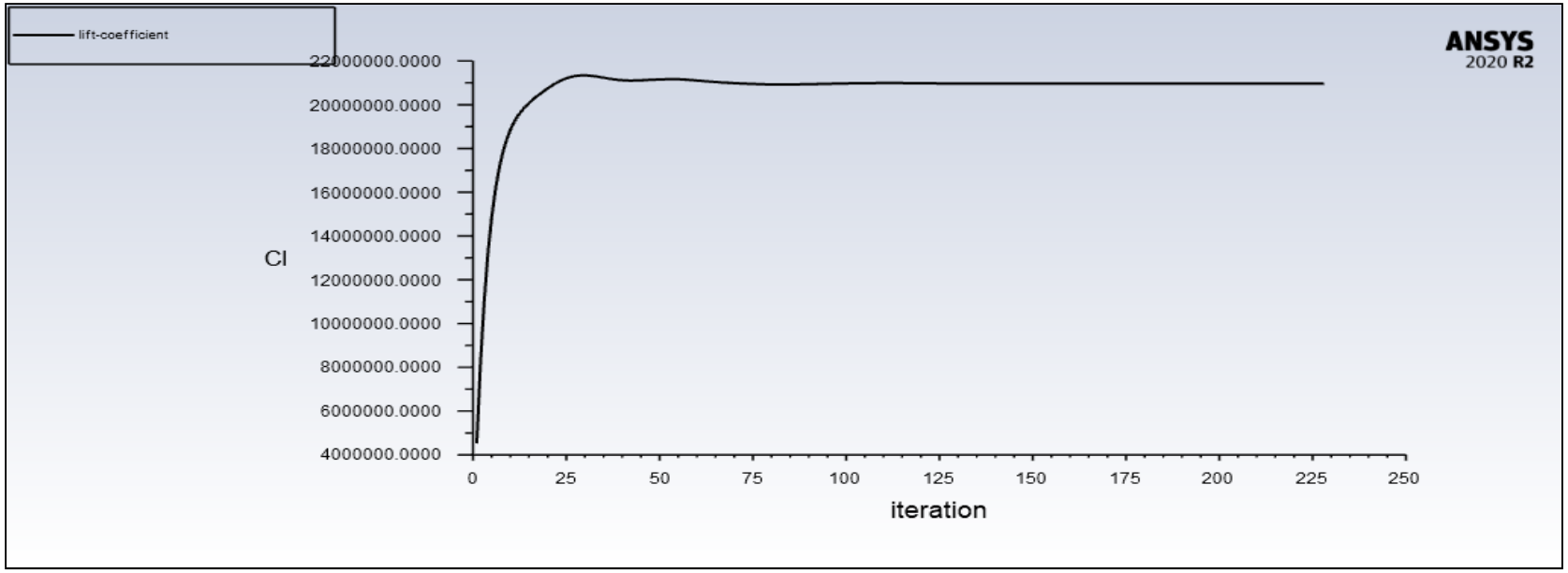

MODEL 3 - 90° PRESSURE COEFFICIENTS

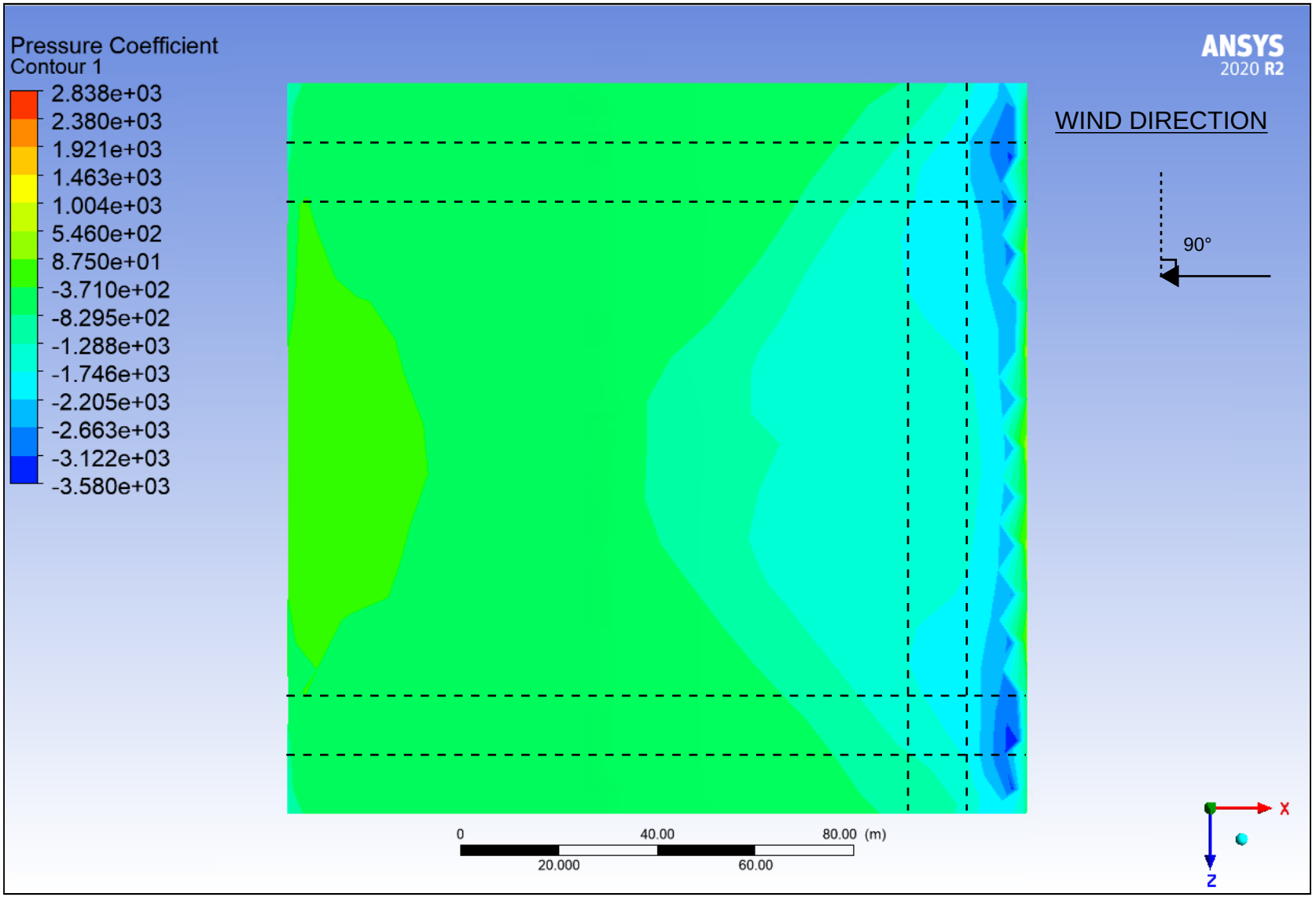

Model 4 Outputs

MODEL 4 - 0° SCALED RESIDUALS AND LIFT COEFFICIENT GRAPHS

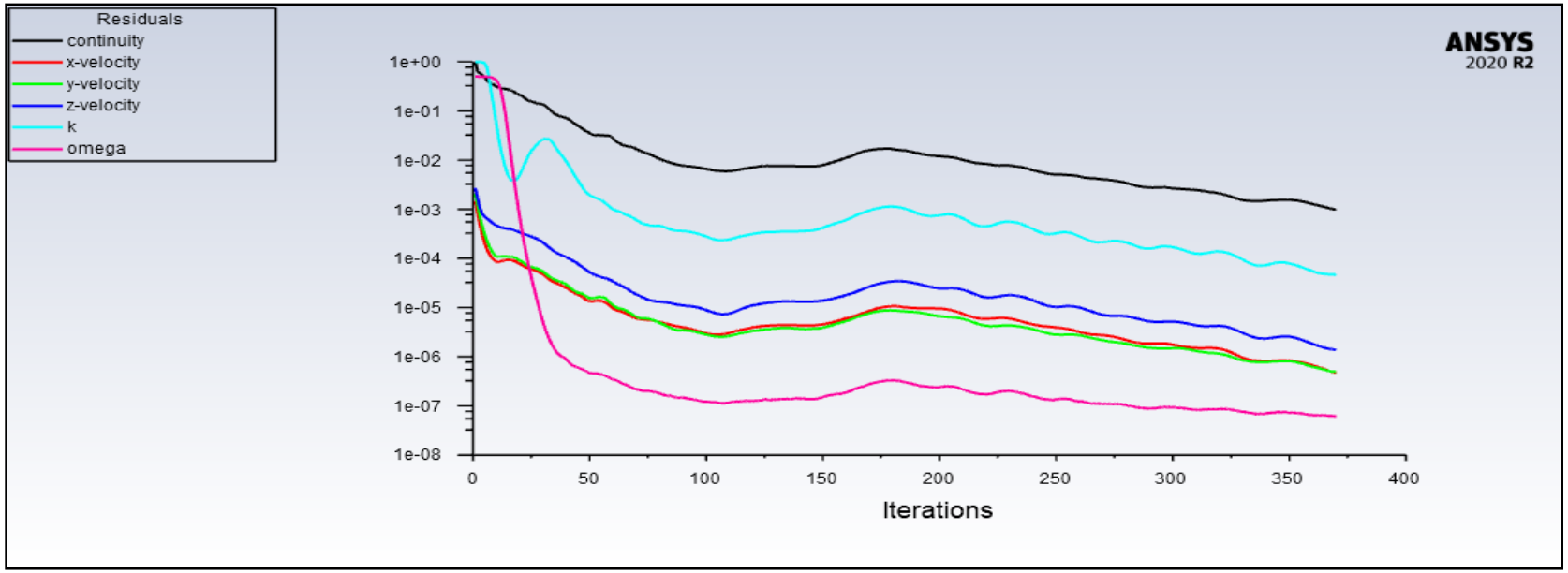

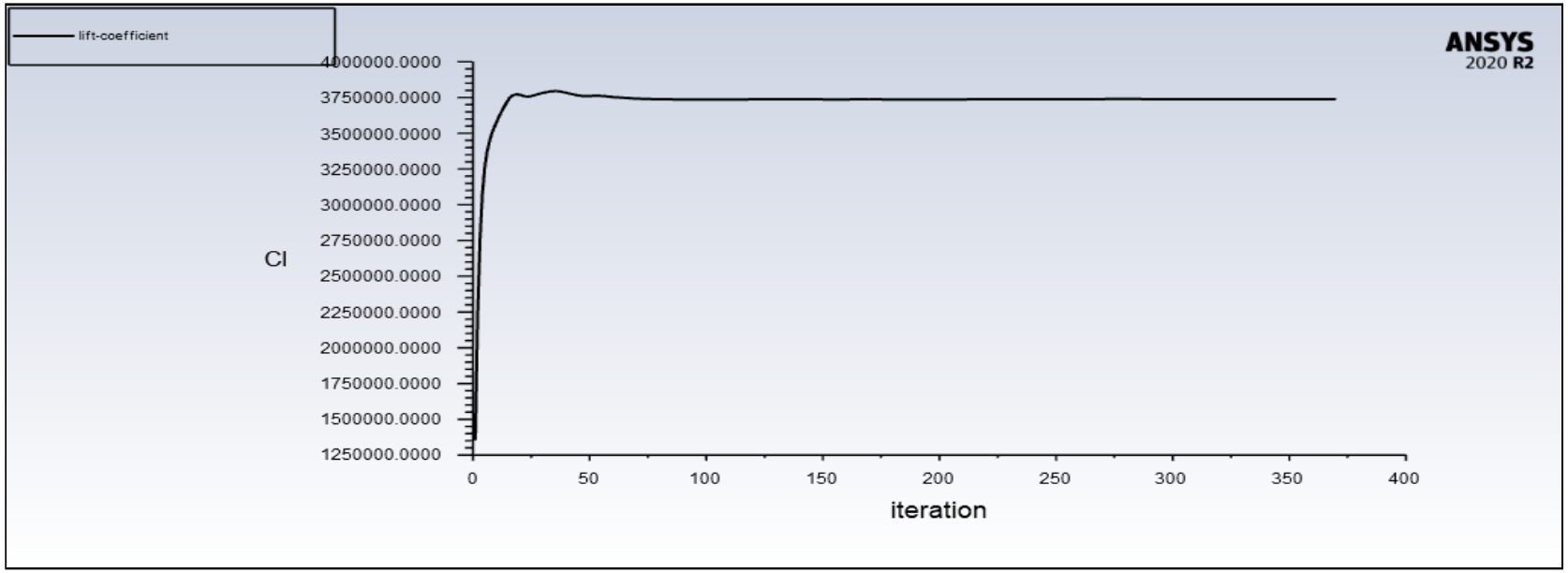

MODEL 4 - 0° PRESSURE COEFFICIENTS

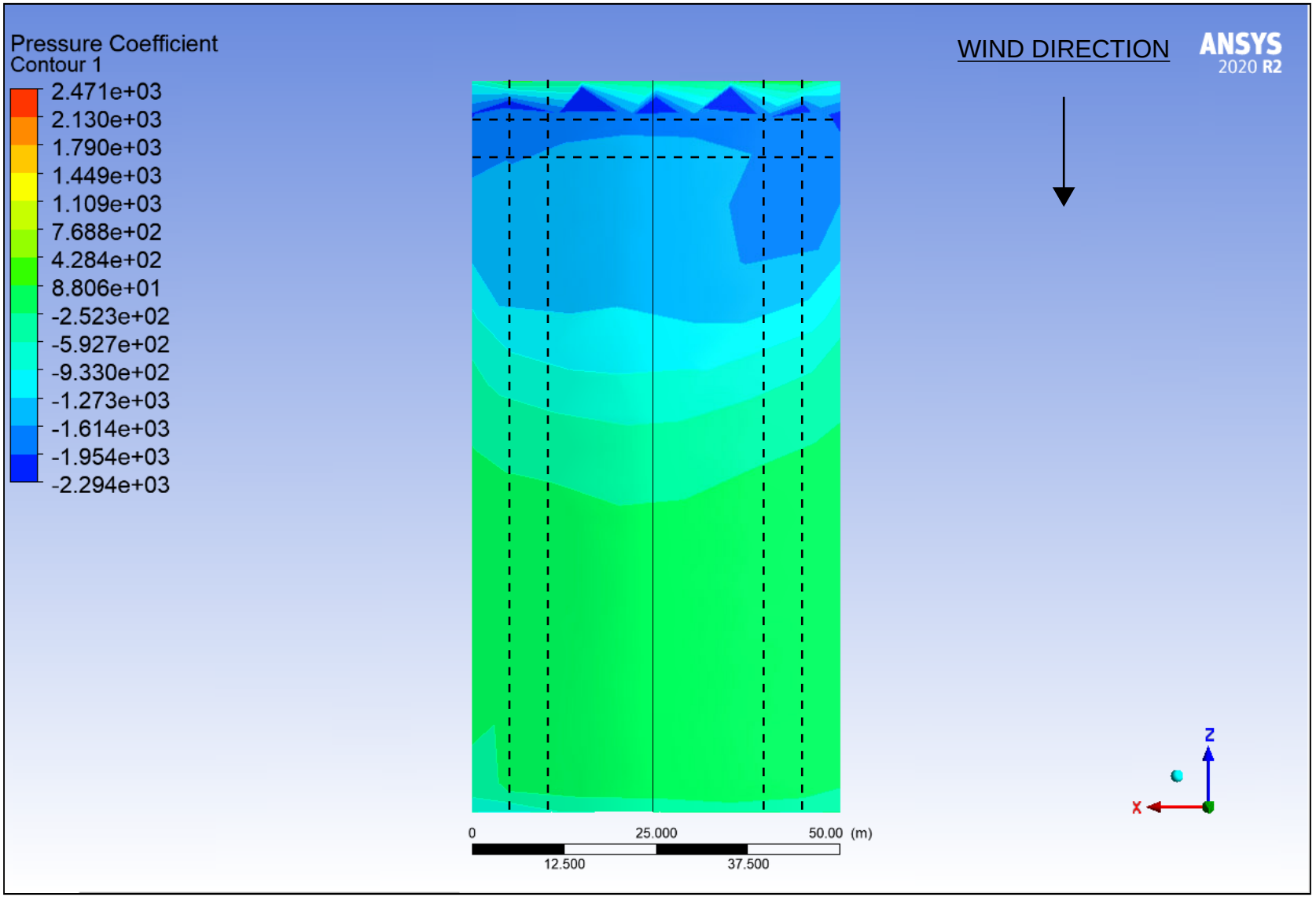

MODEL 4 - 30° SCALED RESIDUALS AND LIFT COEFFICIENT GRAPHS

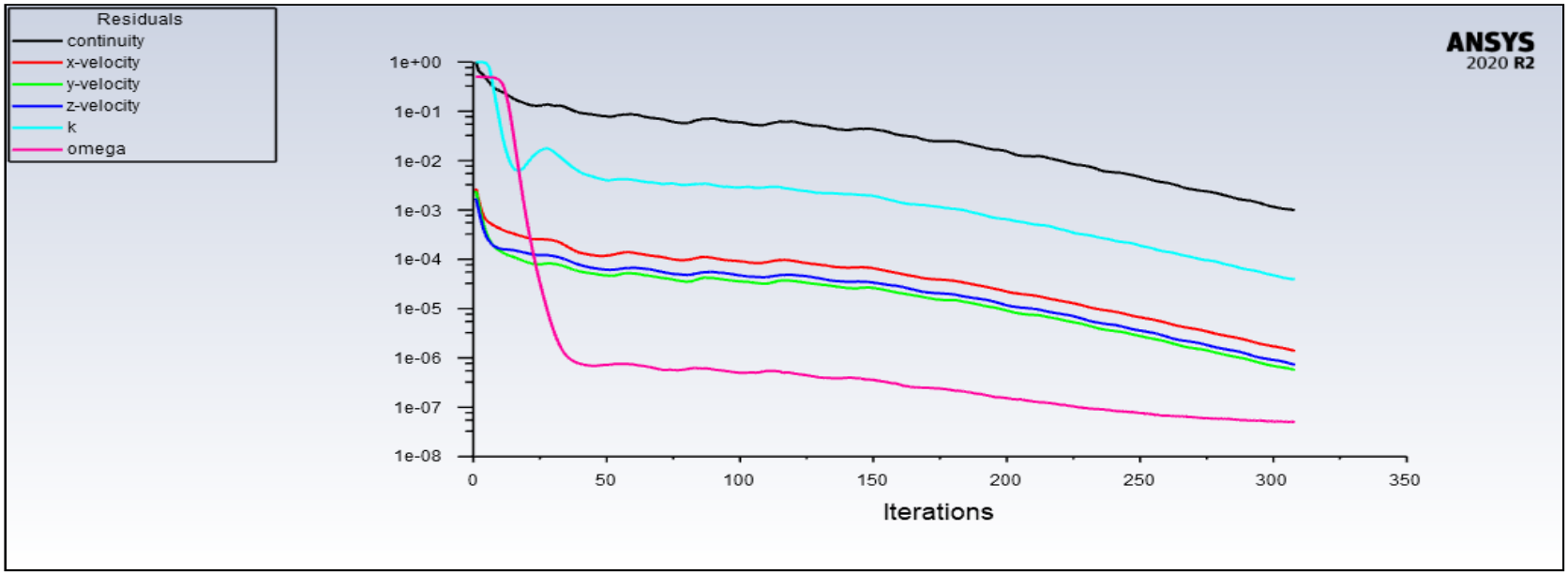

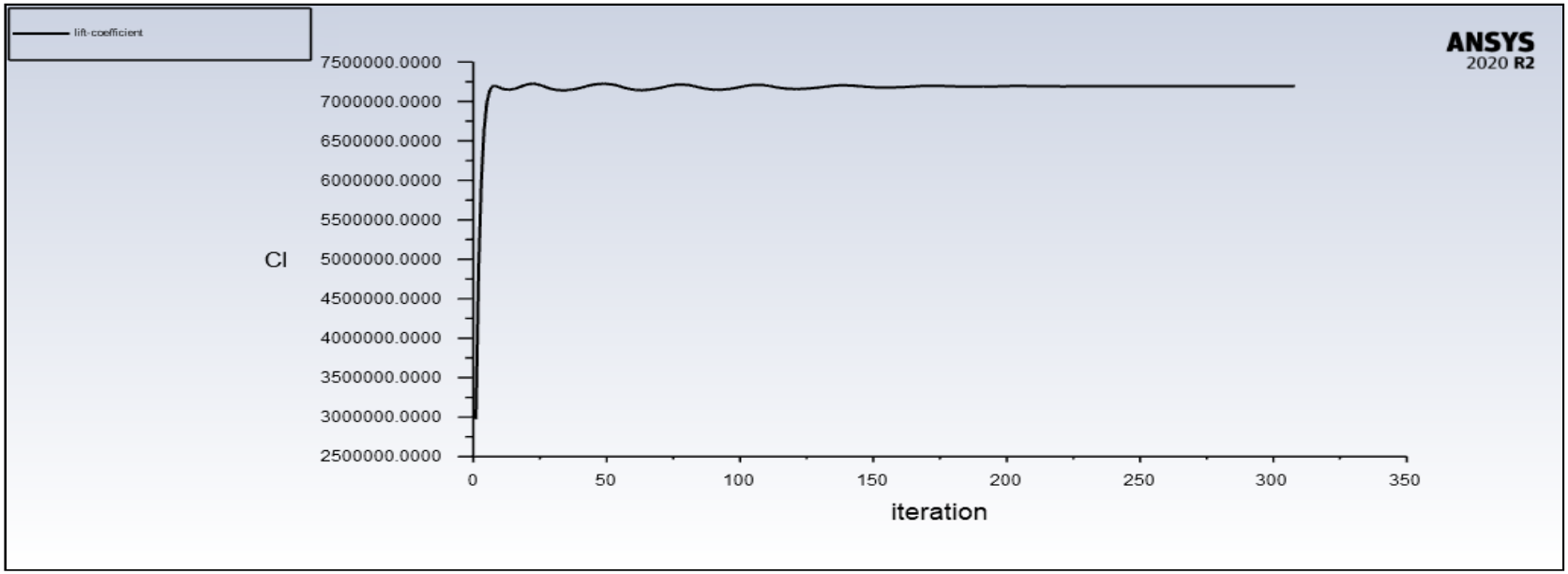

MODEL 4 - 30° PRESSURE COEFFICIENTS

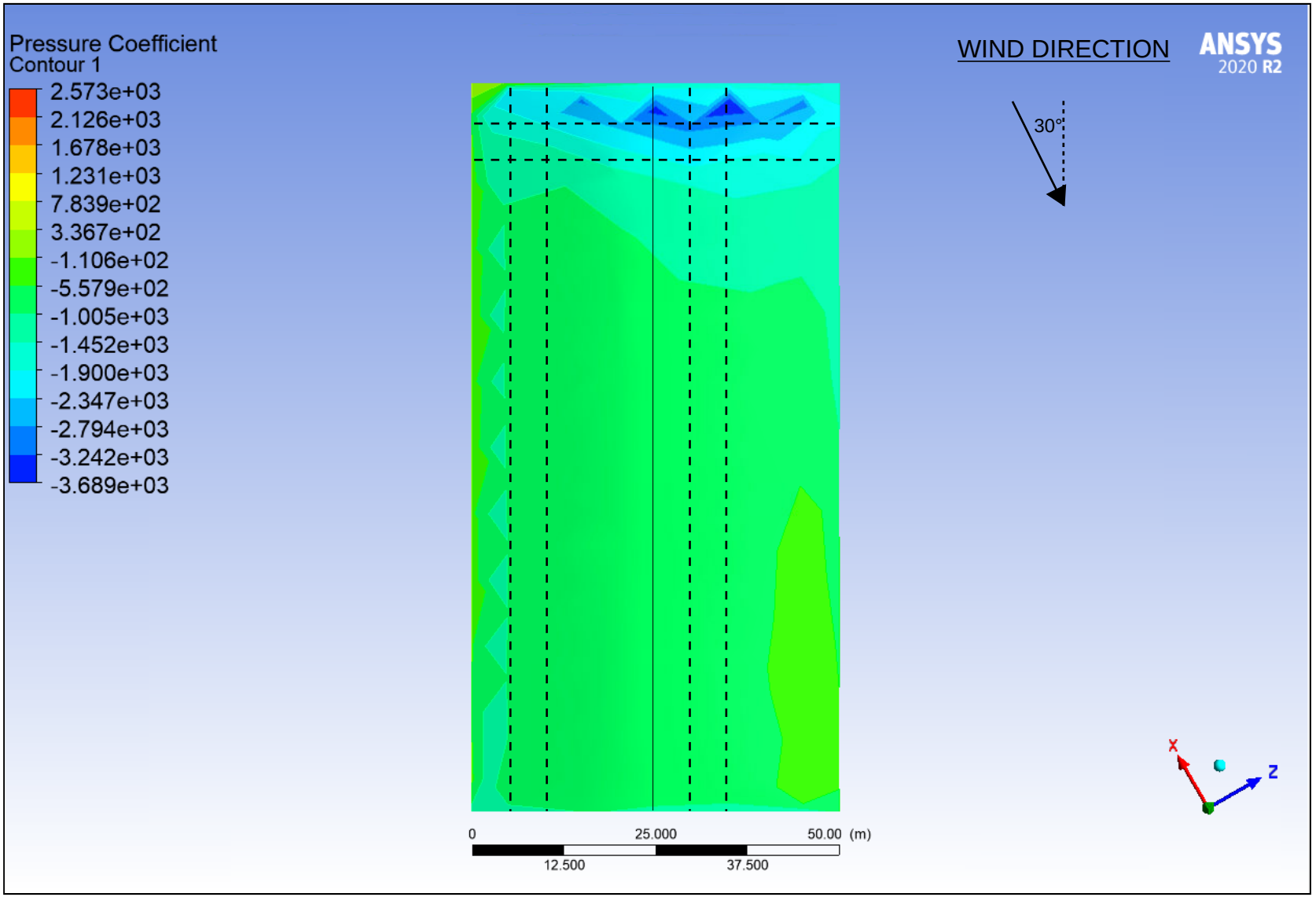

MODEL 4 - 45° SCALED RESIDUALS AND LIFT COEFFICIENT GRAPHS

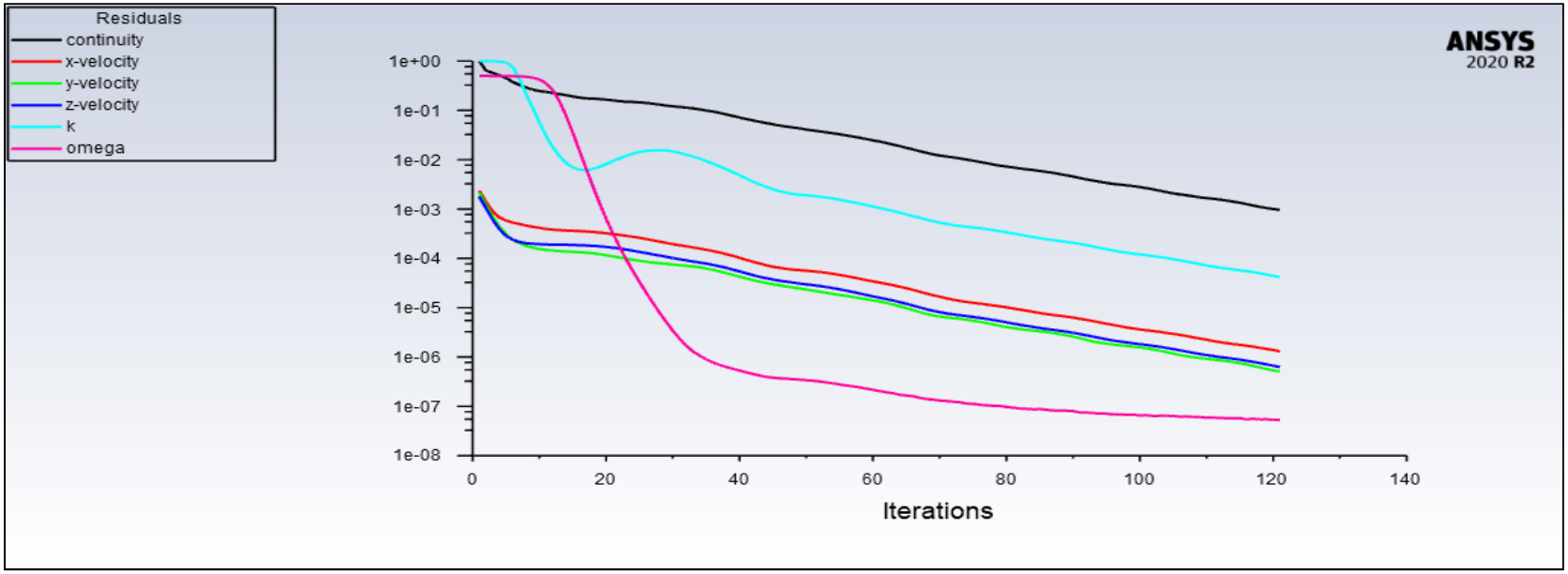

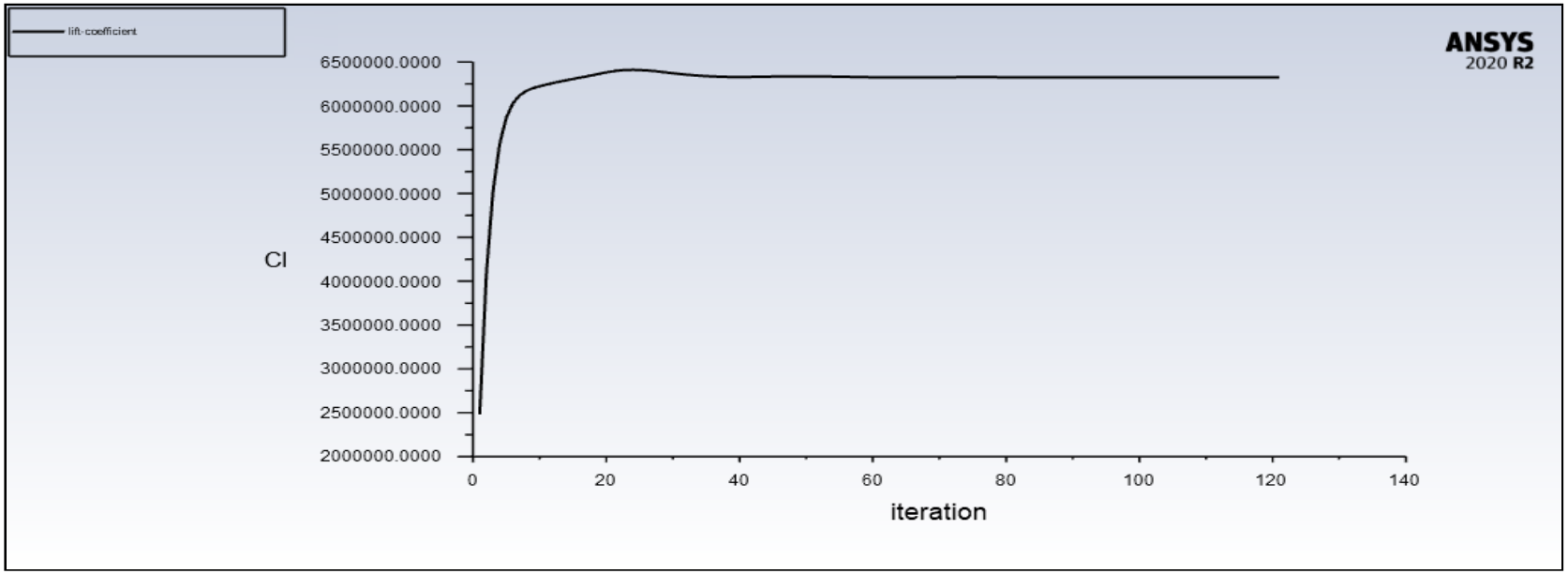

MODEL 4 - 45° PRESSURE COEFFICIENTS

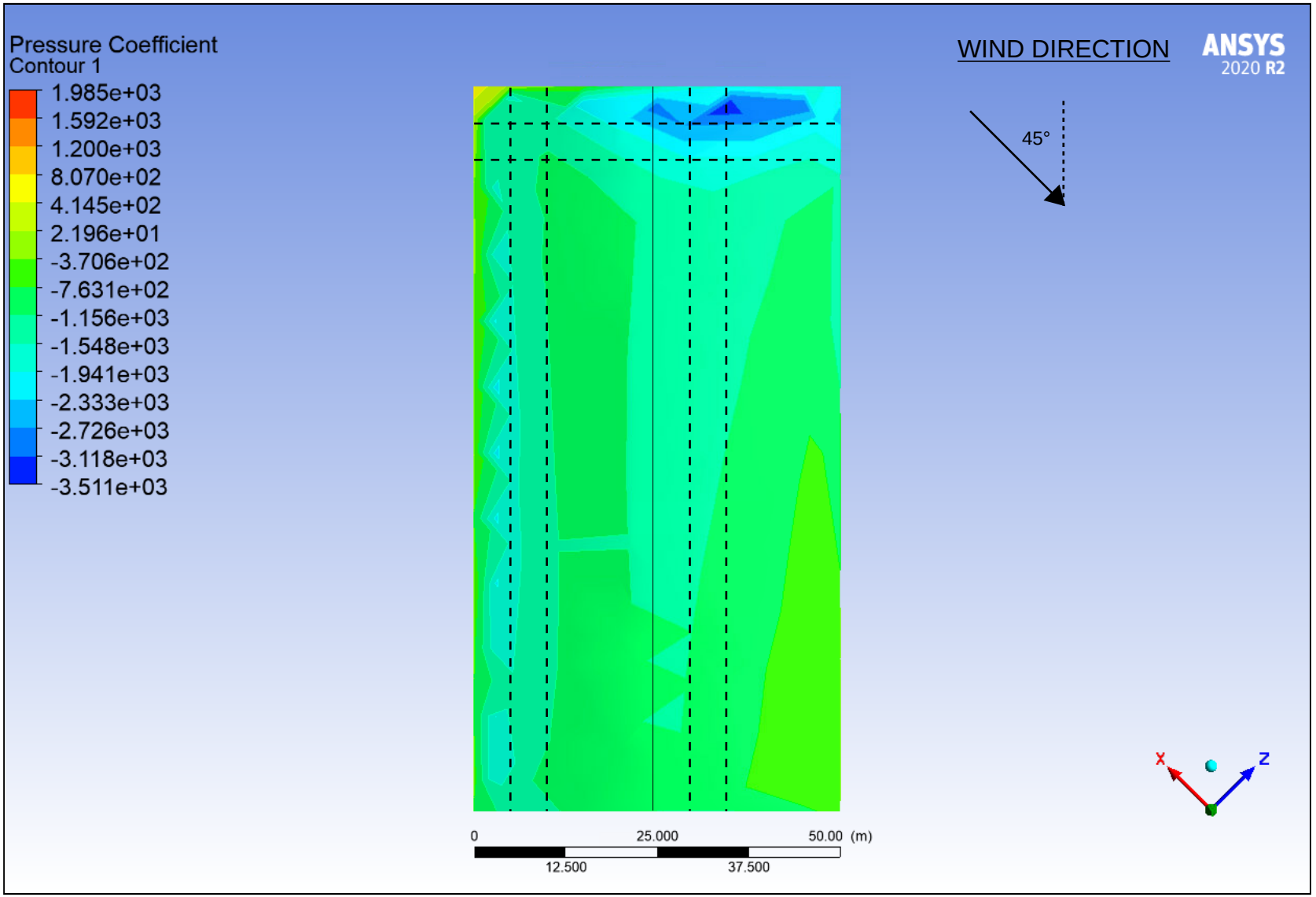

MODEL 4 - 60° SCALED RESIDUALS AND LIFT COEFFICIENT GRAPHS

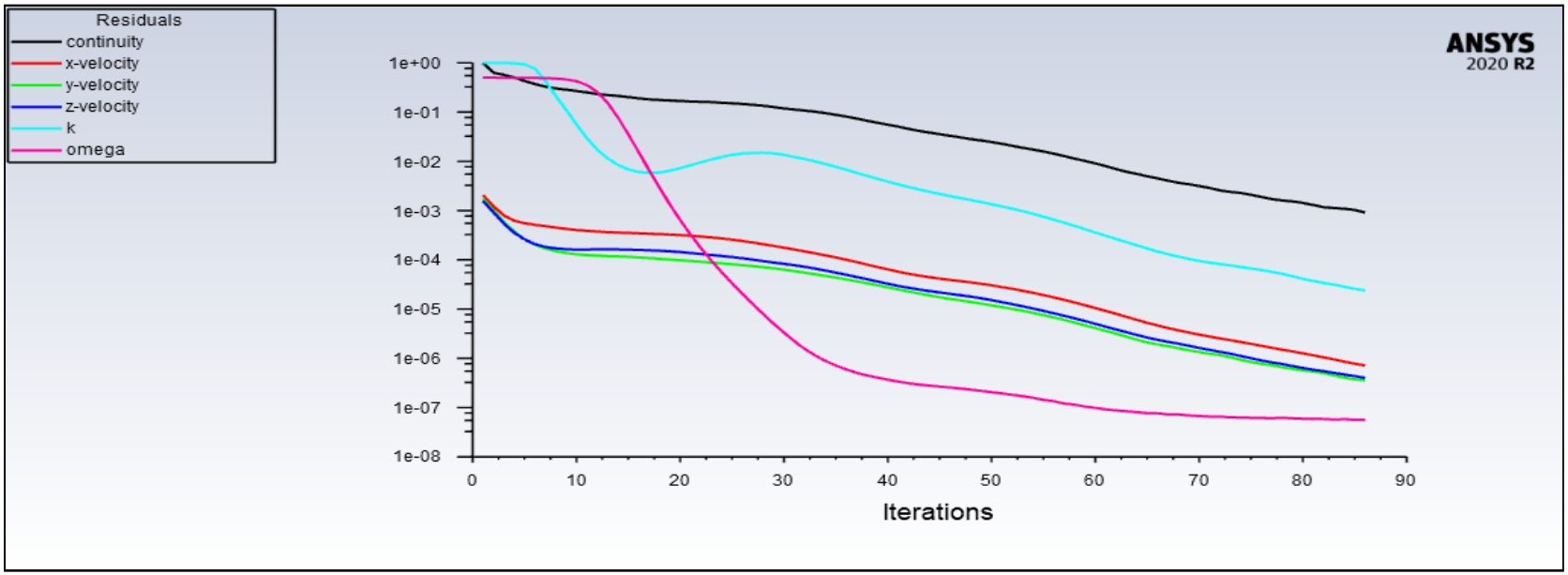

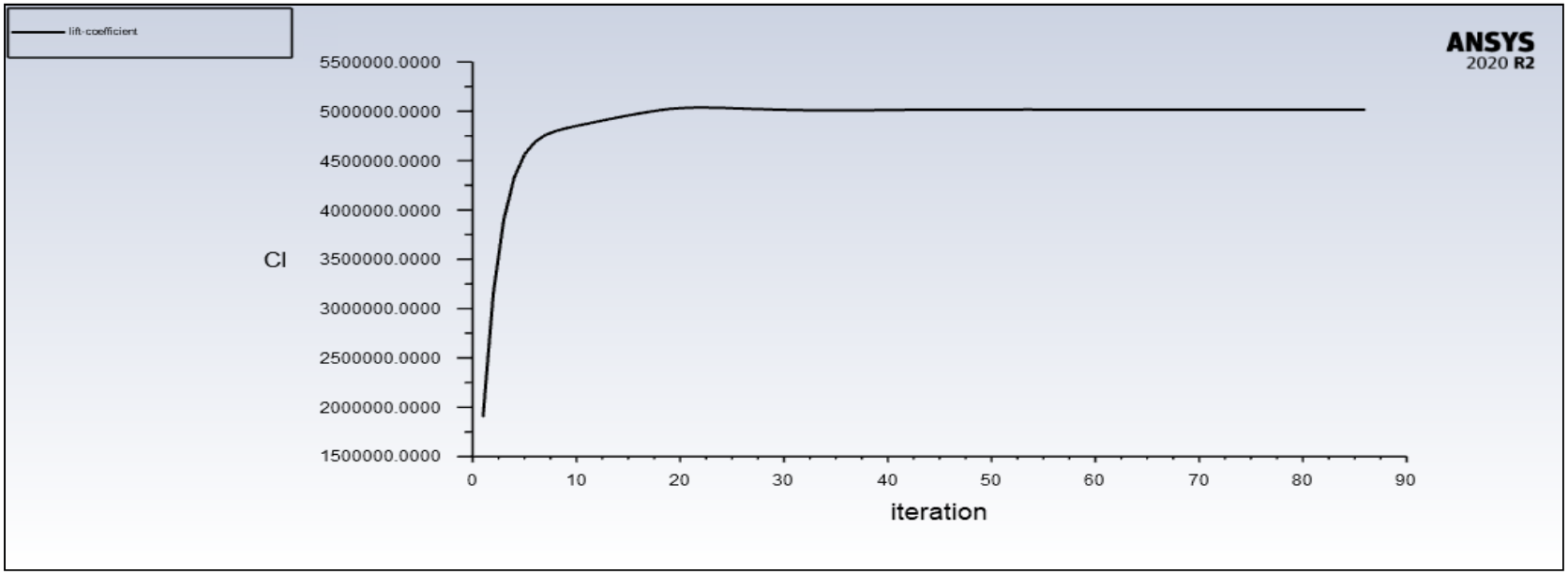

MODEL 4 - 60° PRESSURE COEFFICIENTS

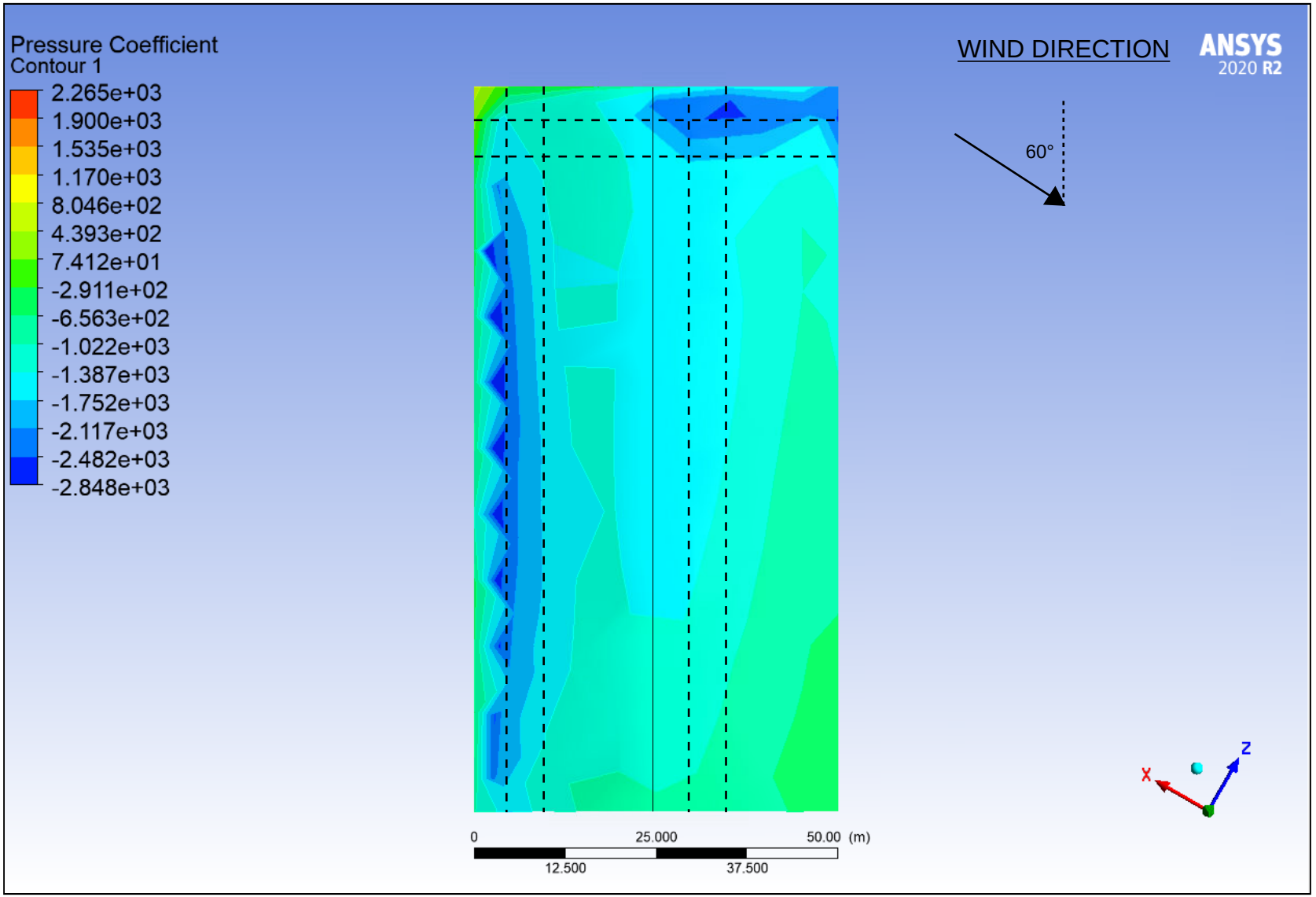

MODEL 4 - 90° SCALED RESIDUALS AND LIFT COEFFICIENT GRAPHS

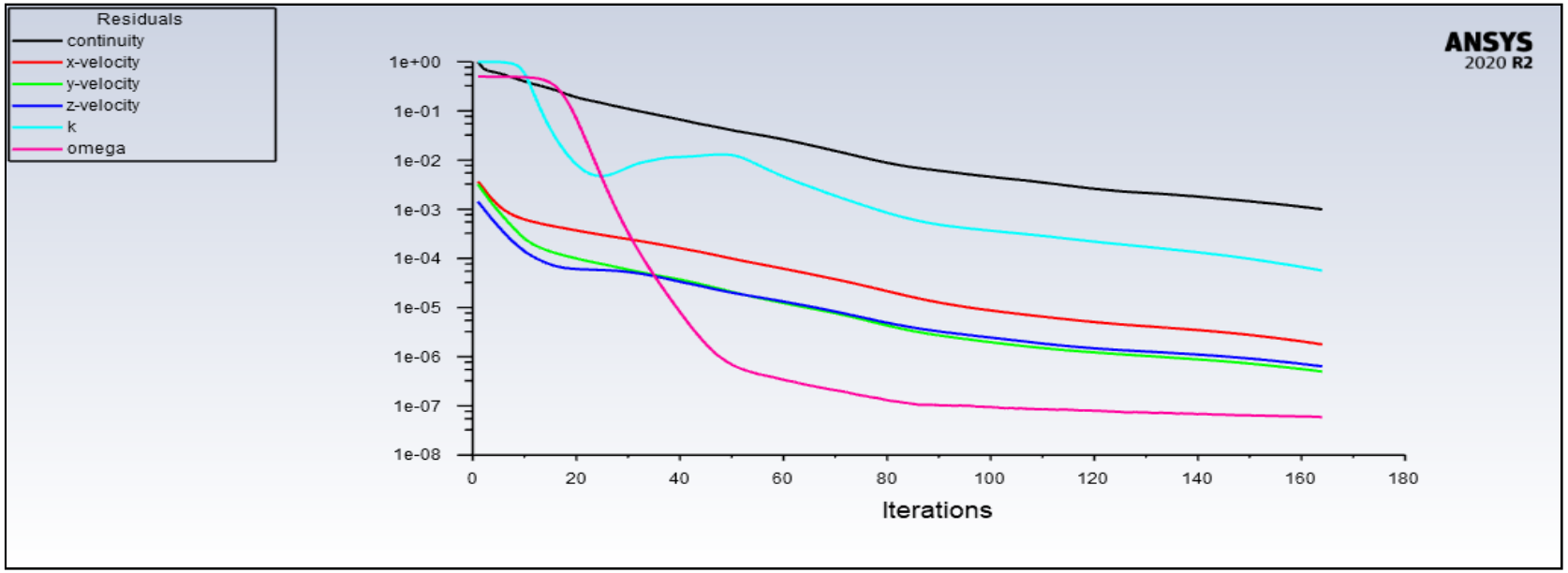

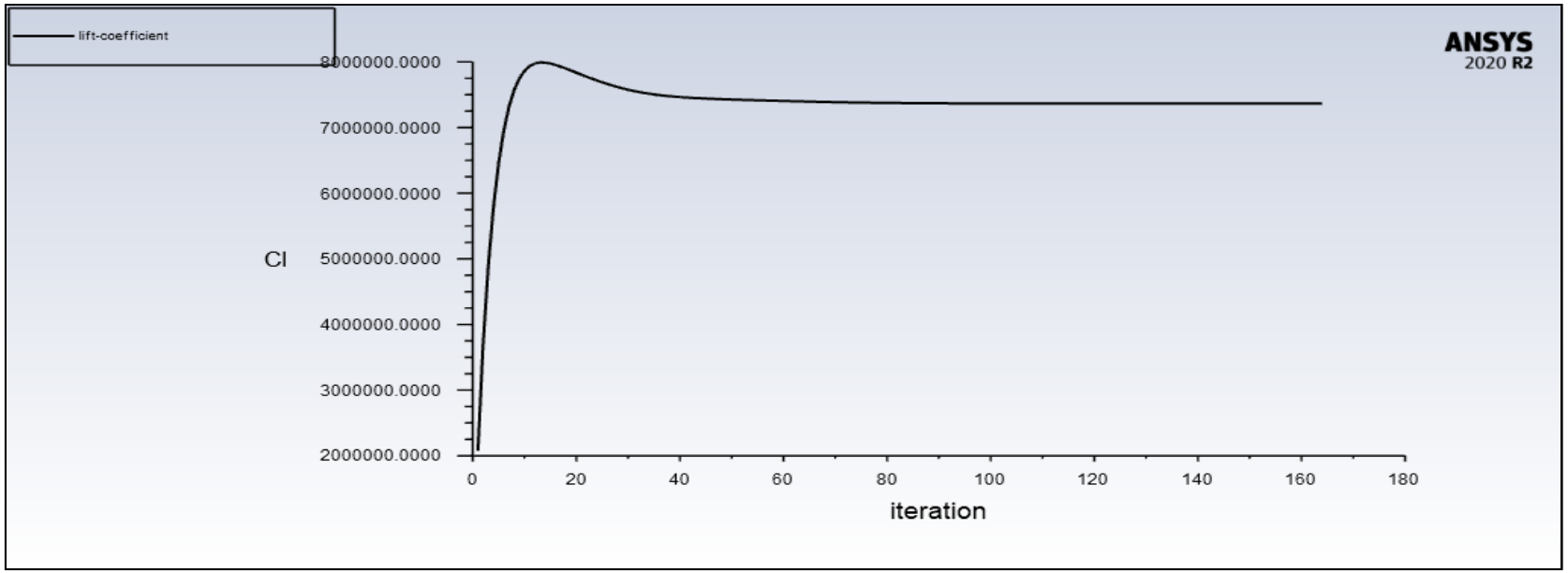

MODEL 4 - 90° PRESSURE COEFFICIENTS

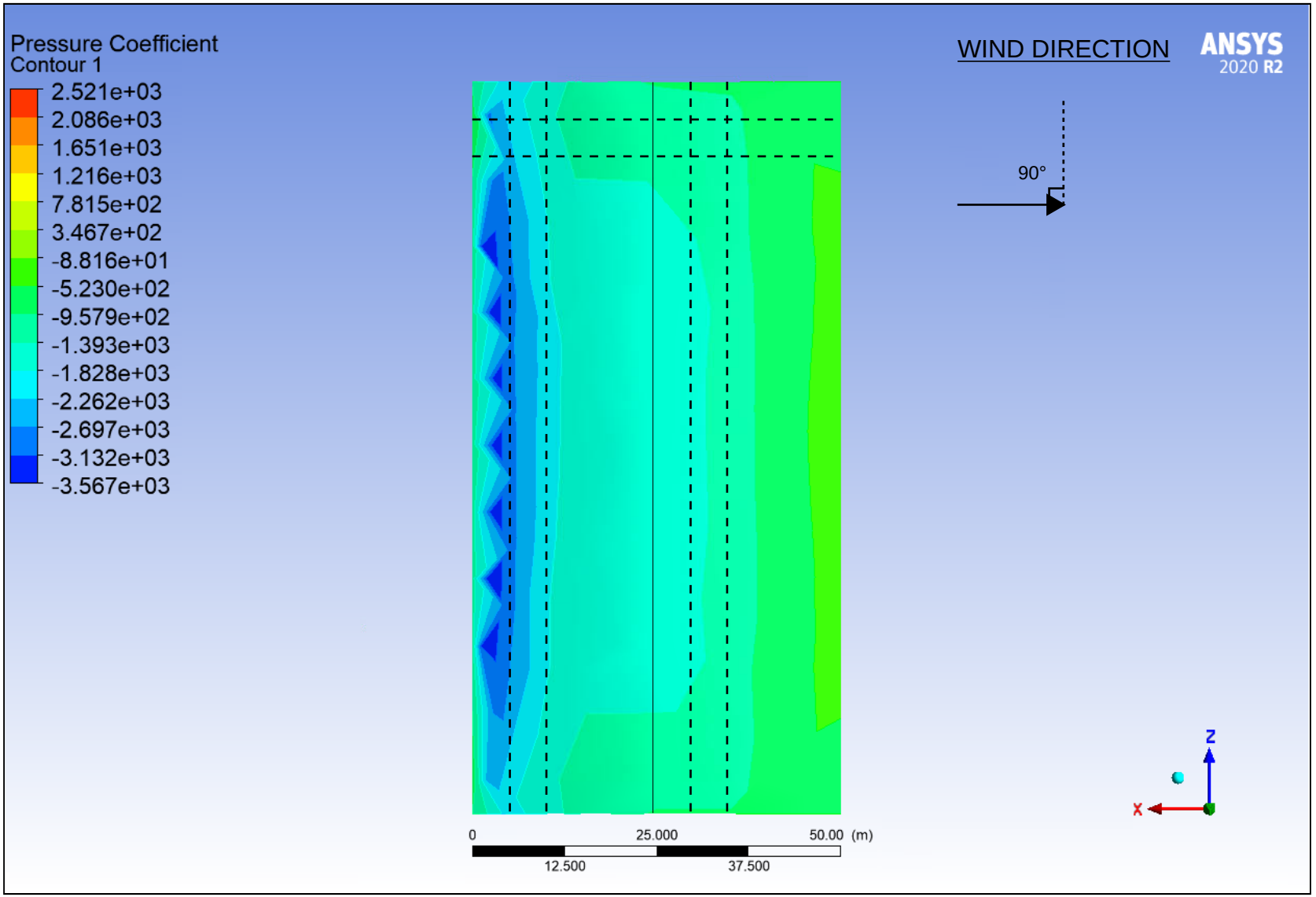

Model 5 Outputs

MODEL 5 - 0° SCALED RESIDUALS AND LIFT COEFFICIENT GRAPHS

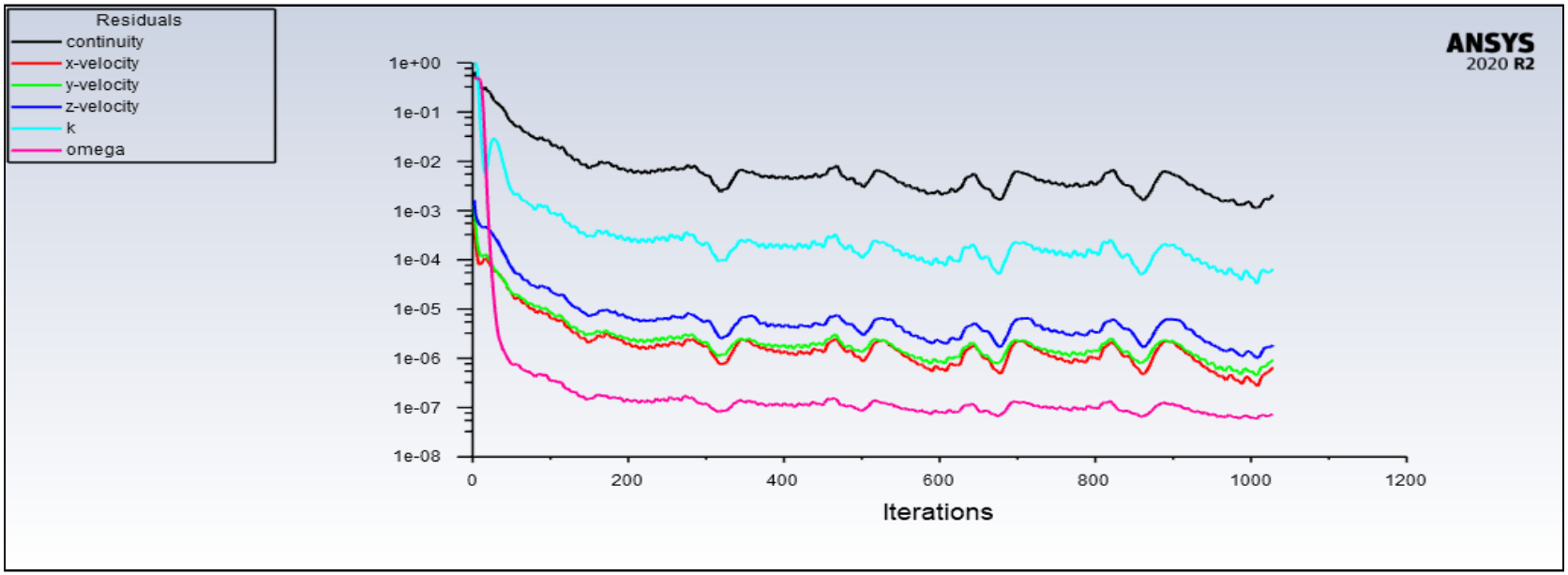

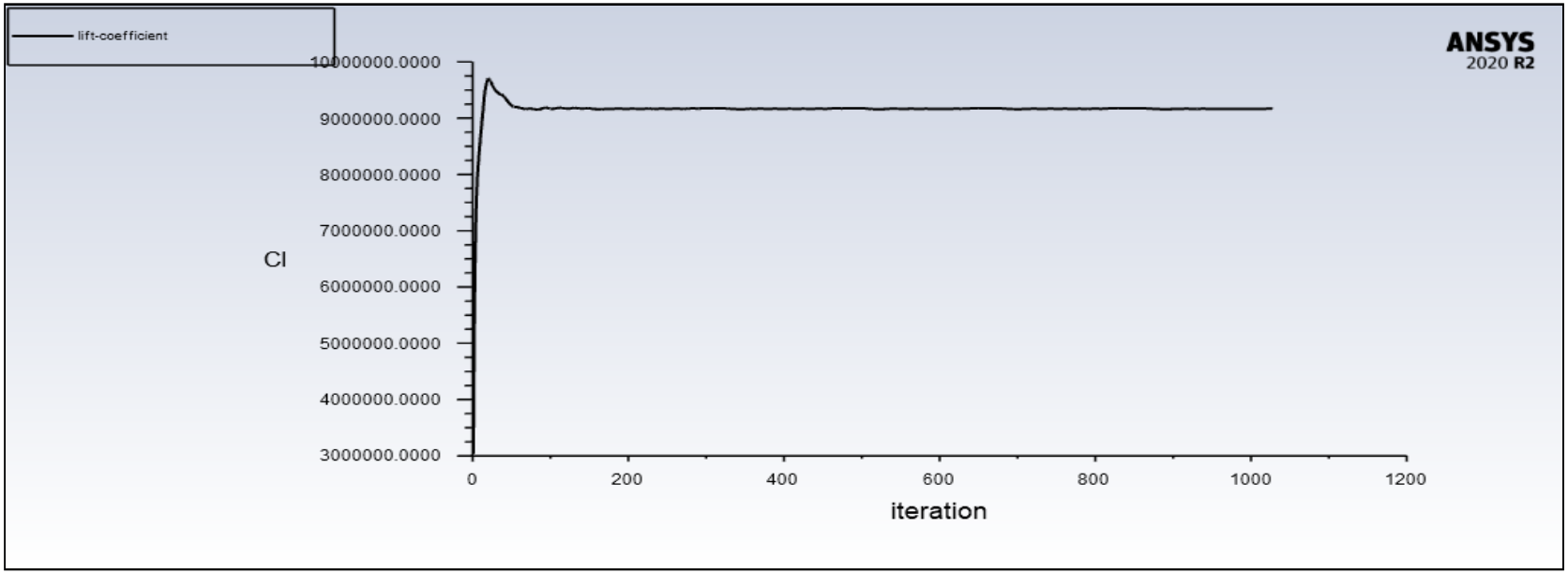

MODEL 5 - 0° PRESSURE COEFFICIENTS

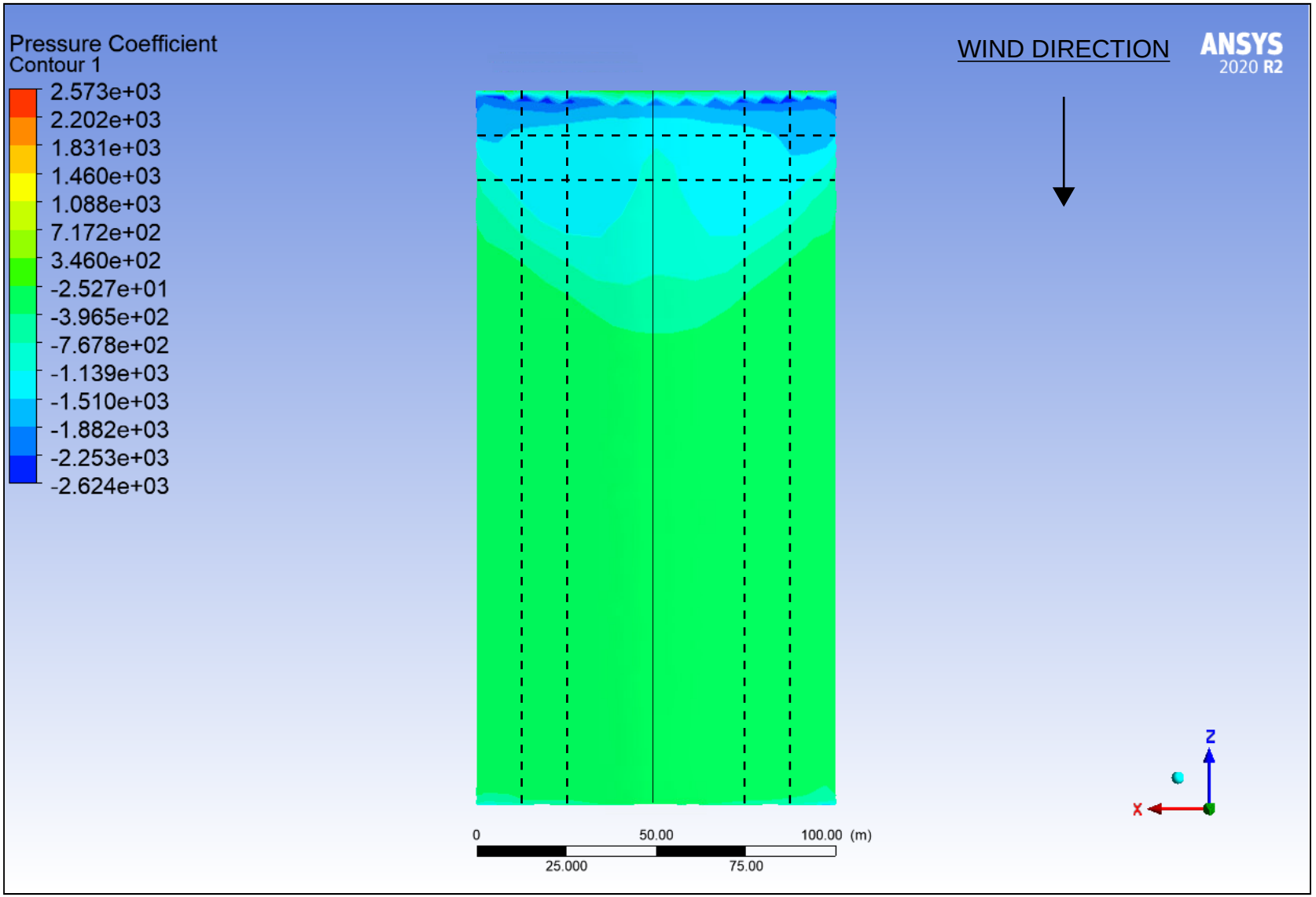

MODEL 5 - 30° SCALED RESIDUALS AND LIFT COEFFICIENT GRAPHS

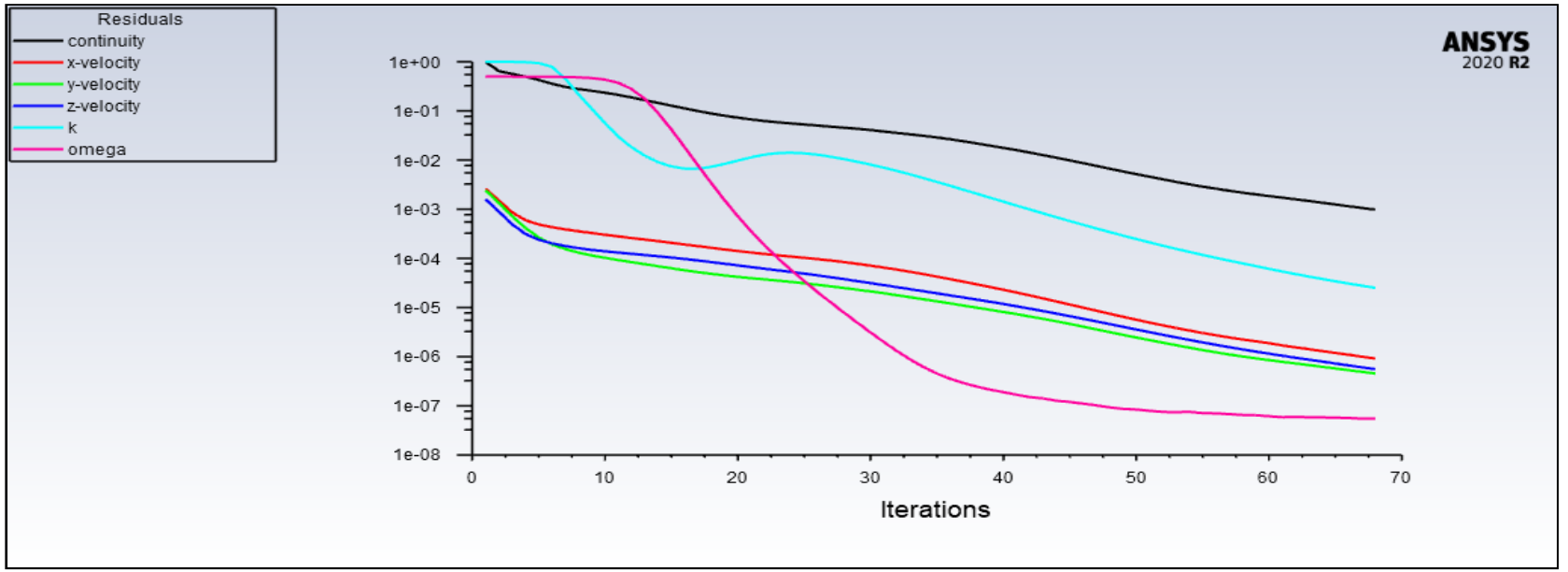

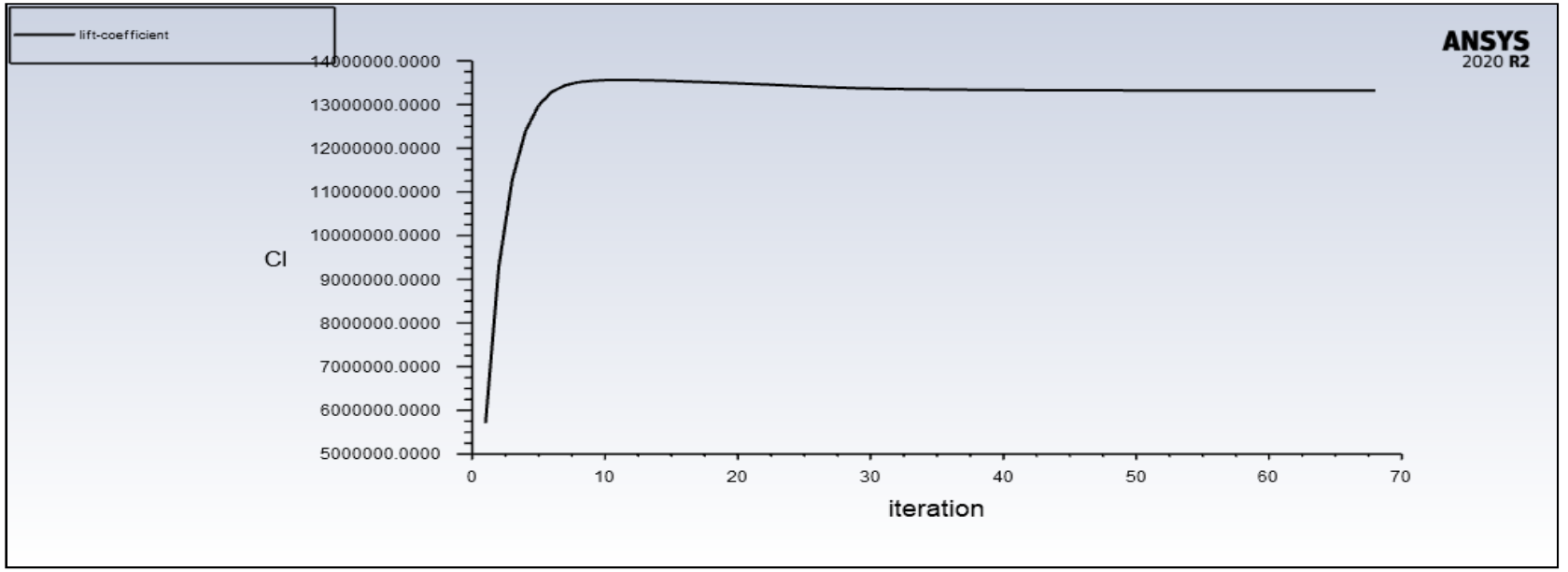

MODEL 5 - 30° PRESSURE COEFFICIENTS

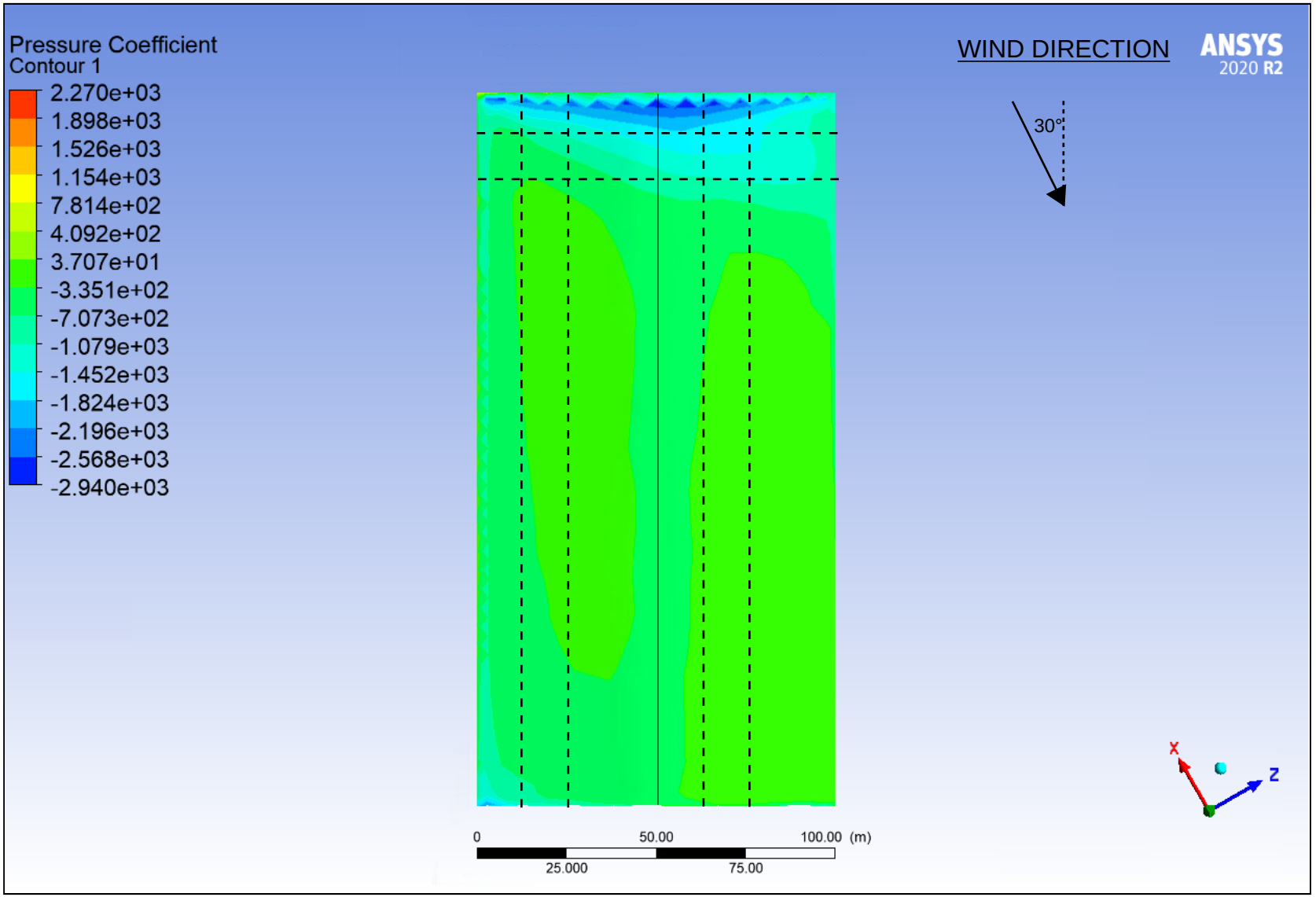

MODEL 5 - 45° SCALED RESIDUALS AND LIFT COEFFICIENT GRAPHS

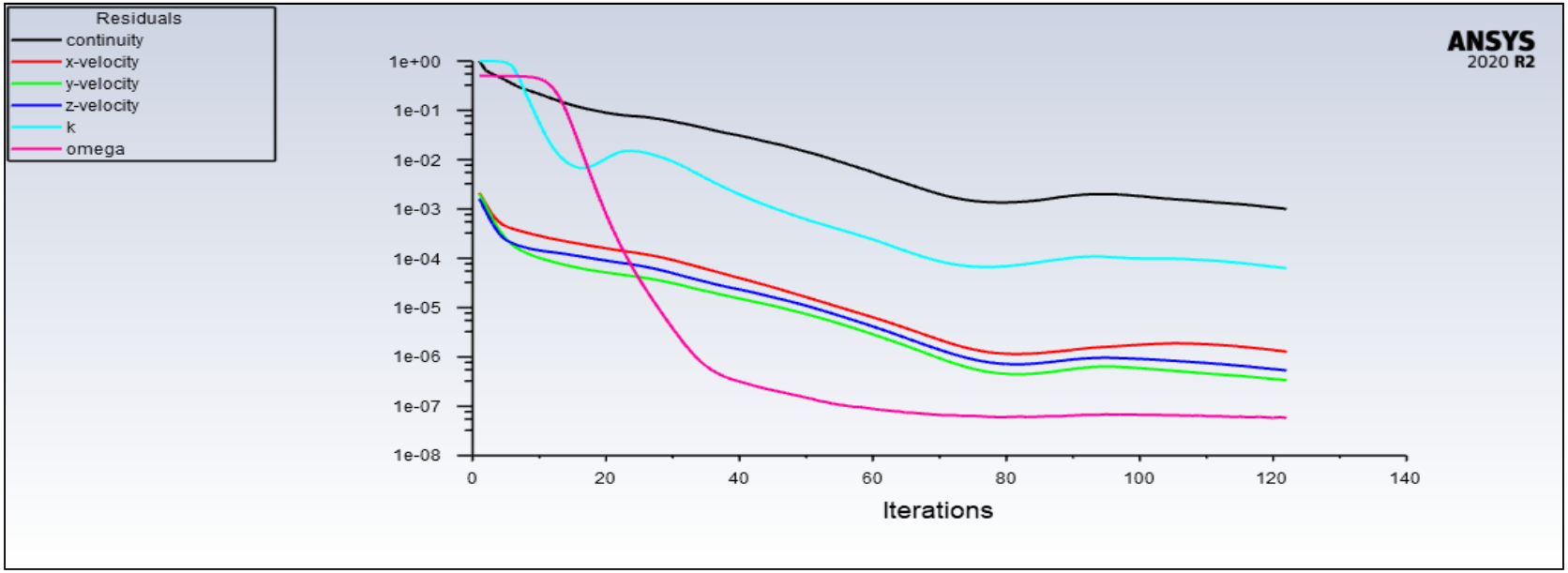

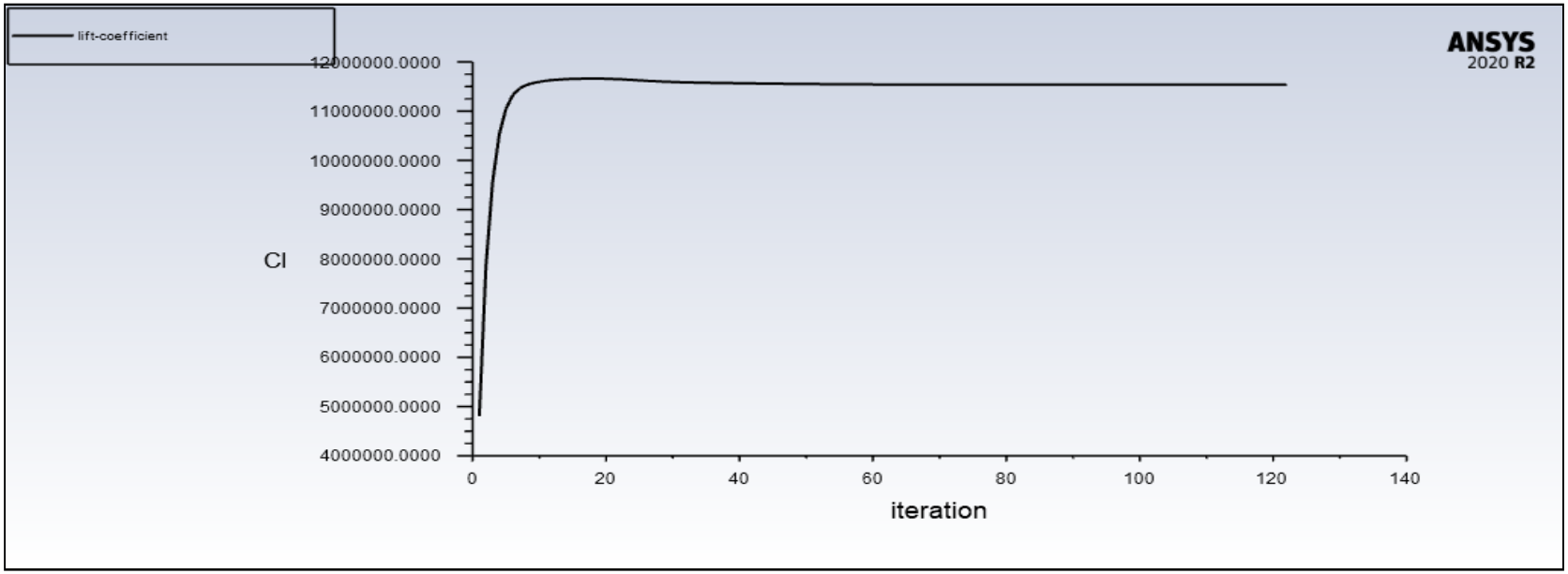

MODEL 5 - 45° PRESSURE COEFFICIENTS

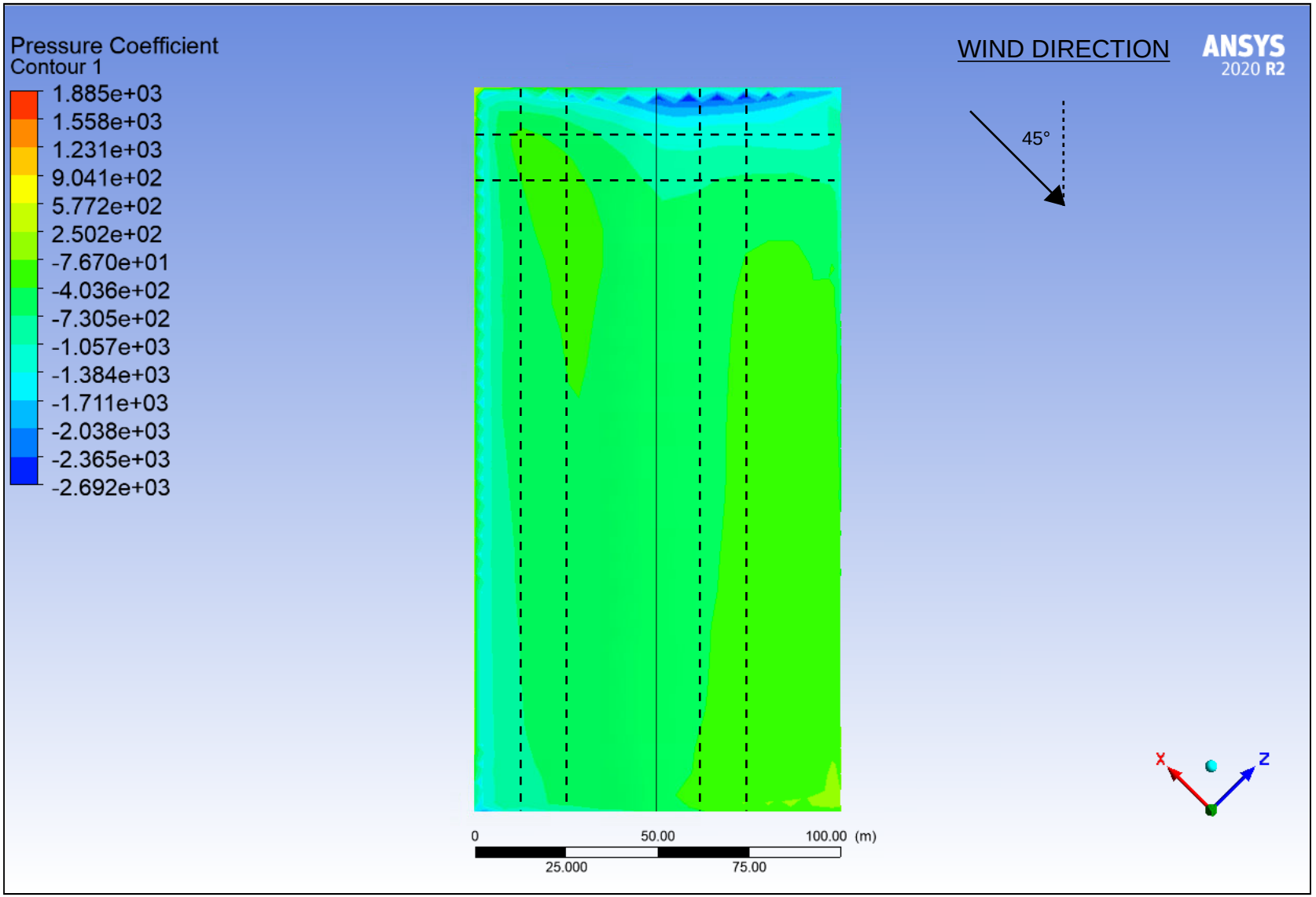

MODEL 5 - 60° SCALED RESIDUALS AND LIFT COEFFICIENT GRAPHS

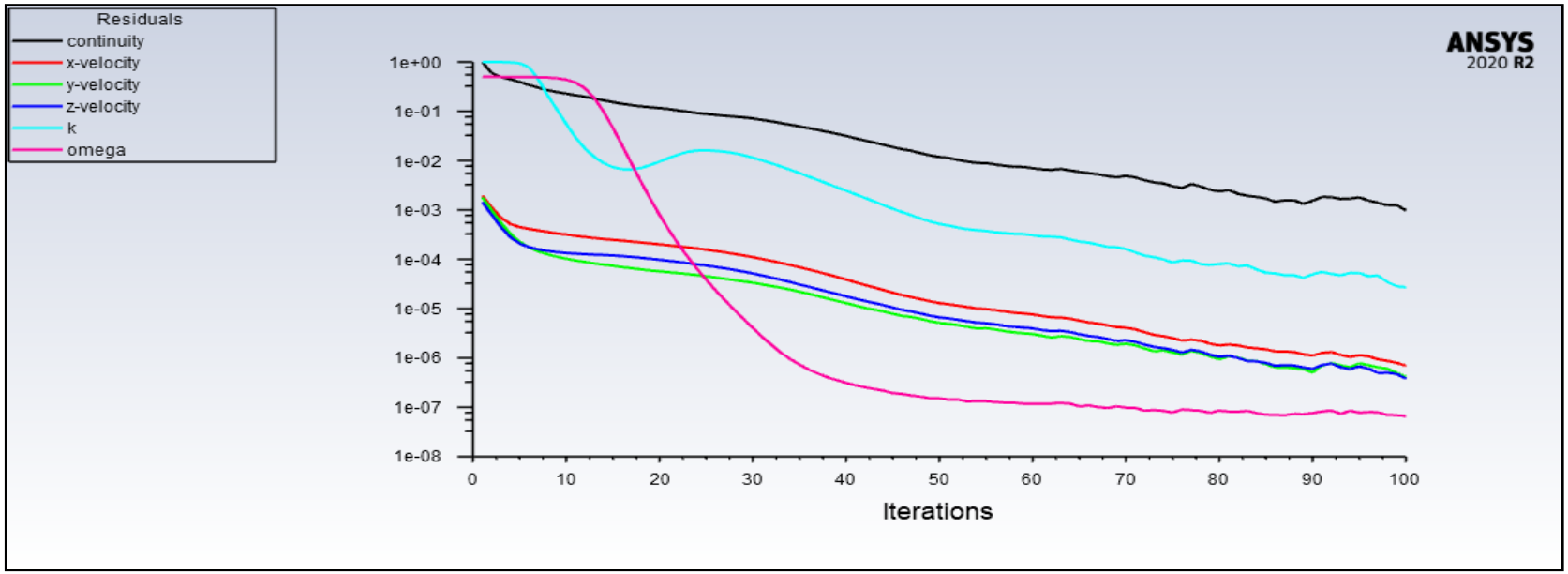

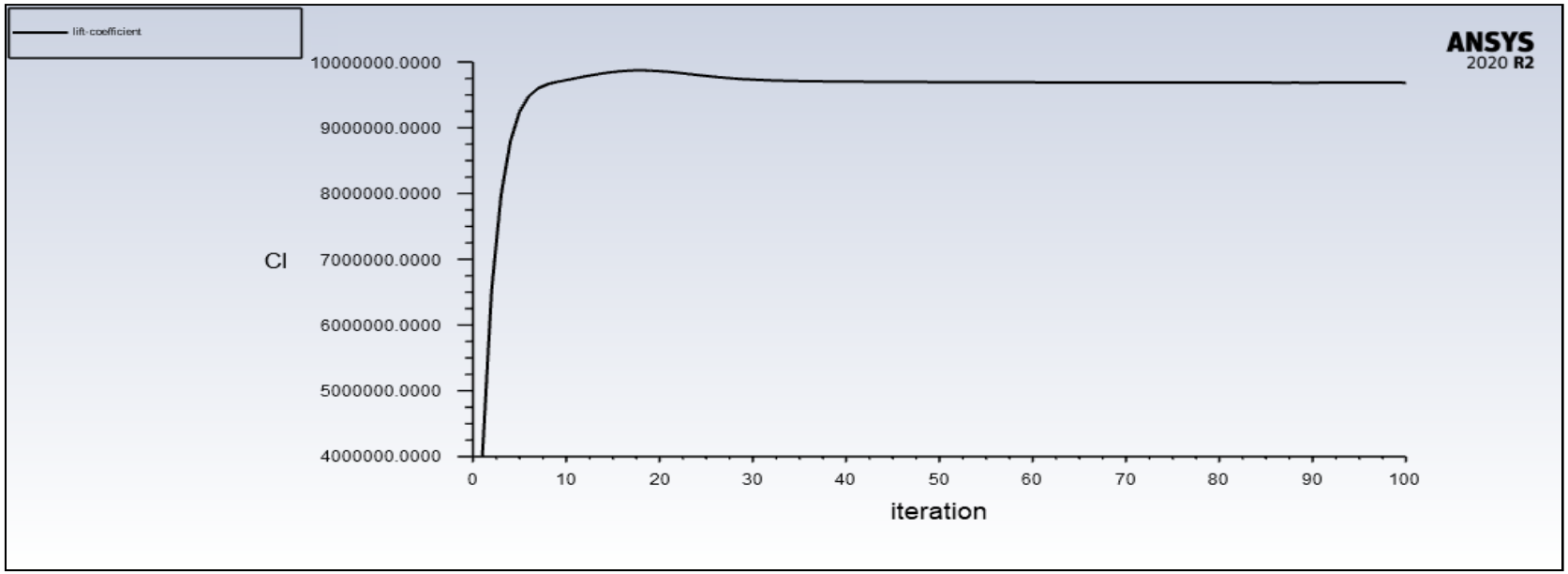

MODEL 5 - 60° PRESSURE COEFFICIENTS

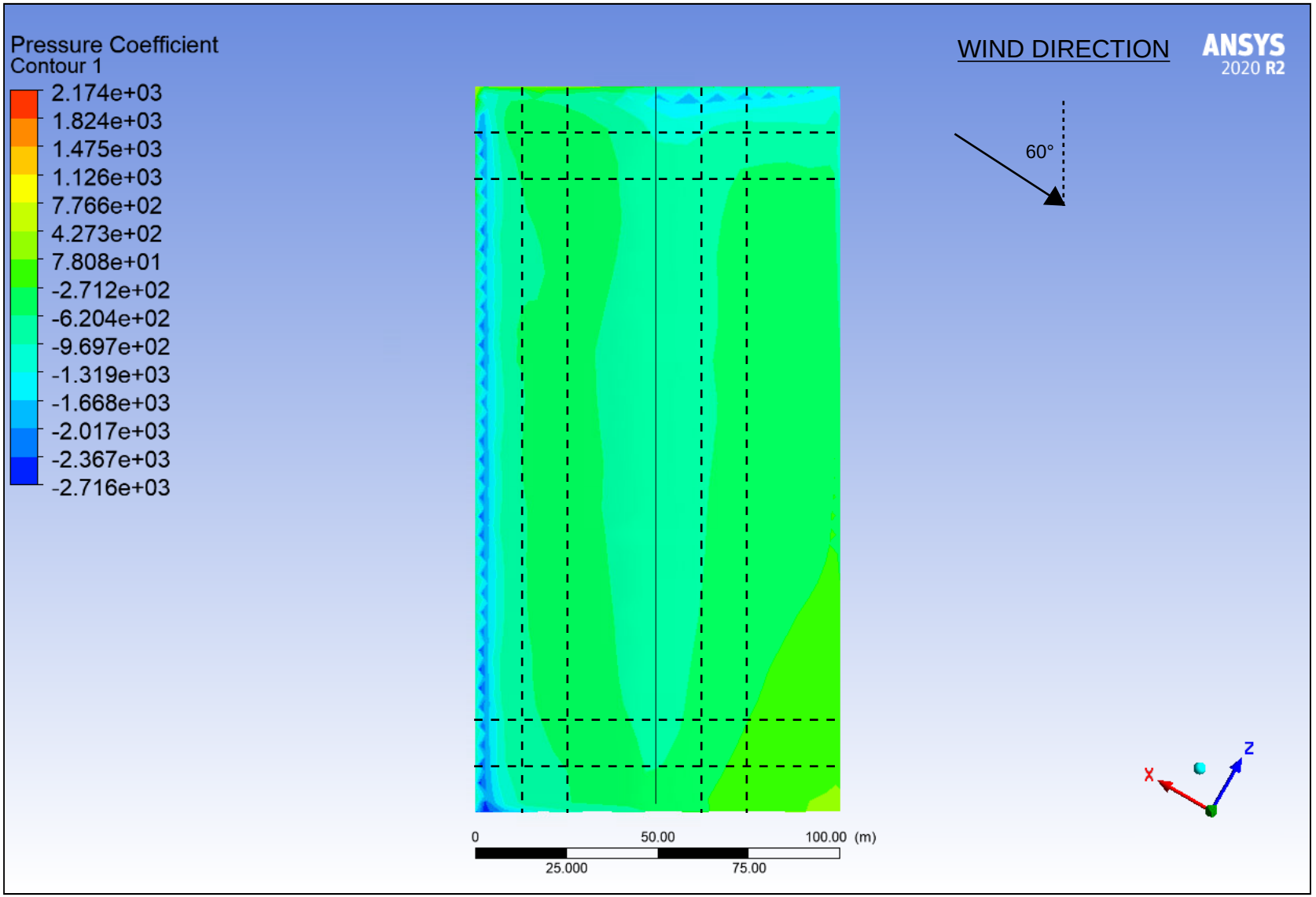

MODEL 5 - 90° SCALED RESIDUALS AND LIFT COEFFICIENT GRAPHS

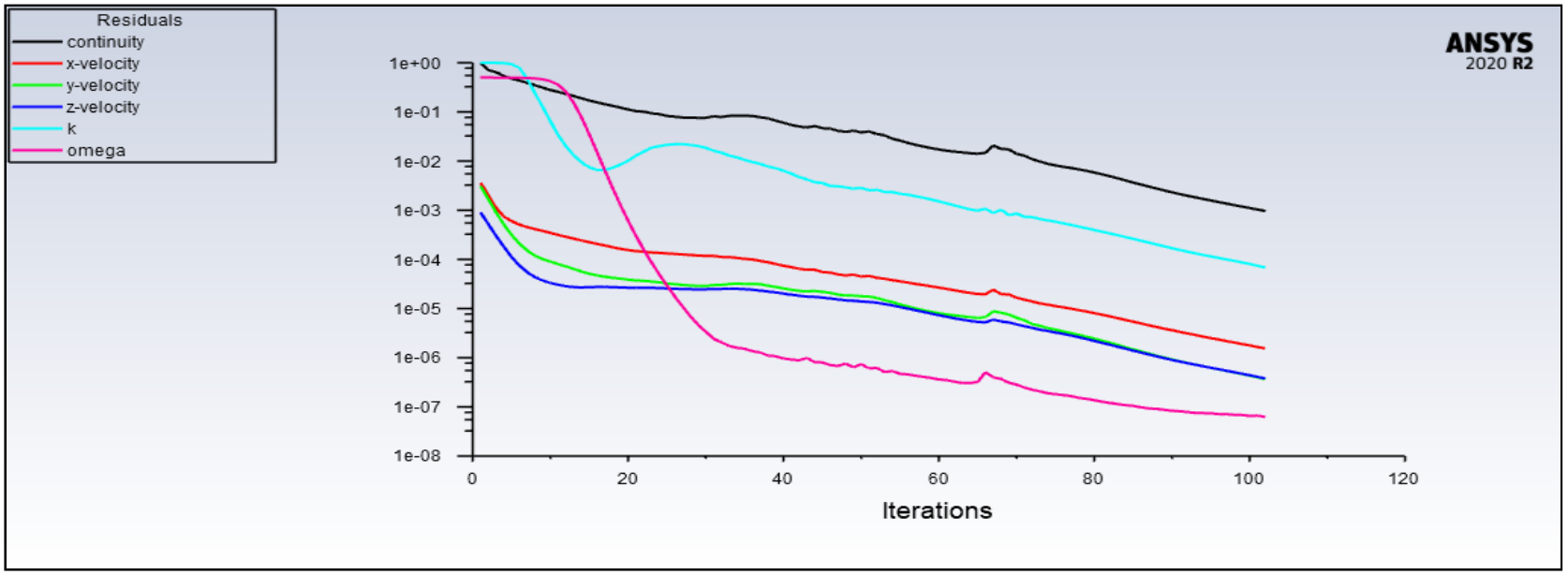

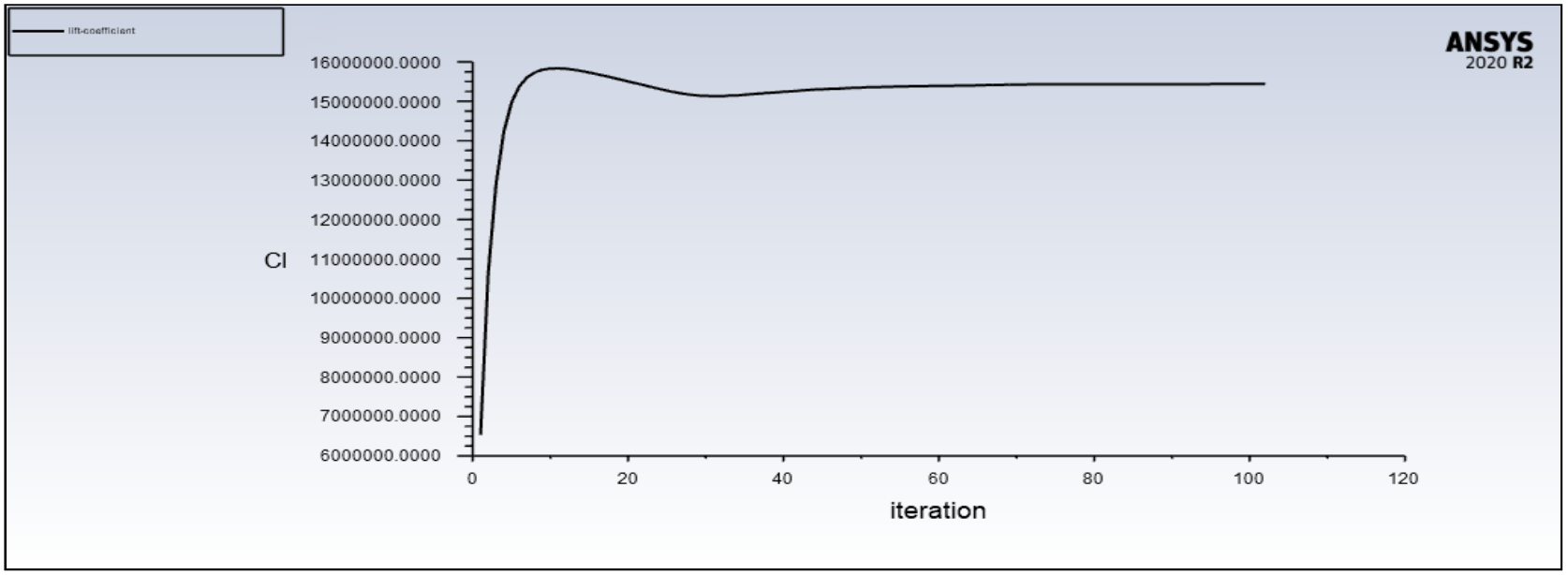

MODEL 5 - 90° PRESSURE COEFFICIENTS

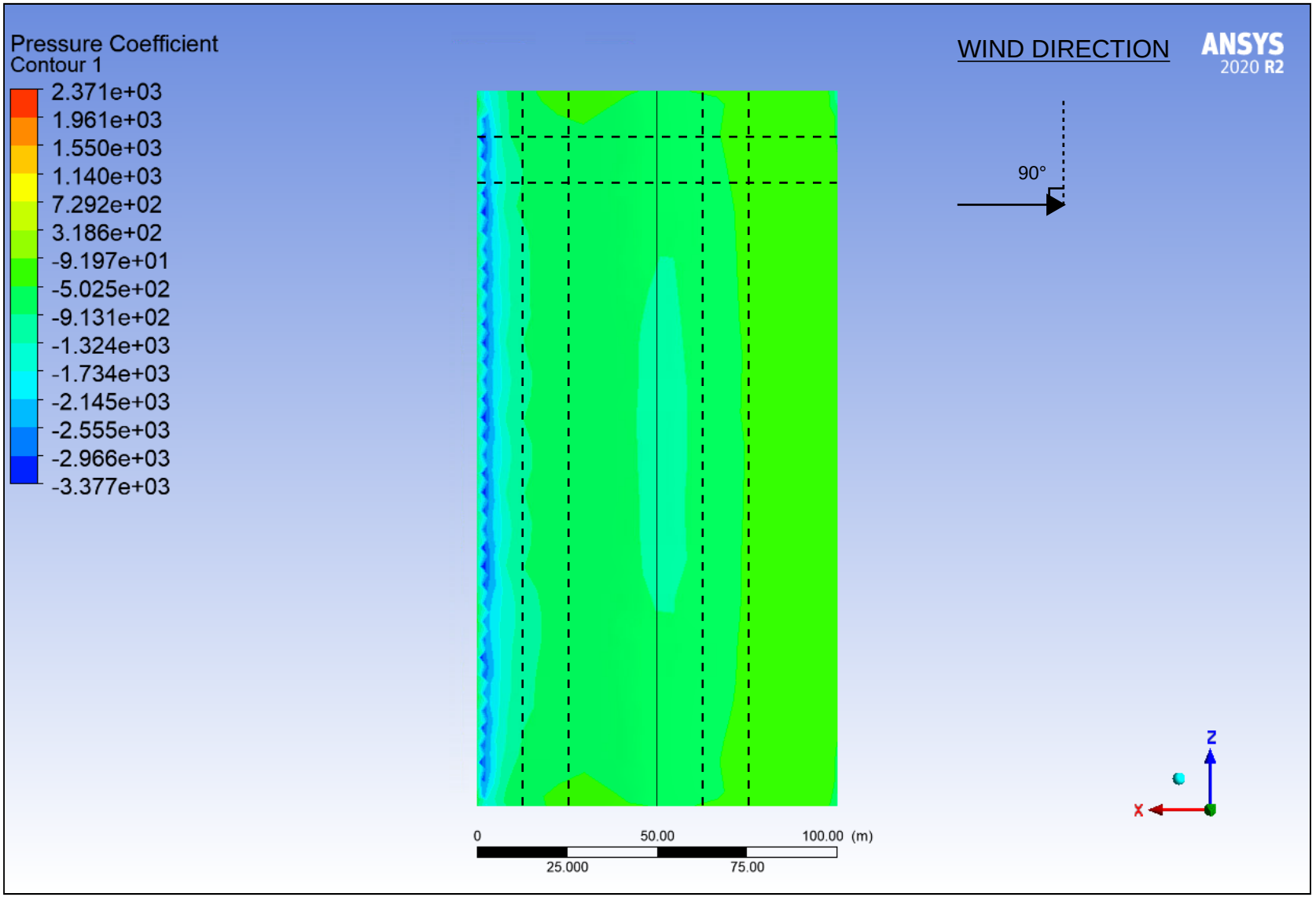

Model 6 Outputs

MODEL 6 - 0° SCALED RESIDUALS AND LIFT COEFFICIENT GRAPHS

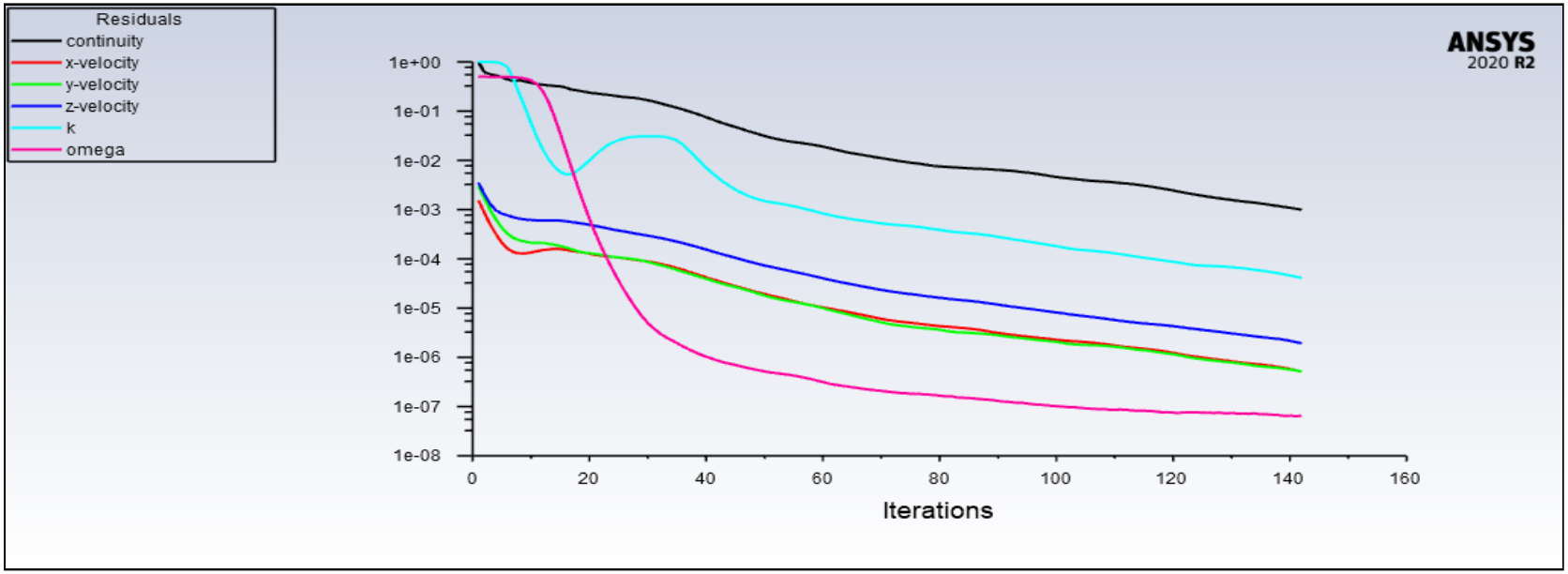

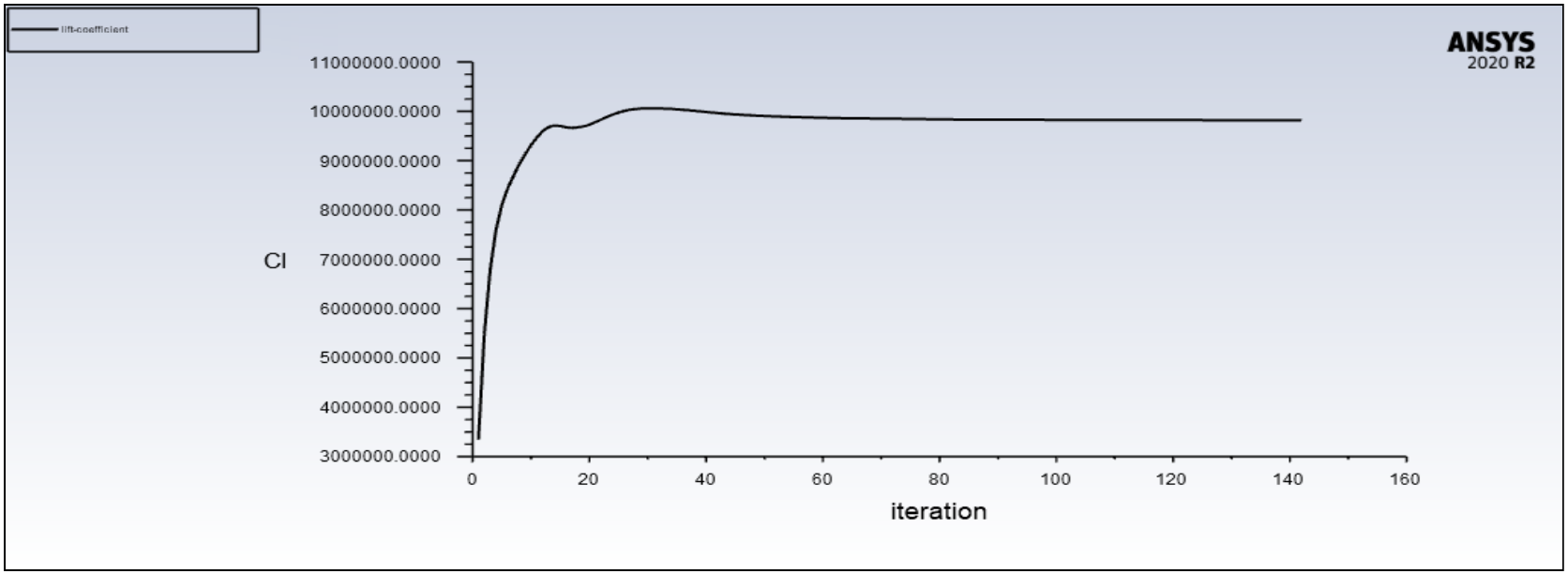

MODEL 6 - 0° PRESSURE COEFFICIENTS

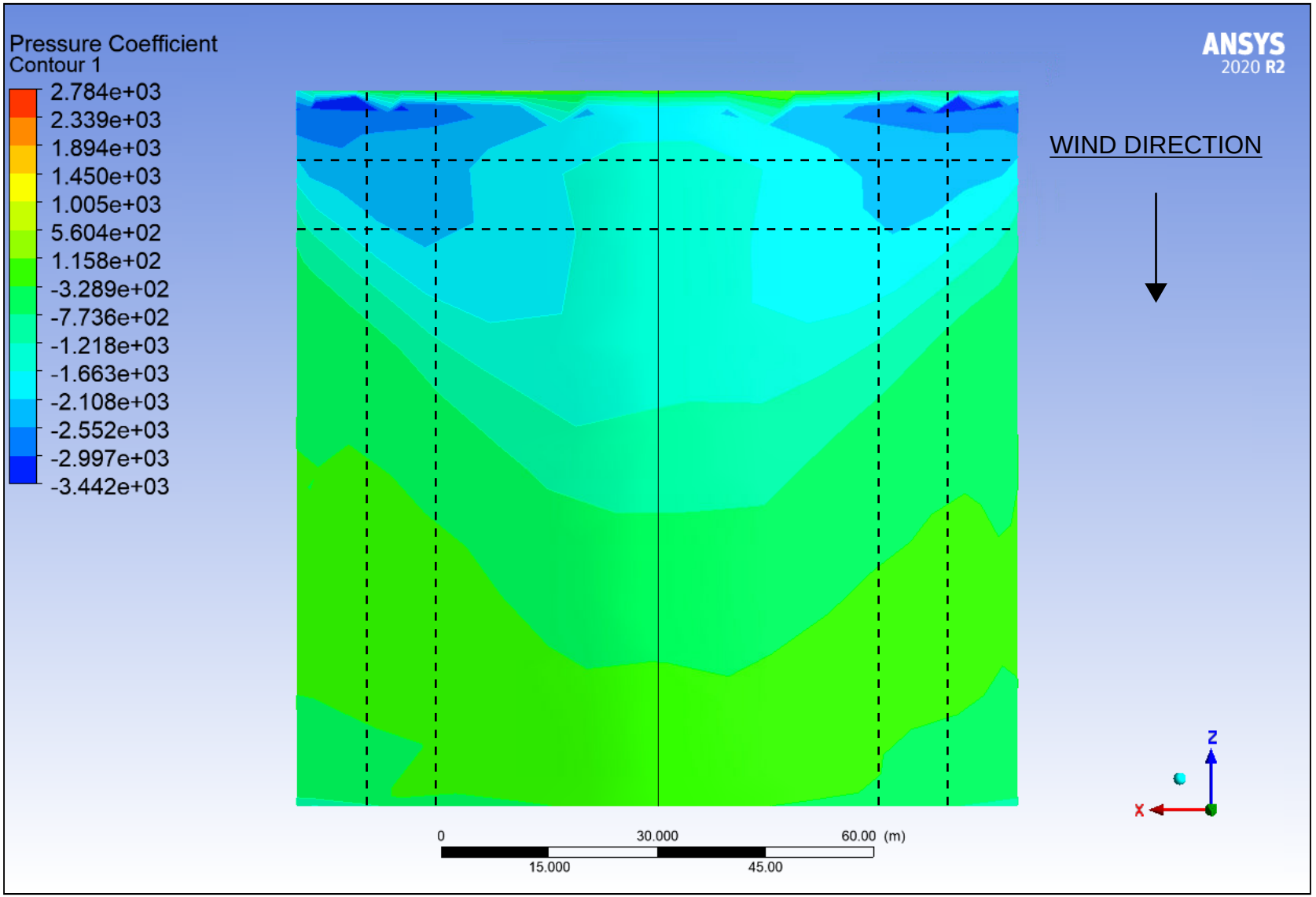

MODEL 6 - 30° SCALED RESIDUALS AND LIFT COEFFICIENT GRAPHS

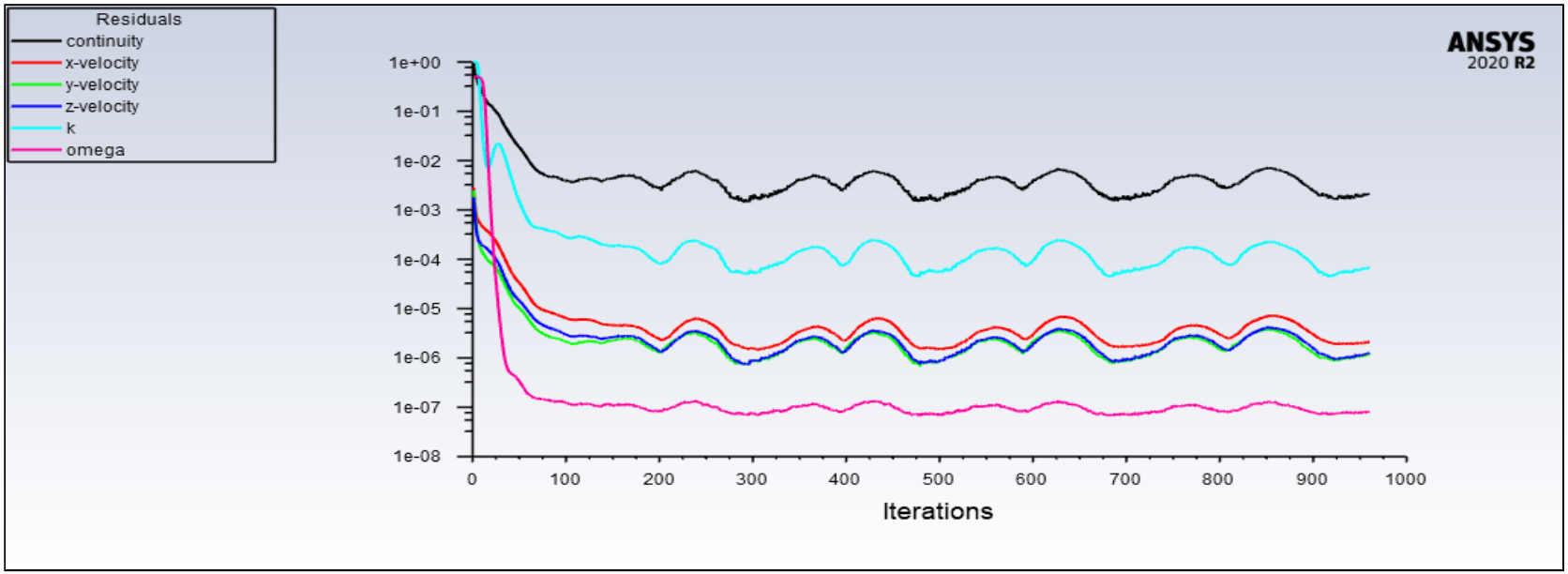

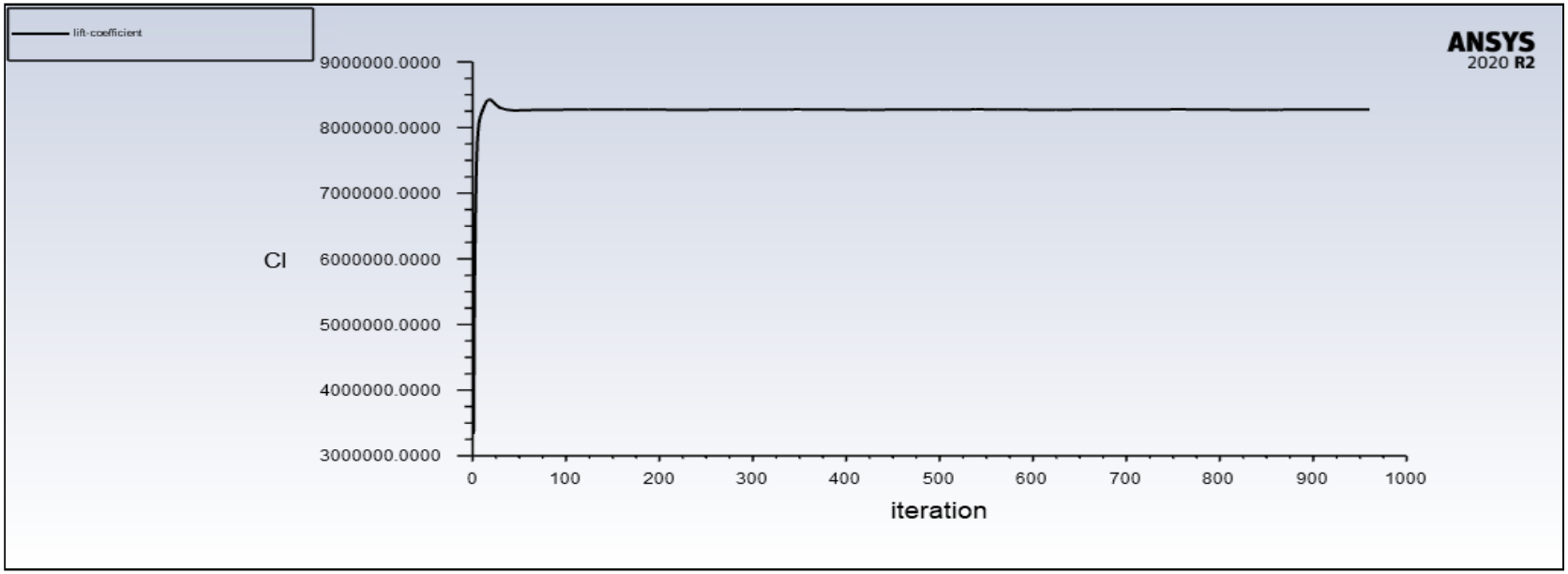

MODEL 6 - 30° PRESSURE COEFFICIENTS

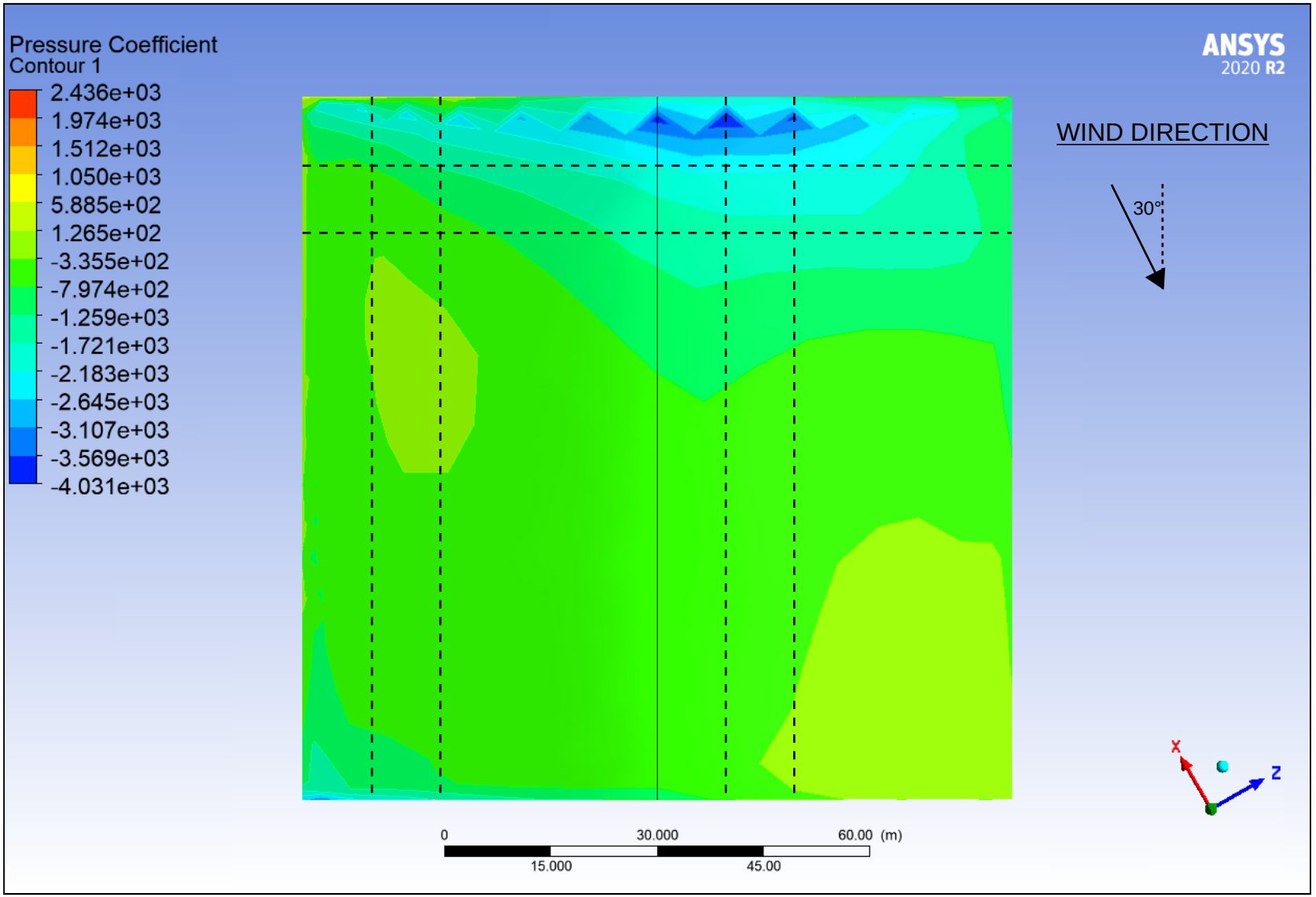

MODEL 6 - 45° SCALED RESIDUALS AND LIFT COEFFICIENT GRAPHS

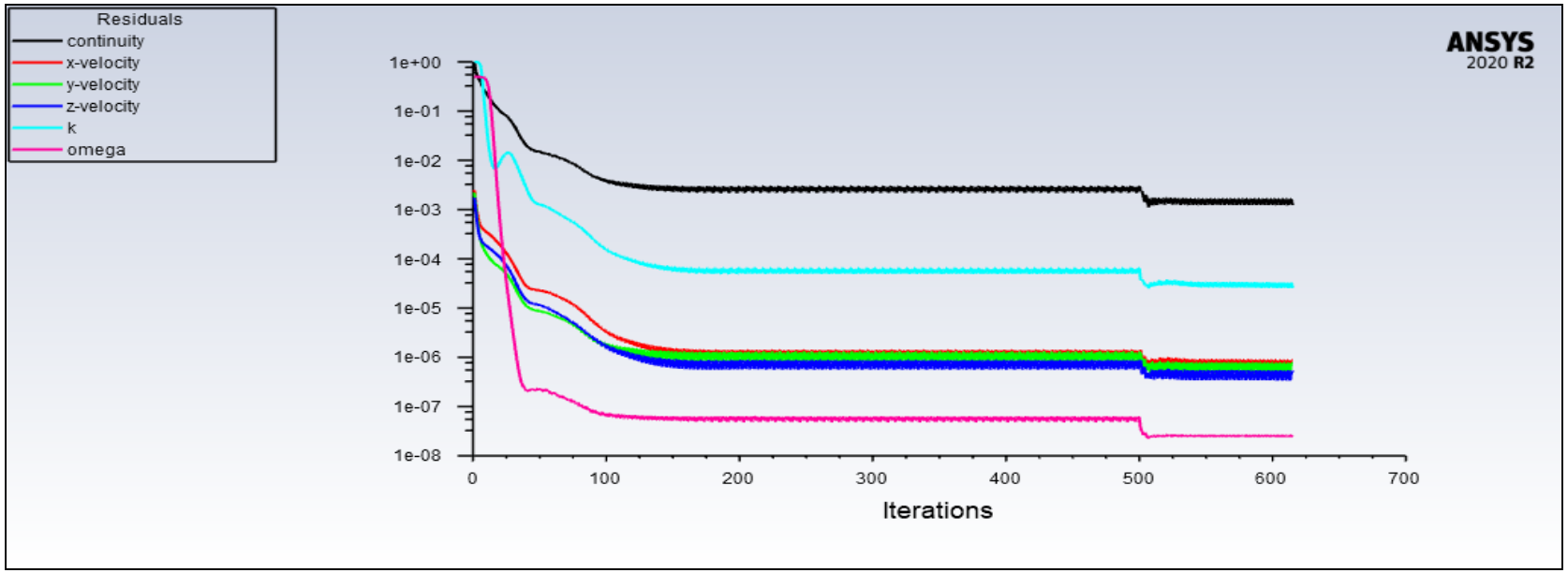

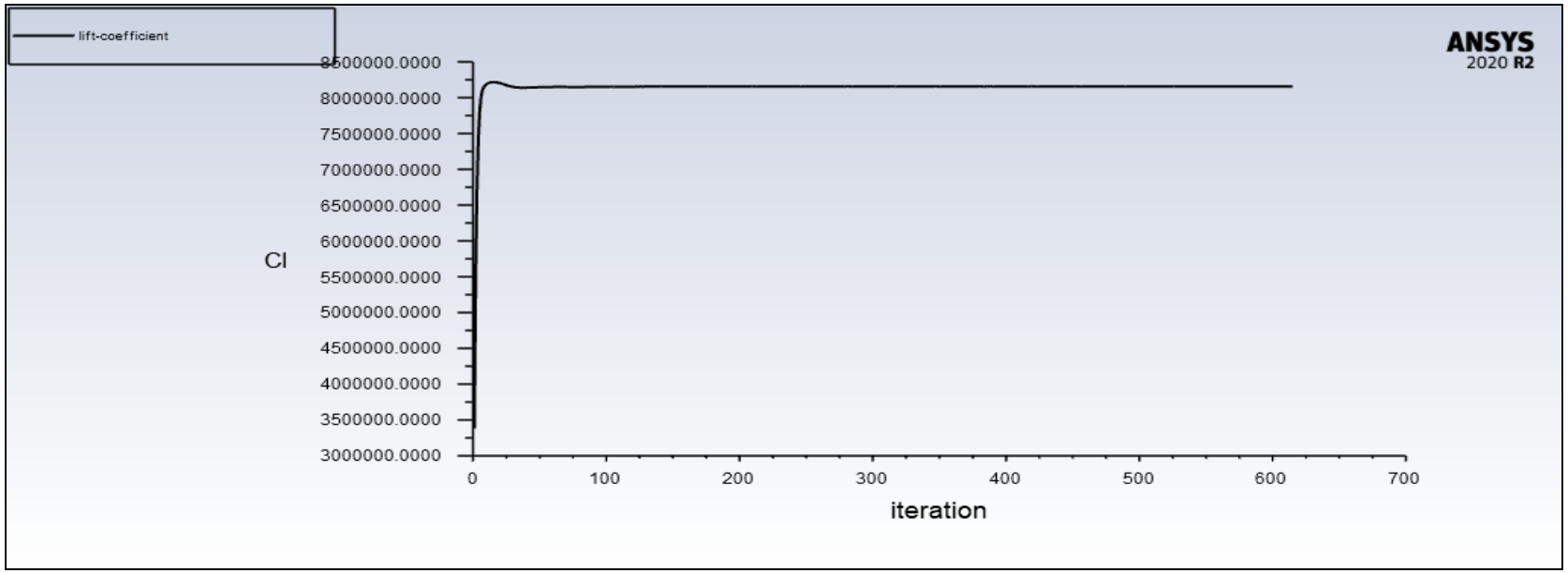

MODEL 6 - 45° PRESSURE COEFFICIENTS

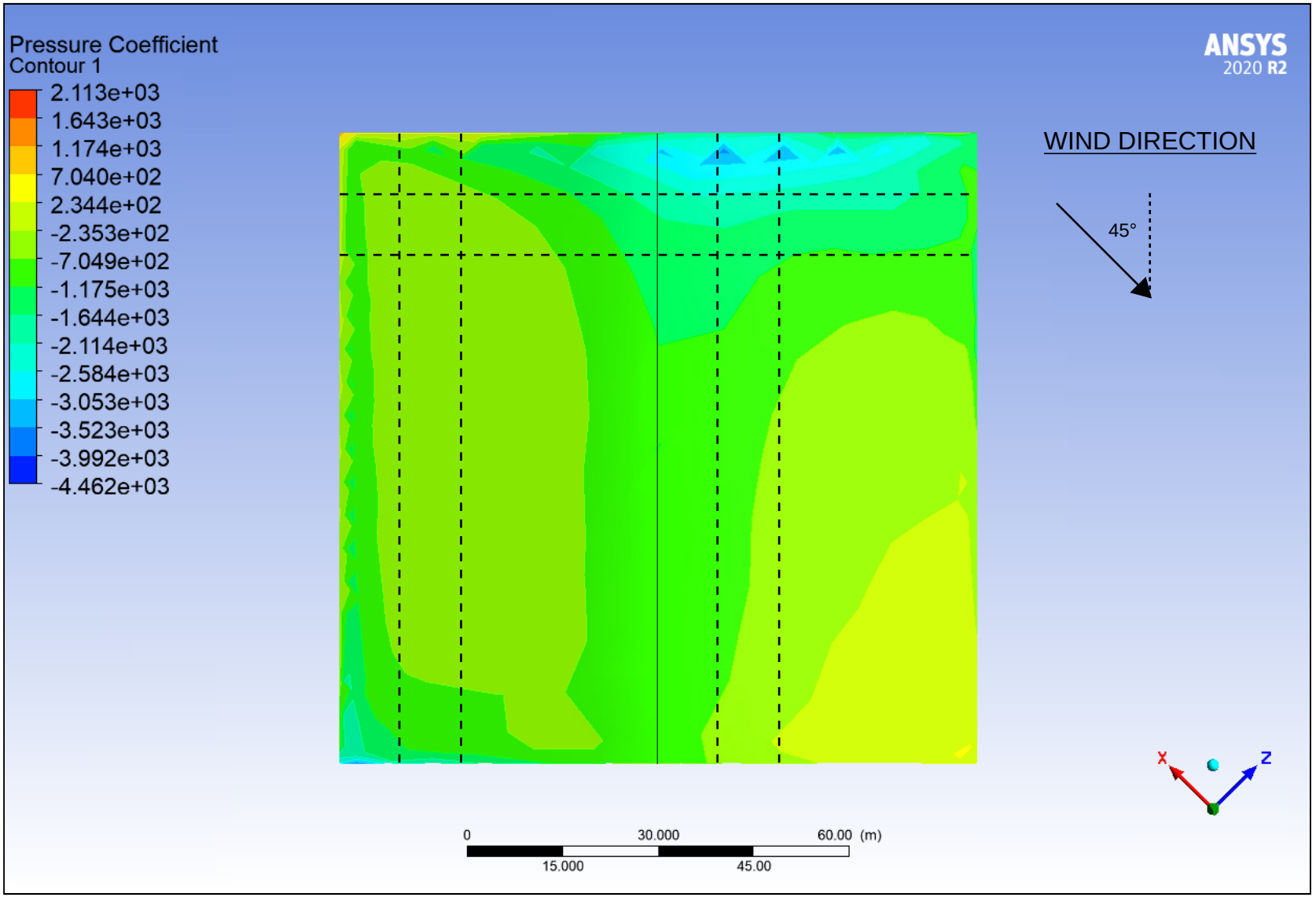

MODEL 6 - 60° SCALED RESIDUALS AND LIFT COEFFICIENT GRAPHS

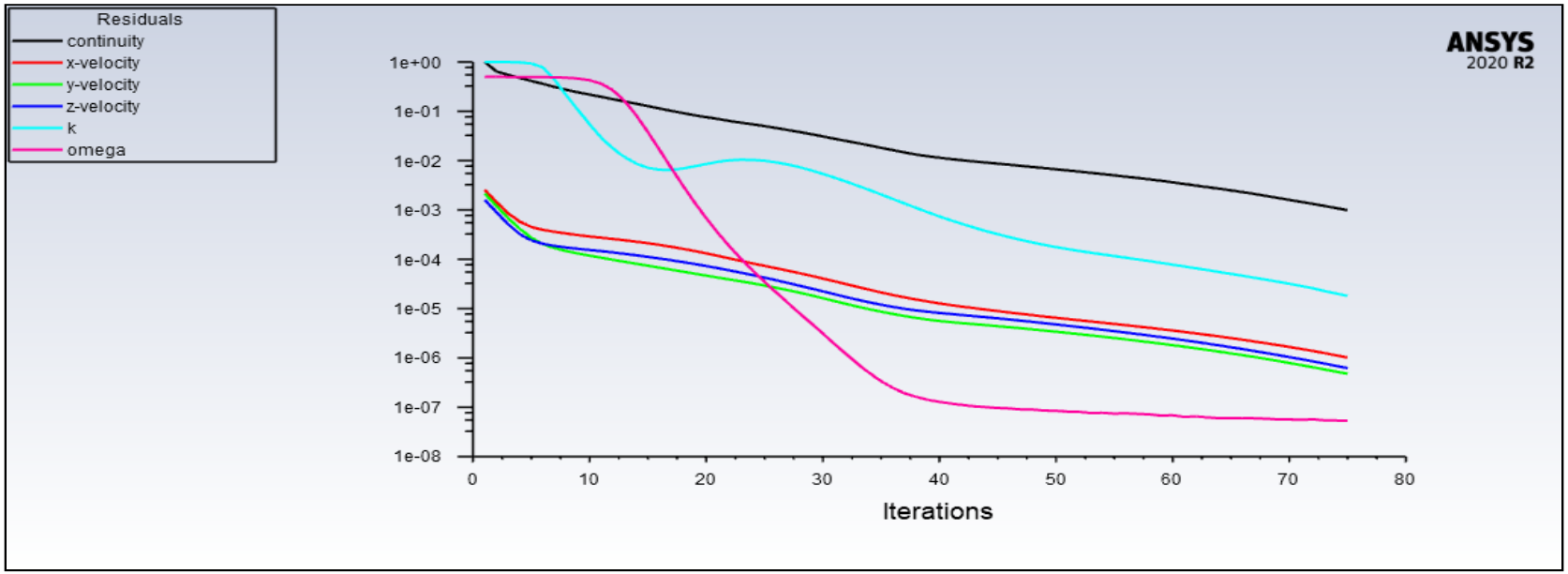

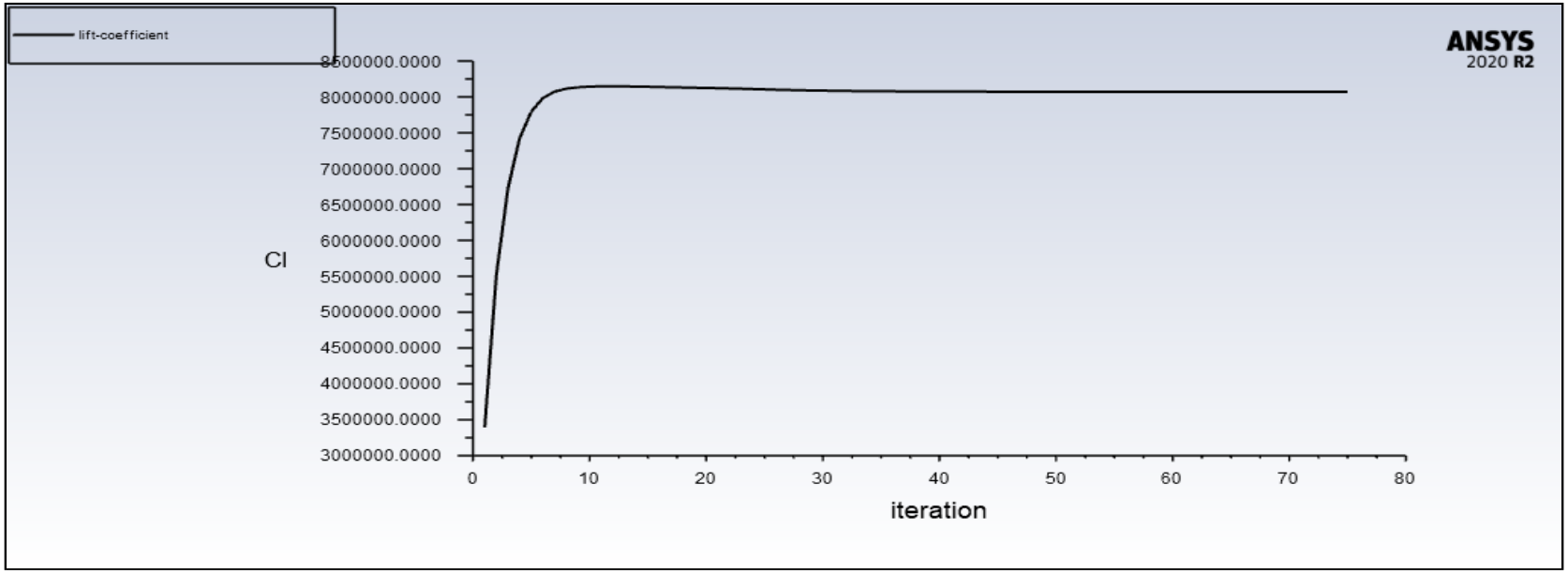

MODEL 6 - 60° PRESSURE COEFFICIENTS

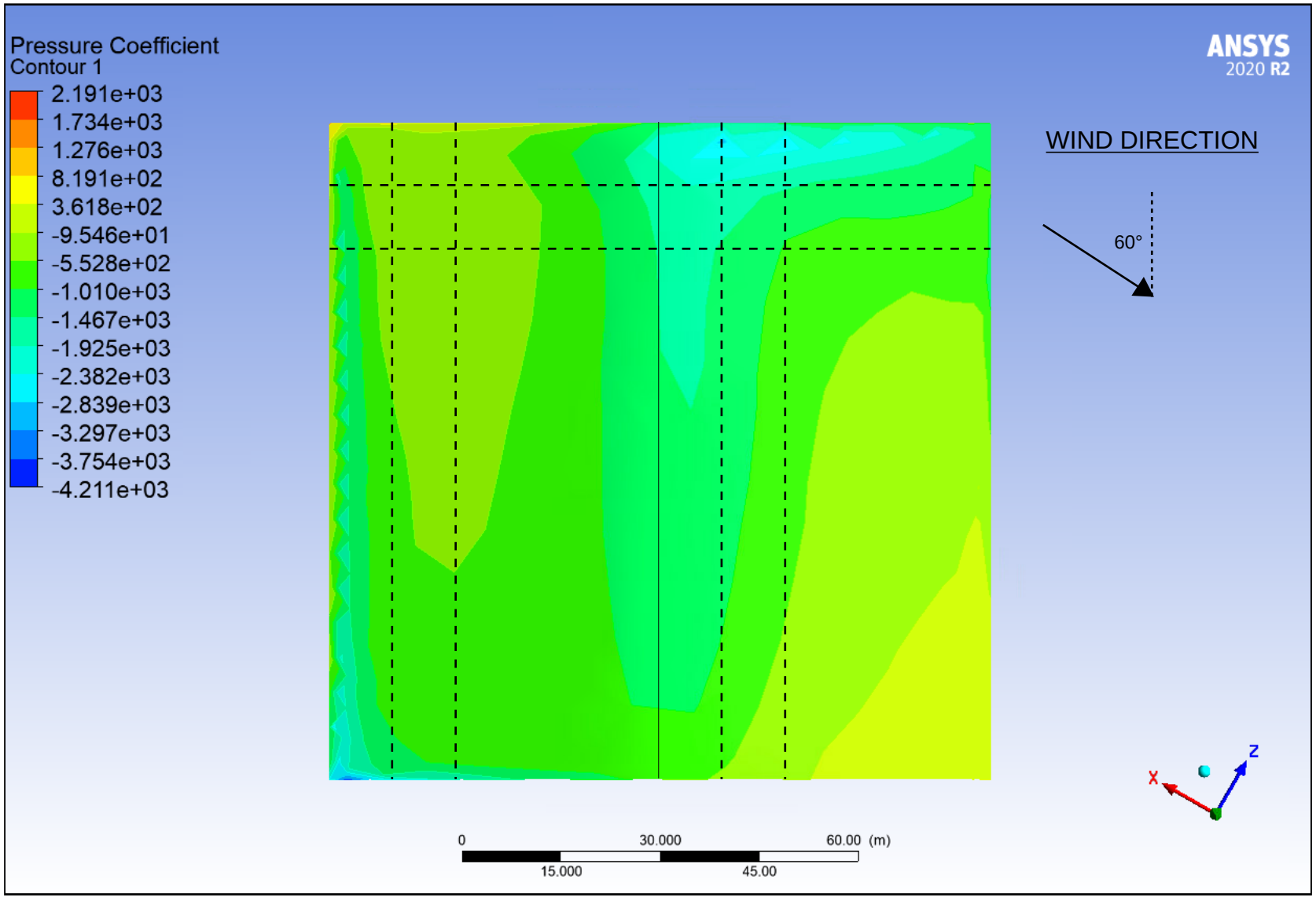

MODEL 6 - 90° SCALED RESIDUALS AND LIFT COEFFICIENT GRAPHS

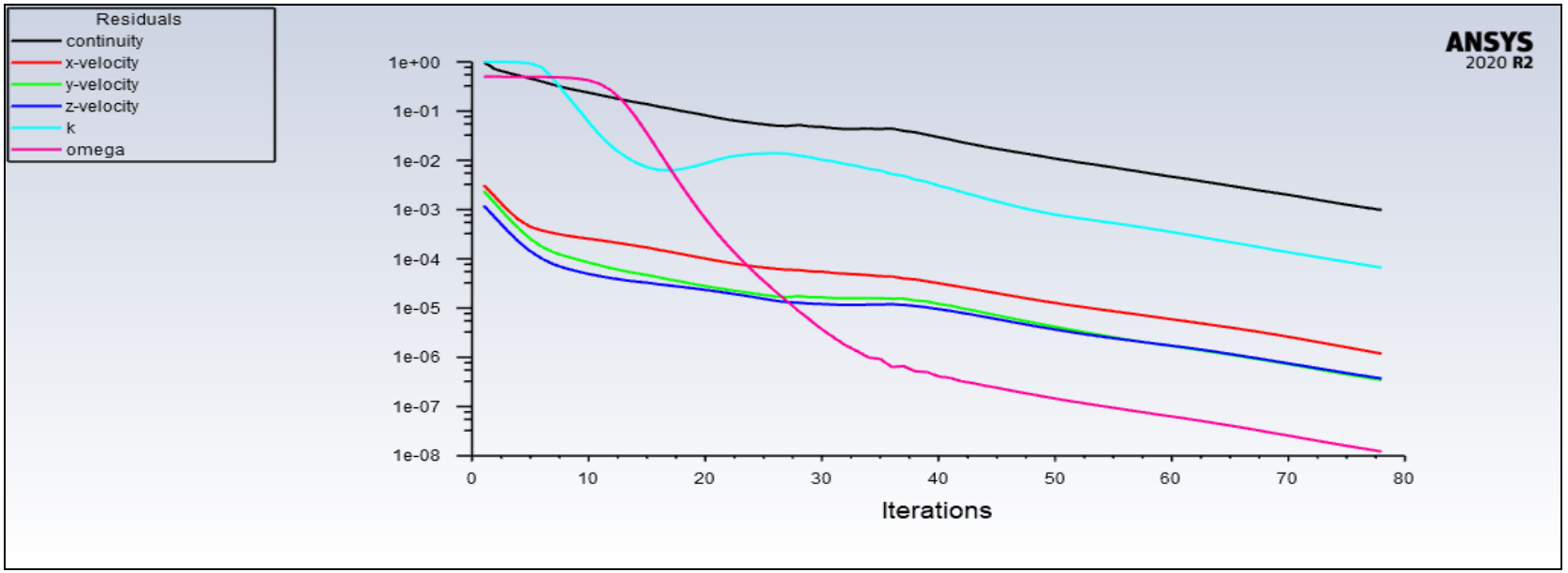

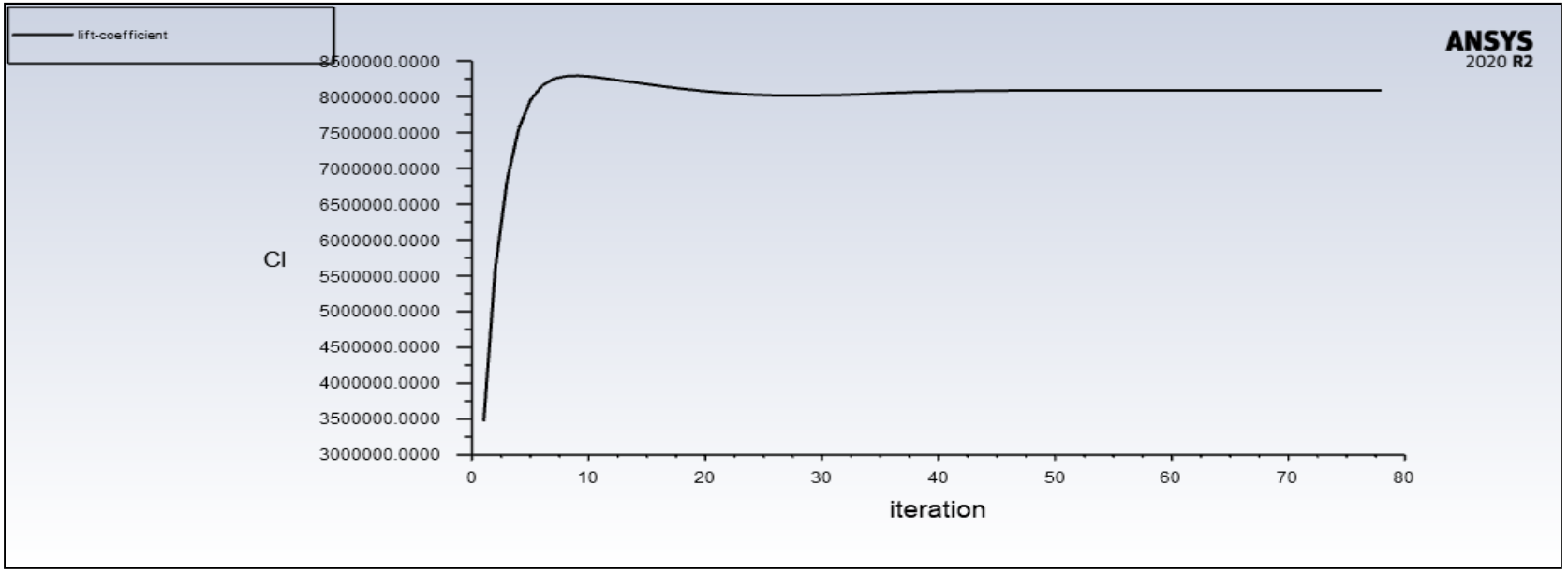

MODEL 6 - 90° PRESSURE COEFFICIENTS

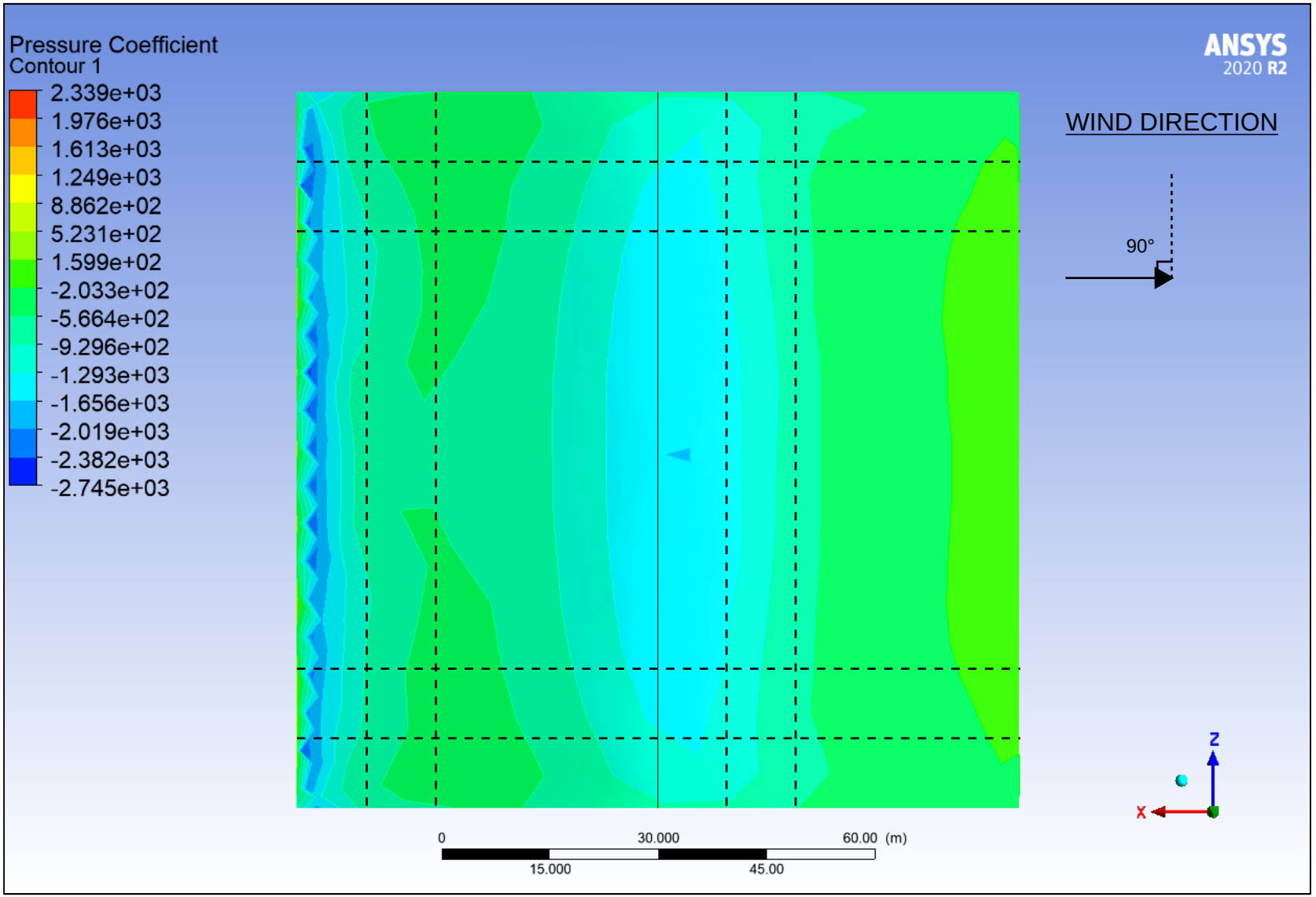

APPENDIX C

Appendix C: Project Communication Log

Project Title:	Analysis Of Local Pressure Factors On Low-Rise Industrial Buildings Using Computation Fluid Dynamics		
Student Name:	Will Davis	**Supervisor Name:**	Prof. Dr Md. Abul Kalam
Date	**Event**	**Topic of Communication**	**Outcome**
23/09/2023	Email	Description of report topic and outline. Attachment of first report draft for review.	Supervisor made minor grammatical track changes on report.
26/10/2023	Email	Confirmation of face-to-face meeting.	No meeting took place.